

NASA TMX-69881

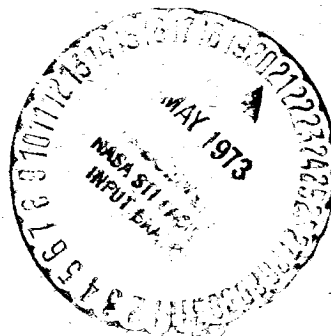
# NIMBUS II USERS' GUIDE

(NASA-TM-X-69881)  
(NASA) 235 p

NIMBUS 2 USERS' GUIDE

N73-72517

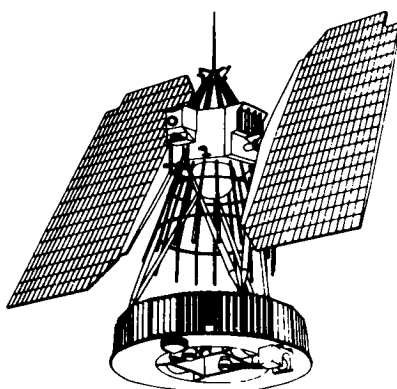
00/99    Unclass  
          02560



GODDARD SPACE FLIGHT CENTER  
GREENBELT, MARYLAND

# **NIMBUS II USERS' GUIDE**

JULY 1966



Prepared by  
ARACON Geophysics Company  
Concord, Massachusetts  
A Division of Allied Research Associates, Inc.

For the  
**Nimbus Project**  
**Goddard Space Flight Center**  
**Greenbelt, Maryland**



## FOREWORD

The Nimbus II USERS' GUIDE has been prepared for the purpose of providing the requisite information and guidance to all potential users of Nimbus II data.

Part I (Sections 1 through 5), of this document provides background information about the Nimbus II system in general and discusses the experimental sensory subsystems and the class of data to be anticipated from them. Some subsystems are treated only briefly; appropriate reference to other documents is given for those needing more details.

Part II (Sections 6 through 9), of the USERS' GUIDE deals with the format of Nimbus II data; data processing, archiving and availability; and information relative to retrieval services.

Most importantly, the USERS' GUIDE describes the contents and format of the Nimbus II data catalogs issued at approximately monthly intervals. The individual catalogs are not completely self-explanatory, so that the USERS' GUIDE is a necessary adjunct to the catalogs.

The preparation of the Nimbus II USERS' GUIDE was accomplished largely by the ARACON Geophysics Division of Allied Research Associates, Inc., Concord, Massachusetts under Contract NAS 5-10114 with the Goddard Space Flight Center, NASA, Greenbelt, Maryland. Sections 3 and 4 of the USERS' GUIDE were prepared by the HRIR and MRIR Experimenters, Lonnie L. Foshee and Andrew W. McCulloch, respectively, of the Laboratory for Atmospheric and Biological Sciences, Goddard Space Flight Center. The ARACON technical effort was conducted primarily by John B. Howe, Leon Goldshlak, Milton M. Hopkins, Jr., Donald R. Jones and Romeo R. Sabatini. John Lindstrom was the Data Utilization Systems Manager and Ralph Shapiro was the Operations Manager for the Nimbus Project.

Harry Press  
Nimbus Project Manager  
Goddard Space Flight Center

## CONTENTS

FOREWORD . . . . .	iii
--------------------	-----

### PART I

<u>Section</u>	<u>Page</u>
1 NIMBUS II SYSTEM . . . . .	1
1.1 Nimbus II Spacecraft . . . . .	1
1.2 Orbit. . . . .	1
1.3 Spacecraft Attitude . . . . .	1
1.4 Ground Station Complex . . . . .	4
1.5 Data Utilization Center. . . . .	5
2 ADVANCED VIDICON CAMERA SYSTEM (AVCS). . . . .	7
2.1 Description of the AVCS. . . . .	7
2.2 AVCS Calibration . . . . .	11
2.3 Data Display Format . . . . .	12
3 HIGH RESOLUTION INFRARED RADIOMETER (HRIR) EXPERIMENT . . . . .	19
3.1 Introduction . . . . .	19
3.2 The High Resolution Infrared Radiometer . . . . .	19
3.3 The HRIR Subsystem and Ground Processing Equipment. . .	22
3.4 HRIR Data Processing . . . . .	23
3.4.1 Photofacsimile Film Strips. . . . .	23
3.4.2 Gray Scale Calibration. . . . .	27
3.4.3 Digital HRIR Data Processing. . . . .	28
3.4.4 Analog Recording . . . . .	30
3.5 Automatic Gridding of HRIR Data . . . . .	31
3.6 Calibration. . . . .	32
3.6.1 Effective Spectral Response . . . . .	32
3.6.2 Effective Radiance . . . . .	35
3.6.3 Equivalent Blackbody Temperature . . . . .	35

## CONTENTS (Continued)

Section		Page
4	MEDIUM RESOLUTION RADIOMETER (MRIR) EXPERIMENT . . . . .	39
4.1	Description of the Experiment. . . . .	39
4.2	Calibration . . . . .	44
4.3	Data Processing . . . . .	62
	4.3.1 General. . . . .	62
	4.3.2 Analog . . . . .	63
	4.3.3 Digital MRIR Data Processing. . . . .	63
	4.3.4 Photo Display. . . . .	64
5	AUTOMATIC DATA TRANSMISSION SYSTEMS: AUTOMATIC PICTURE TRANSMISSION (APT) AND DIRECT READOUT INFRARED RADIOMETER (DRIR) . . . . .	69
5.1	Automatic Picture Transmission (APT). . . . .	69
	5.1.1 Data Code Experiment. . . . .	71
5.2	Direct Readout Infrared (DRIR) . . . . .	72
6	DATA PROCESSING, ARCHIVING AND ACCESS . . . . .	73
6.1	AVCS Data Processing. . . . .	73
6.2	AVCS Data Archiving and Access . . . . .	73
6.3	HRIR Data Processing . . . . .	74
6.4	HRIR Data Archiving and Access . . . . .	75
6.5	MRIR Data Processing. . . . .	75
6.6	MRIR Data Archiving and Access . . . . .	76
6.7	HRIR and MRIR Computer-Produced Standard Format Data Archiving and Access. . . . .	76
6.8	HRIR and MRIR Non-Standard Format Data Archiving and Access. . . . .	78
6.9	APT and DRIR . . . . .	80
6.10	Special Instructions to Users. . . . .	80

## CONTENTS (Continued)

<u>Section</u>	<u>Page</u>
7	NIMBUS II CATALOG . . . . . 81
7.1	General . . . . . 81
7.2	Section I – Introductory Remarks . . . . . 81
7.3	Section II – Daily Sensor "on" Status Charts . . . . . 81
7.4	Section III – APT and DRIR. . . . . 84
7.5	Section IV – Orbital Data . . . . . 84
7.6	Section V – Sensory Information Processing . . . . . 84
8	COMPUTERIZED DATA RETRIEVAL SYSTEM . . . . . 85
8.1	Basic Concepts . . . . . 85
8.2	Inputs to SIP Program . . . . . 85
8.2.1	Swath . . . . . 85
8.2.2	Sector. . . . . 86
8.2.3	HRIR Data Block. . . . . 86
8.3	Output – Data Log Section of Catalogs. . . . . 86
8.4	Data Retrieval . . . . . 87
8.4.1	Swath Information in Data Log. . . . . 87
8.4.2	Sector Information in Data Log . . . . . 87
8.5	Data Retrieval . . . . . 88
8.5.1	Output Format . . . . . 90
8.5.2	Retrieval Parameters . . . . . 90
8.5.3	Logical Combinations of Parameters . . . . . 91
9	CLASSIFICATION OF DATA CONTENT . . . . . 93
9.1	Introduction . . . . . 93
9.2	Cloud Features . . . . . 93
9.2.1	Vortical Clouds . . . . . 101
9.2.2	Major Cloud Bands . . . . . 120
9.2.3	General Cloud Features (Neither Vortical Nor Major Bands). . . . . 131

## CONTENTS (Continued)

<u>Section</u>	<u>Page</u>
9.3 HRIR Data . . . . .	163
9.4 Terrestrial Features . . . . .	188
9.4.1 Water Body . . . . .	196
9.4.2 Desert . . . . .	196
9.4.3 Mountain . . . . .	196
9.4.4 Coastline . . . . .	197
9.4.5 Other Geomorphology . . . . .	197
9.4.6 Miscellaneous . . . . .	197
9.5 Indistinguishable Features . . . . .	198
9.6 Pictures of Poor Quality or No Discernible Features. . . . .	198
9.7 Classification and Cataloging Descriptors for Nimbus C Satellite. . . . .	199
9.8 Phenomenon Continuation Code . . . . .	204
9.9 Codes for Remarks Section of Data Log. . . . .	206
9.9.1 Data Content Confirmation Code . . . . .	206
9.9.2 Quality Control Codes . . . . .	207
9.9.3 Cloud Amount Code . . . . .	208
APPENDIX A – Format of NMRT-HRIR . . . . .	209
APPENDIX B – Digital MRIR Data Processing. . . . .	215
APPENDIX C – Glossary and Abbreviations . . . . .	221

## SECTION I

### NIMBUS II SYSTEM

#### 1.1 Nimbus II Spacecraft

The Nimbus II spacecraft is essentially the same as Nimbus I (Reference 1). The major differences between the two spacecraft are the addition of a Medium Resolution Radiometer (MRIR) to the sensory ring of Nimbus II and the provision for immediate broadcast of nighttime High Resolution Infrared Radiometer (HRIR) data which can be received by modified APT (Automatic Picture Transmission) ground station equipment. Nimbus II contains Advanced Vidicon Camera System (AVCS), APT and HRIR systems. The basic Nimbus II spacecraft is illustrated in Figure 1-1.

#### 1.2 Orbit

Nimbus II was launched on 15 May 1966 from the Western Test Range in California, by a Thrust Augmented Thor (TAT)/Agena B vehicle. A near-circular orbit was achieved, with an apogee height of 637 nm (1179 Km), a perigee height of 591 nm (1095 Km), and an inclination of 100.311 degrees (79.689 degrees retrograde). The nodal period is 108.17 minutes. Ascending nodes occur at 32 minutes before noon local mean solar time. The orbit is very nearly sun-synchronous; the drift rate of the orbital plane relative to the earth-sun line is approximately half a degree per month.

Current orbital elements will appear in the monthly editions of the Nimbus II catalogs.

#### 1.3 Spacecraft Attitude

Nimbus is an earth-oriented satellite and contains an active stabilization system which maintains a nearly constant attitude relative to the earth. The satellite is stabilized about a set of right-hand orthogonal axes (Figure 1-2). These axes are defined as follows:

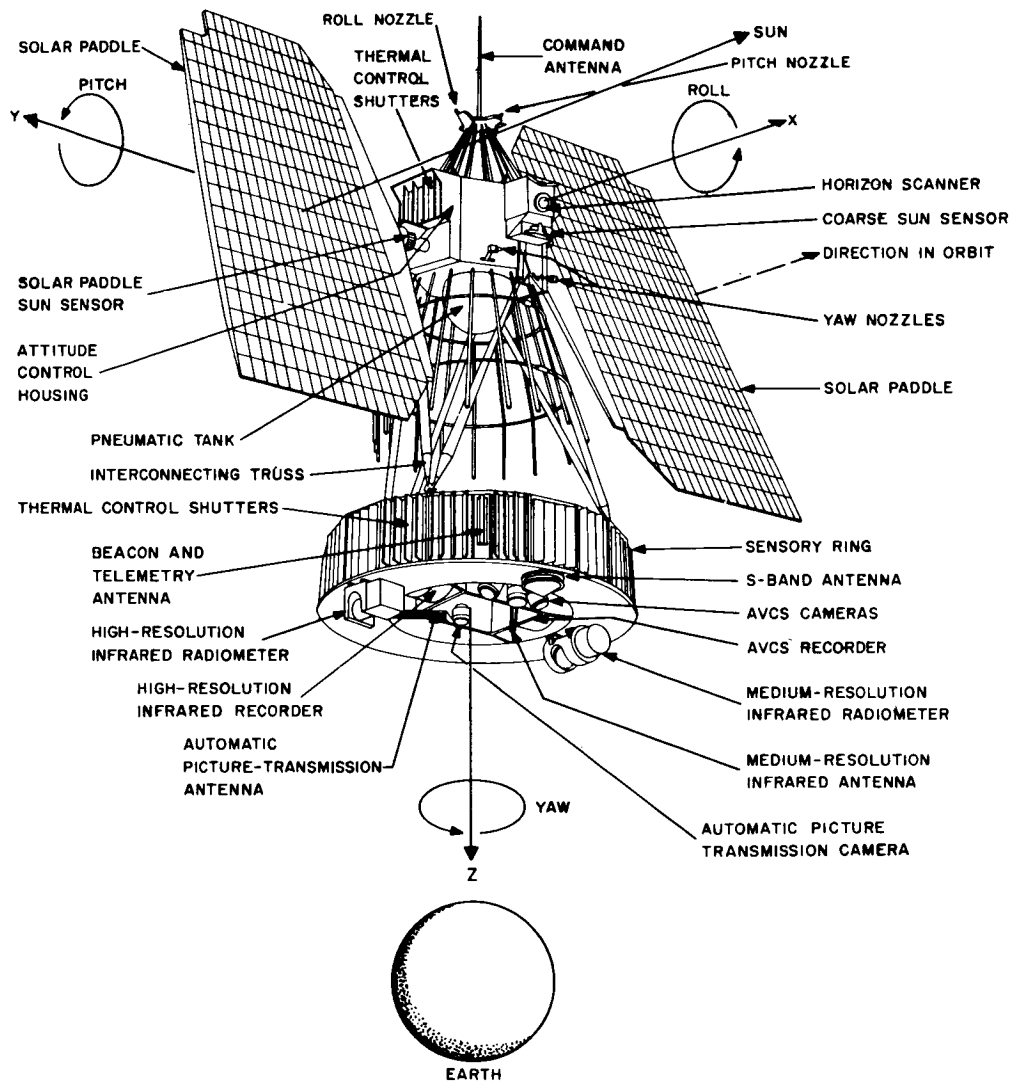


Figure 1-1-Nimbus II Spacecraft

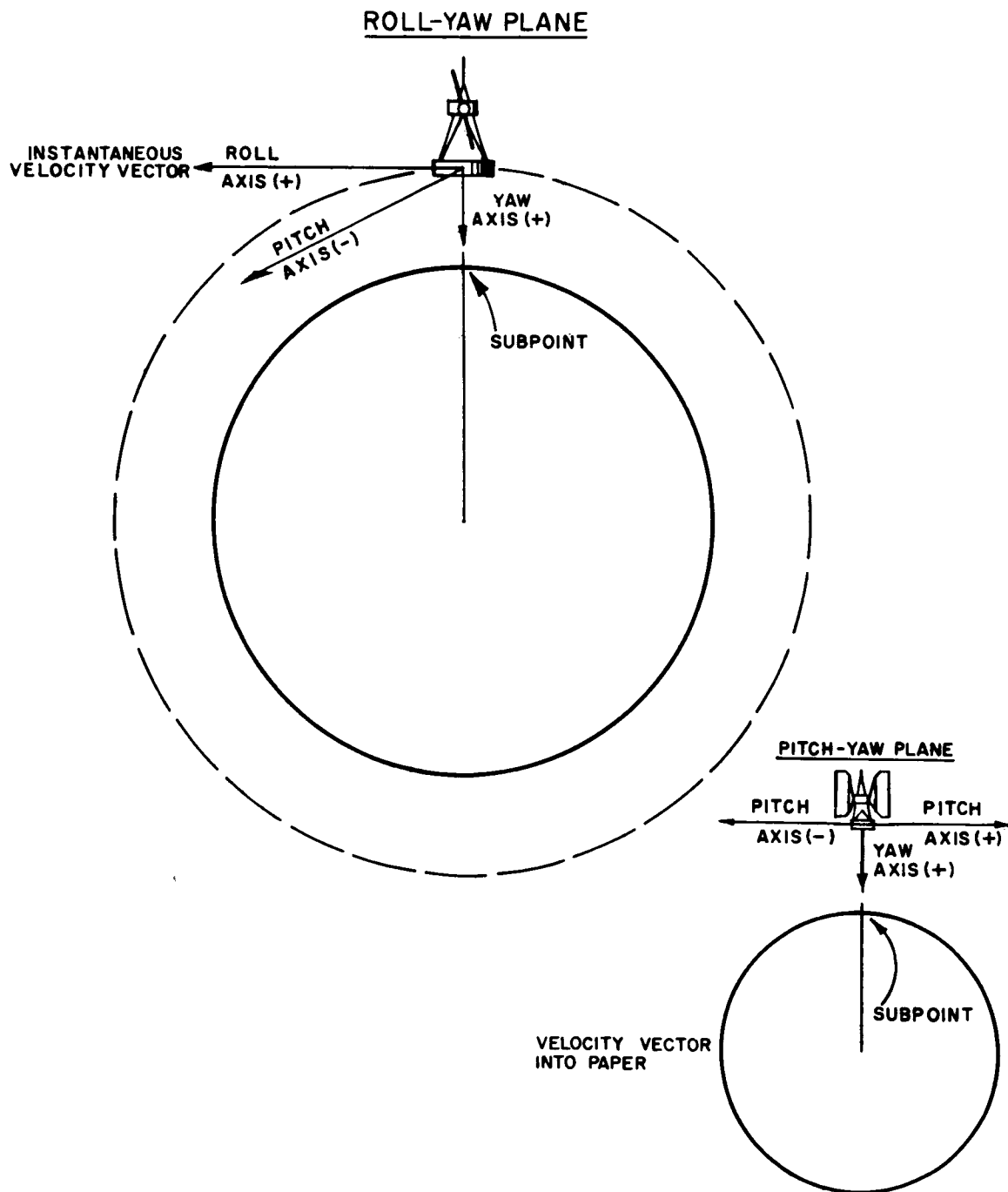


Figure 1-2-Nimbus Attitude Axes



- a. the yaw axis is the local vertical through the satellite,
- b. the roll axis is in the general direction of the velocity vector; it is the local horizontal through the satellite in the orbital plane.
- c. the pitch axis is perpendicular to the orbital plane.

Under ideally stabilized conditions, roll, pitch, and yaw are zero. Actual deviations from idealized attitude are difficult to measure routinely from processed telemetry data. These data are recorded separate from the pictures and are normally not available to general users. In general, pitch and roll attitude errors can be expected to be below one degree, while yaw errors are largely below three degrees. In some instances, attitude may be inferred from information contained in the televised images (Reference 2).

#### 1.4 Ground Station Complex

Data Acquisition Facility (DAF) stations in Fairbanks, Alaska, (ULASKA) and Rosman, North Carolina (ROSMAN), command the satellite and acquire engineering (telemetry) and meteorological data. These two DAF stations are part of the Space Tracking and Data Acquisition Network (STADAN) operated by the Goddard Space Flight Center (GSFC), Greenbelt, Maryland. The data acquired at Fairbanks is recorded and relayed to the Nimbus Data Handling System (NDHS) at GSFC over a microwave link generally at reduced rates compared to s/c to ground transmission rates. Raw data is relayed directly via microwave from the Rosman station to NDHS.

Fairbanks acquires the spacecraft on an average of 10 (of the 13 or 14) orbits each day. Rosman acquires an average of four orbits a day; two of these are missed by Fairbanks while the other two are seen by both Rosman and Fairbanks. Both the DAF stations have 85-foot-diameter parabolic antennas with attached command antennas to track, command, and interrogate the spacecraft.

All spacecraft tracking, data-acquisition, commanding, and data-handling operations are controlled from elements within GSFC. The spacecraft's location is computed at all times at the GSFC Computing Center. At the GSFC, the Nimbus Technical Control Center (NTCC) controls and coordinates operational activities of the spacecraft. The NTCC has responsibility for evaluation of the spacecraft performance and the determination of all commands to be transmitted to the spacecraft. Also at the GSFC are the computer and other supporting facilities to process the spacecraft meteorological and engineering data received from the two DAF stations. These facilities are managed and operated by the NDHS.

### 1.5 Nimbus Data Utilization Center (NDUC)

The functions of the NDUC are:

1. Near-real-time handling of data: accountability and quality control; classification and documentation of the data; and photographic processing and storage.
2. Production of monthly users' catalogs containing information on AVCS, HRIR, MRIR, APT, and DRIR (Direct Readout Infrared) data. These catalogs will be published monthly during the spacecraft life and within 30 days of the end of each catalog period. See Section 7.
3. Cataloging, indexing, storage and retrieval, and reproduction of Nimbus II HRIR, AVCS, and MRIR sensory data. Limited storage of APT and DRIR data will also be maintained.
4. Retrieval and reproduction of Nimbus II data to satisfy experimental and selected special requests (Public Information Office), etc.

The establishment and operation of the NDUC is performed under a NASA contract by ARACON Geophysics Division of Allied Research Associates, Inc., Concord, Massachusetts.

Nimbus II data processing procedures carried out by the NDUC commence at the point of receipt of gridded AVCS, HRIR, and MRIR film from the NDHS, or receipt of locally-acquired APT and DRIR data from photo facsimile equipment. On-line handling of these data is performed as they are received in "interrogation format." Photographic processing of the AVCS pictures is accomplished in NDHS by a kinescope-Bimat Film processing system. This system produces a completely processed negative and positive transparency simultaneously.

HRIR data are read out on Westrex facsimile equipment which provides an indexed positive and/or negative transparency. The NDHS uses a rapid processor to develop the positive. An undeveloped archival negative is forwarded to the NDUC photographic laboratory for final processing.

MRIR data are produced as a print and a 4" x 5" negative in the NDHS using an EIS Universal Kinescope (digital) - polaroid camera back system.

AVCS and HRIR film data are subjected to the following procedures by the NDUC:

1. Quick look quality control check – review for adequate processing, sync tears, wow and flutter, and any other photographic, optical or electrical malfunctions.
2. Coverage validation and data accountability – review of geographical areal coverage vs. desired coverage as programmed, proper frame indexing, and total count.
3. Splicing and sequencing data to provide contiguous information.
4. Label and legend check – review of all annotation placed upon each strip of film.
5. Grid verification check – confirmation of gridding accuracy and detection of severe attitude errors.
6. Photographic quality control – densitometric measurements are made to assure that electronic and photographic processing meet the required standards.

Data which do not meet the quality control requirements of NDUC will be reprocessed by NDHS where possible or will be "flagged" in the monthly catalogs.

AVCS data will be archived by the National Weather Records Center through the National Environmental Satellite Center (NESC), Suitland, Maryland. HRIR and MRIR data will be archived at GSFC.

A major task of the NDUC is that of meteorological and geomorphological classification of the Nimbus II AVCS and HRIR data. This effort is outlined in some detail in Section 9. From these and associated efforts are derived the material which is contained in the monthly catalogs, the contents of which are described in Section 7.

## SECTION 2

### ADVANCED VIDICON CAMERA SYSTEM (AVCS)

#### 2.1 Description of the AVCS

The Nimbus II AVCS provides television pictures of clouds in the earth's atmosphere and, in clear areas, of terrestrial features on the earth's surface. These data are obtained only during daylight hours.

The AVCS consists of three vidicon cameras and associated electronics. The central camera is oriented downward along the yaw axis (nominally the local vertical) while each of the side cameras are mounted in the yaw-pitch plane at an angle of 35 degrees to the central camera. Figure 2-1 shows schematically the geometric relations of the cameras. Figure 2-2 shows the Nimbus television coverage, an area of approximately 1,900 by 400 nautical miles. Successive frames are taken at 91-second intervals providing about 20 percent overlap of earth coverage at 600 nautical mile altitudes. Complete daylight orbital coverage can be obtained with 32 consecutive picture triplets. Successive orbits, displaced about 27 degrees westward in longitude at the equator, provide adjacent pictorial data, with increasing overlap from the equator towards the poles. Figure 2-3 is a montage of all AVCS pictures taken by Nimbus II on 20 June 1966. Daily montages such as this are used in NDUC for the data classification work described in Sections 8 and 9. (Gaps in coverage near 60° North latitude are caused by the interruption of picture taking during ULASKA interrogations).

The three cameras use 1-inch vidicons with 800-line resolution. The size of the resolution element varies from 1/2 mile at the nadir to approximately 1.5 miles at the corners, at a 600-nautical-mile altitude. The three cameras are driven by a common timer which provides the picture sequence. A 40-millisecond exposure time is used, and the image is scanned by the electron beam in 6.5 seconds. The resulting signal is frequency-modulated and recorded on three tracks of a tape recorder, one track for each camera. A fourth track records a continuous timing signal from the spacecraft clock so that picture exposure times can be identified. Sufficient tape is provided for recording 53 pictures (equivalent to about 1-2/3 orbits) which are played back upon ground command. The AVCS data is multiplexed with HRIR data and transmitted on S-band at 1707 mc.

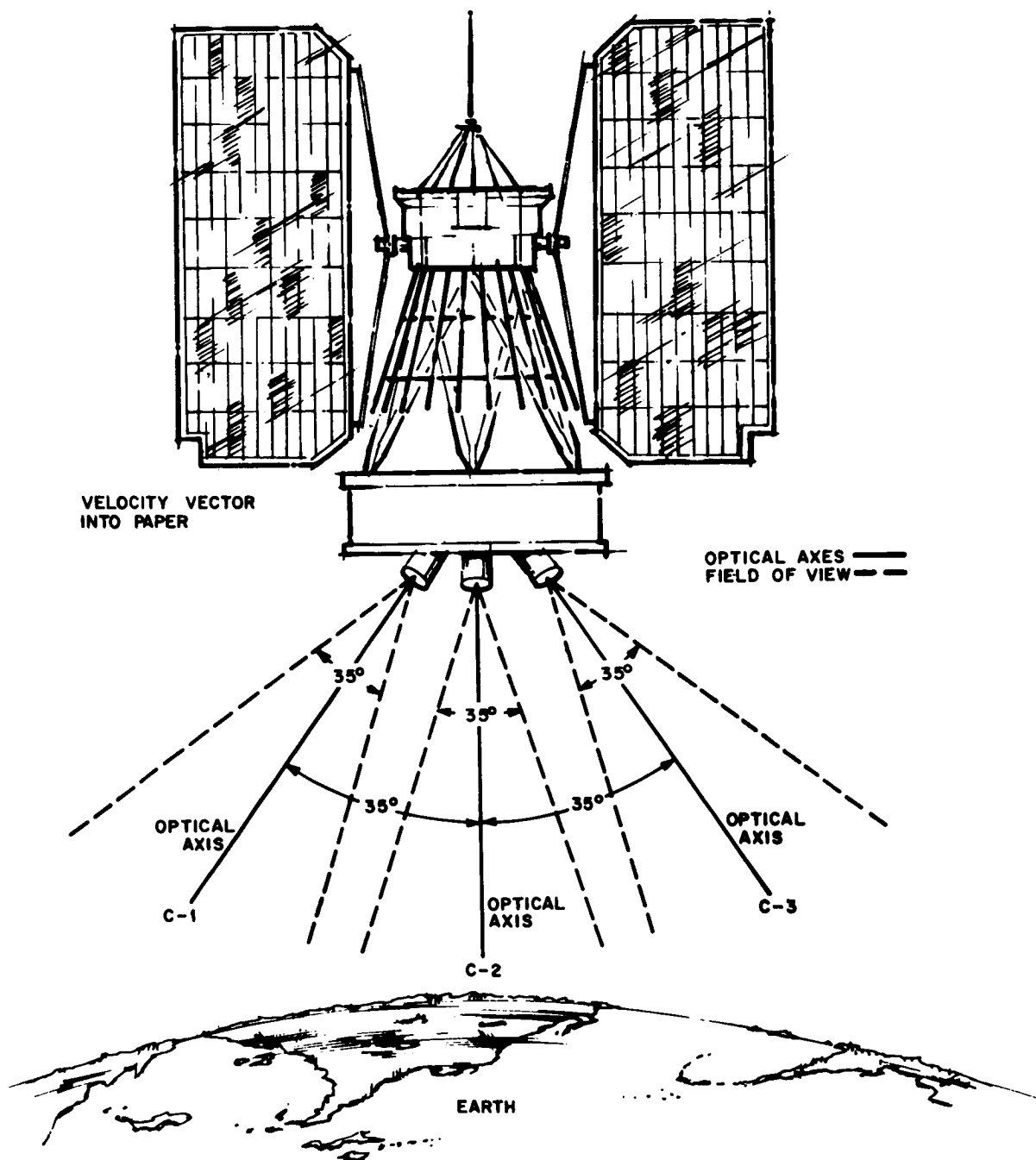


Figure 2-1—Schematic of AVCS Optics

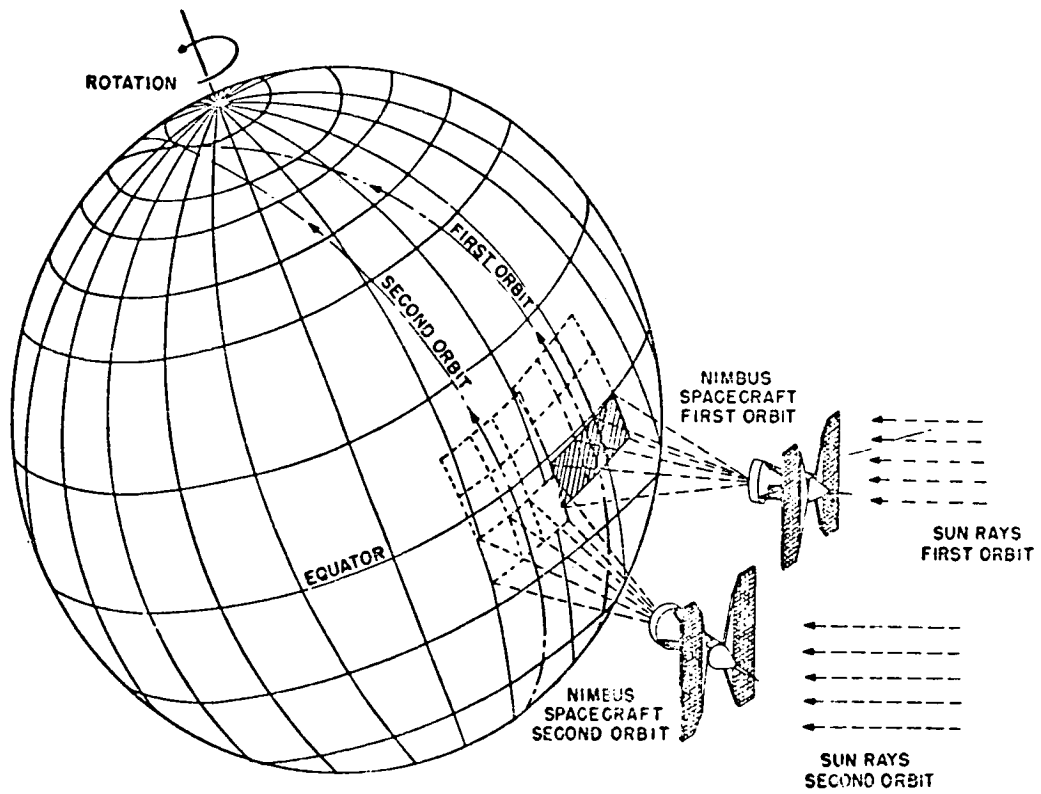


Figure 2-2-AVCS Camera Coverage

# NIMBUS II AVCS DAILY MONTAGE

20 JUNE 1966



Figure 2-3—Montage of AVCS pictures taken on 20 June 1966

A variable iris in each camera is designed to compensate automatically for latitudinal changes in earth illumination. A manual override is available to set the iris into any one of three fixed positions.

## 2.2 AVCS Calibration

Prior to launch each camera of the AVCS was aligned with a test target (of known dimensions) at a known distance from the lens. The target was photographed in both the Direct and Tape mode by each of the three cameras. These target photographs were then used to determine the focal lengths and acceptance angles of each camera. The results are presented in Table 2-1. Differences between the Direct and Tape mode were insignificant and no distinction is made between the two modes.

Table 2-1

Camera Number	1	2	3
f (mm)	18.21	18.21	18.23
Acceptance Angle (side to side) $\pm 0.02$	35	35	35

Angles between the cameras are a nominal 35 degrees (See Figure 2-1).

## 2.3 Data Display Format

Figure 2-4 shows the AVCS format. Pictures from each camera are presented on separate 70-mm film strips. Each AVCS picture includes an image area slightly less than two inches square, a gray scale adjacent to the image area and an index legend. Each image area contains 25 fiducial marks (Figure 2-5) designed to permit quantitative photogrammetric use of the data. These fiducial marks are vacuum-deposited metal lines on the face of each vidicon so that each fiducial represents a definite physical location on the original image plane. The central fiducial, indicated by a cross (+), represents the point where the camera axis intersects the image plane, the picture principal point.

Index legend data provides identifying information for the associated image, as follows:



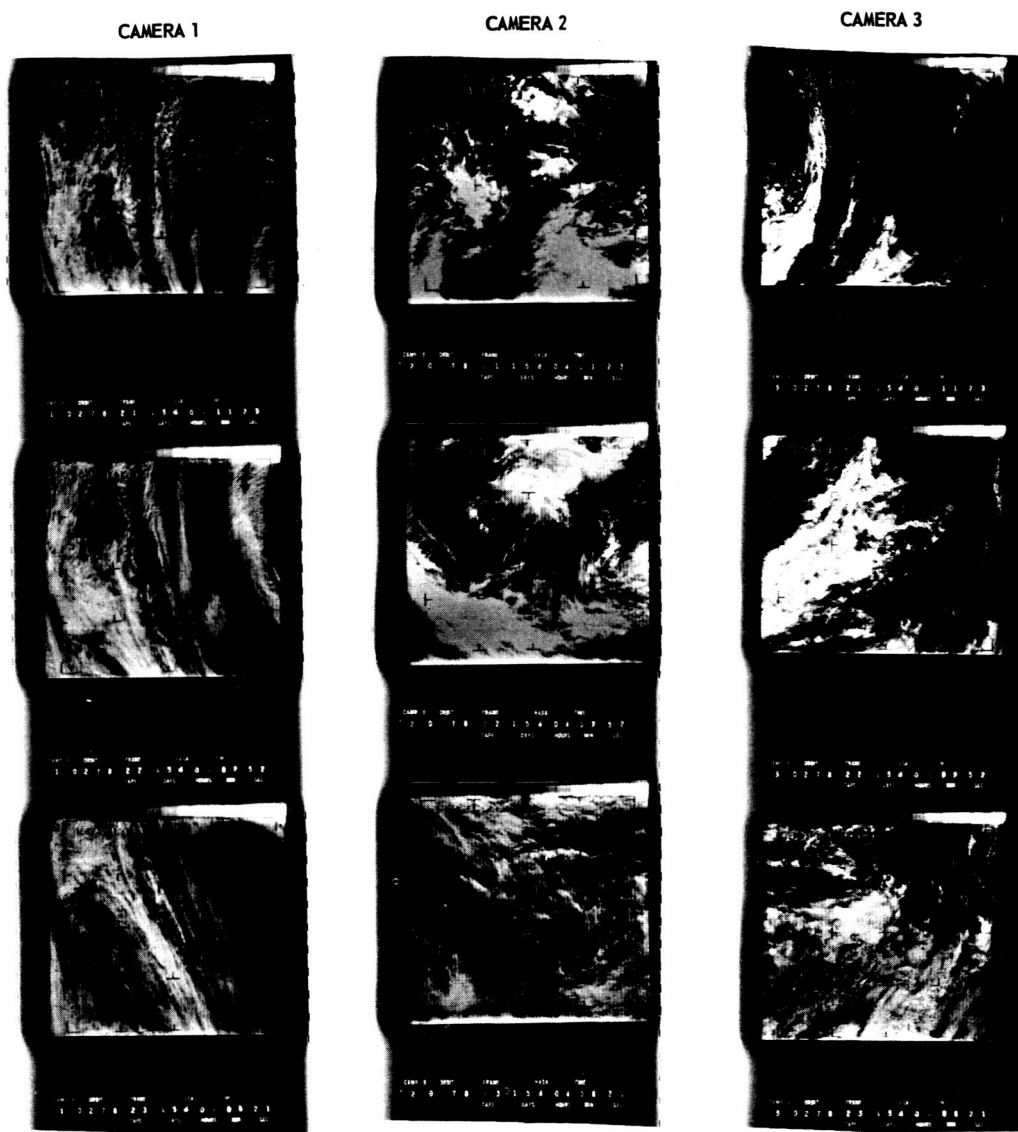


Figure 2-4-AVCS Film Strip Format

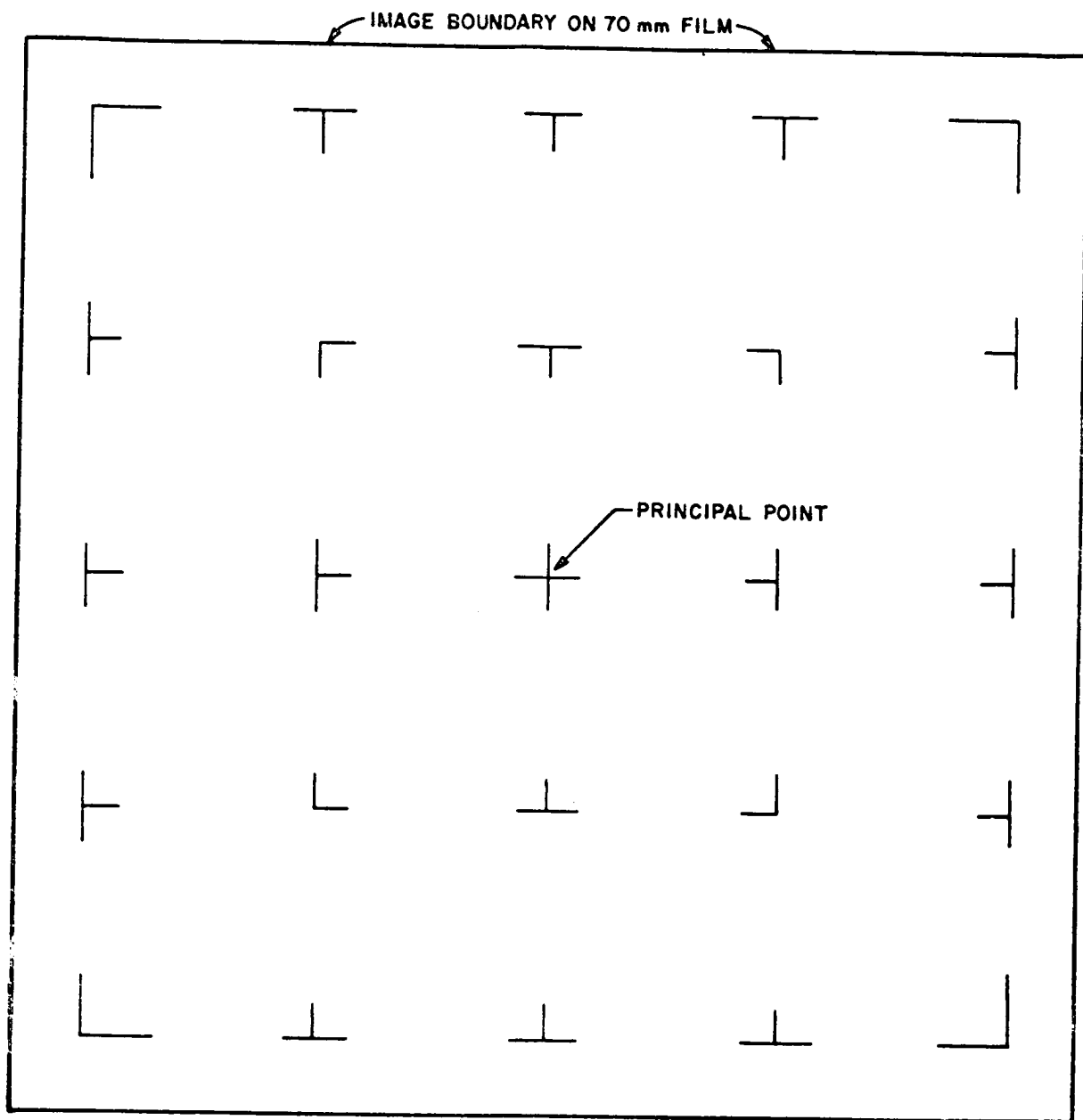


Figure 2-5-Nimbus AVCS Fiducial Matrix  
(This display is enlarged approximately three times the actual image size)

## LEGEND-IMAGE CORRESPONDENCE

An arrow appears at each end of the picture legend, directed towards the picture to which the legend information corresponds; this is normally the picture farthest from the legend.

### CAMR

Abbreviation for camera number identifier illustrated in Figure 2-3. The digit "1", "2" or "3" appears directly below the abbreviation to identify the camera system through which the scene was photographed.

The letter "A", "B", or "C" appears on the same line and immediately following the camera abbreviation on the index legend. This letter is used for ground station housekeeping and may be ignored by the user.

### ORBIT

A four-digit number indicating the interrogation (readout) orbit during which the pictorial data were transmitted to the ground station. This number is frequently not that of the orbit on which the picture was actually taken.

### FRAME

A picture frame identifier affixed during interrogation, which will generally not be the same as the frame numbers assigned during cataloging.

### NASA

National Aeronautics and Space Administration identifier of the source of the data.

### TIME

The picture timing code consisting of four data blocks. The first block of three digits represents the calendar day and can be interpreted by reference to Table 2-2. The following three blocks of two digits each represent picture time in hours, minutes and seconds of Universal Time. Time code blocks are identified beneath the digital information.

TABLE 2-2  
TABULATION OF CALENDAR DAY NUMBER VERSUS DATE  
(FOR OTHER THAN LEAP YEARS)

DAY OF MONTH	JAN	FEB	MAR	APR	MAY	JUN	JULY	AUG	SEPT	OCT	NOV	DEC	DAY OF MONTH
1	1	32	60	91	121	152	182	213	244	274	305	335	1
2	2	33	61	92	122	153	183	214	245	275	306	336	2
3	3	34	62	93	123	154	184	215	246	276	307	337	3
4	4	35	63	94	124	155	185	216	247	277	308	338	4
5	5	36	64	95	125	156	186	217	248	278	309	339	5
6	6	37	65	96	126	157	187	218	249	279	310	340	6
7	7	38	66	97	127	158	188	219	250	280	311	341	7
8	8	39	67	98	128	159	189	220	251	281	312	342	8
9	9	40	68	99	129	160	190	221	252	282	313	343	9
10	10	41	69	100	130	161	191	222	253	283	314	344	10
11	11	42	70	101	131	162	192	223	254	284	315	345	11
12	12	43	71	102	132	163	193	224	255	285	316	346	12
13	13	44	72	103	133	164	194	225	256	286	317	347	13
14	14	45	73	104	134	165	195	226	257	287	318	348	14
15	15	46	74	105	135	166	196	227	258	288	319	349	15
16	16	47	75	106	136	167	197	228	259	289	320	350	16
17	17	48	76	107	137	168	198	229	260	290	321	351	17
18	18	49	77	108	138	169	199	230	261	291	322	352	18
19	19	50	78	109	139	170	200	231	262	292	323	353	19
20	20	51	79	110	140	171	201	232	263	293	324	354	20
21	21	52	80	111	141	172	202	233	264	294	325	355	21
22	22	53	81	112	142	173	203	234	265	295	326	356	22
23	23	54	82	113	143	174	204	235	266	296	327	357	23
24	24	55	83	114	144	175	205	236	267	297	328	358	24
25	25	56	84	115	145	176	206	237	268	298	329	359	25
26	26	57	85	116	146	177	207	238	269	299	330	360	26
27	27	58	86	117	147	178	208	239	270	300	331	361	27
28	28	59	87	118	148	179	209	240	271	301	332	362	28
29	29	(60)	88	119	149	180	210	241	272	302	333	363	29
30	30	89		120	150	181	211	242	273	303	334	364	30
31	31	90		151			212	243		304		365	31

NOTE: This table is for years other than leap years. For leap years, add one to each calendar day number on and after that for March 1.

Picture time codes refer to the picture taking rather than the data readout times. Time code information may be in error, especially near the start and end of picture sequences.

#### DIRECT/TAPE

The picture taking mode indicator. Direct pictures can be acquired only within the interrogation range of a DAF antenna. These pictures by-pass the Nimbus on-board tape recording system and are telemetered directly to the ground.

Tape mode pictures are stored on video tape in the spacecraft and are subsequently read out on command when the satellite comes within communication range of a DAF. Nearly all of the Nimbus II AVCS pictures will be from the tape mode.

Geographic referencing of the data involves establishment of the correspondence between points in the object scene (surface of the earth) and those in the image plane (AVCS pictures). This is facilitated by perspective latitude-longitude grids superposed on the AVCS image by the NDHS computer and hardware complex. Most AVCS pictures from Nimbus II will be provided in gridded form. In some instances, however, pictures may not be gridded.

AVCS grid points are electronically integrated with the video signal at the ground station. Each grid point consists of black and white elements, so that the grid point is visible regardless of the background gray level or the picture polarity (negative or positive).

Figure 2-6 illustrates the AVCS perspective latitude-longitude grids. The discrete grid points form grid lines, with all latitude grid lines at two-degree intervals. Longitude lines are composed of points spaced at one-degree intervals, and the spacing between longitude lines varies from the equator to the poles as indicated in Table 2-3.

TABLE 2-3  
Longitude Gridding Intervals

Latitude (Degrees)	Longitude Interval (Degrees)
0-59.99	2
60-79.99	6
80-84.99	18
85-90*	36

\*Exception: Any frame containing the pole is gridded in longitude at 36 degree intervals only.

An arrowhead appears at a latitude-longitude intersection somewhere near each picture center, pointing to the north. The latitude of this intersection also determines the longitude grid interval of the picture in accordance with Table 2-3.

The latitude and longitude of the grid line intersection at the arrowhead appears in the upper left corner of the image area as six characters. Latitude is indicated by the first two digits. The third character indicates the hemisphere, "N" for northern or "S" for southern. Longitude is given by the last three digits as 000 through 360 degrees EAST. West longitudes are not used in the AVCS grids. The gridding system may be changed slightly during the life of Nimbus II. Any such changes will be described in the Monthly Catalogs.

The processing, archiving, and availability of AVCS films is described in Section 6.

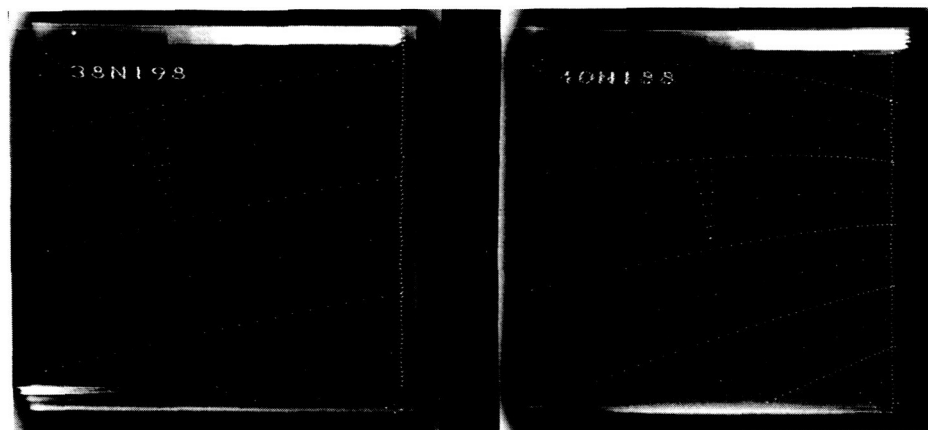


Figure 2-6—Sample AVCS Grids. (Pictures were taken at night, therefore north is toward bottom of frame).

## SECTION 3

### HIGH RESOLUTION INFRARED RADIOMETER (HRIR) EXPERIMENT

#### 3.1 Introduction

The Nimbus High Resolution Infrared Radiometer (HRIR) was designed to perform two major functions: first, to map the Earth's cloud cover at night to complement the television coverage during the daytime portion of the orbit, and second, to measure the temperatures of cloud tops and terrain features.

Measurements taken during the daytime do not reveal true surface temperatures since the radiometer operates in the 3.5 to 4.1 micron region and reflected solar radiation is added to the emitted surface radiation. However, reflected sunlight in this spectral region does not saturate the radiometer output and usable pictures can be made.

#### 3.2 The High Resolution Infrared Radiometer

The single-channel scanning radiometer is shown in Figure 3-1. It contains a lead selenide (PbSe) photoconductive cell which is radiation cooled to  $-75^{\circ}\text{C}$  and operates in the 3.5 to 4.1 micron "window" region. The white collars shown in the figure are sunshields to prevent solar radiation from entering the radiometer during spacecraft sunrise and sunset. The scan mirror is located between the sunshields. The cylindrical projection at one end contains the motor which drives both the scan mirror and the chopper. The front of the pyramidal horn which is part of the radiative cooling assembly can be seen. The electronics are located around this horn.

The radiometer, which weighs 11.3 pounds and consumes 4 watts of power, can measure radiance temperatures between  $210^{\circ}\text{K}$  and  $330^{\circ}\text{K}$  with a noise equivalent temperature difference of  $1^{\circ}\text{C}$  for a  $250^{\circ}\text{K}$  background. The radiative cooling system is shown in Figure 3-2. Cooling is accomplished by means of a black cooling patch at the bottom of a highly reflective gold-coated horn. The horn is oriented to view cold space during the entire orbit and the patch is suspended by thin wires to reduce heat conduction from the housing. The detector is connected to the cooling patch by a high thermal conductance transfer bar.

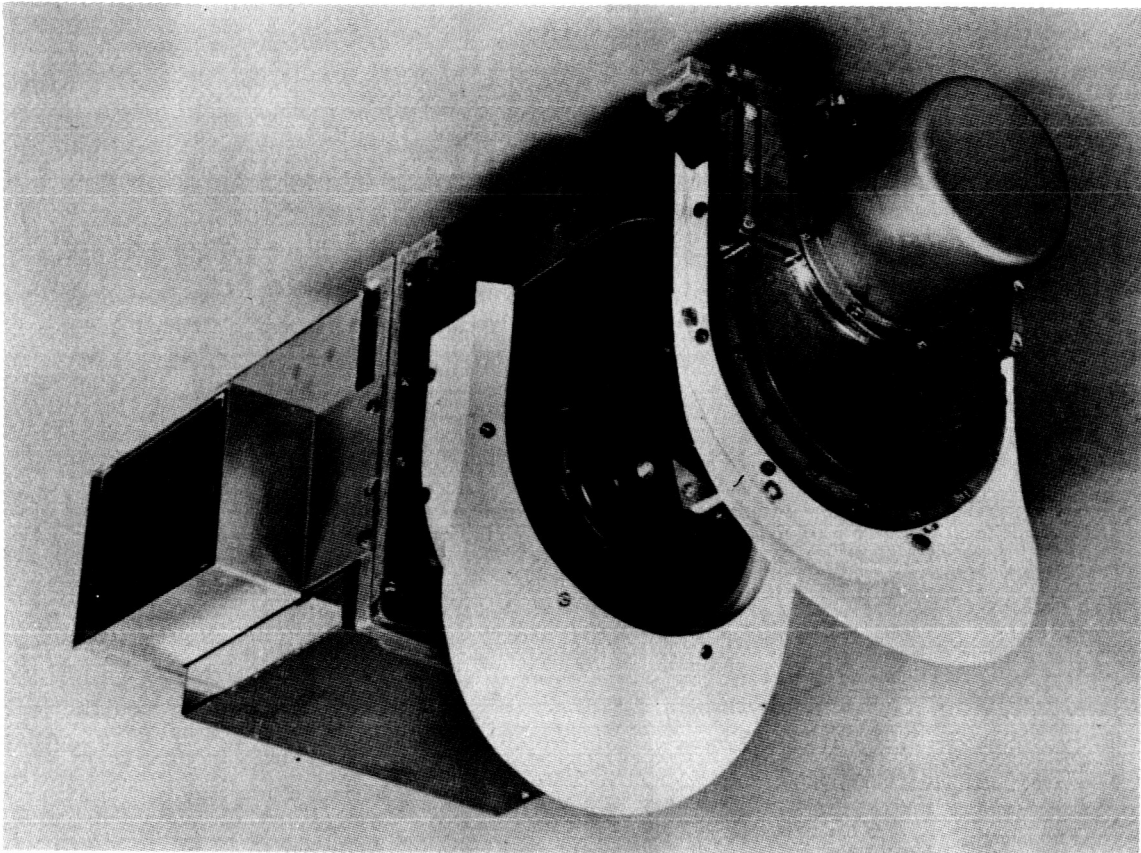


Figure 3-1—Nimbus II HRIR Radiometer

### HRIR RADIATION COOLING

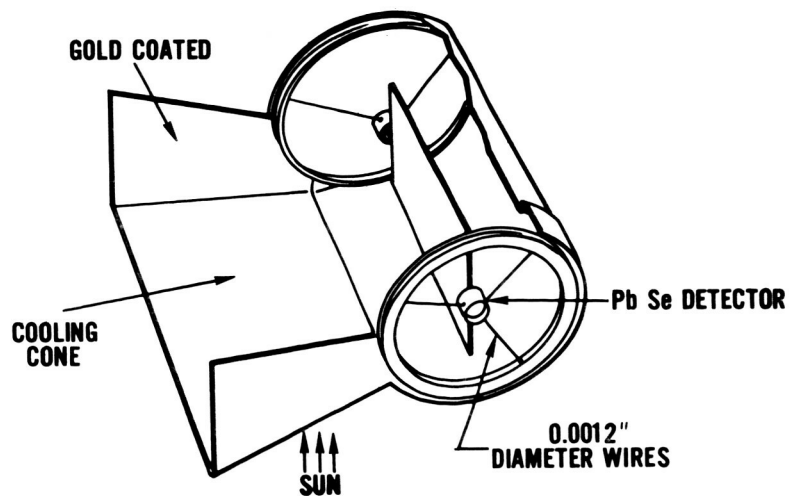


Figure 3-2—Radiative cooling system for the HRIR lead selenide detector.



The radiometer has an instantaneous field of view of about  $1/2$  degree, which at an altitude of 600 nm (1110 km) corresponds to a subsatellite ground resolution of 5 nm (8 km). Figure 3-3 illustrates the HRIR optical system. The scan mirror is inclined 45 degrees to the axis of rotation which is coincident with the spacecraft velocity vector (assuming no yaw attitude error). The optical scan path thus lies in a plane perpendicular to the orbital motion. The radiation reflected from the scan mirror is chopped at the focus of a 4-inch f/1 modified Cassegrainian telescope. It is then refocused at the detector by means of a reflective relay which contains the 3.5 to 4.1 micron filter. The scan rate of 44.7 revolutions per minute was chosen so that contiguous scanning would occur in the neighborhood of the subsatellite track, with increasing overlap toward the horizon.

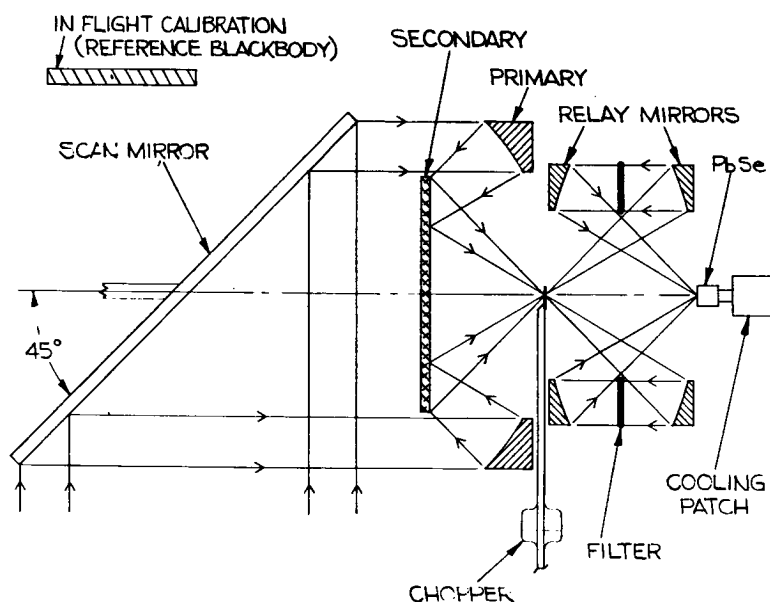


Figure 3-3—Schematic of the HRIR optical system.

In contrast to television, no image is formed within the radiometer; the HRIR sensor merely transforms the received radiation into an electrical (voltage) output with an information bandwidth of 280 cycles per second. A Visicorder oscillograph trace of a portion of an actual Nimbus I analog record is shown in Figure 3-4. The radiometer scan mirror continuously rotates the field of view of the detector through 360 degrees in a plane normal to the spacecraft velocity vector. The detector views the in-flight blackbody calibration target (which is a part of the radiometer housing), outer space, Earth, outer space, and returns again to intercept the in-flight blackbody target. The space and housing-viewed parts of the scan, which can be identified without difficulty, serve as part of the in-flight

**NIMBUS I HRIR**  
326 R/O 328  
SEPT 19, 1964  
EAST OF PHILIPPINES

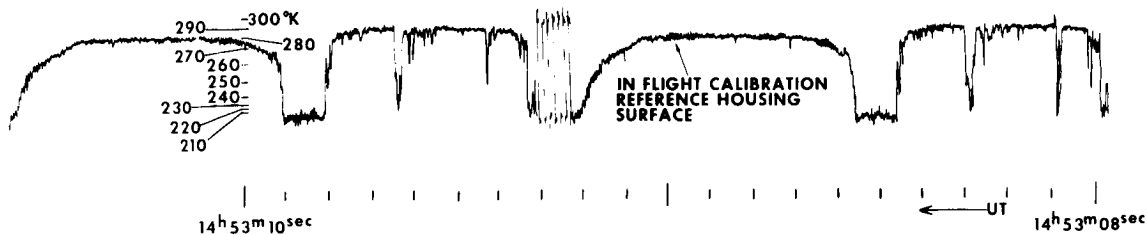


Figure 3-4—Portion of an analog record showing nearly two HRIR scan cycles.

check of calibration. Information on housing temperatures, which are monitored by thermistors, are telemetered to the ground stations and for calibration purposes are constantly compared with the temperatures obtained from the radiometer housing scan. The space scan serves as the zero reference point. During the space sweep a permanent magnet on the scan mirror gear triggers an electronic gate and a multivibrator so that the seven pulses shown in Figure 3-4 are generated. These pulses are used to synchronize automatic display equipment on the ground.

### 3.3 The HRIR Subsystem and Ground Processing Equipment

A simplified block diagram of the HRIR subsystem is shown in Figure 3-5. The radiometer video output (0 to -6.4 v dc) is fed to an FM modulator which converts the radiometer voltage to frequency modulated signals (8.25 to 10 kcs) that are recorded on one track of a 4-track tape recorder. Simultaneously, 10-kilocycle AM timing signals from the Nimbus spacecraft clock are placed on a second track on the tape. When these two tracks are completely recorded, the direction of the tape travel is automatically reversed and the recording continues on the other two tracks. The recorder accepts data at a tape speed of 3.75 inches per second and upon command plays back all four channels simultaneously at 30 inches per second. The 8 to 1 playback speedup causes a directly proportional increase in the FM signal frequencies (66 to 80 kc). The four tape recorder outputs (two video and two time code) are fed into the four channels of the HRIR multiplexer where each channel is translated to its assigned position in the HRIR subsystem base band (i.e., 55 to 69.5 kc and 127.5 to 141.5 kc for the two video channels). The four channels are combined in an adder circuit with the AVCS multiplexed signals and the composite signal is fed to the Nimbus S-band transmitter for transmission to the Data Acquisition Facility (DAF).

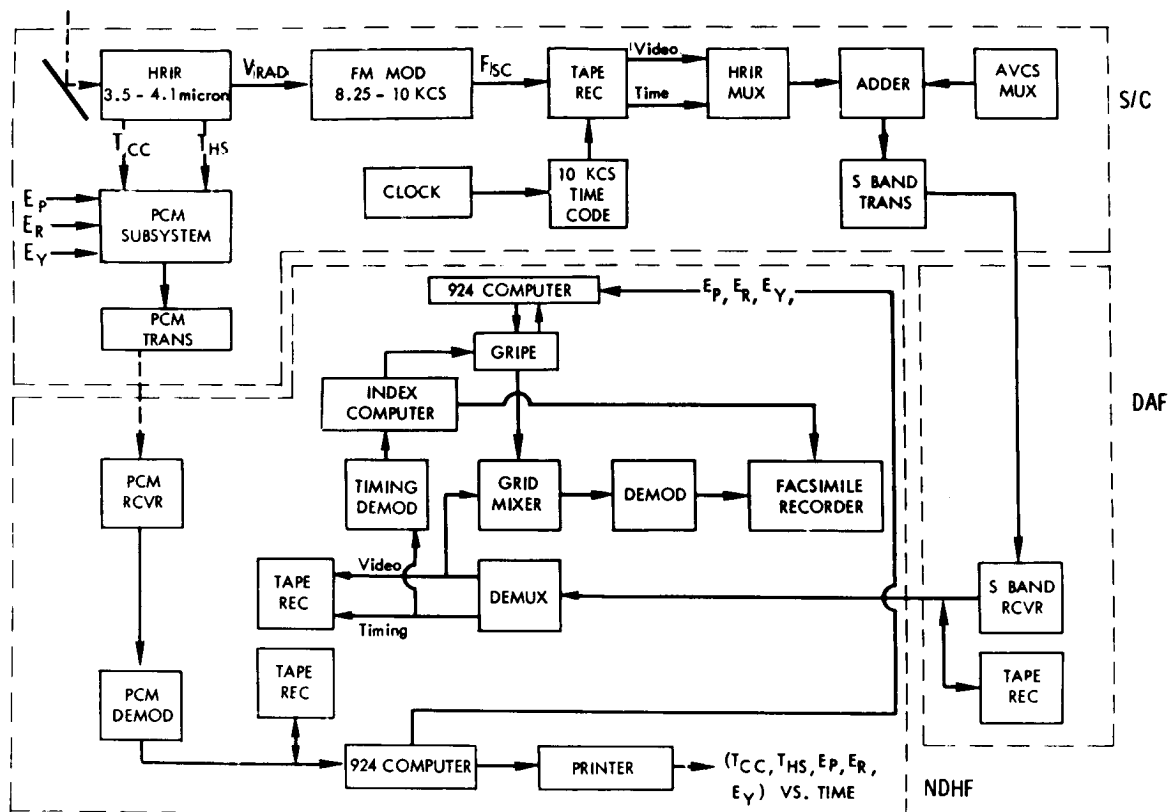


Figure 3-5—Simplified block diagram of the HRIR Subsystem.

### 3.4 HRIR Data Processing

#### 3.4.1 Photofacsimile Film Strips

At the DAF, the HRIR information is demultiplexed and recorded on magnetic tape. It is then transmitted to the Goddard Space Flight Center, where the FM signal is demodulated, synchronized, and displayed by a photofacsimile recorder. The facsimile recorder converts the radiometer output electrical signals into a continuous strip picture, line by line, on 70 mm film. Blanking circuits in the recorder reject unwanted sections of each line scan; only the Earth scan and, for calibration purposes, very small portions of the space scan and the radiometer housing scan are recorded on the film strip. The processing time between spacecraft playback command and display for one full nighttime orbit is about 30 minutes.

All of the Nimbus II HRIR data are displayed on photofacsimile film strips. Each block of data on a film strip is provided with an index display which identifies the data. The index display contains three pieces of information: the readout

orbit number, the approximate beginning (for forward mode) or ending (for reverse mode) time, and the playback mode. Figure 3-6 (a) shows a block of Nimbus I "forward mode" data, i.e. data read out with the tape recorder traveling in the same direction as it traveled while the data were being recorded. The orbit number 301 refers to the number of the orbit at the time the data were read out from the satellite. The time is the first time code associated with the data "read" from the magnetic tape and is the time of a satellite clock when recording of the data began in the satellite. The time given in the index display is 17:12:26 UT on the 261st day of the year or September 17, 1964. The letters "FWD" indicate the "forward" playback mode.

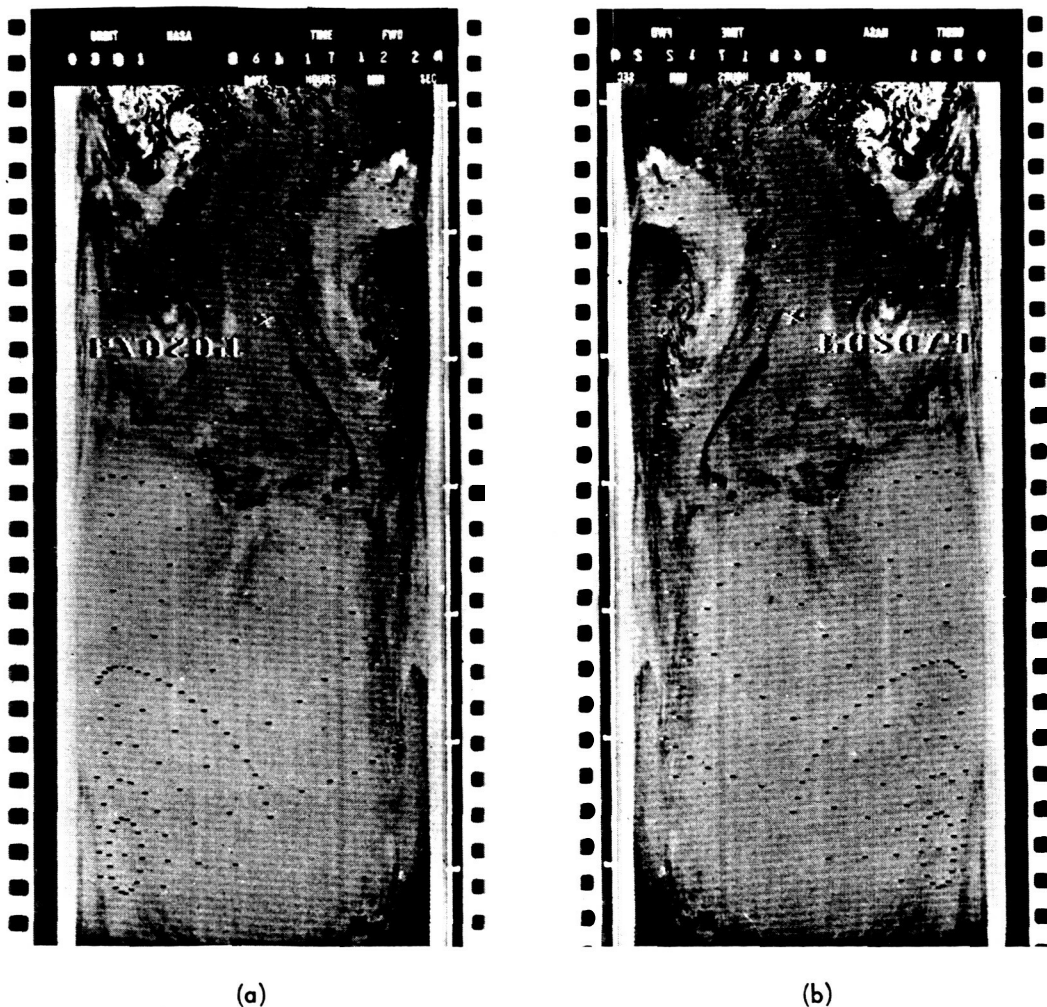


Figure 3-6—A block of Nimbus I Forward mode data showing (a) the film strip positioned for reading the index display, and (b) the film strip with the nighttime data correctly oriented for viewing with north and east toward the top and right, respectively.

A series of time marks in increments of two minutes is found on the right side of the film. These marks represent even minutes of time. The first time mark is the first even minute after the index display time; i.e. 17:14 UT, the second is 17:16, etc., and the last time mark is 17:26. The data do not begin at the time given in the index display but begin from 40 to 120 seconds later. The time marks are used to determine the beginning time of the data. In producing the film the index display is first presented; then, the film is advanced rapidly about 0.5 of an inch. It remains in this position normally for approximately six seconds during which time the photofacsimile recorder is phased so that the correct video is presented on the film, i.e., the  $138.24^\circ$  of mirror rotation is centered around the subsatellite point. Normally from 40 to 64 seconds of the data are lost during this phasing period, and the data on the film begin an equivalent length of time after the index time. There are cases in which the phasing time is as long as 120 seconds. If the first even minute, after the index display time occurs during the phasing period, the first time mark can be positioned erroneously. When this happens, the spacing between the first and second time marks is different from subsequent spacings. However, by working backwards from the second time mark, the correct time for the beginning of the data and the time for data prior to the second mark can be found. The time identifies the data to have been recorded during orbit 298, although they were read out during orbit 301.

The data are correctly oriented when the film is viewed from the opposite side (i.e., shiny side toward the viewer), keeping the index display at the top for forward mode data as shown in Figure 3-6 (b). From left to right, across the film, the  $138.24^\circ$  of arc, centered at the subsatellite point, includes space, Earth, and space; plus 2mm of the radiometer housing temperature measured by the radiometer. The width of the space portion of the scan increases with increasing height of the satellite since less of the  $138.24^\circ$  of arc is included in the Earth portion of the scan.

Figure 3-7 (a) shows a block of Nimbus I "reverse Mode" (REV) data, i.e., data read out with the tape recorder traveling in the opposite direction from the direction it traveled while recording the data. The index display at the top of the film shows that the data were read out during orbit 123. The first time code received by the photofacsimile recorder was Day 249 (September 5, 1964) at 16:43:44 UT. This time code is the last time code associated with the data. The time marks are found on the left side of the film when viewed from this position. The first time mark represents the first even minute before the index display time. In this case the first time mark is 16:42, the second is 16:40, etc. The time identifies the data to have been recorded during orbit 122. The data are properly oriented when the film is viewed from the opposite side (shiny side toward the viewer) with the index display at the bottom as shown in Figure 3-7 (b). For properly oriented

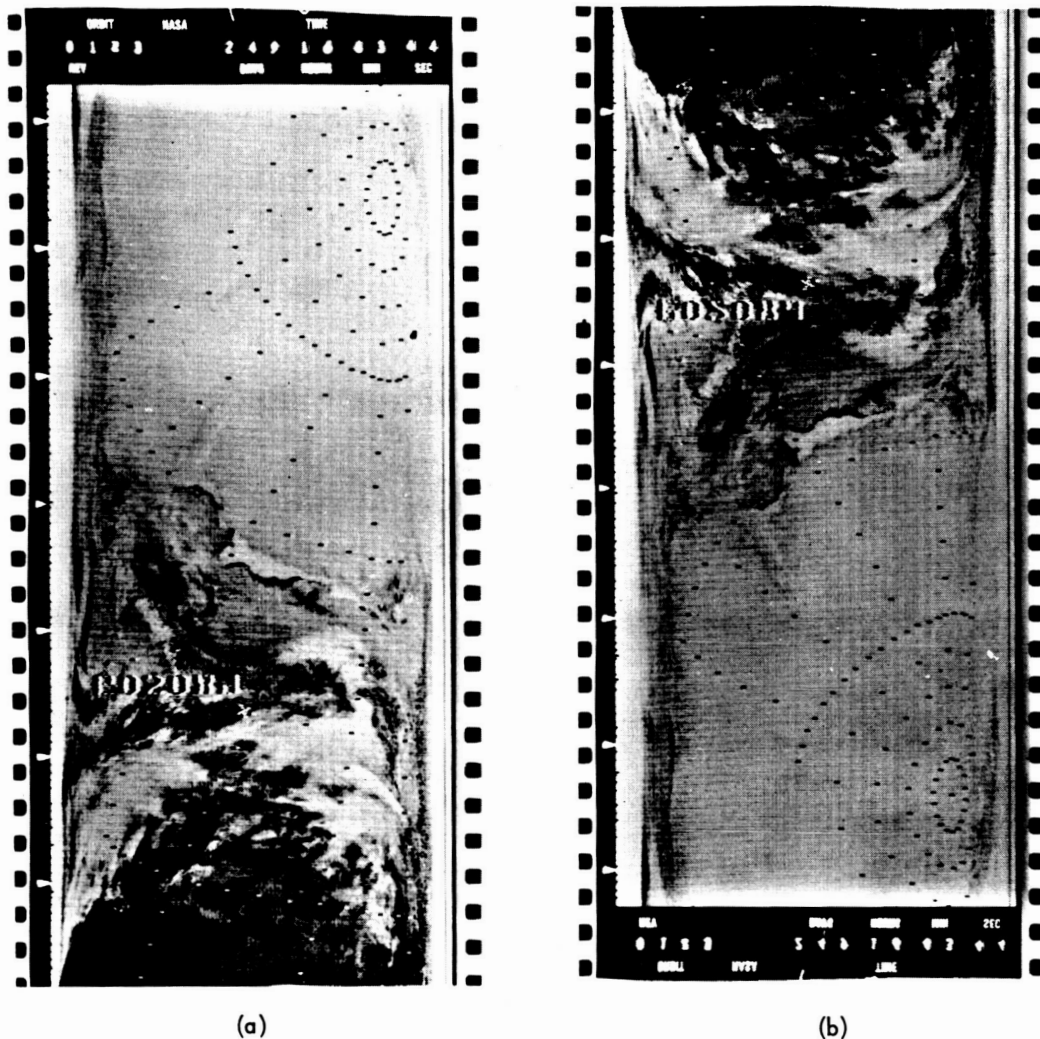


Figure 3-7—A block of Nimbus I Reverse mode data showing (a) the film strip positioned for reading the index display, and (b) the film strip with the nighttime data correctly oriented for viewing with north and east toward the top and right, respectively.

film, the time marks appear on the left for both forward and reverse mode data. From left to right across the film of reverse mode data, 2mm of housing temperature, space, Earth, and space are seen.

It should be emphasized that the information given in the index display and the time marks can be, and often is, in error. Most errors will be flagged in the catalog data log. When an error occurs in the index display time or the time marks, the correct time can often be found by correlating the data showing land features and orbital information. In cases of data not showing land features, a knowledge of the beginning and end times of the recording of the data and length of the playback helps to correlate the data with time. Also helpful are the grids on the film

which are established using the time codes associated with the data, but these grids can also be in error. All available diagnostic sources should be consulted and cross-checked in establishing the beginning and ending times.

As a result of direct sunlight getting into the Nimbus II radiometer, a band 1/4" to 3/4" on the picture over the south polar region is degraded to the point where the information is useless.

### 3.4.2 Gray Scale Calibration

The photofacsimile recorder is provided with the means for automatically producing a ten-step calibration gray scale wedge. Progressive voltage levels, from a manually adjusted ten-step potentiometer network, are sequentially selected by a ten-step motor driven cam operated by a timed program selector switch and are recorded on the film. The ten voltage levels correspond to the ten equivalent blackbody temperatures shown in Figure 3-8. The gray scale wedge shown in Figure 3-8 is for illustrative purposes only, and no attempt should be made to calibrate the positive prints by means of this gray scale. Variations in photographic reproduction and printing make it impossible to calibrate absolutely all data with one gray scale wedge. The photofacsimile recorders were recalibrated after orbit 535, hence two sets of calibration values are included in Figure 3-8.

Unless otherwise specified, a uniform exposure will be employed in producing copies requested by a user, and calibration gray scale wedges will be included with each data orbit to permit the interpretation of the data in terms of absolute equivalent blackbody temperature values. These gray scales are produced and exposed on the film immediately before or after the associated data is recorded; any variation in photographic processing thus affects the gray scale and the data equally.

Cloud top and terrain temperatures can thus be measured with a fair degree of accuracy on negative or positive transparencies by using a densitometer. The pictorial display is invaluable for recognition and qualitative analysis of the meteorological information.

Figure 3-9 is a reproduction of a selected portion of the photofacsimile display of an orbital strip covered by the Nimbus I HRIR near midnight on September 20, 1964, ranging from the Gulf of Alaska at the top to the equator at the bottom. The blackness of each picture element varies directly with the intensity of the radiation sensed by the radiometer (by convention, this is defined as a "positive" HRIR print). The warm waters of the tropical Pacific Ocean can be recognized

Orbits 000-535	Orbits 536-
(Outside Range)	210°K
225°K	225°K
240°K	235°K
252°K	245°K
267°K	250°K
282°K	255°K
301°K	265°K
327°K	280°K
(Outside Range)	295°K
(Outside Range)	310°K

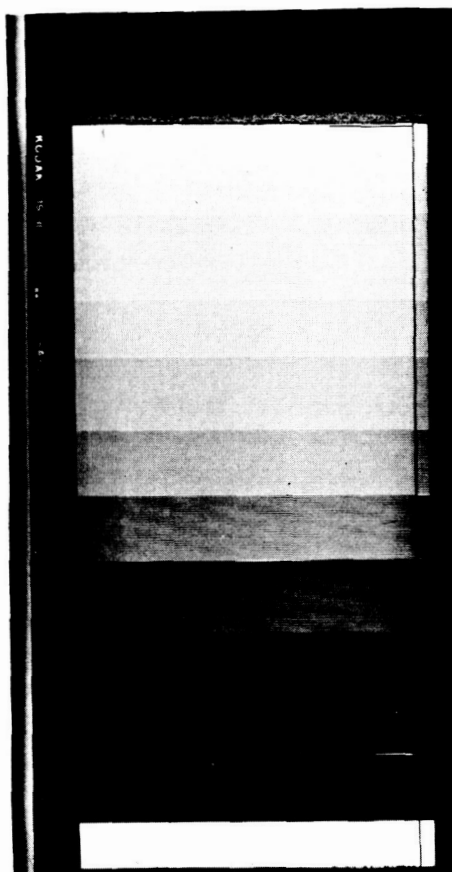


Figure 3-8—The ten-step gray scale wedge for the photofacsimile-produced HRIR positive film strips showing the corresponding equivalent blackbody temperatures, for sensor cell temperature of  $-70^{\circ}\text{C}$ .

in the very dark area near the bottom in contrast to the somewhat cooler temperatures of the North Pacific Ocean shown by the dark patches just north and south of  $40^{\circ}\text{N}$ . The "medium gray" around  $30^{\circ}\text{N}$  is a large mass of very low altitude stratus clouds or fog. The string of small, very bright (cold) spots near  $137^{\circ}\text{W}$  and  $38^{\circ}$  to  $40^{\circ}\text{N}$  indicate isolated, very high altitude cumulus clouds relating to thunderstorm activity.

### 3.4.3 Digital HRIR Data Processing

A much more quantitative picture results when the original analog signals are digitized with full fidelity and the digital data are processed by an IBM 7094 computer where calibration and geographic referencing is applied automatically.



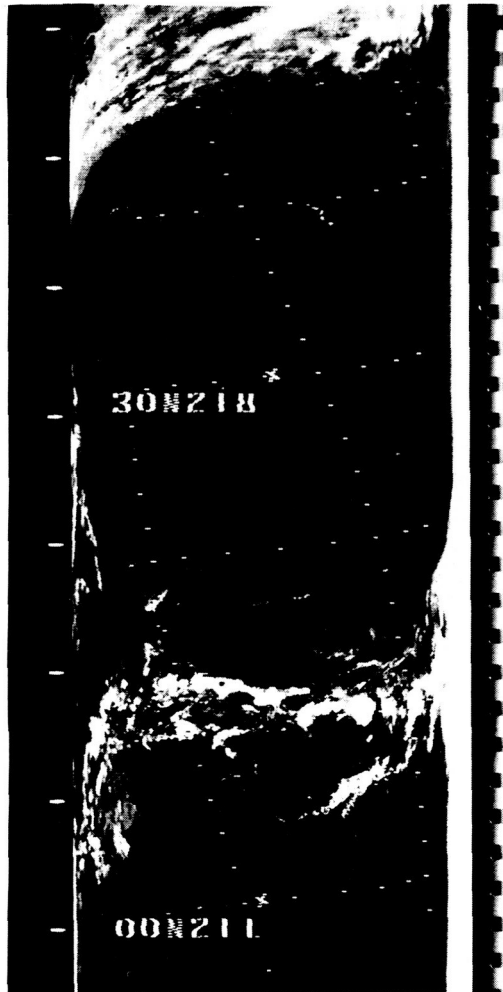


Figure 3-9—An example of automatic gridded HRIR data.

Extracts of such automatic, numeric presentations are shown in Figure 3-10. The very highest cloud in Figure 3-10, located in the Intertropical Convergence Zone ( $11.5^{\circ}$  -  $12^{\circ}$ N and  $145$  -  $146^{\circ}$ W), is characterized by extremely low radiation intensities corresponding to blackbody temperatures of  $190^{\circ}$ K near the center of the cloud top (Figure 3-10).

A simplified block diagram of the A/D processing system is shown in Figure 3-11. The analog magnetic tape is fed to an A/D converter which utilizes a CDC 924 computer to prepare a digital tape. This tape is then operated upon by the 7094 which prepares a reduced radiation data tape called the Nimbus Meteorological Radiation Tape-HRIR (NMRT-HRIR) which can be used to generate grid point maps or to accomplish special scientific analyses. The format of this tape is given in Appendix A.

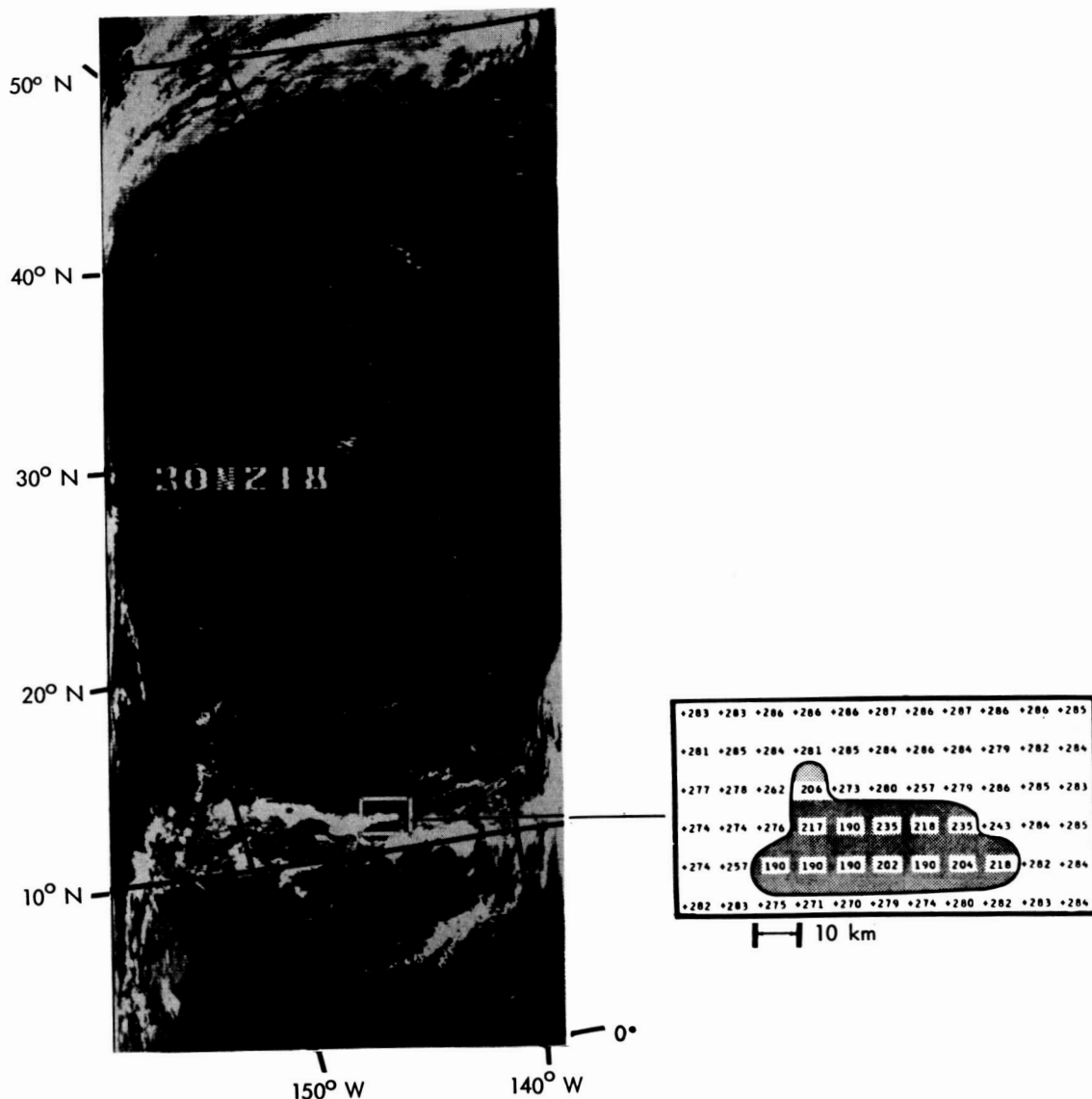


Figure 3-10—A positive print of nighttime Nimbus I HRIR data: (a) Pictorial presentation of cloud and water temperatures over the North Pacific measured by the HRIR at midnight on 20 September 1964. (Dark shades are warm, white shades are cold.) (b) Automatically produced digital map of cloud surface temperatures.

#### 3.4.4 Analog Recording

Analog records can be made from the original spacecraft interrogation record; these Visicorder oscillograph records permit accurate measurement of temperature as a function of time and sensor scan angle. (Fig. 3-4). However, the sheer volume of the data prohibits the use of this method except for special cases.

## NIMBUS II HRIR ANALOG TO DIGITAL DATA PROCESSOR

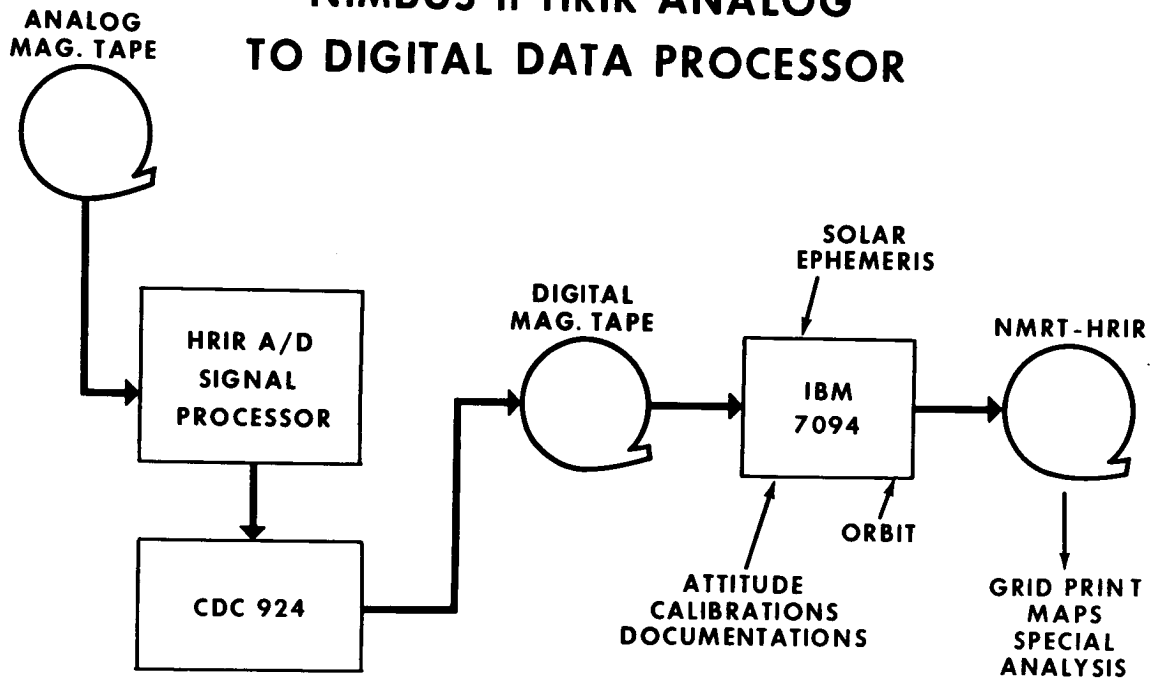


Figure 3-11—Nimbus II HRIR Analog to Digital Data Processor

### 3.5 Automatic Gridding of HRIR Data

The absolute and relative geographical locations of each picture element scanned by the radiometer depend on the stability of the spacecraft. The Nimbus controls system has a demonstrated pointing accuracy of better than  $\pm 1$  degree in pitch and roll and  $\pm 3$  degrees in yaw. A pointing error of 1 degree in pitch or roll corresponds to a subsatellite error of 11 nautical miles (20 km) in the location of a picture element for an altitude of 600 nautical miles (1110 km). On a global basis, this is an acceptable error for most meteorological analysis.

Automatic gridding of the data is accomplished by utilizing the CDC 924 to compute geographic coordinates, and a grid computer and mixer which generate the grid points and add them to the HRIR data in analog form. These grid points are electronically superpositioned on the film. The grid point array makes up lines for every  $10^\circ$  of latitude and longitude, with points spaced at  $2^\circ$  intervals along each line. (There is no change in longitude interval near the poles as there is in AVCS gridding.) The grid points are superpositioned on the film from  $0^\circ$  to  $53.5^\circ$  of scan nadir angle. The annotation for the grid is given at  $60^\circ$  North and South,  $30^\circ$  North and South, and at the Equator. The annotation applies at the small "x" near the center of the film. East longitude is given to the nearest degree from  $0^\circ$  to  $359^\circ$ . In Figure 3-6 (b) the only annotation which appears is at  $60^\circ$ S and  $079^\circ$ E and applies at the small "x" to the left and above the annotation.

A feature of the gridding program provides for the presentation of the annotation for the grids on the film in such a manner that it is properly oriented when the latest recorded data are at the bottom and the earliest recorded data are at the top of the film. For data recorded at night when the satellite travels from north to south, this presentation of the annotation is natural, with north at the top and south at the bottom of the film. However, in the case of daylight recorded data when the satellite travels from south to north, the latest recorded are the northernmost data and a properly oriented film strip shows the annotation upside down. If a data block contains only daytime data, the print, when correctly oriented, shows the annotation upside down. However, if a data block contains both nighttime and daytime data, the print is arranged such that the nighttime data are oriented correctly, forcing the daytime data to appear with the southern most data at the top and northern most data at the bottom.

The grid-point array for reverse mode data is the same as that for forward mode data. In Figure 3-7 (b) the annotation is given at 60°S and 089°E. This annotation applies at the small "x" to the right and above the annotation.

Another example of automatic gridding is shown in Figure 3-9. The line along the right edge of Figure 3-9 indicates the horizon as seen by the radiometer. There is a clear indication of fluctuation in that line after the spacecraft has passed over the high tropical clouds near the equator. This indicates the disturbances which the high altitude, cold clouds presented to the infrared horizon scanner of the Nimbus I controls system, causing the spacecraft to roll slightly as it passed over the equator.

### 3.6 Calibration

In discussing the calibration, three fundamental quantities must be defined: the effective spectral response,  $\phi_\lambda$ ; the effective radiance,  $\bar{N}$ ; and the equivalent blackbody temperature,  $T_{BB}$ .

#### 3.6.1 Effective Spectral Response

The radiation received by the radiometer is reflected by five front-surface aluminized mirrors and transmitted through a filter before reaching the PbSe detector. The effective spectral response,  $\phi_\lambda$ , is defined as

$$\phi_\lambda = R_\lambda F_\lambda A_\lambda \quad (1)$$

where  $R_\lambda$  is the combined spectral reflectivity of all five front-surface mirrors,  $f_\lambda$  is the spectral transmittance of the filter and  $A_\lambda$  is the spectral absorptivity of the detector.

In the actual computation of  $\phi_\lambda$ , the spectral reflectivities,  $R_\lambda$ , of all mirrored surfaces were assumed to be constant over the pass band of the filter and hence were normalized to unity. The resultant equation used in computing  $\phi_\lambda$ , therefore, was

$$\phi_\lambda = f_\lambda A_\lambda \quad (2)$$

The materials used in the optics are given in Table 3-1. The function  $f_\lambda$  was taken from International Telephone and Telegraph Laboratories measurements of the filter used in HRIR Unit F-4, the instrument flown on Nimbus II; and the function  $A_\lambda$  was taken from several typical laboratory curves of PbSe detectors. The effective spectral response is given in Figure 3-12.

Table 3-1  
Nimbus II HRIR Optics

<b>Filter</b>	
Type:	Multilayer wide band-pass interference
Substrate:	Germanium
Transmission:	0.76 (calculated)
<b>Scan Mirror</b>	
Type:	Evaporated SiO over hard-coated aluminum
Substrate:	Aluminum
Reflectivity:	0.96 (estimated)
<b>Cassegrainian telescope (primary and secondary)</b>	
Type:	Front-surface Al with SiO Protective coating
Substrate:	Glass
<b>Relay Optics</b>	
Type:	Front-surface gold coated with SiO protective coatings
Substrate:	Glass
Reflectivity of the 4 mirror surfaces (Cassegrainian telescope and relay optics):	0.92 (estimated)

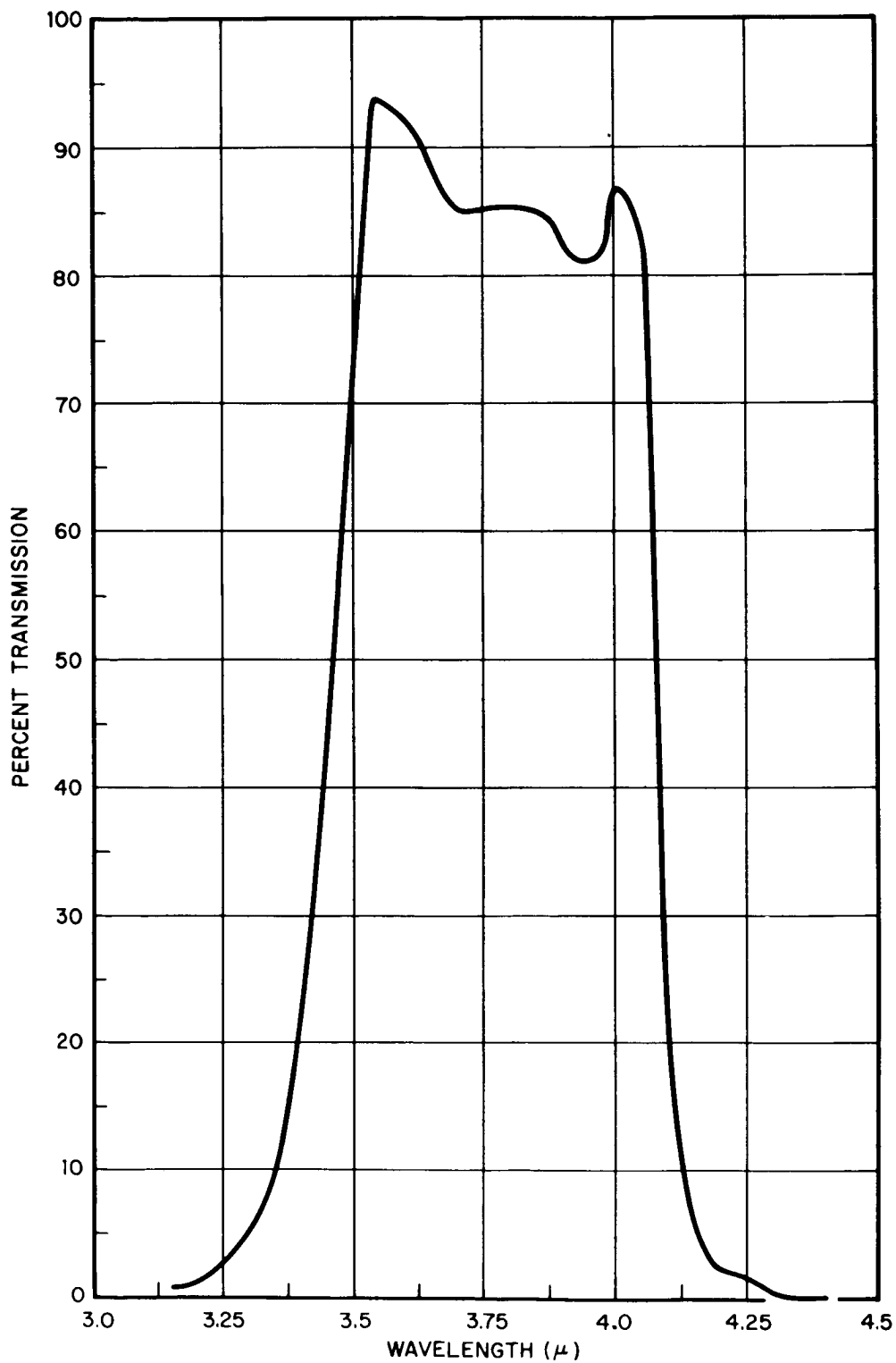


Figure 3-12—The effective spectral response of the HRIR versus wavelength

### 3.6.2 Effective Radiance

Because of its narrow field of view, the HRIR essentially measures beam radiation or radiance toward the satellite along the optical axis. In the preflight laboratory calibration, the field of view of the radiometer was filled by a blackbody target whose temperature could be varied and accurately measured over a range of 190°K to 340°K. From the temperature of the blackbody target,  $T_{BB}$ , the spectral radiance of the target is determined by the Planck function,  $B_\lambda$ . The integration of this function over the effective spectral response,  $\phi_\lambda$ , yields that portion of the radiance of the target to which the radiometer responds, the "effective radiance,  $\bar{N}$ ," given by

$$\bar{N} = \int_0^\infty B_\lambda (T_{BB}) \phi_\lambda d\lambda \quad (3)$$

### 3.6.3 Equivalent Blackbody Temperature

The effective radiance to which the orbiting radiometer responds may be expressed by

$$\bar{N} = \int_0^\infty N_\lambda \phi_\lambda d\lambda \quad (4)$$

where  $N_\lambda$  is the spectral radiance in the direction of the satellite from the Earth and its atmosphere. It is convenient to express the measurement from orbit in terms of an equivalent temperature of a blackbody filling the field of view which would cause the same response from the radiometer. From Equations 3 and 4 it is seen that this "equivalent blackbody temperature" corresponds to the target temperature,  $T_{BB}$ , of the blackbody used in the laboratory calibration. This relationship is expressed schematically in Figure 3-13. Therefore, the radiometer measurements can be expressed either as values of effective radiance,  $\bar{N}$ , or as equivalent blackbody temperatures,  $T_{BB}$ . The  $\bar{N}$  versus  $T_{BB}$  function from Equation 3 is given in Figure 3-14.

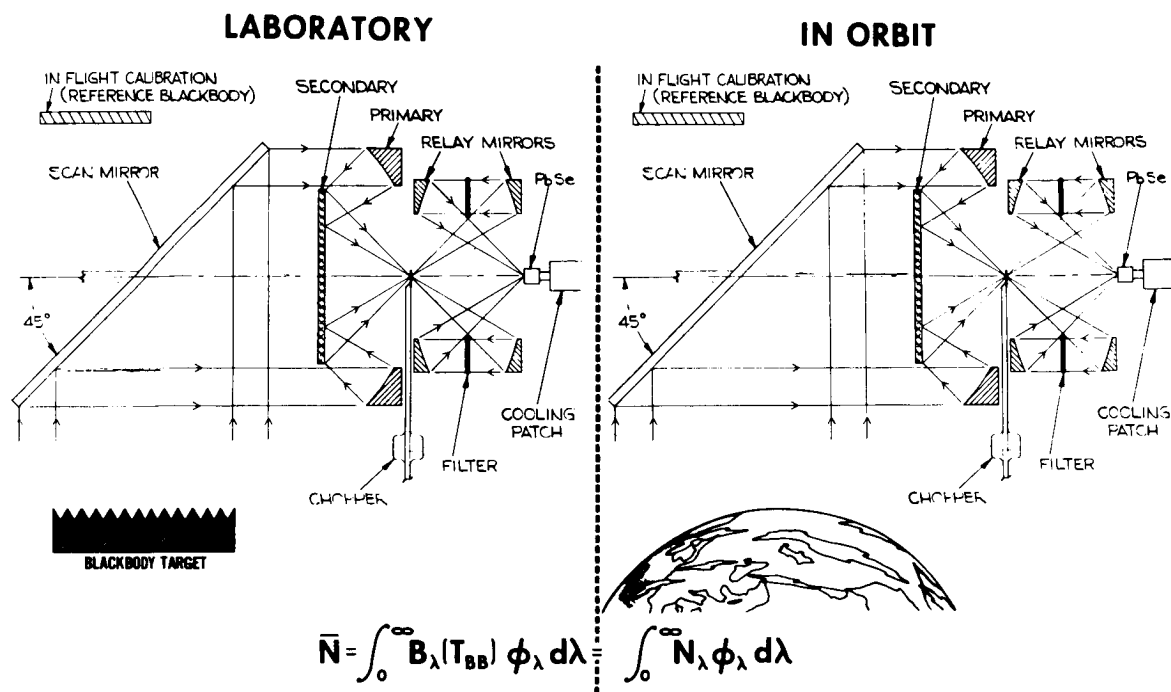


Figure 3-13—Schematic illustration of the relationships between laboratory calibration and  $T_{BB}$  measurements made in orbit:

The only independent varying parameter of consequence in the calibration was the cooled PbSe cell temperature. All other temperature and voltage variations were automatically compensated for and/or regulated within very narrow limits. Therefore, separate calibrations were made for several different cell temperatures. The blackbody target temperature,  $T_{BB}$ , was varied between 190°K and 340° in 10°K steps and the radiometer output voltages were recorded for a given cell temperature. Then the PbSe cell was stabilized at a new temperature and the target temperature was cycled again from 190°K to 340°K.

After the radiometer was integrated in the spacecraft and subjected to vacuum-thermal environmental testing, a check of calibration was performed. These data were obtained approximately eight months after the original laboratory calibration of the radiometer. Essentially the same techniques were employed in the calibration check as were used in the original laboratory calibration. The blackbody target temperature was varied from 190°K to 340°K in 20°K steps and the subcarrier frequencies from the FM modulator were recorded on the spacecraft HRIR tape recorder (cf. Figure 3-5). After one full target temperature cycle, the data were played back through the entire system and transmitted via the S-band transmitter in the spacecraft. The data were received at the ground station, demultiplexed,



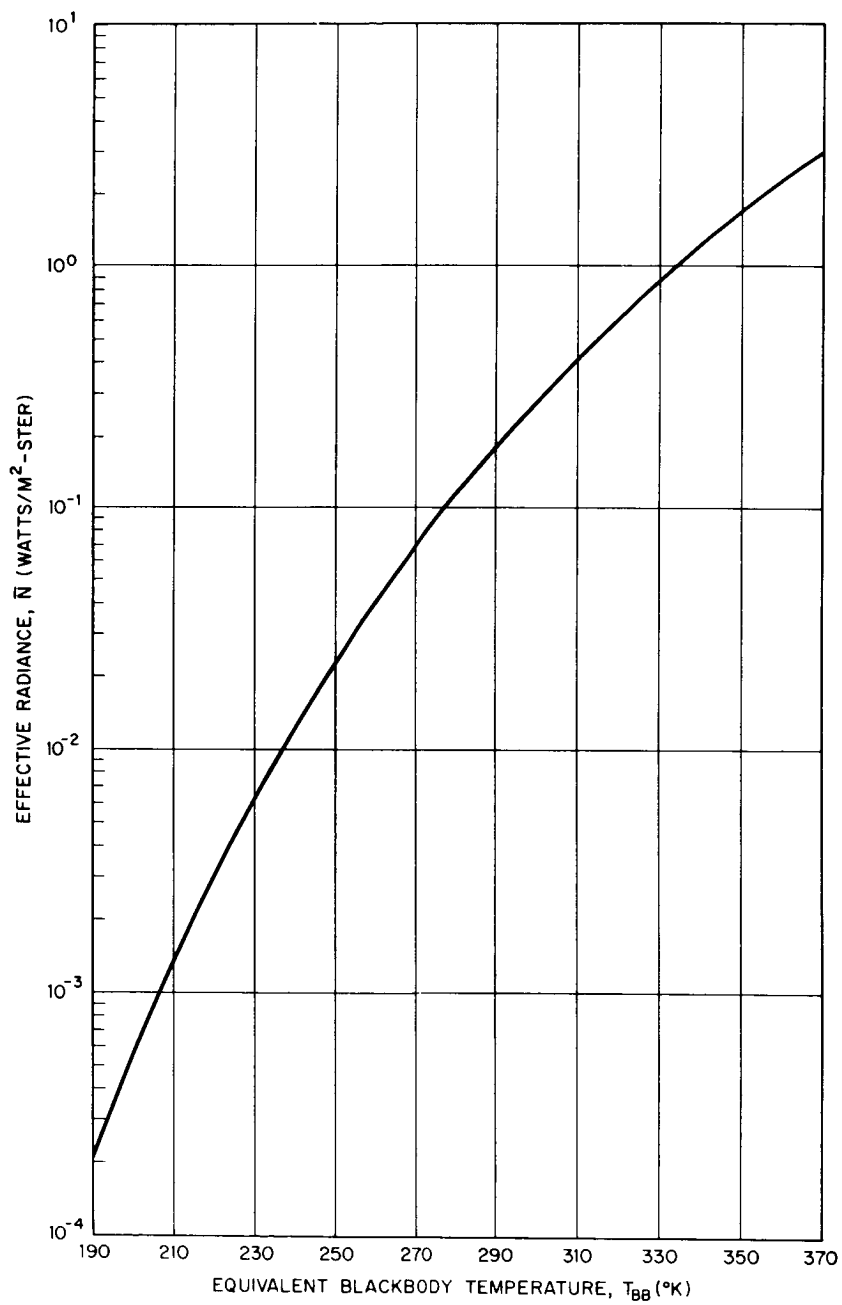


Figure 3-14— $\bar{N}$  versus  $T_{BB}$ .

demodulated and displayed in the form of an analog trace on an oscillographic record, thus simulating as fully as possible, on a system basis, the orbital conditions. Close examination of both sets of calibration data revealed no significant changes over the eight months' period during which the radiometer underwent testing and integration with the spacecraft; therefore, we have high confidence in the validity of the calibration. The definitive calibration data for the HRIR F-4 unit which is installed on Nimbus II is shown in Figure 3-15. A plot of detector cell temp. vs. orbit will be included in the monthly Users' Catalog. Parametric curves for different values of the PbSe cell temperature are given. Values of  $T_{BB}$  can be converted to  $\bar{N}$  from Figure 3-14. In orbit the calibration is checked at one target temperature during each scan by means of a blackbody target of known temperature mounted on the upper side of the radiometer (Figure 3-3).

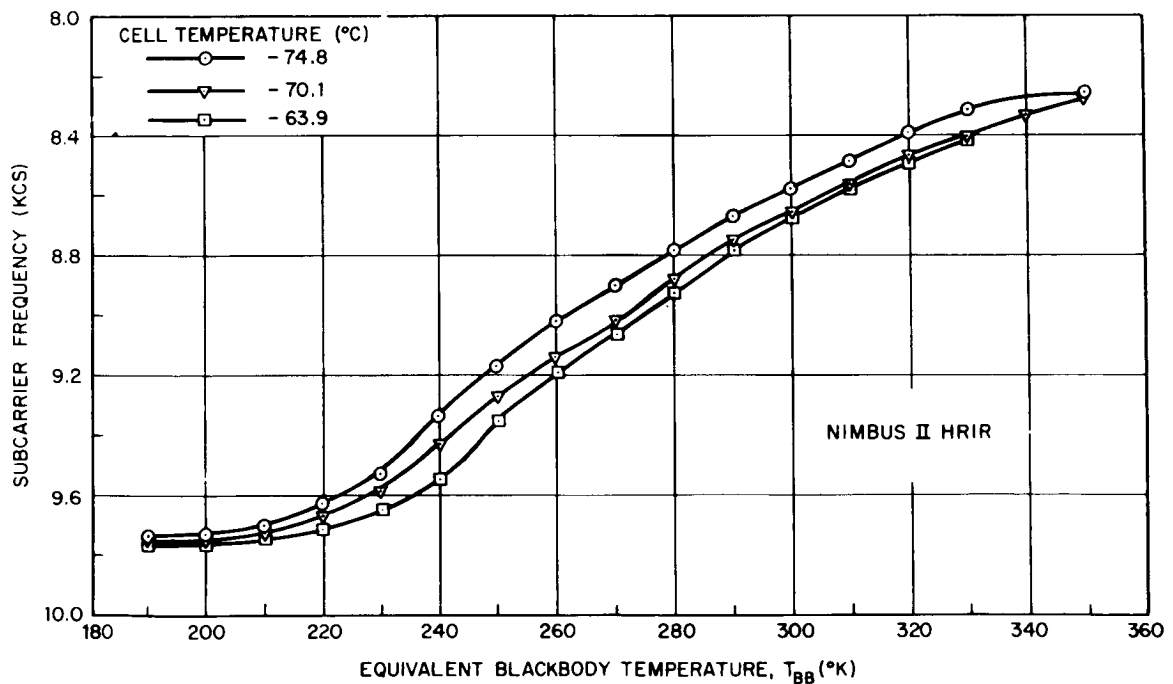


Figure 3-15—HRIR Calibration Nimbus II HRIR.

## SECTION 4

### MEDIUM RESOLUTION INFRARED RADIOMETER (MRIR)

#### 4.1 Description of the Experiment

This experiment is designed to measure electromagnetic radiation emitted and reflected from the earth and its atmosphere in five selected wavelength intervals. The scientific basis for the experiment and the results from earlier measurements of this type acquired from the TIROS series have been well documented. (References 3-35). For this reason the objectives will only be summarized here. Since the radiometer includes one channel having a response extending into the visible, the term Medium Resolution Infrared Radiometer is somewhat inaccurate. However, because the use of the term "MRIR" has historically become so firmly entrenched, this familiar designation will be used to identify the experiment discussed below.

For meteorological purposes, data for heat balance of the earth-atmosphere system will be obtained as well as water vapor distribution, surface or near surface temperatures, and seasonal changes of stratospheric temperature distribution. The Nimbus circular, polar orbit is ideally suited to this experiment since global coverage is necessary to accomplish the stated objectives. In addition, the three-axis stabilization of the Nimbus spacecraft permits the acquisition of data in a systematic way at continuously varying angles of view in a simple geometrical pattern.

The five wavelength regions, each with a brief description of its purpose, are as follows:

6.4 to 6.9 microns - This channel covers the 6.7 micron water vapor absorption band. Its purpose is to provide information on water vapor distribution in the upper troposphere and, in conjunction with the other channels to provide data concerning relative humidities at these altitudes.

10 to 11 microns - Operating in an atmospheric "window," this channel measures surface or near-surface temperatures over clear portions of the atmosphere. It also provides cloud cover and cloud height information (day and night).

14 to 16 microns - This channel, centered about the strong absorption band of CO<sub>2</sub> at 15 microns, measures radiation which emanates primarily

from the stratosphere. The information gained here is of primary importance in following seasonal stratospheric temperature changes.

5 to 30 microns – This channel measures the emitted long wavelength infrared energy and, in conjunction with the reflected solar radiation channel furnishes data on the heat budget of the planet.

0.2 to 4.0 microns – This channel covers more than 99% of the solar spectrum and yields information on the intensity of reflected solar energy from the earth and its atmosphere.

The instrument devised for this experiment is shown in Figure 4-1. The radiant energy from the earth is collected by a flat scanning mirror inclined at  $45^\circ$  to the optical axis. The mirror rotates and scans in a plane perpendicular to the direction of motion of the satellite. Hence, in every  $360^\circ$  scan it covers the earth from horizon to horizon, views space twice, and "looks" at its own housing once. Figure 4-2 shows a typical earth scan as presented on a strip chart recorder. The portions of the scan labelled "Space, Spacecraft, Scanner Housing, Space" yield in-flight calibration data (discussed in detail below). The incident flux is then focused onto a thermistor bolometer detector through appropriate optical filtering which limits the radiation to the desired wavelengths. The energy is modulated by a mechanical chopper to produce an a.c. signal from the detector. Figure 4-3 shows an optical diagram of the system. Used in this manner, the chopper becomes the reference temperature for the radiometer. Since the chopper temperature can reasonably be expected to vary during orbit, and because the detector signal represents the difference in energy between the target and the chopper, some method of determining the absolute temperature of the target as the chopper changes temperature is necessary. This is accomplished by introducing an electronic offset which is controlled by thermistors monitoring the chopper temperature. This offset voltage is added to or subtracted from the signal in direct proportion to the chopper temperature so that a target of a given temperature will always produce the same absolute voltage output.

The electrical signal from the detector is then amplified and synchronously demodulated to yield an analog output of 0 to -6.4 volts to cover the desired range of target temperatures (or of radiance in the 0.2-4.0 micron interval) for each channel. These analog signals are sampled  $33\frac{1}{3}$  times per second and converted to 7-bit digital data. Each data word bit is then recorded on seven channels of an 8-track tape recorder such that the data word bits are stored in parallel. On command for playback the data are reconverted to serial form and transmitted to the Data Acquisition Facility (DAF) using a special MRIR transmitter with a carrier frequency of 137.2 Mc. After receipt at the ground, the data are transmitted to the Goddard Space Flight Center for final processing.

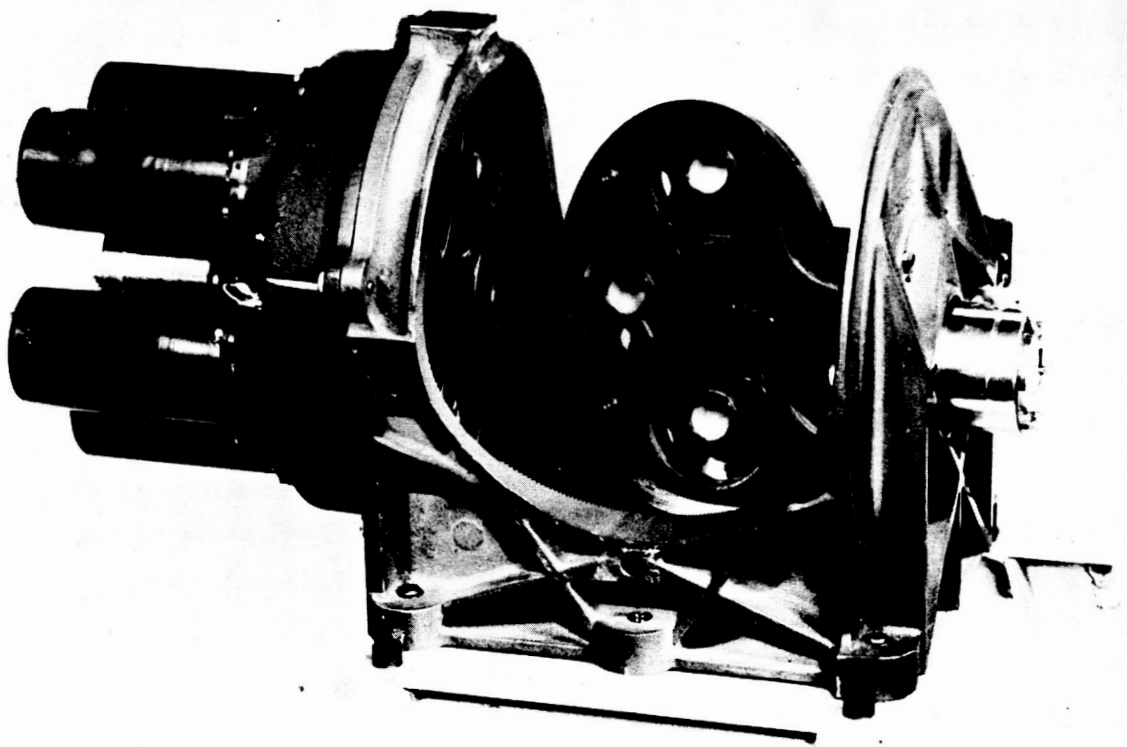


Figure 4-1-MRIR Radiometer

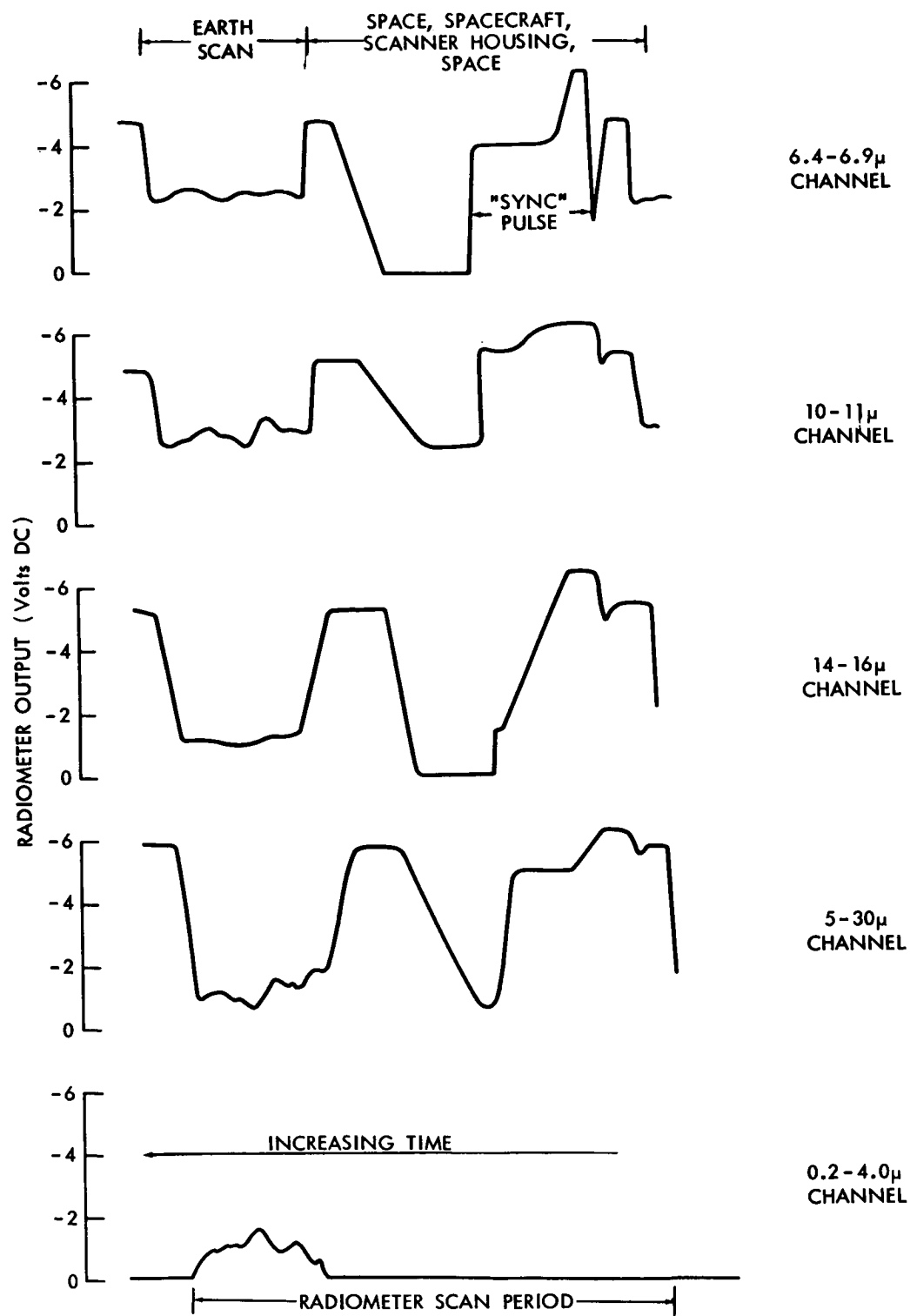


Figure 4-2—Typical Scan Pattern for MRIR in Orbit

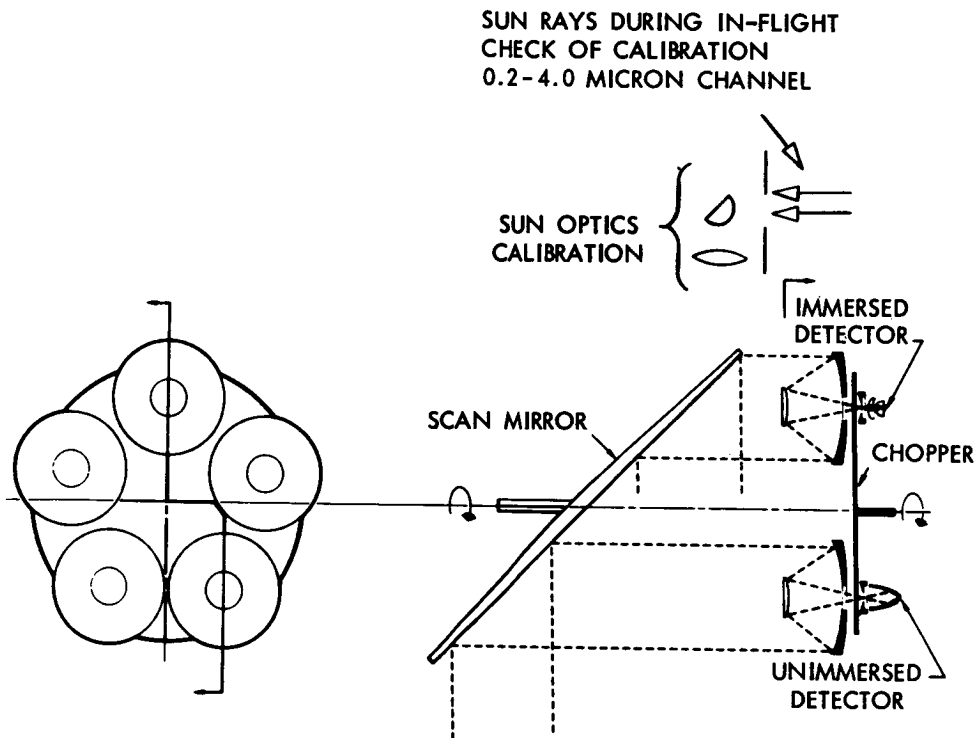


Figure 4-3—Optical Arrangement of NIMBUS Five-Channel Radiometer

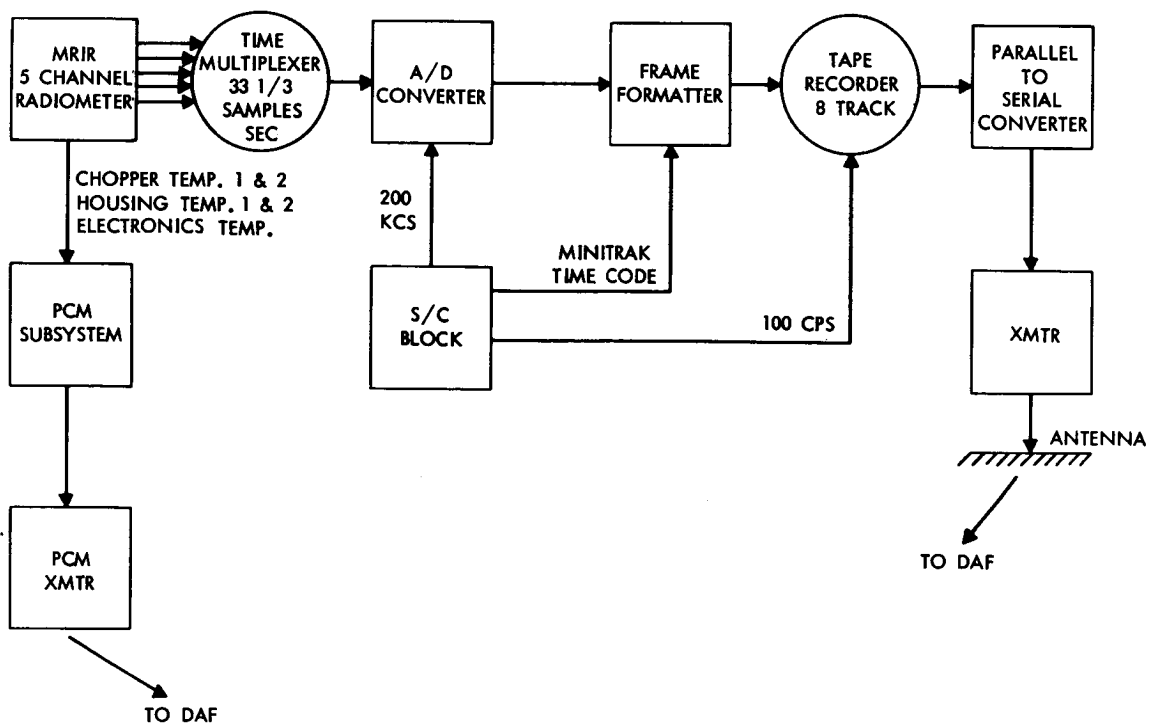


Figure 4-4—Block Diagram of S/C Portion of MRIR System

Timing information is furnished by the Spacecraft clock and mixed with the data such that every 60 milliseconds the time code is inserted. At the ground station the time code is extracted from the data and displayed on the analog record. This display is described in section 4.3.2. Simultaneously the time information is formatted in IBM compatible language and included on the digital tape output (section 4.3.3) for computer processing. Figure 4-4 shows a block diagram of the system. (See Reference 36).

## 4.2 Calibration

The main parameters for calibration of all electromagnetic radiation detection devices are essentially the same. These parameters have been defined in Section 3.6. Briefly, they are the quantities,  $\bar{N}$ ,  $T_{BB}$  and  $\phi_\lambda$ . Here  $\phi_\lambda$  is a composite function involving all of the factors which contribute to the spectral response of the instrument, such as filter transmission, mirror reflectances, and the spectral responsivity of the detector. The effective radiance,  $\bar{N}$ , is defined as

$$N = \int_0^\infty N_\lambda \phi_\lambda d\lambda \quad (1)$$

where  $N_\lambda$  represents the generally non-Planckian radiation from the earth and its atmosphere. For the infrared channels,  $T_{BB}$  then becomes the equivalent blackbody temperature as defined in Section 3.6, and used in the laboratory calibration. Figures 4-5 through 4-8 give  $\bar{N}$  vs.  $T_{BB}$  curves for each infrared channel of the MRIR. Figures 4-9 through 4-13 show the effective spectral response functions,  $\phi_\lambda$ , of each channel of the instrument. The total instrument spectral response function for each channel was measured utilizing a Perkin-Elmer model 112U spectrometer with a radiation thermocouple as a reference. Because of low signal-to-noise ratios, especially at the longer wavelengths, some error was introduced into these measurements. However, departures from the spectral characteristics of the filter are, in general, small and upon integration to obtain  $\bar{N}$ , errors of no more than 1% are encountered.

For laboratory calibrations a cone-shaped blackbody target whose surface was treated with a diffuse black paint was used for the infrared channels, and a calibrated light source was used for the short wave channel. The target assembly is shown in Figure 4-14.



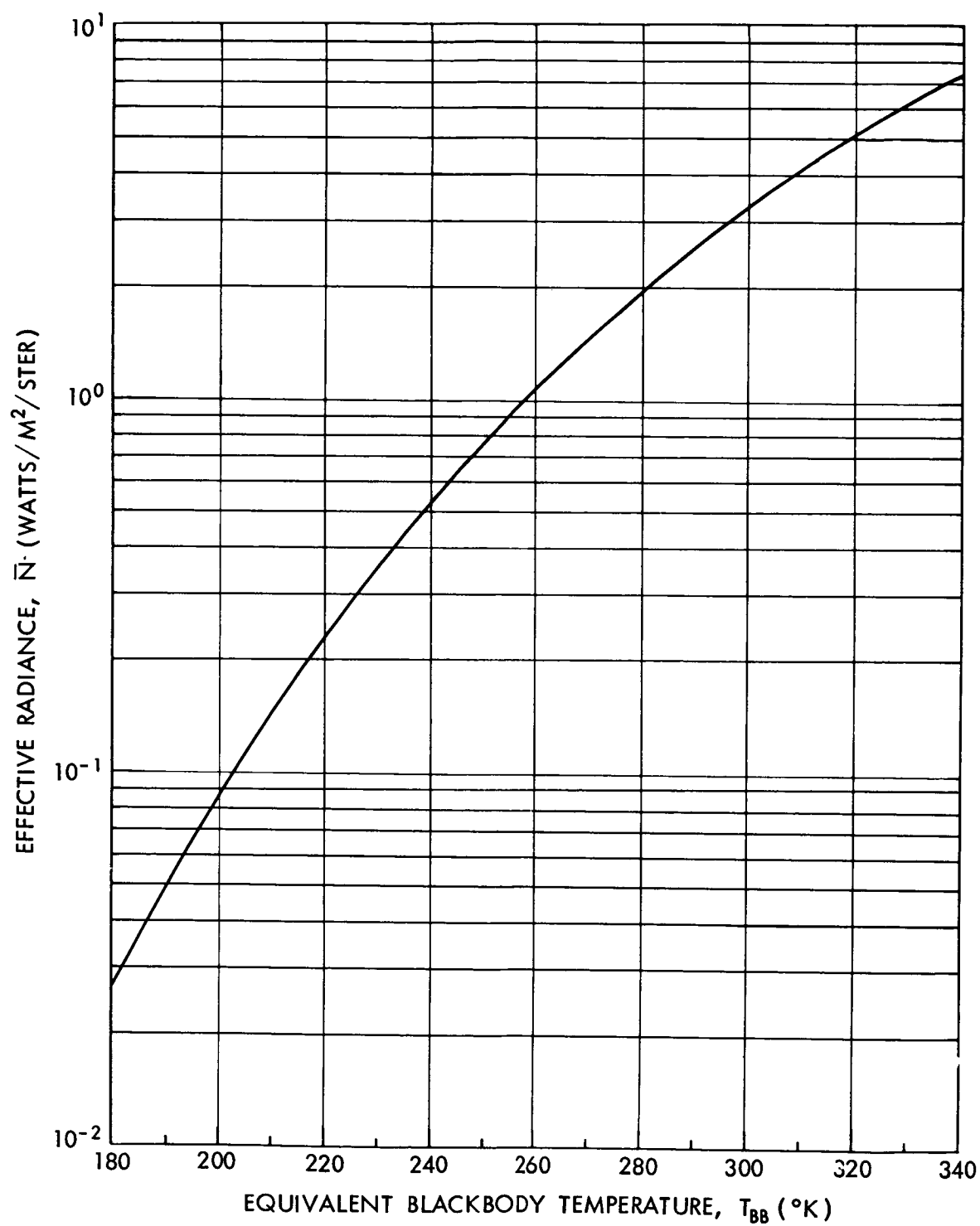


Figure 4-5— $\bar{N}$  vs.  $T_{BB}$  for 6.4-6.9 Micron Channel

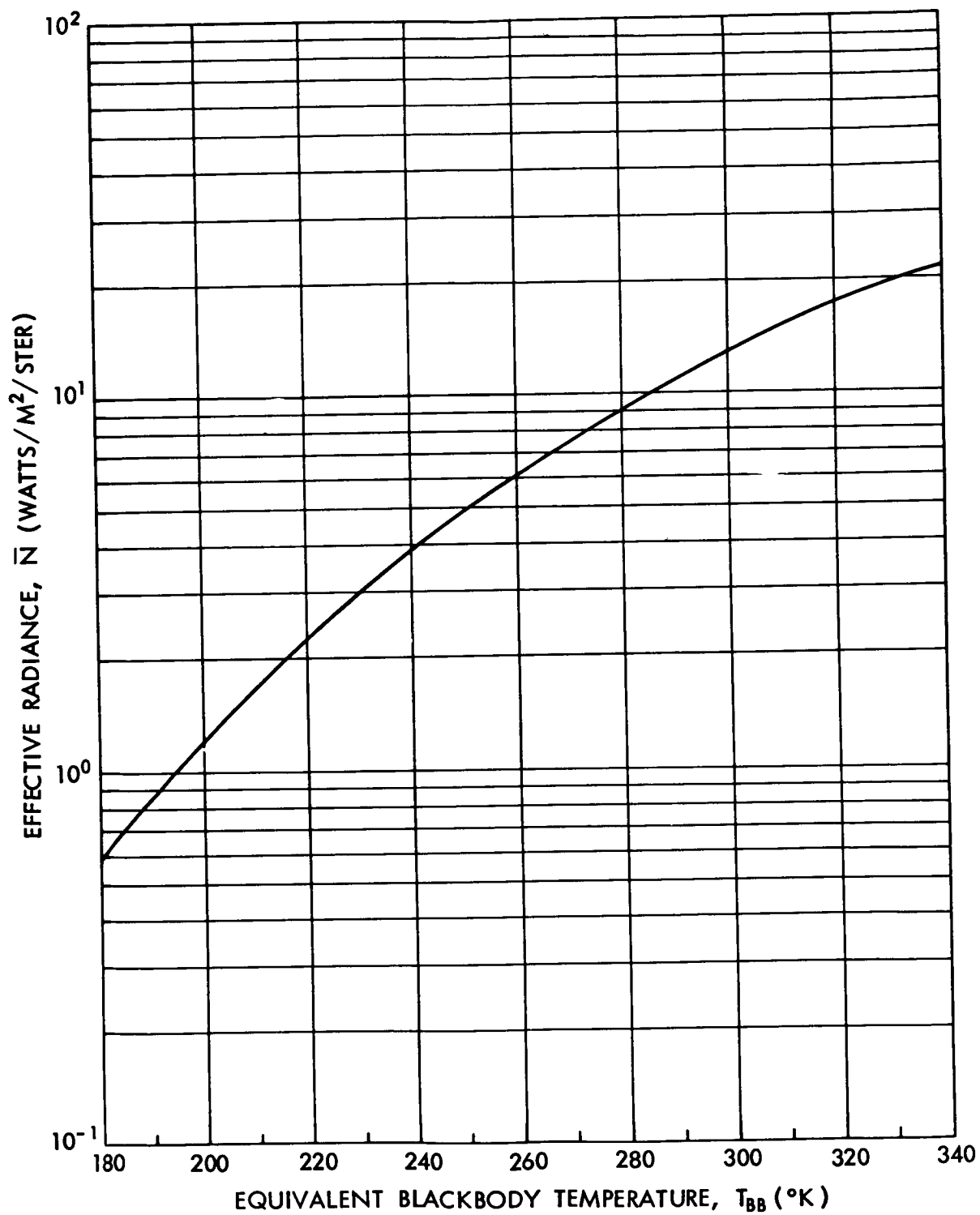


Figure 4-6- $\bar{N}$  vs.  $T_{BB}$  for 10-11 Micron Channel

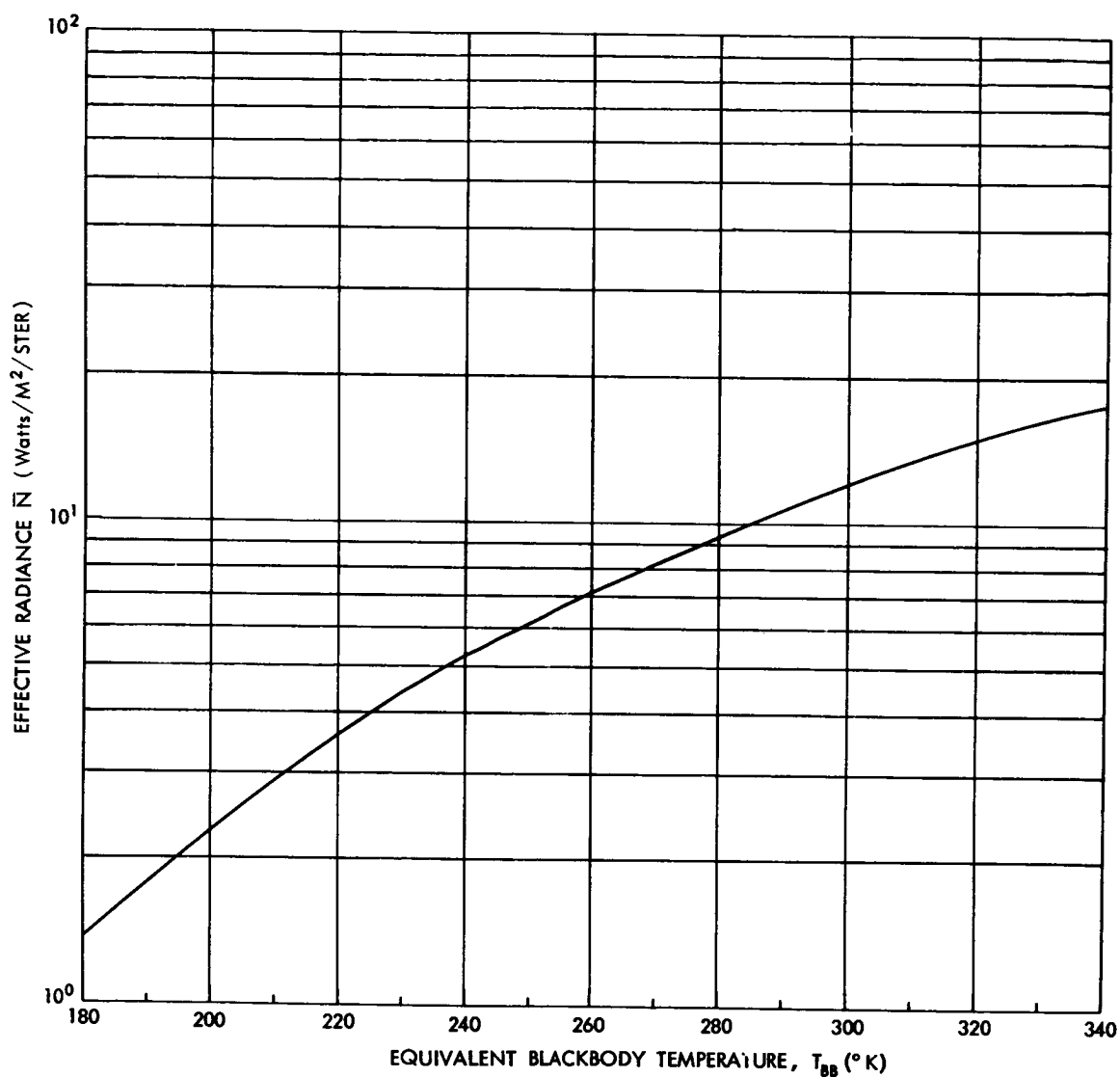


Figure 4-7— $\bar{N}$  vs.  $T_{BB}$  for 14-16 Micron Channel

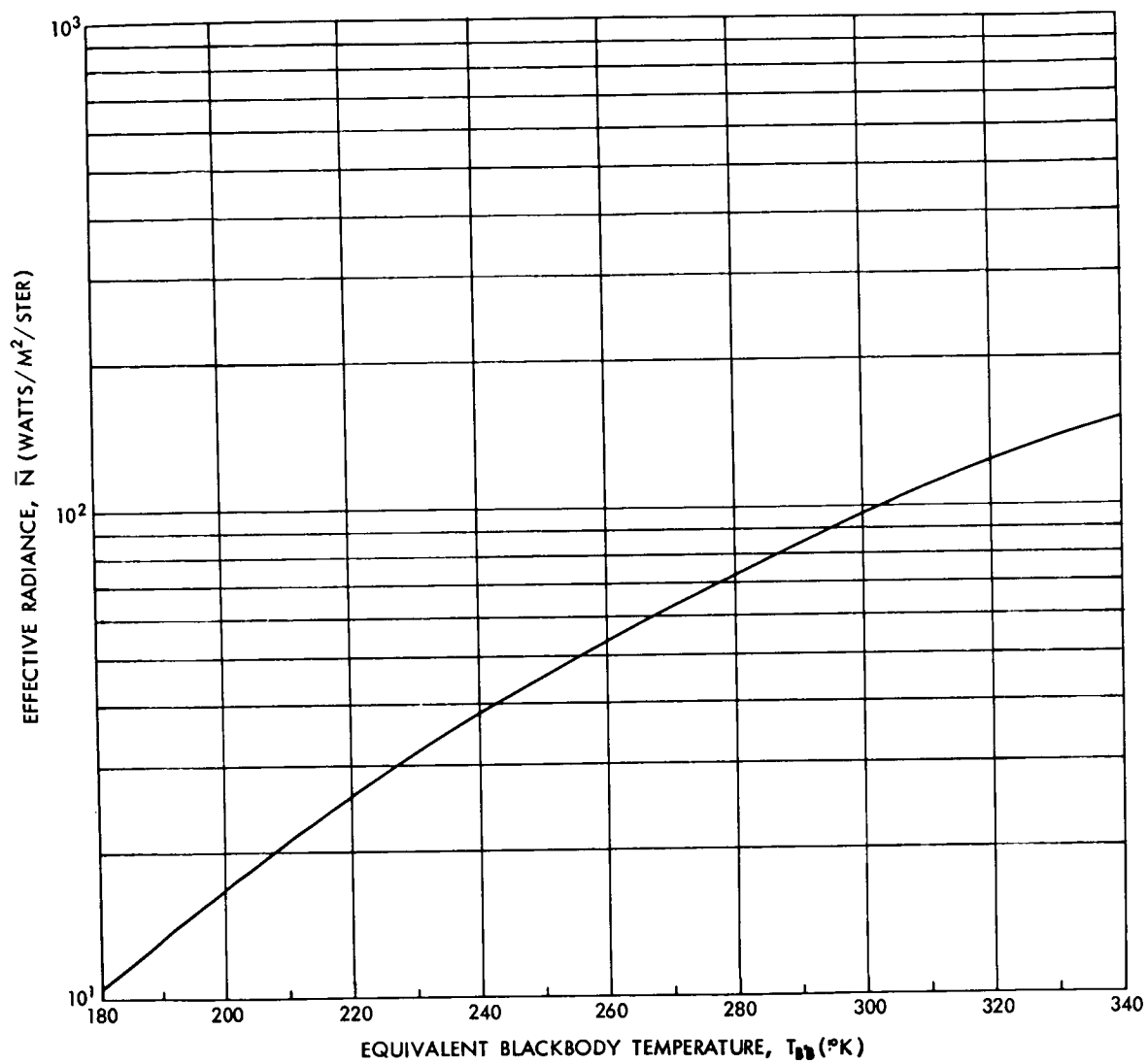


Figure 4-8— $N$  vs.  $T_{BB}$  for 5-30 Micron Channel

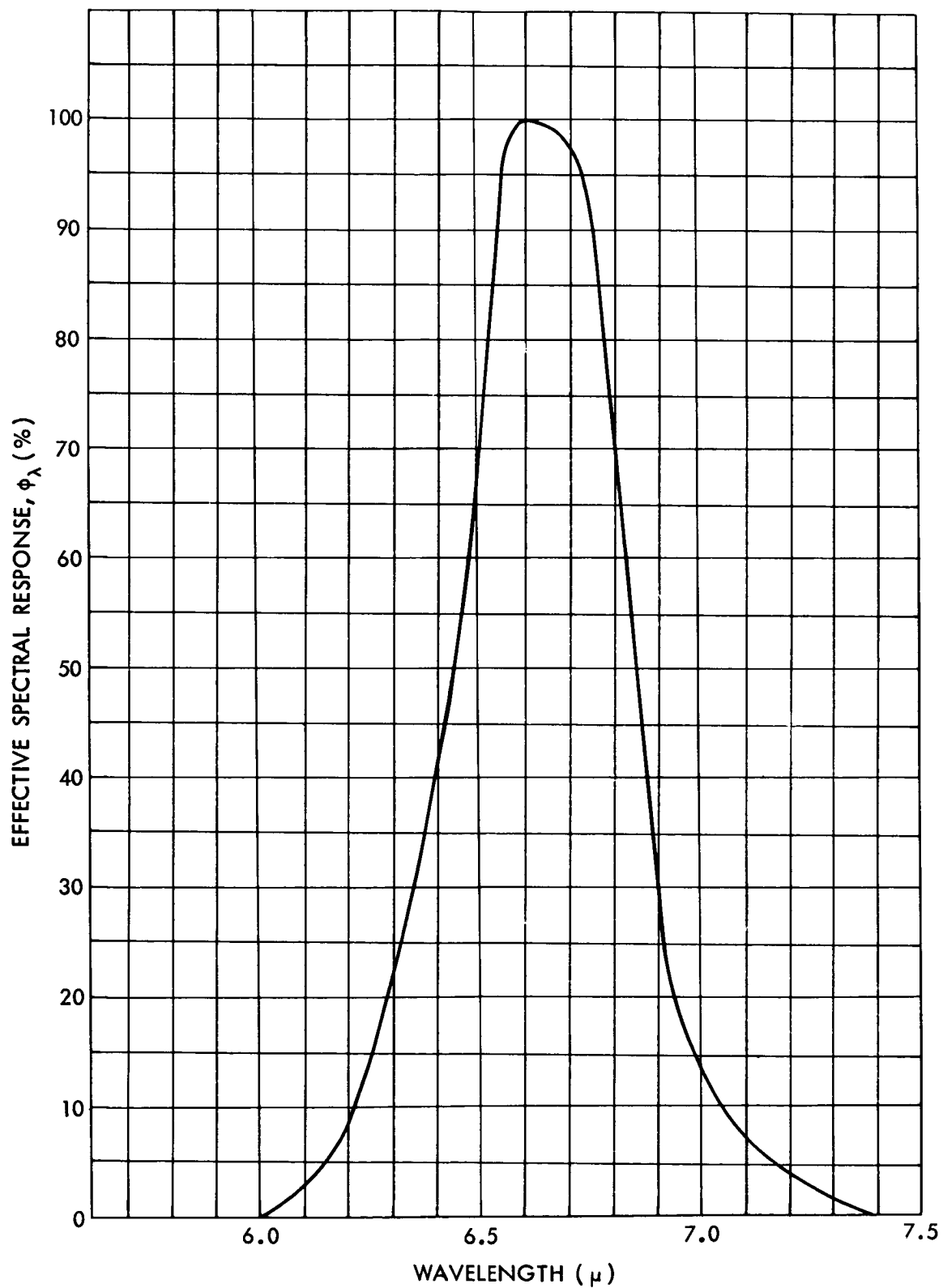


Figure 4-9—Effective Spectral Response of 6.4-6.9 Micron Channel

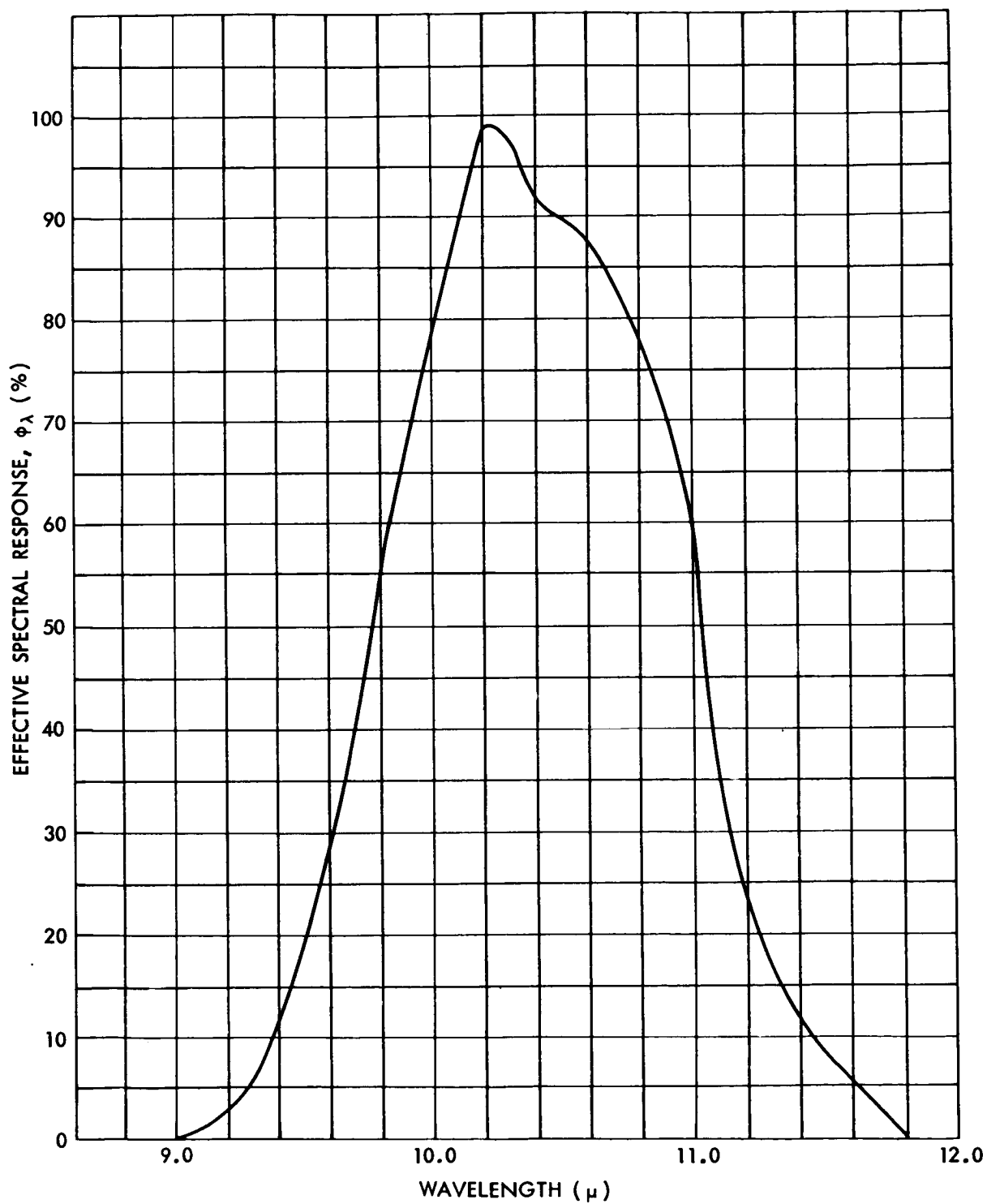


Figure 4-10—Effective Spectral Response of 10-11 Micron Channel

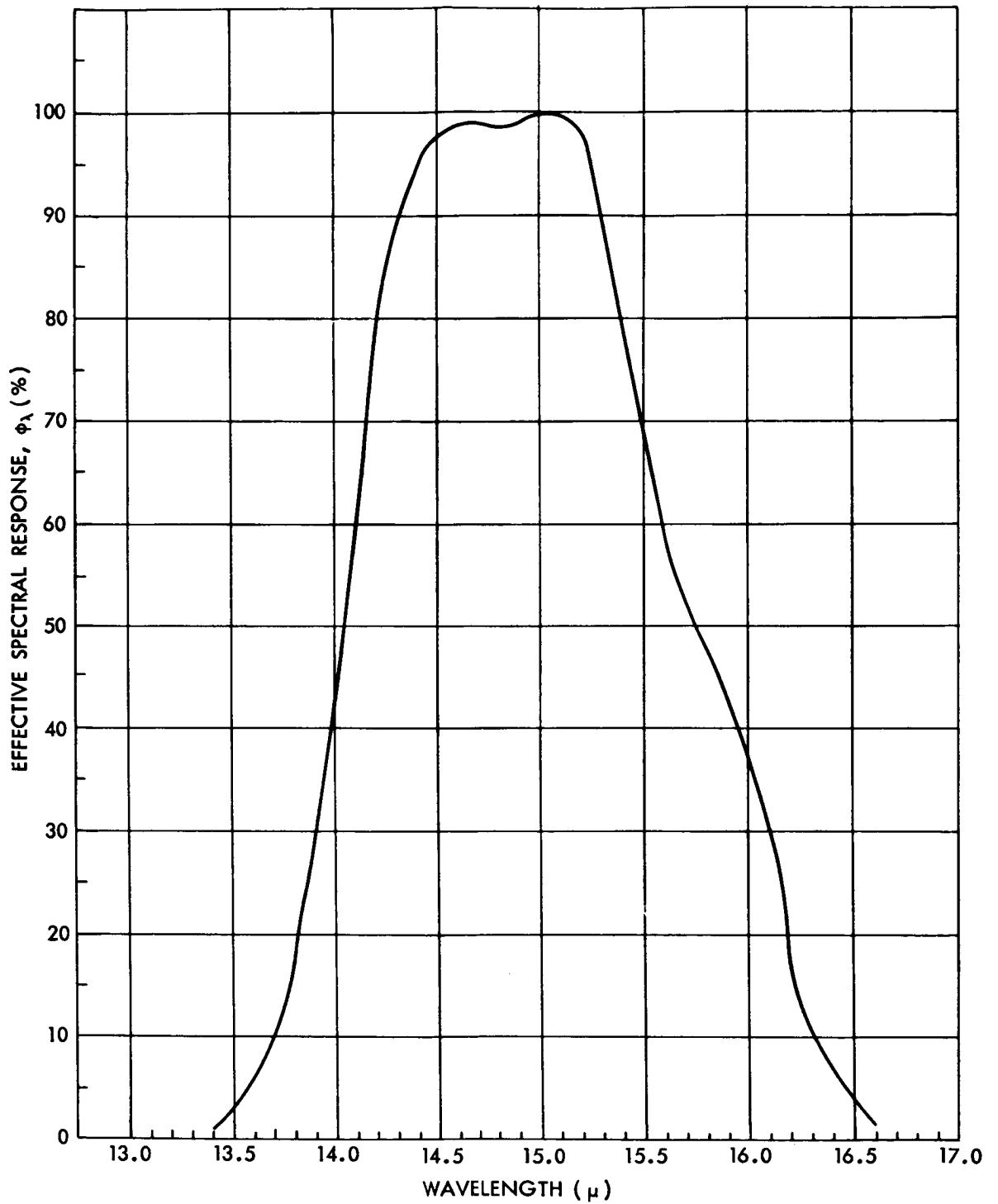


Figure 4-11—Effective Spectral Response of 14-16 Micron Channel

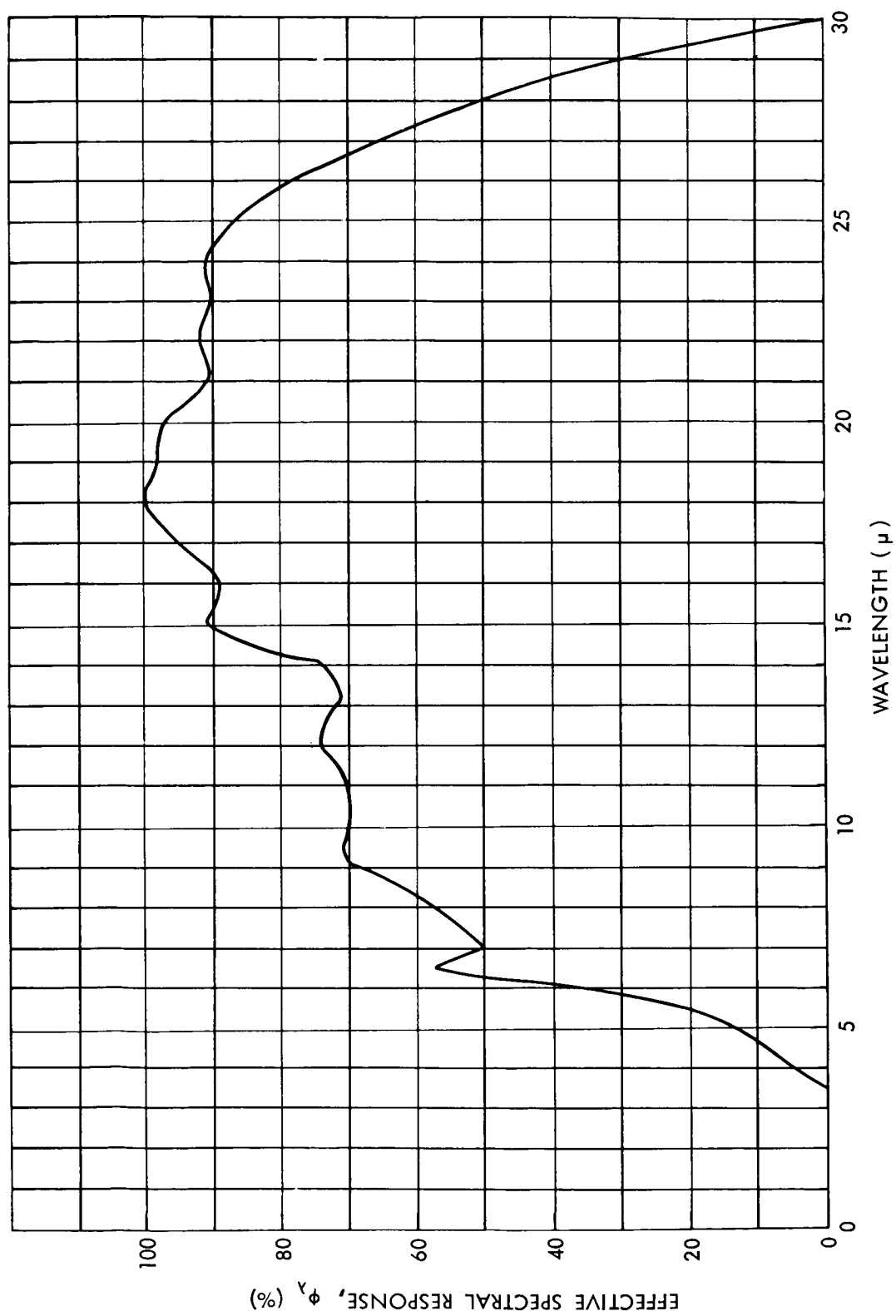


Figure 4-12-Effective Spectral Response of 5-30 Micron Channel



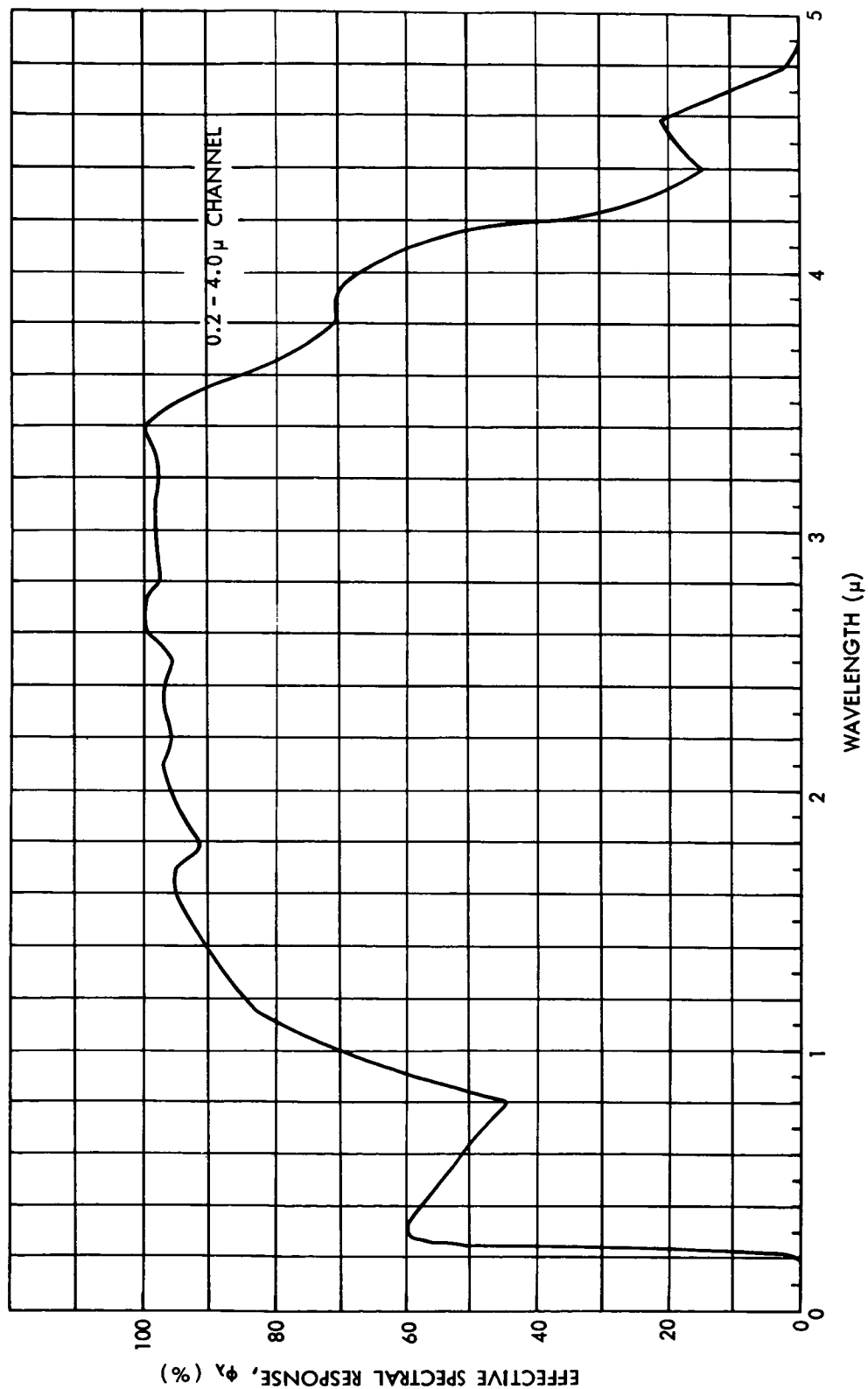


Figure 4-13—Effective Spectral Response of 0.2-4.0 Micron Channel

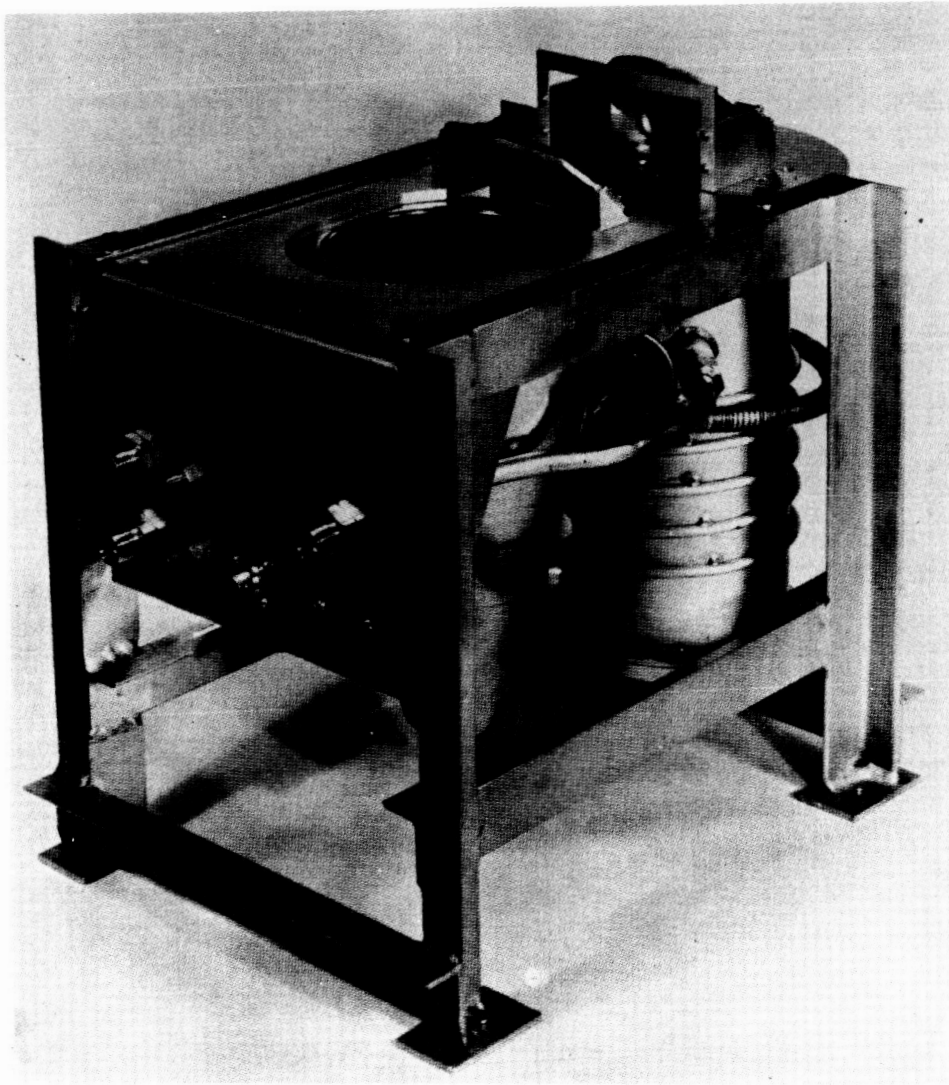


Figure 4-14-MRIR Calibration Target Assembly

The blackbody cone can be cooled by liquid nitrogen to 180°K or below and then heated with nichrome wire to any temperature within the overall dynamic range of the radiometer. The heater coil is designed so that during the warming cycle thermal gradients from the apex to the aperture are maintained within  $\pm 1/2^\circ\text{C}$ .

The radiometer is mounted such that the blackbody and the short wave radiation targets fill the fields of view of the appropriate channels. The output of the radiometer is recorded on a strip chart recorder, and a calibration curve, such as that shown in Figure 4-15, is constructed.

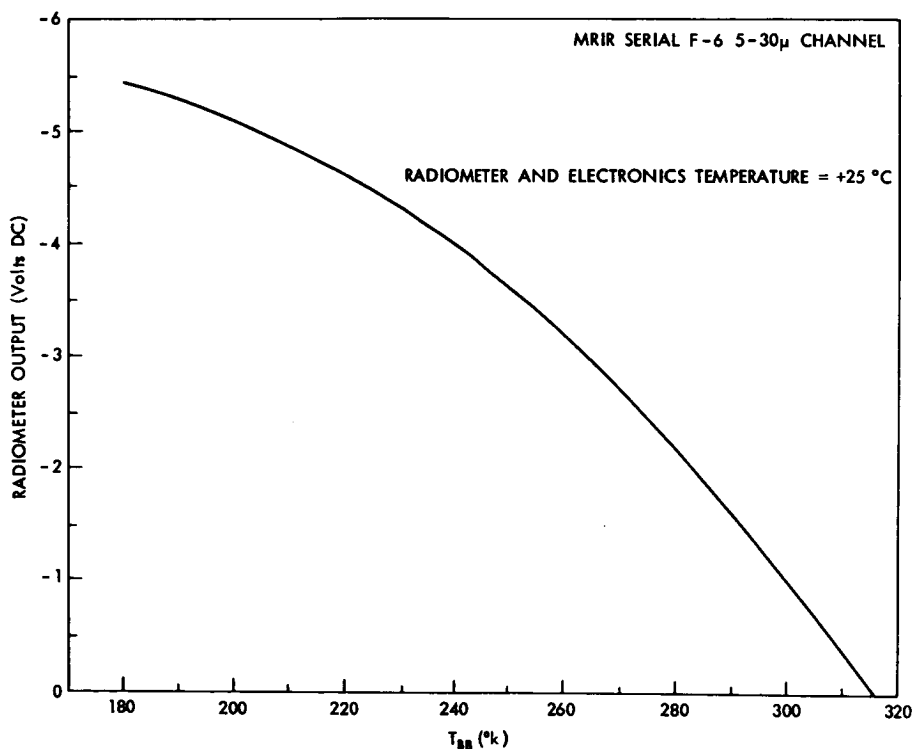


Figure 4-15—Typical Calibration Curve (IR Channels)

The short wave channel is calibrated by means of a diffuse target whose absolute calibration was determined by comparison with a standard of spectral radiance furnished by the National Bureau of Standards. The calibration of the diffuse target was carried out at a number of color temperatures and given in terms of spectral radiance,  $N_\lambda$  vs. input voltage to the target lamp. By varying the input voltage, a calibration curve of radiometer output voltage (0 to -6.4 v) vs.  $N_\lambda$  is generated with the aid of Equation (1). A typical calibration curve for this channel is given in Figure 4-16. In order to calculate the reflectance of

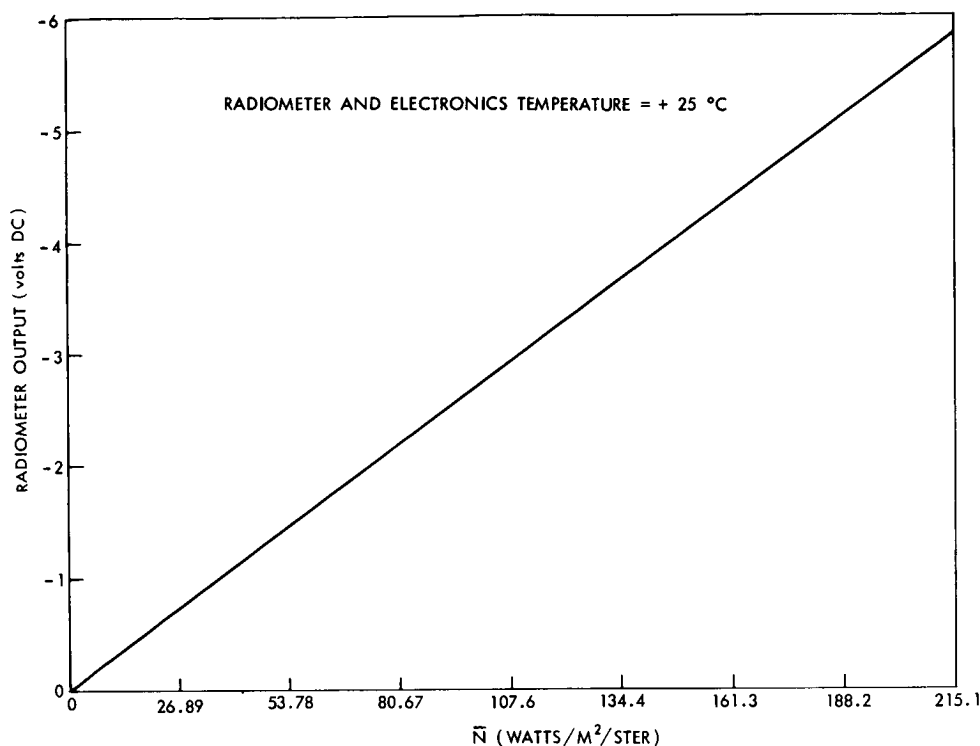


Figure 4-16—Typical Calibration Curve (0.2-4.0 Micron Channel)

incident solar radiation of a spot on earth viewed by the radiometer, one must know the effective solar constant  $\bar{H}^*$ , i.e., the integral over all wavelengths of the solar spectral irradiance at the top of the atmosphere,  $\bar{H}_\lambda^*$ , multiplied by the effective spectral response of the channel, given by

$$\bar{H}^* = \int_0^\infty H_\lambda^* \phi_\lambda d\lambda \quad (2)$$

where

$$\int_0^\infty H_\lambda^* d\lambda = 2.0 \text{ g-cal cm}^{-2} \text{ min}^{-1} = 1395 \text{ watts meter}^{-2} \quad (3)$$

A calculation of  $\bar{H}^*$  was made using the solar spectral irradiance data given in "The Handbook of Geophysics" (Reference 37), and the effective spectral response curve given in Figure 4-13, resulting in the value

$$\bar{H}^* = 844.8 \text{ watts meter}^{-2} \quad (4)$$

The effective average radiant reflectance in the direction of the satellite,  $\bar{r}$ , of a surface filling the field of view of the radiometer and illuminated by unattenuated solar radiation can be defined by

$$\bar{r} = \frac{\pi \bar{N}}{\bar{H}^* \cos \zeta^*} \quad (5)$$

where  $\zeta^*$  is the solar zenith angle.

Calibration of the instrument was performed in vacuum at radiometer temperatures of 0°C, 10°C, 25°C, 40°C and 50°C. Two sets of calibration data were obtained at these temperatures, one with the radiometer and its electronics module at the same temperature; the second set of data was obtained with the electronic module temperature held constant at 25°C and the radiometer cycled through the same range. The second calibration is to allow for interpolation should the radiometer and its electronics module operate at different temperatures on the spacecraft. The values obtained from these calibrations are tabulated in Tables 4-1 and 4-2. These tables refer to radiometer serial number F-6 which is installed on Nimbus II.

The points tabulated in Tables 4-1 and 4-2 are actual measured values. There is some scatter due to experimental error, therefore some smoothing of the data is desirable. For example, utilizing the  $\bar{N}$  vs.  $T_{BB}$  curves (Figures 4-7 through 4-8), a linear least squares fit of the points may be readily obtained and then converted to Voltage vs.  $T_{BB}$  curves if desired.

Throughout the integration of the experiment into the spacecraft many checks of calibration were performed. During this time no significant change from the initial calibration was detected.

During flight the calibration of the instrument can be checked by two measurements in each channel.

In the infrared channels these points occur when the scanner is "looking" into cold space and when it is "looking" at the radiometer housing. Two house-keeping telemetry points monitor the housing temperatures and these may be compared to the radiation temperature as indicated by the radiometer output during that portion of the scan. The expected response to deep space is known (see 0°K points in Tables 4-1 and 4-2), so the two measurements should be sufficient to reconstruct the calibration curve if any instrumental degradation should occur in the space environment.

TABLE 4-1  
CALIBRATION DATA FOR MRIR S/N F-6 RADIOMETER CHOPPER  
AND ELECTRONICS AT INDICATED TEMPERATURE

CHANNEL		6.4-6.9 MICRONS					10-11 MICRONS					14-16 MICRONS					5-30 MICRONS					0.2-4 MICRONS					N FOR SOLAR CHANNEL 0
		OUTPUT SIGNAL (VOLTS DC)					OUTPUT SIGNAL (VOLTS DC)					OUTPUT SIGNAL (VOLTS DC)					OUTPUT SIGNAL (VOLTS DC)					OUTPUT SIGNAL (VOLTS DC)					
		0	10	25	40	50	0	10	25	40	50	0	10	25	40	50	0	10	25	40	50	0	10	25	40	50	
RAD CHOPPER AND ELECT	TEMP. (°C) → TARGET TEMP. (°K) ↓	0	-4.65	-4.75	-4.80	-4.65	-5.15	-5.60	-5.70	-5.85	-5.80	-6.00	-5.95	-6.00	-5.70	-5.20	-4.50	-5.80	-5.80	-5.90	-5.90	-6.10	0	0	0	0	0
	180	-4.60	-4.70	-4.75	-4.60	-5.05	-5.35	-5.45	-5.55	-5.50	-5.70	-4.95	-5.00	-4.70	-4.25	-3.65	-5.30	-5.30	-5.40	-5.40	-5.60	-0.65	-0.65	-0.70	-0.70	-0.70	
	190	-4.50	-4.60	-4.70	-4.50	-5.00	-5.25	-5.35	-5.50	-5.40	-5.50	-4.60	-4.70	-4.45	-4.00	-3.40	-5.20	-5.20	-5.25	-5.25	-5.45	-1.35	-1.35	-1.40	-1.40	-1.45	
	200	-4.35	-4.50	-4.55	-4.45	-4.80	-5.20	-5.25	-5.35	-5.30	-5.30	-4.30	-4.30	-4.10	-3.60	-3.10	-5.00	-5.00	-5.10	-5.10	-5.20	-2.00	-2.00	-2.15	-2.10	-2.15	
	210	-4.20	-4.30	-4.40	-4.25	-4.60	-5.00	-5.05	-5.20	-5.15	-5.20	-3.85	-3.90	-3.70	-3.22	-2.75	-4.80	-4.80	-4.90	-4.90	-5.00	-2.65	-2.65	-2.90	-2.85	-2.90	
	220	-4.00	-4.00	-4.10	-4.00	-4.25	-4.80	-4.85	-5.00	-5.05	-5.00	-3.45	-3.45	-3.20	-2.80	-2.40	-4.60	-4.60	-4.60	-4.65	-4.70	-3.30	-3.30	-3.65	-3.60	-3.60	
	230	-3.55	-3.55	-3.65	-3.60	-3.65	-4.60	-4.65	-4.70	-4.70	-4.70	-2.80	-2.80	-2.95	-2.70	-2.30	-1.90	-4.30	-4.30	-4.30	-4.35	-4.00	-4.00	-4.10	-4.10	-4.35	
	240	-3.05	-3.05	-3.10	-3.00	-3.00	-4.35	-4.35	-4.40	-4.40	-4.40	-2.25	-2.30	-2.10	-1.80	-1.40	-1.40	-4.05	-4.05	-4.00	-4.00	-4.70	-4.70	-4.85	-5.10	-5.10	
	250	-2.25	-2.25	-2.35	-2.20	-2.20	-4.00	-4.00	-4.05	-4.05	-4.05	-1.65	-1.60	-1.40	-1.15	-0.90	-0.90	-3.65	-3.65	-3.60	-3.60	-5.45	-5.45	-5.55	-5.85	-5.85	
	260	-1.40	-1.40	-1.35	-1.20	-1.20	-3.70	-3.70	-3.65	-3.65	-3.65	-0.90	-0.90	-0.75	-0.50	-0.25	-3.30	-3.30	-3.25	-3.20	-3.20						
	270	-0.10	-0.10	-0.10	-0.00	-0.10	-3.20	-3.20	-3.20	-3.20	-3.15	-0.15	-0.15	-0.00	-0.20	-	-2.85	-2.80	-2.75	-2.75	-2.75						
	280	-	-	-	-	-	-2.75	-2.75	-2.65	-2.65	-2.65	-	-	-	-	-	-3.25	-2.33	-2.25	-2.25	-2.25						
290	-	-	-	-	-	-2.20	-2.20	-2.10	-2.05	-2.05	-	-	-	-	-	-1.85	-1.80	-1.65	-1.65	-1.65							
300	-	-	-	-	-	-1.65	-1.60	-1.50	-1.40	-1.50	-	-	-	-	-	-1.30	-1.20	-1.05	-1.05	-1.15							
310	-	-	-	-	-	-1.00	-0.90	-0.75	-0.75	-0.75	-	-	-	-	-	-0.65	-0.50	-0.35	-0.35	-0.45							
320	-	-	-	-	-	-0.25	-0.20	-0.00	-0.00	-0.00	-	-	-	-	-	-0.35	-0.20	-0.00	-0.00	-0.10							

TABLE 4-2

CHANNEL RADIOMETER CHOPPER → TEMP (°C)	6.4-6.9 MICRONS					10-11 MICRONS					14-16 MICRONS					5-30 MICRONS					0.2-4 MICRONS					N FOR SOLAR CHANNEL	
	OUTPUT SIGNAL (VOLTS DC)					OUTPUT SIGNAL (VOLTS DC)					OUTPUT SIGNAL (VOLTS DC)					OUTPUT SIGNAL (VOLTS DC)					OUTPUT SIGNAL (VOLTS DC)						
	0	10	25	40	50	0	10	25	40	50	0	10	25	40	50	0	10	25	40	50	0	10	25	40	50		
TARGET TEMP (%) ↓	0	-4.80	-4.80	-4.80	-4.70	-4.85	-5.70	-5.80	-5.70	-5.70	-5.85	-6.25	-6.10	-5.65	-5.10	-4.20	-5.90	-5.95	-5.85	-5.85	-5.95	0	0	0	0	0	0
180	-4.75	-4.75	-4.70	-4.65	-4.80	-5.45	-5.50	-5.45	-5.45	-5.55	-5.20	-5.07	-4.70	-4.10	-3.45	-5.45	-5.45	-5.35	-5.35	-5.45	-0.65	-0.70	-0.65	-0.65	-0.65	26.89	
190	-4.65	-4.70	-4.65	-4.55	-4.75	-5.40	-5.45	-5.35	-5.35	-5.50	-4.90	-4.80	-4.40	-3.85	-3.20	-5.30	-5.30	-5.20	-5.20	-5.35	-1.40	-1.35	-1.40	-1.35	-1.40	53.78	
200	-4.55	-4.60	-4.55	-4.45	-4.65	-5.25	-5.30	-5.25	-5.25	-5.35	-4.50	-4.45	-4.10	-3.55	-2.90	-5.10	-5.10	-5.05	-5.00	-5.15	-2.05	-2.00	-2.15	-2.05	-2.05	80.67	
210	-4.40	-4.40	-4.35	-4.25	-4.45	-5.10	-5.10	-5.10	-5.05	-5.15	-4.10	-4.00	-3.65	-3.15	-2.65	-4.90	-4.90	-4.85	-4.80	-4.95	-2.75	-2.70	-2.85	-2.75	-2.75	107.60	
220	-4.10	-4.15	-4.10	-4.00	-4.10	-4.95	-4.95	-4.90	-4.85	-4.95	-3.60	-3.55	-3.20	-2.70	-2.25	-4.65	-4.65	-4.55	-4.50	-4.70	-3.45	-3.35	-3.55	-3.45	-3.45	134.40	
230	-3.75	-3.70	-3.65	-3.55	-3.70	-4.65	-4.70	-4.65	-4.60	-4.65	-3.05	-3.00	-2.70	-2.25	-1.80	-4.40	-4.40	-4.35	-4.30	-4.25	-4.20	-4.10	-4.30	-4.15	-4.15	161.30	
240	-3.10	-3.15	-3.10	-2.90	-3.10	-4.40	-4.45	-4.40	-4.35	-4.40	-2.40	-2.35	-2.10	-1.65	-1.35	-4.10	-4.10	-4.05	-3.95	-3.90	-4.05	-4.90	-4.80	-5.00	-4.85	188.20	
250	-2.35	-2.40	-2.35	-2.15	-2.35	-4.05	-4.10	-4.00	-4.00	-4.05	-1.65	-1.70	-1.45	-1.10	-0.80	-3.75	-3.75	-3.70	-3.65	-3.55	-3.65	-5.65	-5.50	-5.80	-5.60	215.10	
260	-1.40	-1.40	-1.40	-1.15	-1.40	-3.70	-3.70	-3.65	-3.55	-3.65	-0.95	-0.95	-0.75	-0.45	-0.25	-3.35	-3.30	-3.20	-3.10	-3.25							
270	-0.10	-0.15	-0.10	-0.00	-0.10	-3.30	-3.25	-3.20	-3.10	-3.20	-0.15	-0.20	-0.00	-	-	-2.90	-2.85	-2.75	-2.65	-2.80							
280	-	-	-	-	-	-2.80	-2.80	-2.70	-2.55	-2.65	-	-	-	-	-	-2.45	-2.35	-2.25	-2.10	-2.25							
290	-	-	-	-	-	-2.25	-2.25	-2.15	-2.00	-2.10	-	-	-	-	-	-1.85	-1.80	-1.70	-1.60	-1.65							
300	-	-	-	-	-	-1.65	-1.65	-1.55	-1.40	-1.45	-	-	-	-	-	-1.35	-1.20	-1.05	-1.00	-1.05							
310	-	-	-	-	-	-1.00	-0.95	-0.85	-0.70	-0.70	-	-	-	-	-	-0.65	-0.55	-0.40	-0.30	-0.40							
320	-	-	-	-	-	-0.25	-0.20	-0.05	-0.00	-0.00	-	-	-	-	-	-0.30	-0.20	-0.05	-0.00	-0.05							

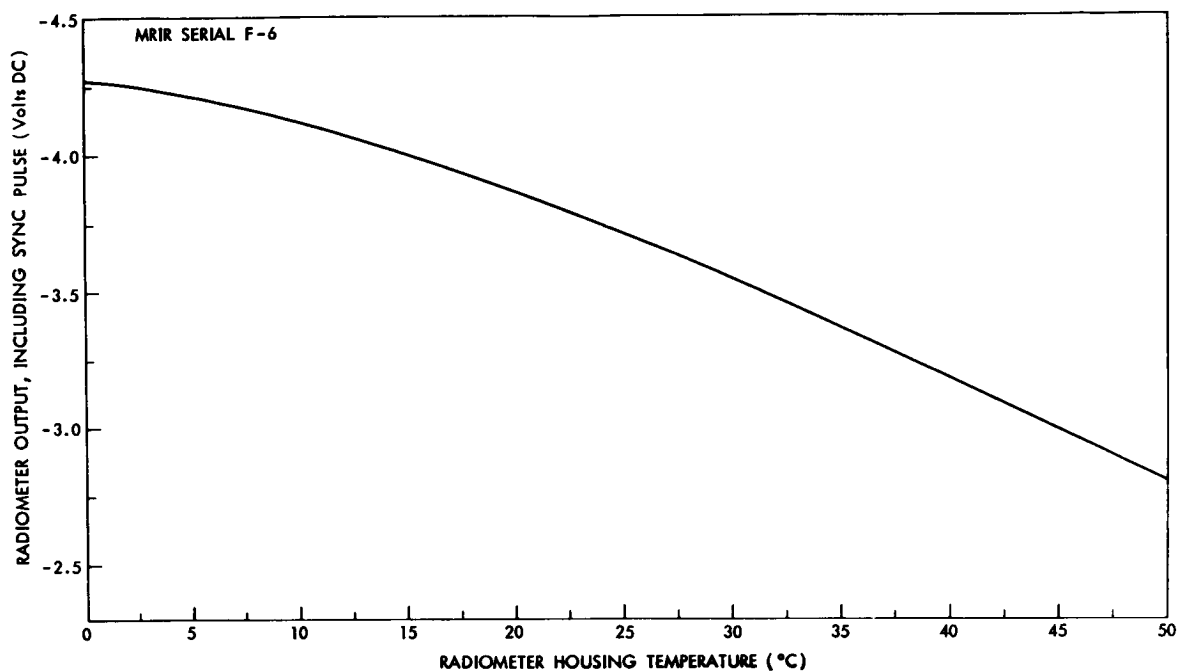


Figure 4-17-Output Voltage of 6.4-6.9 Micron Channel When Field of View is Filled by Scan Housing and Sync Pulse is Applied

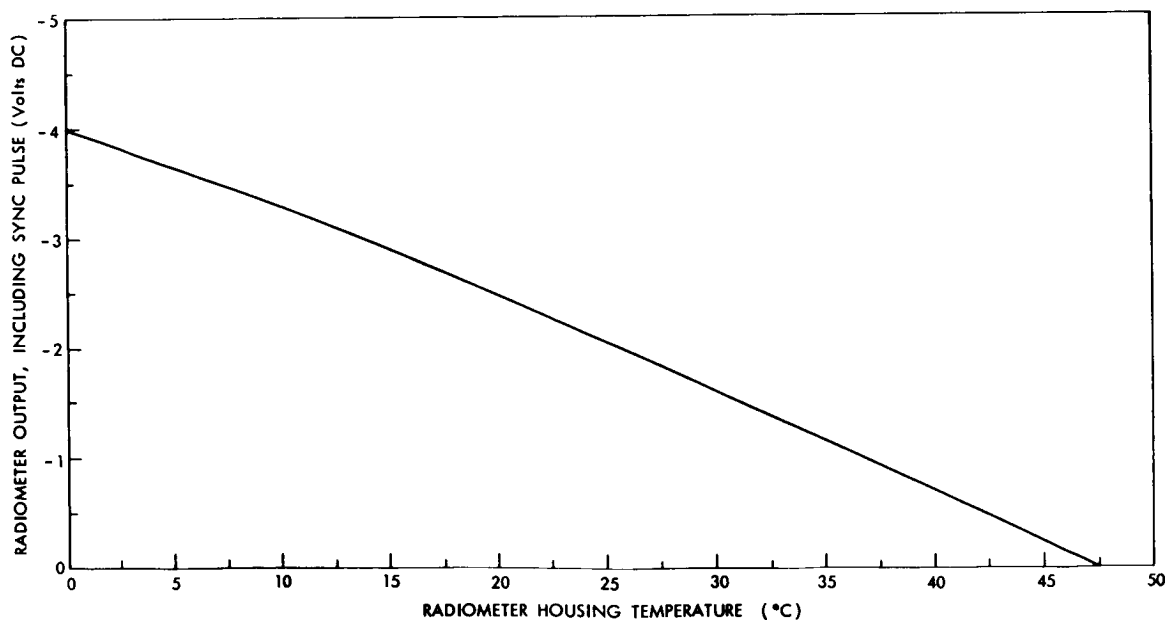


Figure 4-18-Output Voltage of 14-16 Micron Channel When Field of View is Filled by Scan Housing and Sync Pulse is Applied



Two of the infrared channels (those centered at 6.6 and at 15 microns) are not expected to record target temperatures above 270°K. Signals that otherwise would be positive voltages from these two channels while viewing the relatively warm housing are electronically clamped at 0 volts (cf. Figure 4-2) and, hence, can not be used for calibration purposes. To obtain a check of calibration in these two channels an electronic input ("sync" pulse) which is present in all of the thermal channels is utilized. This voltage consists of a pulse added to the signal and to the offset voltage once per scan just as the scan mirror enters the housing (cf. Figure 4-2). This pulse is a precise voltage primarily designed to calibrate the electronic gain of the system, but since it is added to the signal its height above the zero volt level will be proportional to the housing temperature. Figures 4-17 and 4-18 are curves of the "sync" pulse amplitude vs. housing temperature for these two channels. Also, these values are listed in Table 4-3.

Table 4-3  
"SYNC" Pulse Levels for 6.4-6.9 and  
14-16 Micron Channels Versus Radiometer Temp.

CHANNEL  RADIOMETER TEMP. (°C)	SYNC PULSE LEVEL (VOLTS DC)	
	6.4-6.9 MICRONS	14-16 MICRONS
0	-4.30	-4.00
5	-4.25	-3.70
10	-4.10	-3.30
15	-4.00	-2.90
20	-3.85	-2.45
25	-3.70	-2.00
30	-3.55	-1.60
35	-3.35	-1.15
40	-3.20	-0.75
45	-3.00	-0.20
50	-2.80	0.00

In addition to the housing temperature monitors, the temperature of two locations in the chopper housing and one in the electronics module are monitored. The housekeeping telemetry values are tabulated in Table 4-4.

Table 4-4  
Temperature Telemetry Values for MRIR Radiometer

TEMP. °C	TELEMETRY VALUES (VOLTS DC)				
	CHOPPER 1	CHOPPER 2	HOUSING 1	HOUSING 2	ELECTRONICS MODULE
0	-4.55	-4.55	-4.55	-4.55	-4.55
5	-3.80	-3.85	-3.85	-3.80	-3.80
10	-3.20	-3.15	-3.20	-3.20	-3.25
15	-2.65	-2.65	-2.65	-2.65	-2.70
20	-2.20	-2.20	-2.25	-2.25	-2.30
25	-1.85	-1.85	-1.90	-1.85	-1.90
30	-1.55	-1.55	-1.55	-1.55	-1.60
35	-1.30	-1.30	-1.30	-1.35	-1.35
40	-1.10	-1.15	-1.10	-1.10	-1.10
45	-0.95	-0.95	-0.95	-0.95	-0.95
50	-0.80	-0.80	-0.80	-0.80	-0.80

### 4.3 Data Processing

#### 4.3.1 General

The spacecraft tape recorder for MRIR uses a continuous-loop tape with a capacity for approximately one complete orbit's worth of data. When data is recorded continuously for more than one orbit, old data is therefore progressively erased from the tape, so that at any given instant the tape contains data for only the immediately preceding orbital period. Upon the command to playback, the tape is speeded up 26 times and its contents are transmitted in approximately

4 minutes. Thus the earth coverage of the data received at NDHS will depend on the location, relative to the orbit, of the DAF station.

After the data from the spacecraft are transmitted to GSFC, they are processed by a Telemetry 670 computer. The Telemetry 670 has three distinct outputs for data analysis which will be discussed in the following sections: (1) a strip chart recording of analog output as a function of time for detailed study of specific phenomena; (2) a digital tape compatible with the IBM 7094 for automatic mapping and analysis; and (3) a photo display of each channel for each orbit.

#### 4.3.2 Analog Outputs

These will be in the form of strip charts from an eight-channel Brush Mark 200 recorder. Each chart will contain an entire orbit of data from each channel with timing information recorded on the sixth channel. The data will be recorded as voltage from 0 to -6.35 volts d.c. and the calibration data shown in Tables 4-1 and 4-2 will apply.

It should be pointed out that all values have been rounded to the nearest 0.05 volts since this is the smallest increment which can be processed by the MRIR digital telemetry. A sample of the time information placed on the analog record is shown in Figure 4-19. The time code consists of a sequence start pulse which is full amplitude (-6.40 volts). Following this is a series of pulses whose amplitudes represent units of time. Each pulse is quantized to one of ten discrete levels. The digital magnitude is equal to twice the voltage amplitude of the pulse (i.e., 3 volts corresponds to 6 time units). Following the sequence start pulse three consecutive pulses (0 is included), represent the day. The next two pulses represent hours and the last two show minutes. The days, hours, and minutes codes are separated by two small pulses of voltage amplitude less than 0.5 volts. The leading edge of the sequence start pulse represents the time mark that is given by the code which follows it and the sequence start pulses repeat once per minute. In addition, one-second marker pulses are displayed on another channel of the strip chart recorder for time interpolation if desirable. For convenience these are shown in Figure 4-19 for only ten second intervals, however, they will be every second on the actual recording.

#### 4.3.3 Digital MRIR Data Processing

The digital magnetic tape output of the Telemetry 670 computer represents a primary source of raw experimental data from the MRIR radiometer, and is one of the principal inputs to future data reduction processes. The format of this tape is described in Appendix B.

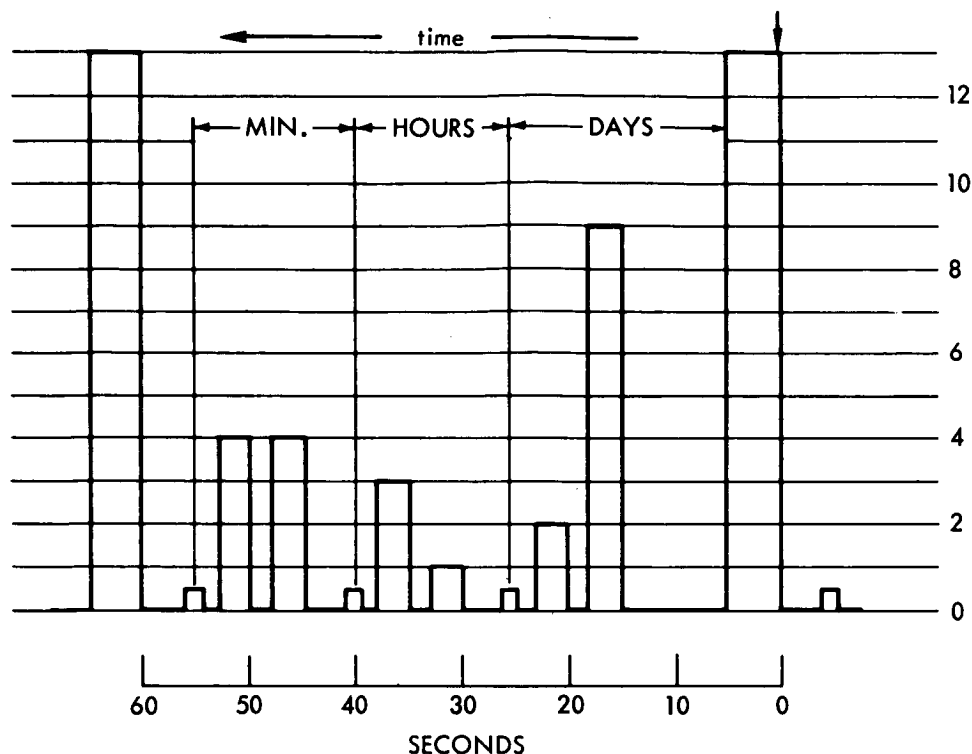


Figure 4-19—Analog record time display. The point in time, "092<sup>d</sup> 13<sup>h</sup> 44<sup>m</sup>," occurs at the vertical arrow.

#### 4.3.4 Photo Display

As part of the "on-line" processing, the digital output of each channel will be transmitted to a cathode ray tube photo display which will index each data word as to its X-Y coordinates by synchronizing with spacecraft time and the radiometer "sync" pulse described in section 4.2. The "Z" axis modulation is determined by the amplitude of the radiometer output. The format of this photo display is shown in Figure 4-20. The annotation, time bench marks, and gridding are produced prior to interrogation by a CDC 924 computer, punched on paper tape, and fed to the Telemetry 670. The calibration gray scale is generated within the Telemetry computer and displayed on the CRT coincidentally with the data. Because the same shades of gray represent different target temperatures (or effective radiance for the 0.2-4 $\mu$  channel) for different channels, they are labeled only by arbitrary intensity levels. Table 4-5 gives the correlation between these levels and  $T_{BB}$  (or  $\bar{N}$ ) for each channel.

The CRT display itself is rigidly controlled electronically by monitoring the phosphor intensity of each spot as the picture is generated on the screen. Because of this the main errors to be expected in an attempt to analyze the photo



Table 4-5  
Grey Level Values for Pictorial Display

GREY LEVEL	CHANNEL TARGET VALUES				
	6.7 $\mu$	10-11 $\mu$	14-16 $\mu$	5-30 $\mu$	0.2-4.0 $\mu$
	$^{\circ}\text{K}$	$^{\circ}\text{K}$	$^{\circ}\text{K}$	$^{\circ}\text{K}$	$\bar{N}(\text{WM}^{-2} \text{ STER}^{-1})$
1	270	310	245	305	0
2	263	300	241	294	21.27
3	256	288	237	283	42.81
4	249	277	233	272	57.17
5	242	266	229	261	85.89
6	235	255	225	254	107.4
7	228	244	221	239	129.0
8	221	233	217	228	150.5
9	214	222	213	217	172.0
10	207	211	209	206	193.6
11	200	200	205	195	215.1

display quantitatively will occur in the picture development itself. The picture will be made by photographing the CRT face with a Polaroid camera using 4"  $\times$  5" film pack which provides both a positive print and negative transparency. The 4"  $\times$  5" negative will be archived for future reproduction.

It has been found that during an orbit some fluctuation of the instrument calibration occurs. This is usually small with the exception of the region near and over the South Pole. Here as the spacecraft enters satellite day, sunlight is shining into the radiometer scanner housing causing areas within the field of view to be warmed. This creates a spurious signal making the Polar region appear warmer than it should. This can be compensated for by correlation with in flight calibration in the computer processed data and in studying the analog records. The photographic data, however, are not corrected for this anomaly hence an apparent warm band appears over the South Pole in the 14-16 micron channel and to a lesser extent in the 10-11 micron channel in all of the pictures.

For this reason and because of the above mentioned smaller fluctuations, quantitative data cannot be obtained from the pictures with any degree of accuracy. Errors as large as 25°C in the 14-16 band and up to 10°-12°C in the 10-11 micron channel are possible in the Polar region. Elsewhere the errors encountered can be as great as 5-8°C in all of the infrared channels.

## SECTION 5

### AUTOMATIC DATA TRANSMISSION SYSTEMS: AUTOMATIC PICTURE TRANSMISSION (APT) AND DIRECT READOUT INFRARED RADIOMETER (DRIR)

#### 5.1 Automatic Picture Transmission (APT)

The Nimbus II APT camera consists of a wide angle lens (6.0 mm focal length) with an 85° side to side field of view, and a special 800-line storage vidicon. The camera is oriented along the downward yaw axis. Picture scanning rate is four lines per second. 200 seconds are thus required to complete one picture scanning sequence. An additional eight seconds are required for phasing, start tones, and peripheral electronic chores so that the APT picture-taking interval is 208 seconds. The camera is located on the bottom of the H-frame inside the sensory ring; the transmitter (136 mc, 5 watts) is in the sensory ring. The camera photographs an area 1200 by 1200 nautical miles (side to side) from the 600-nm nominal altitude. (Note Figure 5-1).

A continuous broadcast of scanned pictorial information is transmitted from the satellite. This broadcast is available to anyone within satellite acquisition range who has the appropriate receiving and recording equipment.

Standard ground terminal equipment includes a facsimile recorder modified for continuous-tone reproduction. Ten levels of gray can be resolved in the pictures.

A more complete discussion of the APT system may be found in Reference 38. Data handling and geographic referencing techniques may be found in the APT USERS' GUIDE (Reference 39 and 40).

APT systems have already been flown experimentally on two satellites: TIROS VIII and Nimbus I. The TIROS VIII APT camera operated from 21 December 1963 until May 1964; the Nimbus I, from 28 August to 21 September 1964. Both flights demonstrated both the technical feasibility of the APT system and the great value of APT data to local meteorological stations. These facts are being further demonstrated by the operational APT systems of ESSA-2 and Nimbus II.



DATA ACQUISITION  
 RANGE OF A SINGLE  
 APT GROUND STATION  
 SHOWING PICTURE  
 COVERAGE FROM THREE  
 TYPICAL 500 N.M. ORBITS

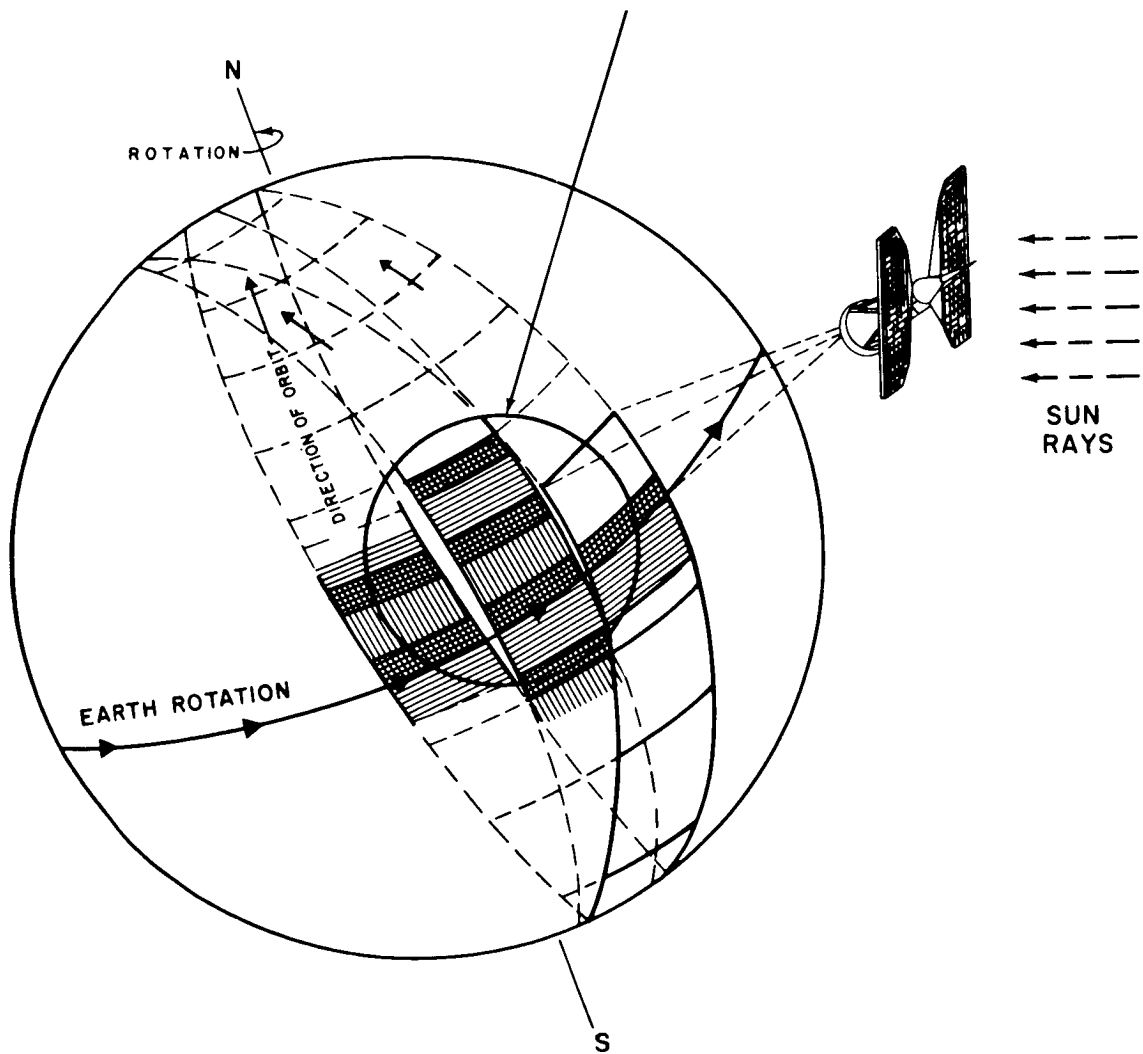


Figure 5-1-APT Coverage Schematic

### 5.1.1 Data Code Experiment

To reduce the amount of orbital data to be transmitted via teletype from central data processing facilities at GSFC or NESC to all APT stations, a Data Code Experiment has been devised to transmit a considerable portion of this data directly from the spacecraft.

The Nimbus II Data Code is an experimental communications subsystem developed to provide users of Automatic Picture Transmission (APT) and Direct Readout Infrared Radiometer (DRIR) data with updated ephemeris information required for the acquisition and geographical location of the APT and/or DRIR data. The Data Code information is provided as an integral part of the APT signal and so is automatically received while acquiring the APT picture.

The primary purposes of the Data Code experiment are to:

1. Automatically provide the times at which APT pictures are taken, thus eliminating the effort and inaccuracies inherent when each picture time must be manually determined at each ground station.
2. Provide, when combined with an initial or infrequently updated ephemeris message received through the mails or normal communications channels, sufficient current orbital information to APT ground stations to permit acquisition and geographical location of APT and/or DRIR data.
3. Eliminate the need for transmission of lengthy, daily ephemeris messages which overload already crowded conventional communications channels, and require APT stations to monitor such communications to insure receipt of the necessary orbital data. With the use of Data Code, all necessary updating information is provided automatically when an APT picture is received.
4. Provide local APT stations with an adequate basis for data acquisition and location, even if conventional communications are inadequate. Once having received an accurate ephemeris message for any satellite, the Data Code information permits updating of the required information for relatively extended periods of time.

The details of the foregoing procedures are contained in Reference 41, copies of which have been distributed to all presently known APT stations, and thus will not be described here.

## 5.2 Direct Readout Infrared (DRIR)

The striking success of the Nimbus I High Resolution Infrared Radiometer (HRIR) in depicting nighttime cloud cover and temperature distribution (See Section 3) has led to the development of a Direct Readout Infrared Radiometer (DRIR) system for Nimbus II. This system transmits HRIR sensor output through the APT transmitter, so that properly equipped ground stations, when within line of sight of the satellite, will be able to receive the HRIR data in the DRIR mode at the same time that the data is being fed in parallel to the HRIR recorder aboard the spacecraft. Ground station requirements to receive DRIR data can be met by most standard APT stations with suitable modifications, including a change in the rate of the facsimile recorder. Details as to the modifications are published in other NASA-sponsored documents.

The DRIR data will be presented as gray scales from white through gray to black (corresponding to cold, cool and warm radiating surfaces, respectively) on the facsimile paper. For the Fairchild facsimile recorder, the total width of the data is 21.5 cm (8.45 inches). Within this width, the data from earth and atmosphere (from horizon to horizon) will occupy approximately seven cm (2.75 inches), the remainder representing space and the interior of the radiometer housing. The APT facsimile scan rate is modified to synchronize with the scan rate of the HRIR, approximately 44.7 RPM. The facsimile stylus moves across the paper at a constant rate, so distance across the paper is directly proportional to angular rotation of the HRIR scanning mirror. Since the line width (in the direction of paper feed) of the facsimile scan is nominally 0.0254 cm (0.01 inch), the rate of data (paper) advance is  $1.14 \text{ cm min}^{-1}$  ( $0.447 \text{ inch min}^{-1}$ ).

The DRIR data are of slight value until they are geographically referenced. While this might be done by reference to coastline or other identifiable geographical features, or crudely by reference to cloud features which can be associated with those on a recent weather map, these are special cases and are usually of marginal utility. For example, they are seldom if ever applicable over oceans.

Reference 42, Manual Gridding of DRIR Facsimile Pictures, delineates the procedures for gridding. Section 3 of this document describes the HRIR sensory system.

## SECTION 6

### DATA PROCESSING, ARCHIVING, AND ACCESS

#### 6.1 AVCS Data Processing

The photographic processing of the AVCS kinescope pictures is accomplished by a rapid BIMAT system in the NDHS which includes a develop, fix, wash, and dry cycle. This system produces a negative and positive transparency simultaneously, the negative being of archival quality. The 70-mm archival negative, after being arranged in data orbit or swath format, i.e., sequential triplets in a swath from pole to pole, is forwarded to the NESC. At the NESC, the 70-mm negative will be reproduced as 35-mm positive and negative transparencies for archiving.

#### 6.2 AVCS Data Archiving and Access

The 35-mm film data produced by the NESC will be forwarded to the National Weather Records Center (NWRC) in Asheville, North Carolina, for archiving.

Nimbus II pictures will be stored at the Records Center in 100-foot reels. On the film rolls, the picture sequences in chronological order will be grouped together by swath number and by camera. That is, within a particular sequence identified by swath number, all of the pictures taken by the left camera (No. 1) will appear in sequence, followed by the pictures of the center camera (No. 2), and finally by those from the right camera (No. 3). A 100-foot reel will contain approximately eight swaths of AVCS pictures.

These film data can be made available in either positive or negative transparency format in increments of 100-foot rolls, as it is not now possible to furnish copies of individual pictures, swaths, enlargements, or other picture formats. The film can be ordered at cost of reproduction.

Reference to the Nimbus II monthly catalog will enable the user to determine his data requirements as to time and geographical location and in turn the particular swaths of data he requires. Orders and inquiries should be addressed to:

National Weather Records Center  
ESSA  
Federal Building  
Asheville, North Carolina 28801

The following information should be included in correspondence or on orders:

1. Date
2. Swath Number
3. Positive or Negative Transparency
4. Dodged or undodged (See Section 6.10).

Should the user desire to retrieve data by meteorological content, geomorphological content, geographical area and/or season (date and time) (as explained in Section 8 of this document), a request should be forwarded to NASA/Goddard Space Flight Center, Nimbus Code 450, Greenbelt, Maryland 20771. Here, a computer retrieval system will provide the designation of the swaths containing the requested data. This information is mailed to the user, who in turn should place his order to NWRC.

For the interim period between launch of Nimbus II and the issuance of the first Nimbus II Monthly Catalog, the GSFC, upon request, can make available Nimbus II AVCS film data in 70-mm copies on a limited and time available basis. As resources permit, limited quantities of data will be furnished to qualified investigators without charge.

Special requests for Nimbus II AVCS data during the interim period should be addressed to:

National Aeronautics & Space Administration  
Goddard Space Flight Center  
Nimbus Code 450  
Greenbelt, Maryland 20771

It is sufficient to indicate the date and specific geographical area of coverage for these special interim requests. 70-mm film will be made available in the following formats (dodged or undodged) by swath:

Negative Transparencies  
Positive Transparencies  
Positive Contact Prints

### 6.3 HRIR Photographic Data Processing

The NDHS simultaneously produces a work positive and archival negative. The undeveloped archival negative is processed by the NDUC photographic laboratory and will be used to reproduce positive transparencies which in turn can be used to produce negative transparencies.

#### 6.4 HRIR Photographic Data Archiving and Access

User requests for HRIR data will be fulfilled by making reproduction from transparencies which will be stored at the National Space Science Data Center (SSDC), GSFC, Greenbelt, Maryland. Reproductions of the 70-mm film can be made as positive or negative transparencies or as positive paper prints, including enlargements. Single data orbit swaths may be ordered. Most of these data will be of nighttime swaths; however, a considerable number of swaths will be of daytime HRIR. Digital magnetic tapes and analog strip chart records may also be requested.

The HRIR data may be obtained by writing to:

National Space Science Data Center  
Goddard Space Flight Center  
Code 601  
Greenbelt, Maryland 20771

Limited quantities of data will be furnished to qualified investigators without charge. Otherwise, data will be furnished for production and dissemination costs. Whenever it is determined that a charge is required, a cost estimate will be provided to the user prior to filling the data request. The basic unit of data will be the Data Swath. Calibration gray scale wedges will normally be included on both transparencies and prints. When requesting data, the following information should be given:

1. Date
2. Swath Number
3. Data Format, i.e. positive, negative transparencies or positive print.
4. Dodged or undodged (See Section 6.10).

Should the user desire to retrieve HRIR data by meteorological content, geomorphological content, geographical area and/or season (as explained in Section 8 of this document), a request should be forwarded to the Goddard Space Flight Center, Nimbus Code 450, Greenbelt, Maryland 20771. Here, a computer retrieval system will provide information as to the swaths containing the requested data. This information will be relayed to the GSFC Space Science Data Center who in turn will provide the requested data to the user. The user request should include the data format required.

#### 6.5 MRIR Photographic Data Processing

The NDHS processes a 4" x 5" negative which is used by the NDUC photographic laboratory to produce positive and negative transparencies. The data will not be rearranged in swath format.

## 6.6 MRIR Photographic Data Archiving and Access

Positive and negative transparencies will be stored at the National Space Science Data Center, GSFC, Greenbelt, Maryland to fulfill users requests. Reproductions of these data can be made as positive and negative transparencies and enlarged prints and requests should be forwarded to the address given in Section 6.4 above. Digital magnetic tapes and analog strip chart records may also be requested. Limited quantities of data will be furnished to qualified investigators without charge. Otherwise, data will be furnished for production and dissemination costs. Whenever it is determined that a charge is required, a cost estimate will be provided to the user prior to filling the data request. The basic unit for furnishing data will be the Interrogation Orbit Record, which normally contains data recorded in the spacecraft during the orbital period immediately prior to the interrogation. (See Section 4.3.1).

Section II and V of the Nimbus II Monthly Catalogs will indicate the coverage of archived MRIR data, which will enable the user to determine his specific data requirements. Initially, the MRIR data content will not be extracted in the same manner as HRIR and AVCS data and thus the retrieval system outlined in Section 8 and 9 will not be available. It is possible that, at a later date, classification and retrieval of MRIR data will be performed. In any event, the classification given concurrent AVCS and HRIR data can be used as a guide.

## 6.7 HRIR and MRIR Computer-Produced Standard Format Data Archiving and Access

The Nimbus radiation data are available in various "hard copy" formats suitable for presenting limited portions of the data, in addition to the Nimbus Meteorological Radiation Tape (NMRT) containing the originally reduced data in their entirety and suitable for processing by digital computers.

Copies of the data in the various standard formats listed below may be obtained by writing to the following address:

National Space Science Data Center  
Goddard Space Flight Center  
Code 601  
Greenbelt, Maryland 20771

As resources permit, limited quantities of data will be furnished to investigators without charge. Otherwise, data will be furnished for production costs or less. Whenever it is determined that a charge is required, a cost estimate will be provided to the user prior to filling the data request.

#### A. Copies of Nimbus Meteorological Radiation (NMR) Tapes (binary)

The NMR Tape is the product of a computer program whose input is the spacecraft telemetry and attitude data, orbital data, digitized radiation data, and the Nimbus radiometer calibration package. These tapes are usable only on IBM compatible electronic data processing equipment having a core storage capacity of the equivalent of at least 4096 36-bit words.

#### B. Data Listings

Computer programs are available which will produce a printed list of the calibrated information for a specified time period from all sensors together with appropriate locator information.

#### C. Grid Print Maps

A series of programs produce printed and contoured data referenced to a square mesh grid on polar stereographic or Mercator map bases. Grid print maps may be produced for either a single orbit or a composite of several orbits. The following standard options are available and should be specified when requesting grid print maps:

##### 1. Map and Approximate Scale

a. Polar Stereographic, 1/30 million (approx.)

b. Polar Stereographic, 1/10 million (approx.)

c. Multi-Resolution Mercator

1. 5.0 degrees Long. per mesh interval - 1/40 million (approx.)

2. 2.5 degrees Long. per mesh interval - 1/20 million (approx.)

3. 1.25 degrees Long. per mesh interval - 1/10 million (approx.)

##### 2. Maximum Sensor Nadir Angle

3. Field Values and Contouring (unless otherwise specified, all maps will include field values and contouring except Mercator Maps of scales larger than 1/20 million which will contain no field values or contouring).



A data population map, indicating the number of individual measurements contained in each grid point average, as well as a sample latitude-longitude overlay for geographically locating the data, will ordinarily be provided along with each grid print map.

When ordering "hard copy" data, the following identifying information should be given:

1. Satellite (e.g. Nimbus II)
2. Read-Out Orbit No.
3. Radiometer Experiment (HRIR and/or MRIR) and for MRIR Channel No. (e.g. MRIR Channel 2, 10-11 Microns).
4. Calendar Date of Equator Crossing
5. Beginning and Ending Times of Data in GMT
6. Format Desired

When ordering NMR Tapes, only items 1, 2 and 5 above need be given.

#### 6.8 HRIR and MRIR Non-Standard Format Data Archiving and Access

Some flexibility in the computer programs and other forms of data presentation is possible, and users having requirements which cannot be satisfied by the available standard formats should write to the following address for further information:

National Space Science Data Center  
Goddard Space Flight Center  
Code 601  
Greenbelt, Maryland 20771

One non-standard form of both HRIR and MRIR data is an analog record. For the HRIR experiment, the analog record is produced on light-sensitive photo-recording paper displaying the video data and time code. See Figure 3-4 which can be used for correlation purposes.

For the MRIR experiment, the analog record is produced by an ink-stylus recording oscillograph. For each orbit an analog record will be available. This

will consist of an 8 channel strip chart with voltage displayed as a function of time. The arrangement of information is as follows.

<u>Recorder Channel</u>	<u>Information</u>
1	6.4-6.9 micron data
2	10-11 micron data
3	14-16 micron data
4	5-30 micron data
5	0.2-4.0 micron data
6	1 second time markers
7	Time code display
8	Earth scan boundaries.

Because of temperature fluctuations of the instrument throughout the orbit, data from the infrared channels must be corrected by means of the in-flight calibration points (sec. 4.2). To facilitate the data analysis a copy of the Selected Engineering data tape listing will be furnished with each analog record. This listing includes the two housing thermistor readings, the two chopper thermistor readings and the electronics Module Temperature. The column headings are in terms of a "function number" which are identified as follows:

<u>Telemetry Function</u>	<u>Function Number</u>
Housing Temperature 1	428
Housing Temperature 2	429
Chopper Temperature 1	434
Chopper Temperature 2	435
Electronics Module Temperature	437

It should be noted that the housing surface viewed by the radiometer has consistently remained approximately  $2.5^{\circ} \pm 0.75^{\circ}\text{C}$  colder than the indicated thermistor reading; consequently this must be taken into account in correcting the data. This difference was not unexpected and has remained essentially constant since launch. Hence, there has been no apparent optical or electronic degradation of the instrument as of orbit 500.

## 6.9 APT and DRIR

APT pictures and the experimental DRIR data can be acquired locally by appropriate ground facilities. APT and DRIR data are not intended to be distributed beyond the local acquisition facilities. However, should potential users desire information concerning this data for specific applications, they should contact the agencies supervising the various receiving stations.

Many APT and DRIR participants do not have facilities to adequately reproduce the original data nor is there any requirement to save these data once they have served their purpose. NASA cannot be responsible for the availability or dissemination of APT or DRIR data.

It should be pointed out that the same DRIR data can be obtained from NASA in the more sophisticated and higher quality HRIR format.

## 6.10 Special Instructions to Users of AVCS and HRIR Film Data

- a. If the primary interest of the investigator is land and ocean features rather than in clouds, he should so indicate as a guide in achieving the proper density in the photographic processing.
- b. Unless otherwise specified a uniform exposure will be employed, and a calibration gray scale will be included with HRIR data only, to permit the interpretation of the data in terms of absolute radiation values. However, the detail in a single transparency or print can, depending on the users' ultimate application and/or analysis, be further enhanced photographically by automatically "dodging" or varying the exposure over the various light and dark portions of a given strip of data. Persons who so specify, will be furnished data which include the automatic dodging feature.
- c. To the extent of our resources and capabilities, any other special requirements will be considered.

## SECTION 7

### NIMBUS II CATALOG

#### 7.1 General

The Nimbus II Catalog, to be published in monthly installments, will provide a relatively current source of information required for obtaining Nimbus II data. As much automation as possible is used in its preparation, this being required not only for speedy publication but also for use of the same listings for automated data retrieval. There will be five sections in each Nimbus II Catalog edition.

#### 7.2 Section I – Introductory Remarks

Section I will contain significant highlights of the satellite operation during the month which would be of particular interest to users. For example, unusual or major meteorological events may be noted. Also, performance of the various sensory systems and of the spacecraft will be described, particularly when significant deviations from normal operations have been experienced.

#### 7.3 Section II – Daily Sensor "On" Status Charts

Section IIA shows schematically the locations over which the AVCS, MRIR and HRIR sensors were on. A modified Miller Mercator cylindrical projection is used as the base map. The map extends from 85°S to 85°N latitude and spans 900 degrees of longitude. Ten degree latitude-longitude lines are shown – each third (30 degree) line being accentuated.

Ascending nodes and swath numbers are shown on each map representing daytime data. Descending nodes are substituted on maps which contain nighttime data.

Two consecutive facing pages contain the AVCS, MRIR, and HRIR nighttime data for one day (Universal Time). The left hand (even numbered) page shows AVCS and daytime MRIR coverage. The right hand page shows MRIR nighttime and HRIR nighttime coverage.

Section II B will display daytime HRIR data; each page will contain two days data.

Superposed on the maps are representations of those segments of the subpoint track during which the appropriate sensor was on. Swath numbers are labelled at the ascending or descending nodes. Time of ascending node defines the date of the entire swath.

To assist the user in relating an orbital segment on the map with the correct swath number a complete orbital track overlay is included as Figure 7-1 and also as a transparent overlay insert in this document. Tick marks indicate number of minutes before and after ascending and descending node, so that the approximate time of data coverage can be determined for any location.

Figure 7-2 depicts the coverage obtained from the AVCS and HRIR/MRIR systems at a 600 nautical mile altitude. The coverage swaths are drawn on the same projection as that used to show sensor "On" tracks in Section II of the monthly catalogs. This display is provided to permit the user to estimate the extent of sensor coverage from the subpoint track segments shown in the catalogs.

The user may, if he wishes, trace the swath widths in Figure 7-1 on transparent or translucent paper and overlay this on the subpoint tracks to obtain actual sensor coverage on the earth.

Equations (1) and (2) can be used to calculate sensor coverage if higher accuracies are desired.

For AVCS:

$$\phi = \sin^{-1} \left( \frac{R+h}{R} \sin n \right) - n \quad (1)$$

For HRIR:

The altitude is sufficiently high so that the horizons show in the data and

$$\phi = \cos^{-1} \left( \frac{R}{R+h} \right) \quad (2)$$

Where  $\phi$  = geocentric angle between satellite subpoint and edge of sensor coverage, measured in a plane perpendicular to the orbital plane, in degrees.

R = earth radius in nautical miles

# VALIDITY PERIOD

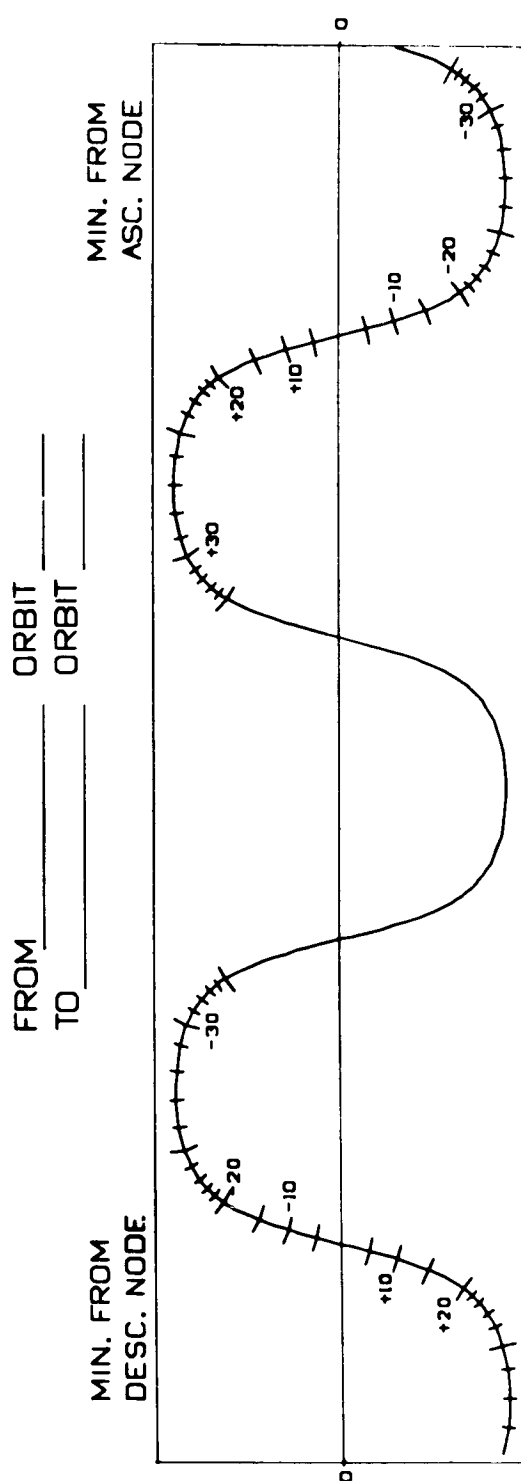
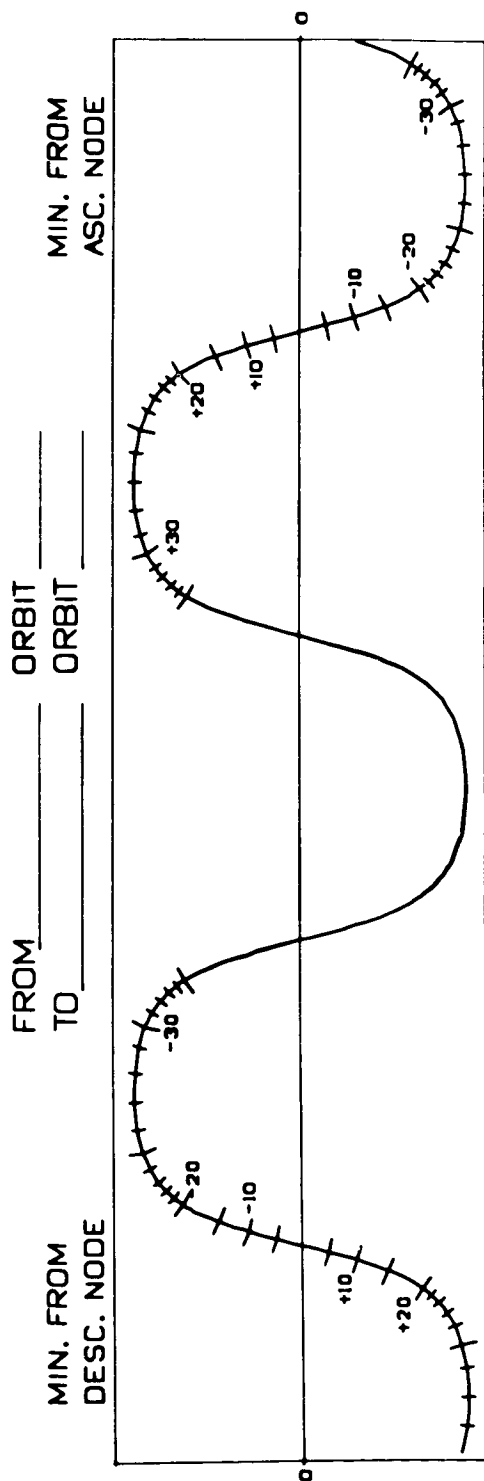


Figure 7-1-Nimbus II Subpoint Track

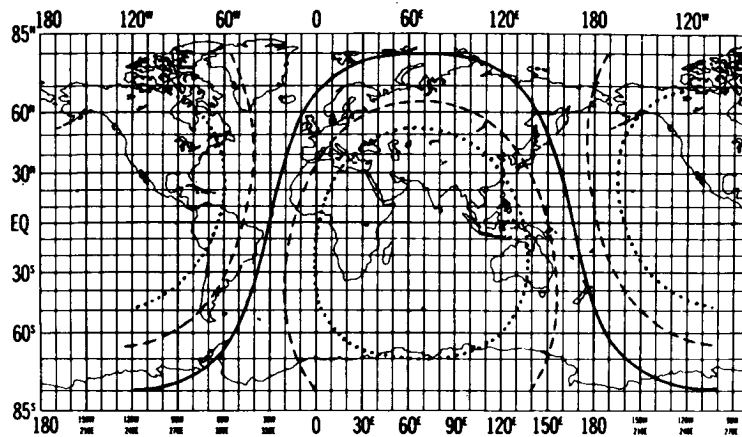


Figure 7-2—Coverage of AVCS (dashed)  
and HRIR (dotted)

$h$  = satellite height in nautical miles

$n$  = angle, measured at the satellite, between local vertical and extreme coverage limit of camera 1 or 3. Equal to 52.5 degrees assuming no attitude error.

#### 7.4 Section III – APT and DRIR

Section III is a summary of APT and DRIR operations and performance.

#### 7.5 Section IV – Orbital Data

Section IV is a listing of Nimbus II orbital elements and ascending and descending nodes.

#### 7.6 Section V – Data Log

Section V is the computer printout of the Sensory Information Processor (SIP) Program. This Program, described in Section 8 of this document, lists the classification of AVCS and HRIR (and possibly MRIR) data by meteorological and geomorphological content. This permits retrieval of data by content as well as by time and geographical location. Procedures for automatic data retrieval are outlined in Section 8 of this document.

## SECTION 8

### COMPUTERIZED DATA RETRIEVAL SYSTEM

#### 8.1 Basic Concepts

Much of the material in the Nimbus II catalogs will be computer-generated; the computer program which prints the Data Logs is known as the Sensory Information Processor (SIP) Program. Another major function of this program is the performance of automatic data retrieval. This section of the **USERS' GUIDE** will describe some of the basic concepts and operational details of the SIP Program with which the user should be familiar. A complete technical description of the program will be published by the General Electric Company as part of the documentation for their Nimbus II programming effort, and inquiries as to the availability of that publication should be made through the Nimbus Project Office. The specifications for the program, based on guidelines set down by GSFC, were prepared by ARACON Geophysics Division, Allied Research Associates, Inc.

The functions of the SIP Program are: (1) To assemble, process, and store on magnetic tape information defining the major characteristics of AVCS, HRIR, and (so far as possible) MRIR data; (2) To print out data logs at specified intervals for inclusion in the monthly Nimbus II catalogs; (3) To provide automated data retrieval services.

#### 8.2 Definitions

##### 8.2.1 Swath

A swath of AVCS data is a strip of picture triplets taken during one daytime passage of the satellite from the south polar to the north polar regions. The orbit number changes midway through a full swath (at the equator), and the swath is identified by the higher orbit number. (This holds true even when no pictures are taken north of the equator.) The swath may contain data gaps and will not always cover the entire daylight portion of the orbit. Numbering of the triplets is from north to south, in reverse time sequence; assignment of triplet numbers is made by the NDUC analysts and will not normally correspond with the numbers in the photographically recorded frame legends.



The HRIR swath is normally a strip of photo-facsimile data obtained during the complete nighttime portion of an orbit, from the north polar to the south polar regions. The swath number is therefore the same as the orbit number. Again, there may be gaps and/or limited coverage. In the case of daytime HRIR data, the swath coverage and identification number are the same as for AVCS.

An MRIR swath is defined as the coverage obtained during the one orbital period immediately preceding each interrogation, and is identified by the interrogation orbit number. This system will be adhered to even in cases where data is lost in the later part of a swath so that, for instance, Swath No. 100 might contain data only from orbit 99. MRIR data is not rearranged into nighttime and daytime sections, but remains in interrogation format. (See section 4.3.1 for an explanation of the MRIR record and playback operation.)

### 8.2.2 Sector

Each swath may be divided by the meteorological analysts into two or more sectors such that each sector is, as nearly as possible, homogeneous in its content of meteorological phenomena. This helps to organize the analysts' approach and, more importantly, permits the approximate geographical location of the phenomena by the SIP Program.

### 8.2.3 HRIR Data Block

The HRIR data are presented in a strip which may be broken at points corresponding to tape reversal and track change of the tape recorder on board the spacecraft. While the data transmission from the satellite may be either in forward or reverse direction with respect to the sequence of observation, the ground equipment reassembles the data into its proper order. Apparent gaps appear at the times of tape reversal; however, little data is lost. The segments between reversals are called data blocks, and the blocks are numbered within each swath, number one being the northernmost block.

## 8.3 Inputs

Input for the SIP Program includes cards punched from log sheets filled out by a team of professional meteorologists and geophysicists on the NDUC staff, who identify and classify and extract AVCS and HRIR data from montages of each 24-hour period (See Figure 2-3). The input card format allows for a general description of each AVCS, HRIR and MRIR swath coverage (on-off times) and for

the division of each swath into sectors based on meteorological domains, with a coded description of the geographical zones covered in each sector and coded descriptors of meteorological and geographical phenomena therein. There is also space for plain language or coded remarks. MRIR data will be included in the SIP Programmed Data Logs, but probably without descriptors and zone numbers.

#### 8.4 Output – Data Log Section of the Users' Catalogs

The Data Log section of the Nimbus II catalogs is printed by computer and contains essentially all the information stored in the SIP magnetic tape files. Hence, the following paragraphs, which describe the Data Log format, also define the information which may be used for automated retrieval.

##### 8.4.1 Swath Information in Data Log

The swath heading lines in the Data Log give Swath Number and date (UT date at time of ascending node), plus the following information:

- a. R/O Number(s) – Orbit number(s) during which the data was read out of the satellite.
- b. START and END UT – Times of northernmost and southernmost AVCS triplets, or of northernmost and southernmost end of HRIR data, or of beginning and end of MRIR data.
- c. LAT – Latitude of subpoint at time of southernmost AVCS triplet or of southernmost end of HRIR nighttime data.
- d. LON and A/N (or D/N) UT – Longitude and Universal Time of ascending node (northbound equator crossing) for the orbit having the same number as the swath. Descending node data is given for HRIR nighttime swaths.
- e. REMARKS – which apply to the entire swath.

##### 8.4.2 Sector Information in Data Log

Each sector line in the Data Log gives sector number and span (triplet numbers or HRIR block numbers included in the sector).

In addition each sector line gives the following information:

a. START UT and LAT – Time and subpoint latitude of northernmost AVCS triplet or northern end of HRIR data.

b. HGHT – Height of satellite at start time, in kilometers.

c. ZONES – Geographical zones included in the sector's earth coverage. The zones are arbitrary fixed areas of the earth's surface. The arbitrariness has been tempered by making the zones of varying size and distributing them with some consideration for homogeneous areas of interest. Figure 8-1 defines the zone boundaries. The zones are grouped into superzones, identified by the first digit of the zone number; thus superzone 20 includes zones 21 through 29. If a sector includes more than four zones, the superzone number will be used rather than the zone numbers.

d. OSO – Other sensors on. This column shows which of the other sensors were on during the time span of each sector. This information is derived by the SIP Program from telemetry data and hence does not necessarily indicate that data has been received by NDUC from the indicated sensors for the time span in question. The information is given by single-letter code as follows:

C – AVCS  
H – HRIR  
M – MRIR  
P – APT  
X – DRIR

e. DATA CONTENT DESCRIPTORS – The coding system and classification scheme for these entries are fully described in Section 9 of this document. Numeric rather than mnemonic codes will be used, and each four-digit descriptor code may be followed by an alphabetic continuation code (See Section 9.8).

f. REMARKS – Classification confirmation codes, quality codes, or plain language remarks may appear here, as defined and explained in Section 9.9.

## 8.5 Data Retrieval

The information which is printed out by the SIP Program for the Data Log section of the catalog is maintained on magnetic tape and can be selectively retrieved by the program. The General Electric Company publication referred to in Section 8.1 contains the details of the program input requirements for retrieval; the following sections will give a conceptual outline of the possibilities.

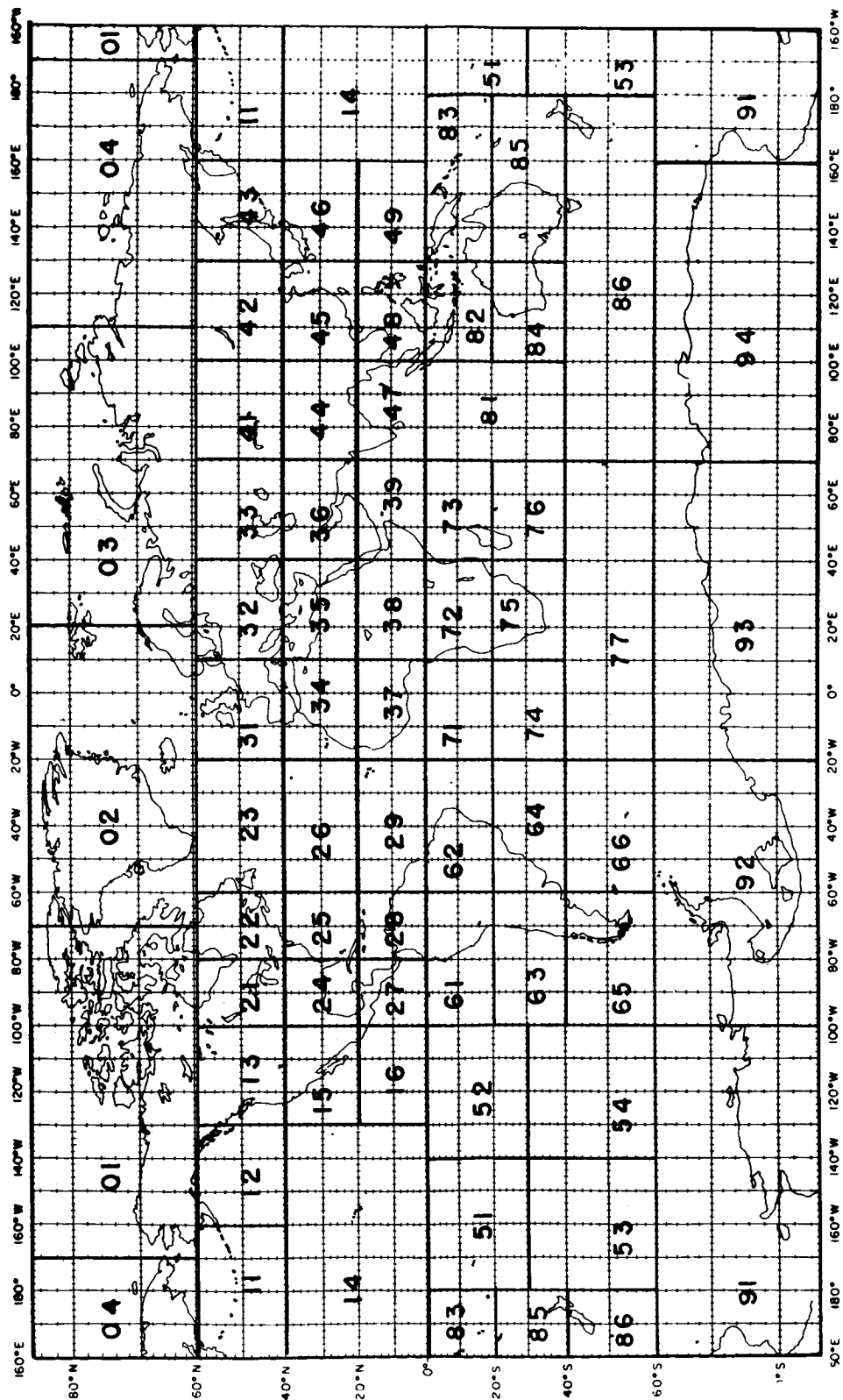


Figure 8-1-Geographical Zones

When the need for retrieval search is expressed or implied by a User's data request, the following procedures will be followed.

1. The User's requirements will be translated into a form suitable for computer search.
2. Search input cards will be prepared.
3. The computer will print the identification and location of data sought, and if desired, the rest of the catalog entry for each item.
4. After inspection, the printout will be forwarded to the User with any necessary explanation.

#### 8.5.1 Output Format

Either of two types of printed output can be requested for a SIP Program retrieval: Extract Index or Extract Catalog. The former is an abbreviated format which extracts and prints out selected parameters of those sectors which satisfy the condensed listing of information pertinent to the request; the latter is in the same format as the catalog Data Log except that only the sectors which satisfy the conditions of the request are printed, together with the appropriate swath heading lines.

#### 8.5.2 Retrieval Parameters

Data can be retrieved on the basis of an individual parameter, logical combinations (see the next section) of parameters, or a range of values for a parameter or parameters. The data retrieval parameters are:

1. Sensor (type)
2. Swath (number)
3. Interrogation (Read-out) Orbit
4. Day (Calendar)
5. Zones (Geographic)
6. Year
7. Other Sensors On (OSO)
8. Data Content Descriptors

The definitions of these parameters have been given in the foregoing paragraphs. Data cannot be retrieved on the basis of information contained in the remarks section of the data log.

As an example of the use of a single parameter for data retrieval, consider this case:

A user requires all meteorological and/or terrestrial data from any sensor, for the lifetime of the satellite, which covers the arctic regions north of the 60th parallel. The SIP retrieval input will specify only the range of the zone numbers. That is the zone number must be greater than 00 and less than 05 (arctic region), and the computer will print out and identify in index or catalog format as specified all sectors for each sensor which contains data in the desired area.

Data content descriptors are organized in logical tree fashion, so that the most detailed descriptors are special cases of more general descriptors. The level of generality is indicated by the number of trailing zeros in the descriptor code. Thus, 4651 is a special case of 4650 which in turn is contained in 4600. The program can be instructed to retrieve all special cases falling under a more general descriptor.

### 8.5.3 Logical Combinations of Parameters

Various retrieval parameters may be strung together, linked by "ands" or "ors," to achieve almost any desired special retrieval. The user must of course be careful to state his desires very clearly so that retrieval can be properly achieved. The range of possibilities can be illustrated by four examples of possible retrieval requests which could be processed:

1. AVCS sectors showing lee wave clouds in the western U. S. during May 1966, but including only the sectors recorded when the MRIR and APT sensors were on.
2. Sectors for any sensor (AVCS, HRIR, or MRIR) in the northern hemisphere, at any time, which contained an extratropical vortex together with an indication of a jet stream.
3. Sectors of HRIR data in the tropical Atlantic or tropical Pacific or tropical Indian Oceans at any time which show quasi-circular cloud masses less than  $6^{\circ} \times 6^{\circ}$  in extent.
4. Sectors of HRIR nighttime data in the western North Atlantic showing relatively cloud-free areas, for September 1966. Since HRIR discriminates poorly between low clouds and the ocean surface this retrieval would probably be handled by first retrieving AVCS sectors which satisfy the conditions, and then manually selecting HRIR data from the same areas on the same dates (12 hours earlier or later).

## SECTION 9

### CLASSIFICATION OF DATA CONTENT

#### 9.1 Introduction

This classification scheme was designed to be used with the computerized data storage and retrieval system designated as the Sensory Information Processor (SIP) and discussed in Section 8. The geophysical data content of the Nimbus meteorological satellite output is divided into six major categories. The first three categories are related to cloud features; the fourth to terrestrial features; the fifth to pictures of doubtful quality; the last to pictures of poor quality or pictures containing no discernible features (see Figs. 9-1 through 9-6). The pictures in the last category are considered to be of no value to researchers or operational users and cannot be retrieved by the computerized system. Each category can be further subdivided into a maximum of seven divisions and each division can have a maximum of seven groups. Each group can be broken down into as many as seven classes. This logical-tree subdivision is thus carried on for four levels. The letters (D) for Division; (G) for Group and/or (C) for Class will appear after most subsection headings to identify the level of classification below each category. The classification of the data content at the first level, although descriptive in nature, is still relatively objective. The classification becomes more subjective and interpretive as one moves down the tree structure to the lowest level. This procedure permits those researchers, who may prefer to retrieve and request data on a descriptive rather than an interpretive basis, to request retrieval at a higher level.

A data content confirmation code (Section 9.9.1) is provided for entries in the remarks section of the Data Log Section of the Nimbus II Users' Catalog (see Section 8). This code will be used to indicate whether or not the data content classification was substantiated by conventional meteorological data.

#### 9.2 Cloud Features

To date, the meteorological community has not adopted a standard set of names, definitions, or descriptions for meteorological phenomena observed in satellite photographs. The names, definitions and descriptions used here may differ from those used elsewhere. A satellite picture or sector will be placed in

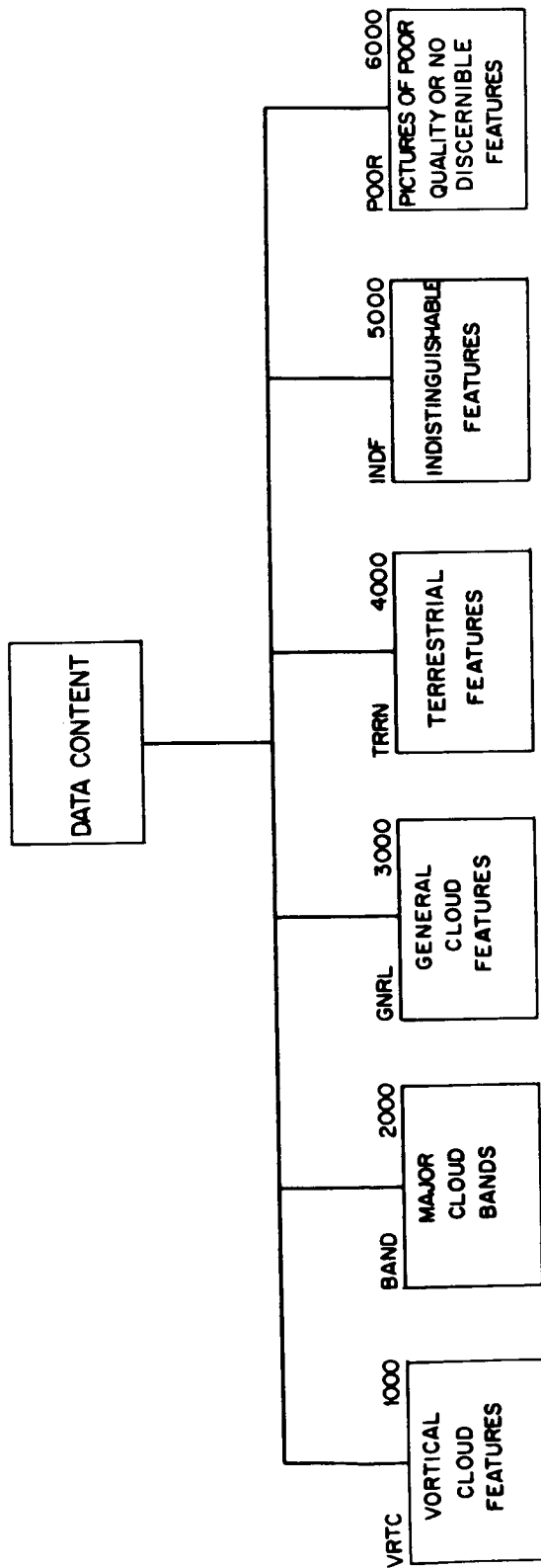


Figure 9-1--Data Content





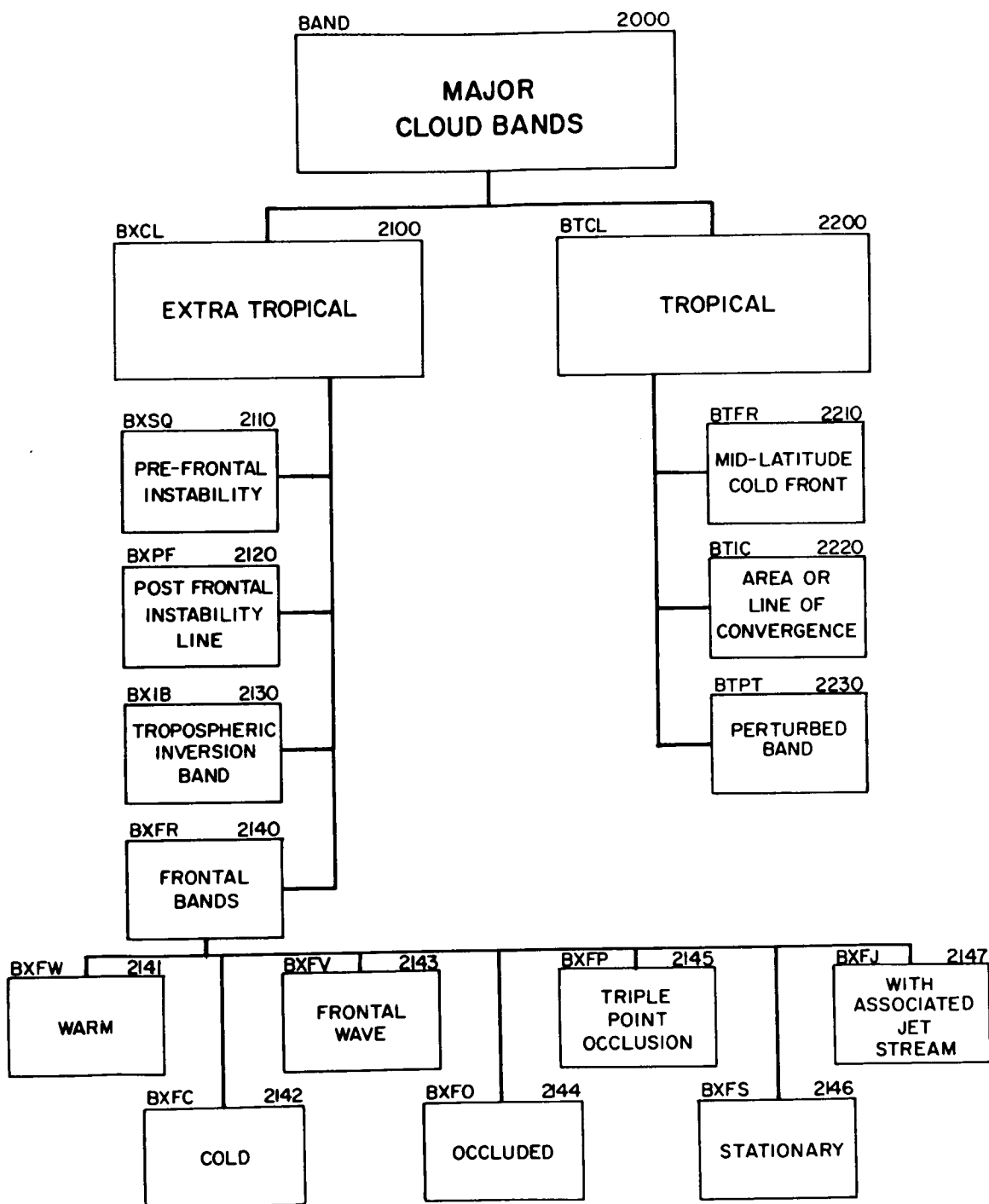


Figure 9-3—Major Cloud Bands

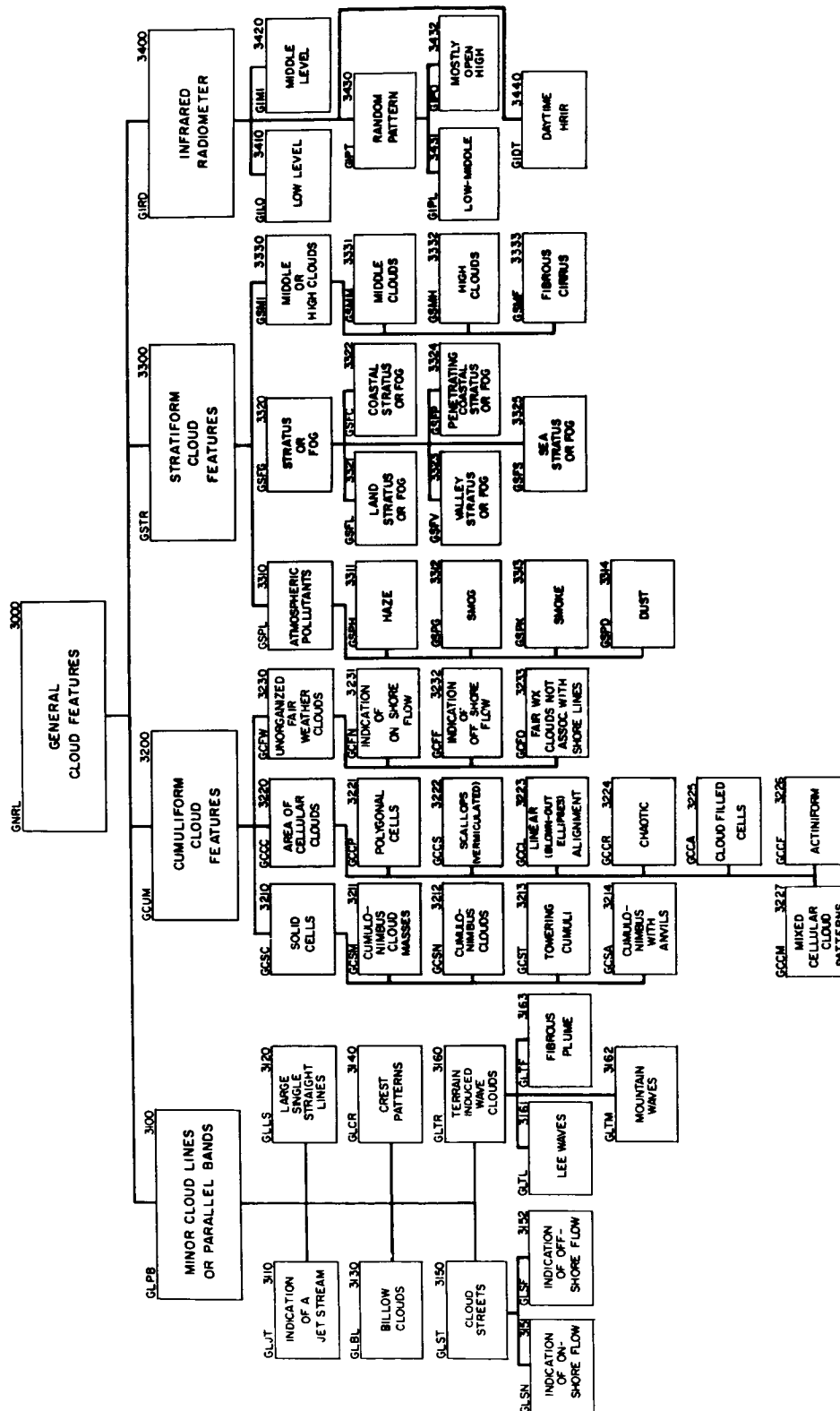


Figure 9-4-General Cloud Features



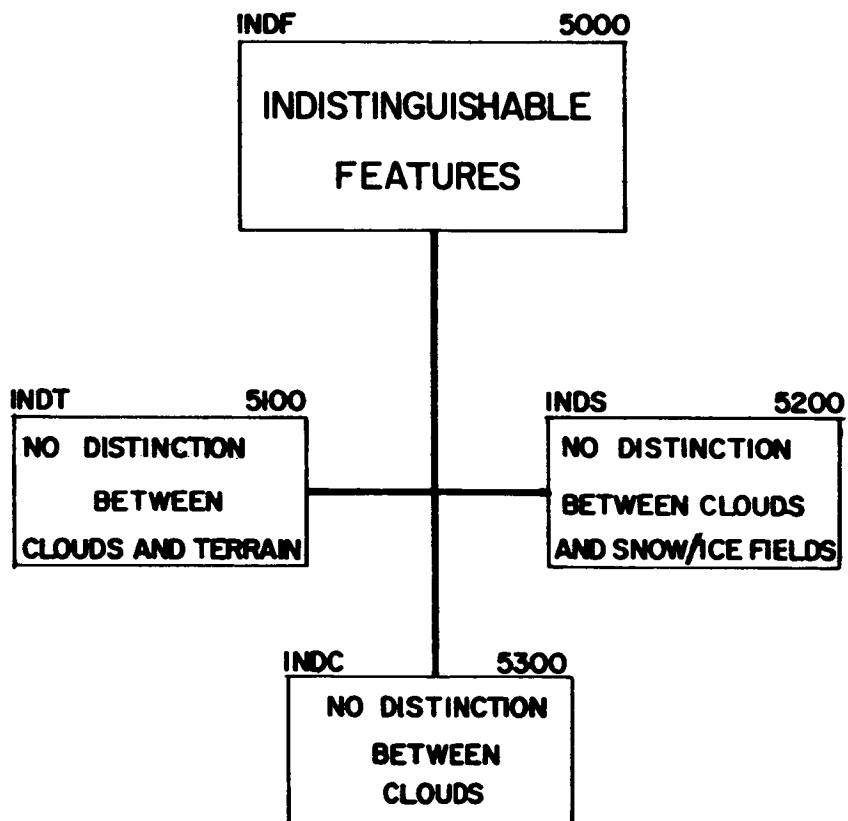


Figure 9-6—Indistinguishable Features

a specific category when it satisfies the description of the category. Whenever a satellite picture satisfies the description of a specific category, but the associated synoptic situation is known to be quite different from that usually associated with the description, the picture will be classified according to its description; then, the appropriate notation will be made in the remarks section of the Data Log Section of the Nimbus II Users' Catalog.

Cloud features are classified primarily on the basis of cloud patterns as seen in the satellite data. The scheme for classifying cloud patterns was chosen to meet the following constraints: (1) relatively high frequency of occurrence; (2) reasonably reliable identifiability; and (3) ease of recognition by an analyst. Whenever sufficient time and data are available, the interpretive classification of cloud features will be validated by correlating the satellite data with current synoptic data. In many cases, some of the subtle features in the conventional analysis, such as short wave troughs may be difficult to establish over areas of limited conventional data. In cases in which the interpretive classification is in doubt and confirmation based on reliable conventional meteorological data is not possible, classification should remain at a higher or more descriptive level.

A lack of contrast between clouds and certain other features in satellite pictures may occasionally make it difficult to distinguish or identify cloud above snow or ice fields (especially in polar or mountainous regions), higher clouds above a uniform undercast, and in some cases clouds above relatively white terrain. A picture will be placed in the category, "Indistinguishable Features" whenever a clear distinction cannot be made between the clouds and other objects.

Cloud Features can be illustrated and initially understood better from television pictures than HRIR data. Accordingly, Nimbus I AVCS pictures will be used in initial illustrations. TIROS television pictures will be used to illustrate cloud features in cases where adequate Nimbus I pictures are not available. Nimbus I AVCS pictures are identified as such in each figure by the letter (N). TIROS pictures are not identified. Selected Nimbus I HRIR data which depict certain cloud features are presented near the end of this section for illustrative purposes.

In most cases the descriptions of various categories and subdivisions are written in terms of how the cloud features appear over the northern hemisphere. These descriptions are also valid for the southern hemisphere if appropriate adjustments are made, as for the clockwise-circulation around southern hemisphere

vortices, and the upside-down appearance of southern hemisphere extratropical cyclones. In a few cases, such as Figure 9-9, the pictures have been turned over and printed upside-down, and so appear to illustrate northern hemisphere meteorological phenomena. In such cases, grid lines and latitude and longitude identifications are also inverted or reversed.

Cloud features are placed in the following three major categories:

- a. Vortical clouds
- b. Major cloud bands
- c. General cloud features.

#### 9.2.1 Vortical Clouds

Vortical cloud patterns include the following:

- a. Circular and/or spiral cloud bands or cloud patterns, usually referred to as vortices, in a wide range of sizes and shapes.
- b. "Comma" or crescent shaped cloud masses, of sizes appropriate to the synoptic scale, having somewhat the appearance of vortices.
- c. Circular or quasi-circular nonbanded cloud masses or "blobs" usually associated with closed cyclonic flow in some layer between the surface and the tropopause.

Curved or linear bands of clouds, usually very much longer than they are wide, are frequently associated with vortical cloud features. In some cases these are frontal bands. Therefore, when these bands are present in vortical patterns, the pattern is classified as a frontal vortex. The classification, non-frontal vortex, is used here to describe those satellite pictures in which there are vortices with no associated cloud bands or those in which the cloud bands are not primarily related to a surface frontal system.

##### 9.2.1.1 Extratropical Vortical Cloud Features (D)

Meteorological satellites have provided photographs of cloud fields associated with an extremely large number of individual extratropical vortical (cyclonic) systems. In examining this large sample, satellite meteorologists have long recognized that certain gross characteristics of these cloud fields are common to meteorologically similar cyclonic systems. Model representations of the cloud field, in the form of schematic illustrations, have been used to illustrate these common cloud characteristics. This philosophy and technique of generalization has been followed in the following presentation.

Most of the illustrations of extratropical vortical cloud features in this section contain both a generalized schematic representation of the cloud features associated with a particular class of extratropical cyclonic systems, and a satellite picture taken from the sample for which the schematic is a generalization. In the present work, the schematics were constructed by extracting from the accompanying picture the gross cloud features which meteorological satellite experience indicates are frequently found in similar cyclonic systems; and by including features which are frequently found but are not necessarily present in the satellite photograph used as an example. Thus, the reader should not expect to find a one-to-one correlation between all the cloud features in the picture and the schematic, but rather a correlation between gross features of the schematic and the picture.

#### 9.2.1.1.1 Frontal Vortices (G)

Class A - "Short Wave Trough" (Beginning of Occlusion) - (Figure 9-7) - These vortices are crescent or comma shaped, bright, heavy overcast, middle and/or high clouds having either an amorphous or "pebbled" appearance, usually without low and/or middle level clouds spiralling into the central region of the pattern from the northwest.

In general, the surface synoptic chart depicts a low pressure system of small to medium scale with a frontal system usually approaching, or in the early stage of occlusion. Occasionally there is no surface front associated with the surface low or trough, but frontogenesis can usually be detected. The 500 mb chart usually depicts a short wave trough displaced somewhat to the north and west of the surface low. A weak to moderate closed circulation may exist at levels below 800 mb. The longitudinal dimension of this cloud pattern is between 210 and 720 nautical miles.

Class B - "Well Developed Short Wave Trough" (Occluding Cyclone) (Figure 9-8) - This vortex is a hook shaped, bright, heavy overcast of middle and/or high clouds with spiralling low and/or middle clouds inside the hook. In Figure 9-8, "inside the hook" is the area north of the base of the fiducial point (+). This pattern differs from the crescent shaped pattern by the presence of spiralling low to middle level clouds inside the hook. The low level clouds are usually cumuliform.

The surface synoptic chart usually depicts an occluding frontal system and the beginning of a cyclonic circulation at the 500 mb level. The 500 mb low pressure region is usually displaced to the north and west with reference to the surface, but to a lesser degree than Class A.

The longitudinal dimension of this cloud pattern is 420 to 960 nautical miles.



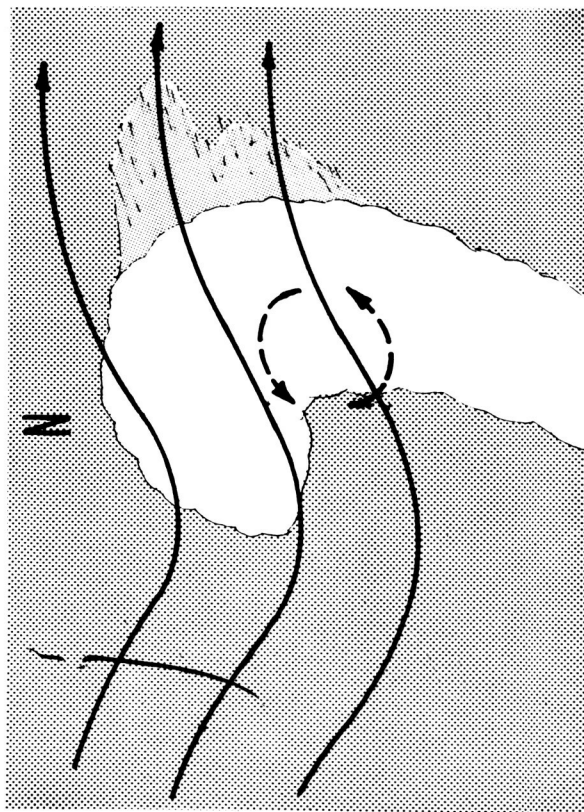
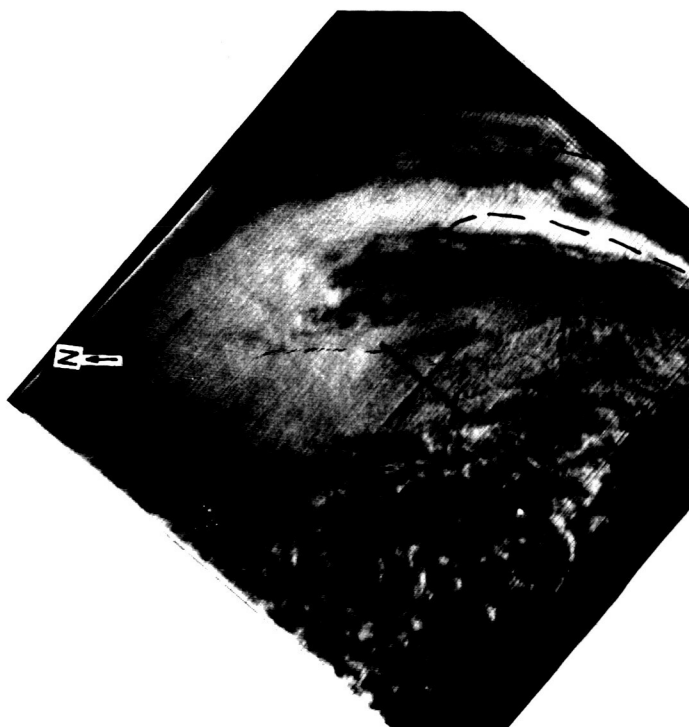


FIGURE LEGEND

- COVERED
- MOSTLY COVERED
- MOSTLY OPEN

DASHED LINES — LOWER TROPOSPHERE FLOW  
 SOLID LINE — MIDDLE TROPOSPHERE FLOW

Figure 9-7—Class A — “Short Wave Trough”

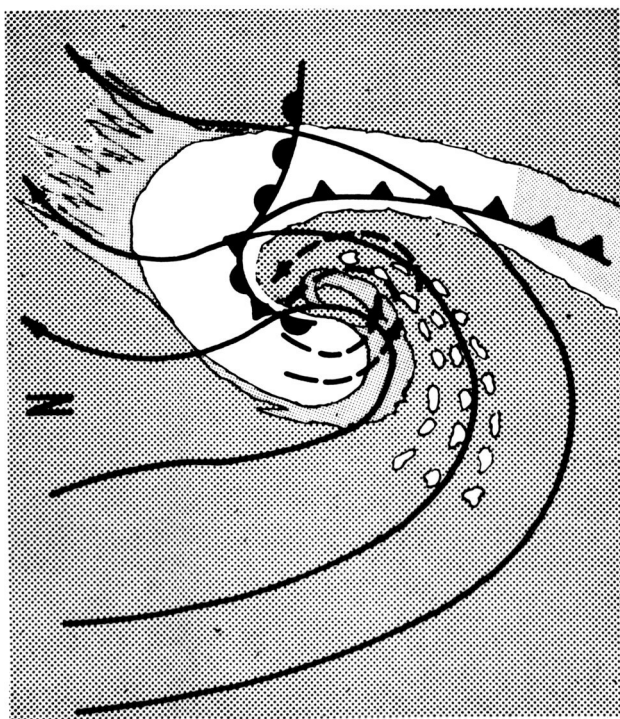


FIGURE LEGEND

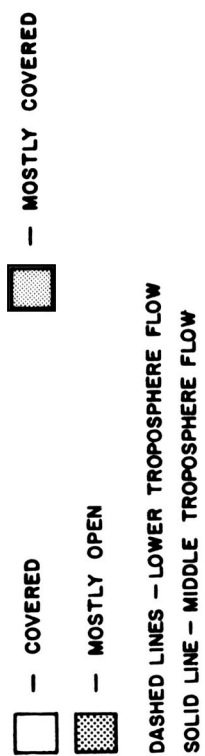


Figure 9-8—Class B — “Well Developed Short Wave Trough” (Occluding Cyclone)

Class C - "Mature Vortex" (Fully Occluded Cyclone) - (Figure 9-9) - These vortices are cyclonically curved, middle and/or high cloud bands, with a heavy overcast area in the northeastern quadrant and a striated, broken area in the northwestern quadrant, usually with low to middle level spiral clouds. The spiral low and/or middle cloud patterns appear near the circulation center.

The closed circulation at the surface and lower levels expands in size compared to classes A and B, and reaches its maximum intensity. Fully occluded frontal systems are usually in evidence. The closed cyclonic circulation at the 500 mb level is usually directly above the surface low pressure area and reaches its maximum intensity. A short wave trough is occasionally imbedded in the southerly flow on the east side of the closed circulation in the midtroposphere.

Typical longitudinal dimensions of these cloud patterns range from 700 to 1000 nautical miles.

Class D - "Decaying Cyclone" - (Figure 9-10) - This vortex depicts spiralling low and/or middle level clouds, with an appearance of decreasing organization.

This is usually a decaying cyclone which may or may not be associated with an active frontal system. In general, there is a closed cyclonic circulation at the 500 mb level. The 500 mb low is more or less directly over the surface low pressure area. The surface and 500 mb low pressure areas are usually much weaker than those of Class C.

Class E - "Tropical Cyclone in Extratropical Latitudes with Associated Frontal Band" - (Figure 9-11) - This is a tropical cyclone which has moved into midlatitude regions and taken on the characteristics of an extratropical vortex, including an associated frontal band. Although the cloud vortex may be similar in appearance to an extratropical vortex, it is placed into this category in order to maintain historical continuity. This classification is further restricted to "named" tropical cyclones whose identity is corroborated by current synoptic data.

A tropical cyclone in extratropical latitudes which does not have an associated frontal band will be classified as a tropical cyclone, rather than a tropical cyclone in extratropical latitudes with associated frontal bands, i.e., not as Class E.

#### 9.2.1.1.2 Non Frontal Vortices (G)

Class I - "Closed Upper Level Circulation Over Land" - (Figure 9-12) - This is a circular middle and/or high cloud mass with essentially continuous

circular striations imbedded in it. This pattern is associated with closed cyclonic circulation aloft (over land), which develops first at midtropospheric levels, and may then penetrate downward. A closed low may be in evidence at both the 500 mb level and the surface.

Class II - "Closed Upper Level Circulation Over Oceans" - (Figure 9-13) - This is a spiral middle and/or high cloud band, but differing from that of Class C in that it lacks an area of striated clouds in the northwestern quadrant; the cloud band is narrower and often more prominent than in the over land category.

The synoptic situation associated with this pattern is the same as that for Class I, but located over subtropical oceanic regions. Those few studied to date have lacked the low level cumulus found in Classes B and C.

Class III - "Short Wave Trough in Polar Flow" - (Figure 9-14) - These are crescent shaped patterns of small to moderate size composed of cumuliform clouds of considerable vertical extent, with some middle and high clouds.

These cloud patterns are associated with a small amplitude, short wave trough imbedded in northwesterly flow at 500 mb. The surface synoptic chart is characterized by a distinct surface wind shift line and a trough in the pressure field.

Class IV - "Terrain Induced Vortices" - (Figure 9-15) - Small scale vortices related to the flow of air over and around islands are sometimes observed in satellite pictures. These cloud features appear as arcs, eddies or complete spiralling patterns downwind from islands. The cloud features are frequently found in an area which is partially cleared of clouds. The cloud features are associated with, or are parts of, a layer of stratocumulus or stratus below an inversion, with low wind speeds and ceilings. These cloud features provide information on the general direction of low level wind flow in the area. Terrain induced vortices are common occurrences downstream from islands of subtropical regions. They have also been noted to the east of the southern tip of Greenland. It is usually easy to differentiate these vortices from those associated with significant storms because of their size, location, and apparent weak intensity.

Class V - "Mesoscale Vortices" - (Figure 9-16) - These cumuliform and cirriform secondary mesoscale vortex patterns, in the polar flow behind major extratropical cyclones, appear to be indicative of 500 mb short wave troughs. These small scale eddies or vortices are usually similar in appearance to the vortical patterns of Classes I, II and especially III. This category is established primarily to accommodate the secondary mesoscale vortices frequently observed near the edge of the Antarctic pack ice.

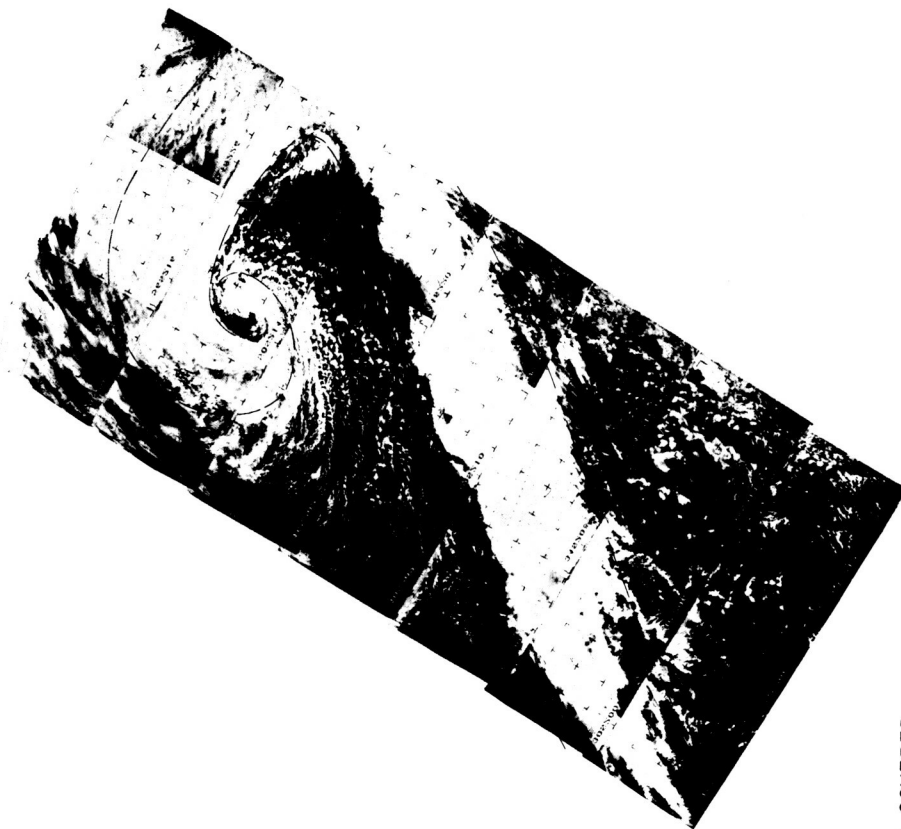
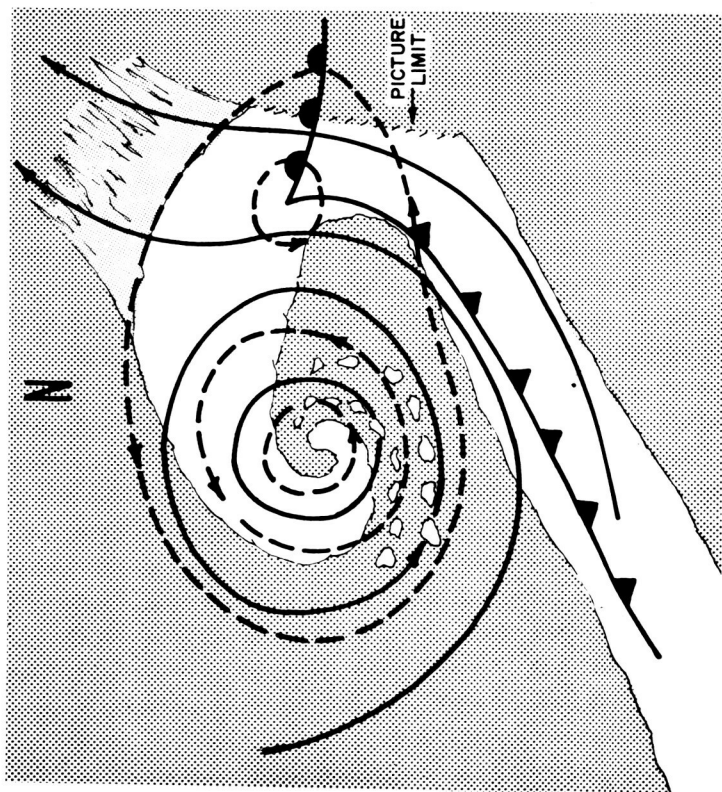


# FIGURE LEGEND

- COVERED
- MOSTLY COVERED
- MOSTLY OPEN
- DASHED LINES — LOWER TROPOSPHERE FLOW
- SOLID LINE — MIDDLE TROPOSPHERE FLOW

Figure 9-9—Class C — “Mature Vortex” (Fully Occluded Cyclone) (N)

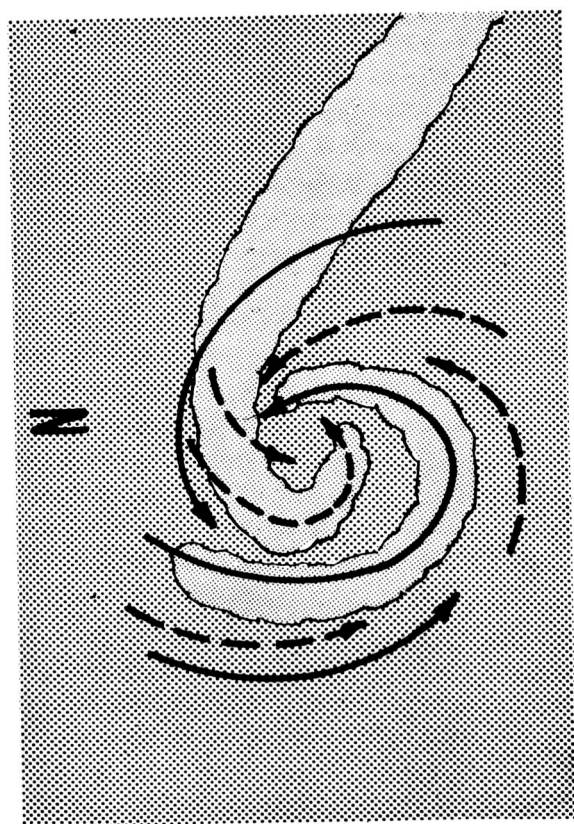
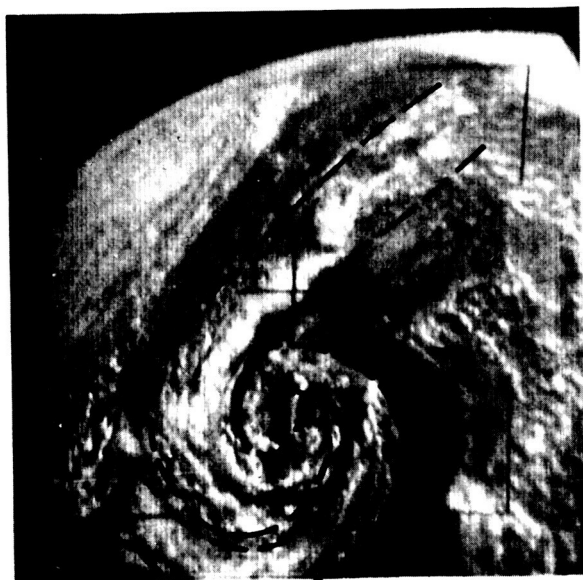


FIGURE LEGEND

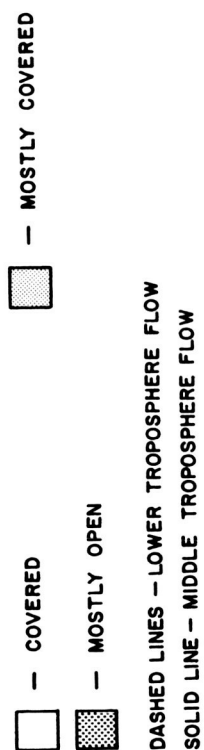


Figure 9.10—Class D — “Decaying Cyclone”

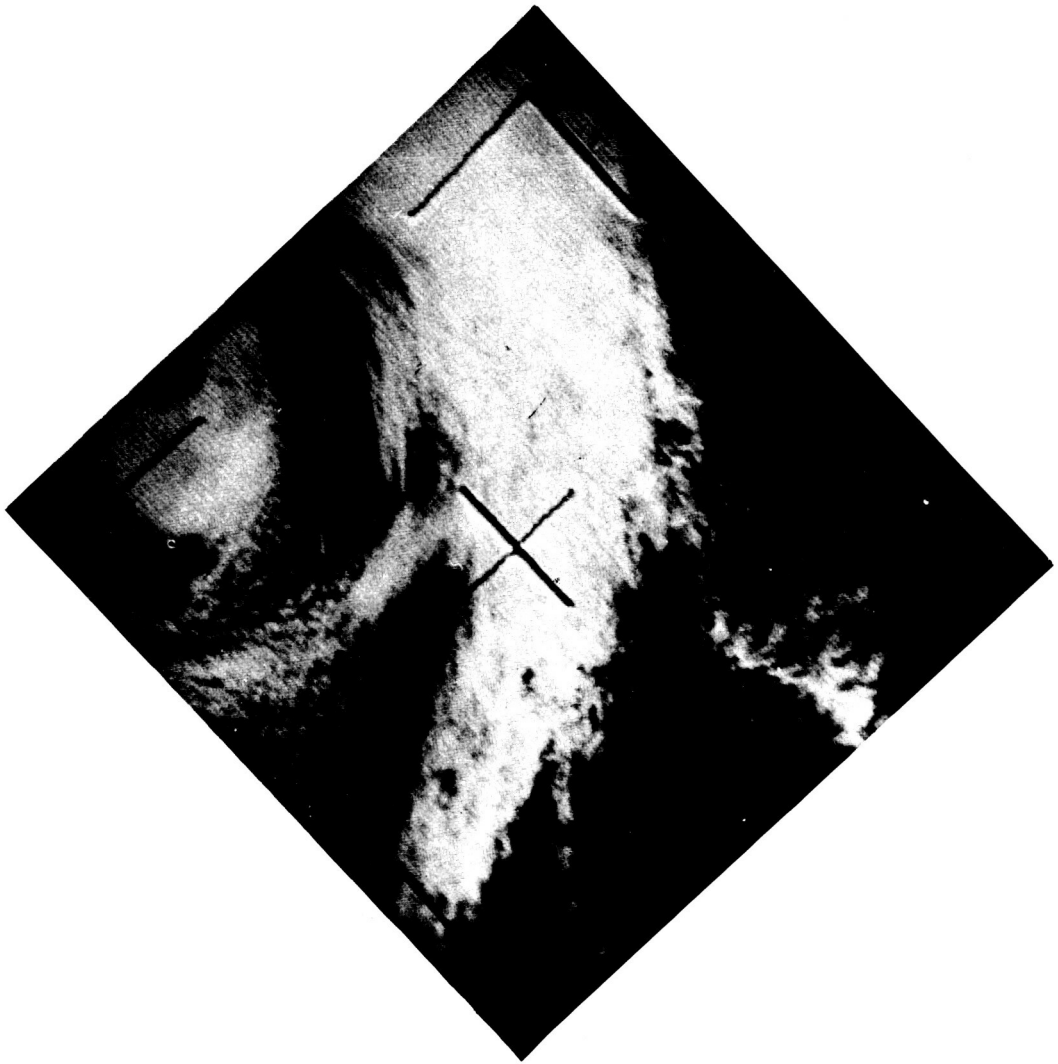


Figure 9-11—Class E – “Tropical Cyclone in Extratropical Latitudes with Associated Frontal Band”

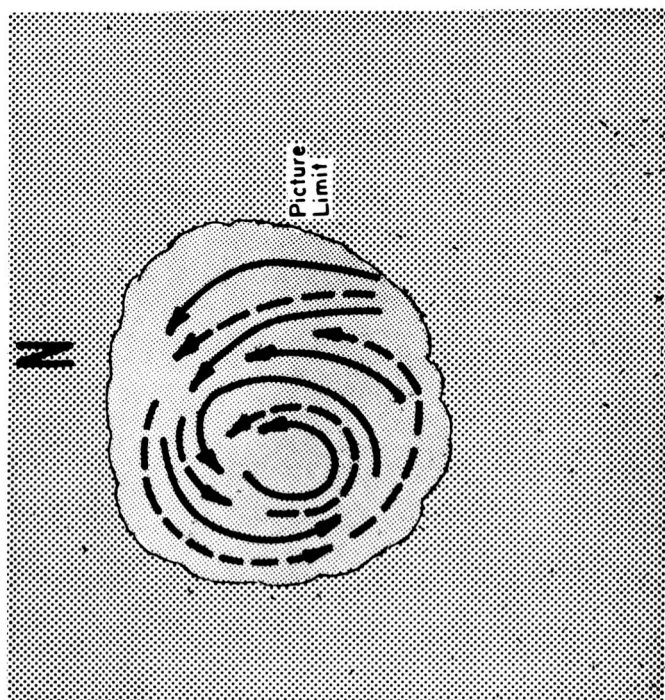


FIGURE LEGEND

- COVERED
- MOSTLY COVERED
- MOSTLY OPEN
- DASHED LINES — LOWER TROPOSPHERE FLOW
- SOLID LINE — MIDDLE TROPOSPHERE FLOW

Figure 9-12-Class I — "Closed Upper Level Circulation Over Land"



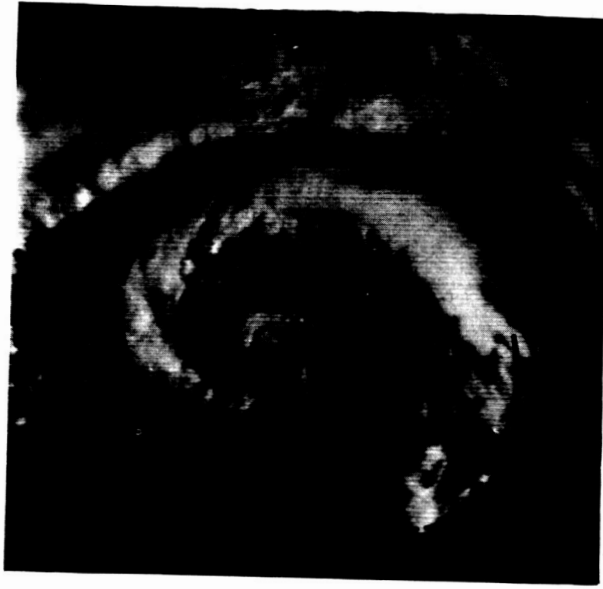
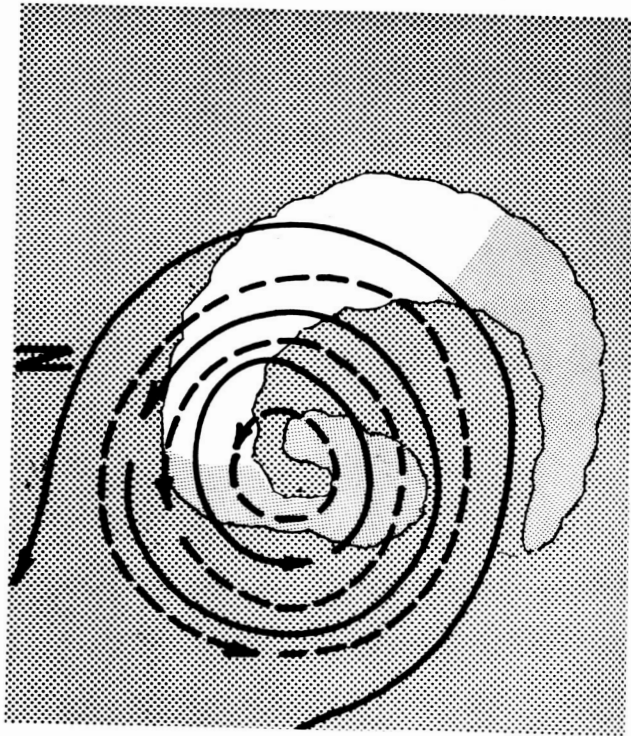


FIGURE LEGEND

- COVERED
- MOSTLY OPEN
- MOSTLY COVERED
- DASHED LINES — LOWER TROPOSPHERE FLOW
- SOLID LINE — MIDDLE TROPOSPHERE FLOW

Figure 9-13—Class II—“Closed Upper Level Circulation Over Oceans”

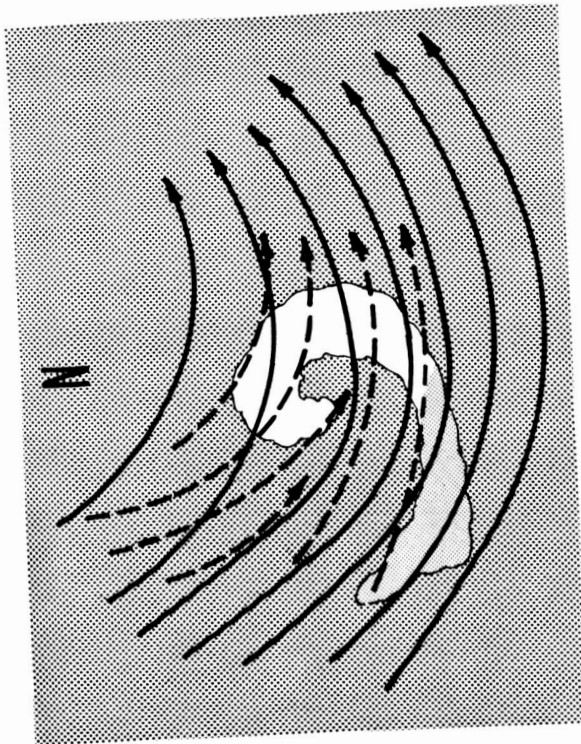
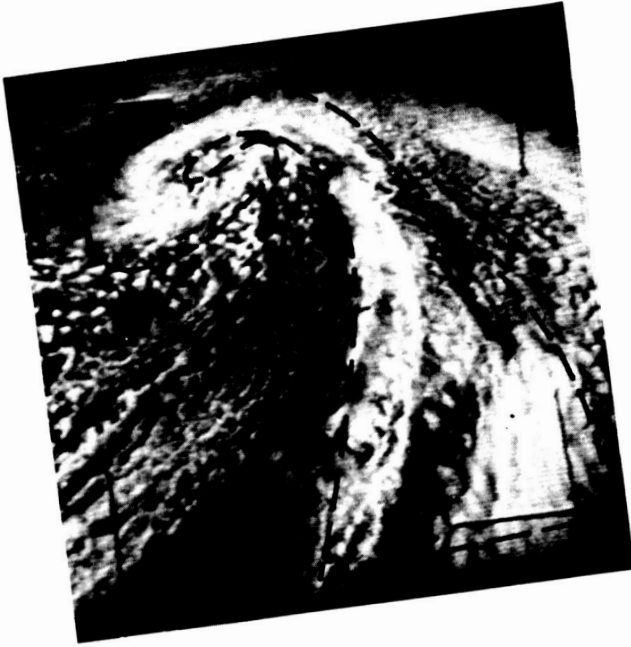


FIGURE LEGEND

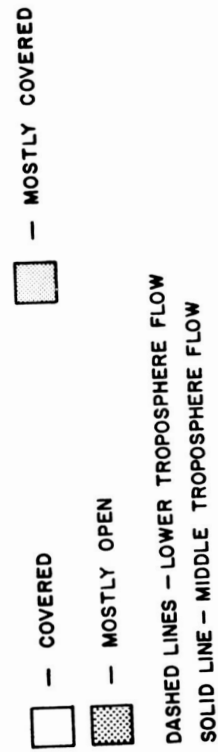
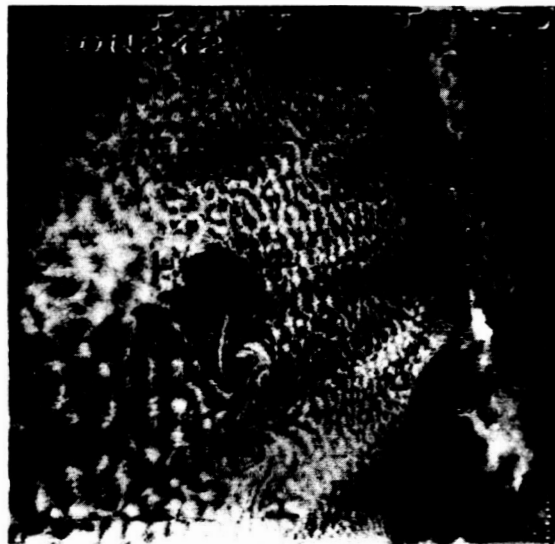


Figure 9.14—Class III — “Short Wave Trough in Polar Flow”



(N)

Figure 9-15—Class IV – "Terrain Induced Vortices"

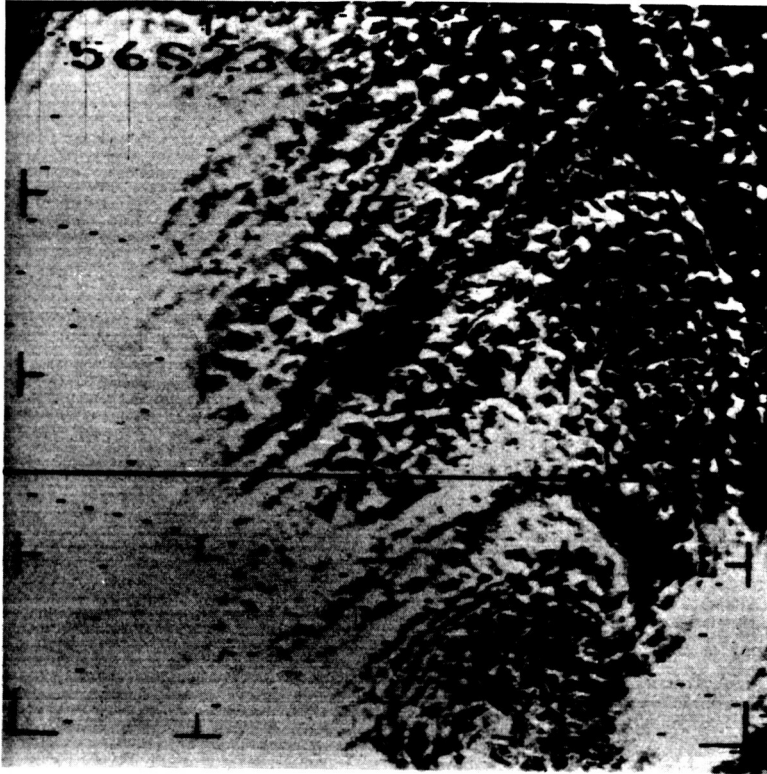


Figure 9-16—Class V – “Mesoscale Vortex” (N)

### 9.2.1.2 Tropical Vortical Cloud Features (D)

#### 9.2.1.2.1 Tropical Cyclones (Fig. 9-17) (G)

Extensive research has led to appreciable progress in determining the wind speeds and intensity of tropical cyclones from the appearance and configuration of the cloud patterns in the satellite pictures. However, objective descriptive techniques which permit quick classification of tropical cyclones according to wind speed and intensity are not currently available. Therefore, all tropical cloud vortices, tropical depressions of greater intensity than a perturbed band, storms, hurricanes, and typhoons are classified as tropical cyclones. Likewise, no attempt is made to classify tropical cyclones according to their stage of development. However, subclassifications are made according to the existence or nonexistence of a cirrus canopy above the vortical cloud pattern, the extent of the area covered by the cyclonic cloud pattern, and whether or not the eye of the cyclone is visible. A separate class is also available for pictures of tropical cyclones which also depict pre-hurricane convective cloud bands or squall lines. In this classification scheme, the dimension of the area of coverage of a tropical cyclone includes the essentially contiguous area of organized concentric or curved cloud bands surrounding the bright cirrus canopy or striations and/or the lower level spiral cloud bands of the central core.

Tropical cyclones are divided into the following groups:

Less than  $4^{\circ} \times 4^{\circ}$  in extent

$4^{\circ} \times 4^{\circ}$  to  $6^{\circ} \times 6^{\circ}$  in extent

Greater than  $6^{\circ} \times 6^{\circ}$  in extent

Each tropical cyclone group is divided into the following classes:

Cirrus canopy indeterminate, eye visible

Cirrus canopy indeterminate, eye not visible

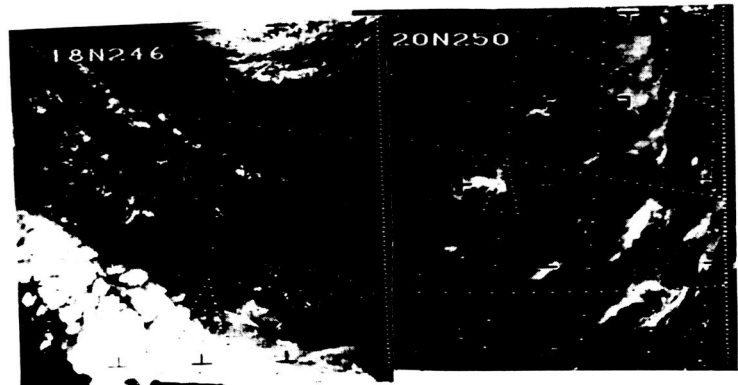
Cirrus canopy, eye visible

Cirrus canopy, eye not visible

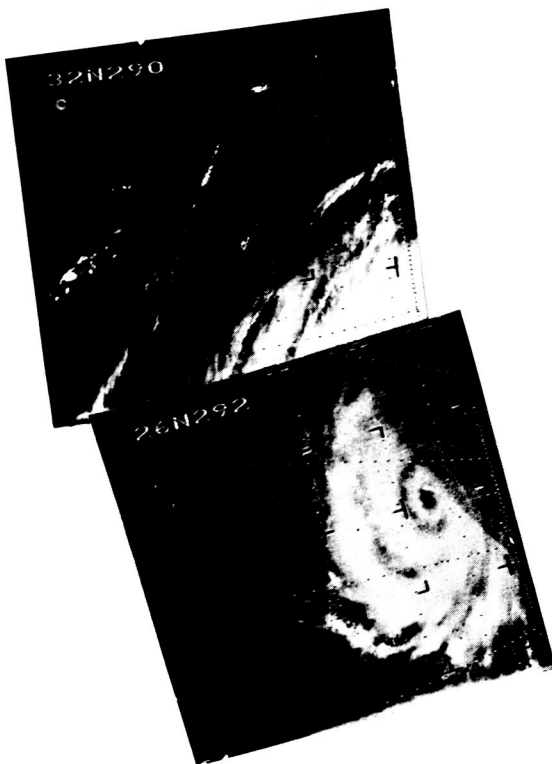
No cirrus canopy, eye visible

No cirrus canopy, eye not visible

With associated squall line.



(a) Less than  $4^{\circ} \times 4^{\circ}$  in Extent (N)  
No Significant Cirrus Canopy



(b)  $4^{\circ} \times 4^{\circ}$  to  $6^{\circ} \times 6^{\circ}$  in Extent (N)  
Partial Cirrus Canopy Eye Visible



(c)  $4^{\circ} \times 4^{\circ}$  to  $6^{\circ} \times 6^{\circ}$  in Extent (N)  
Full Cirrus Canopy, Eye Visible  
With Associated Squall Line

Figure 9-17-Tropical Cyclones

The amount and thickness (transparency) of the cirrus coverage of the central core will be entered in the remarks section of the Data Log Section of the Nimbus II Users' Catalog.

#### 9.2.1.2.2 Tropical Quasi-Circular Cloud Features (Fig. 9-18) (G)

These tropical cloud features are characterized by quasi-circular cloud masses or "blobs" associated with usually closed cyclonic flow in some layer below the tropopause. In some cases, cyclonic flow may exist only in layers above the 500 mb level. Some of these systems may later intensify. The quasi-circular cloud masses are usually cumuliform conglomerates, which may or may not appear as spiral bands, topped by a partial or complete cirrus canopy. These cloud patterns are associated with both lower tropospheric and upper tropospheric troughs and shear systems, as well as easterly perturbations and the ITC. Although surface and low level synoptic charts may indicate that the cloud pattern is associated with a tropical cyclone, the satellite picture cannot be classified as a tropical vortex on the basis of appearance alone. It appears that the size of the cloud mass is an important feature in attempting to identify perturbations and disturbances which will intensify into major tropical cyclones. For this reason, quasi-circular cloud forms are classified according to both the size of the cloud form and the existence or nonexistence of a cirrus canopy. The two groups of tropical quasi-circular cloud features are:

Quasi-circular clouds – less than  $6^{\circ} \times 6^{\circ}$  in extent

Quasi-circular clouds –  $6^{\circ} \times 6^{\circ}$  or greater in extent

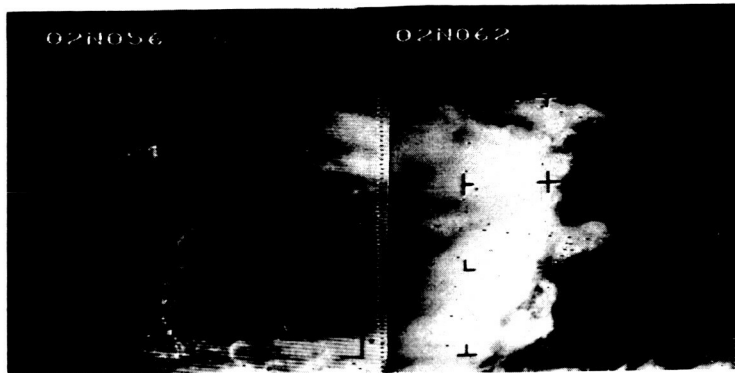
Each quasi-circular cloud group is divided into the following classes:

No cirrus canopy

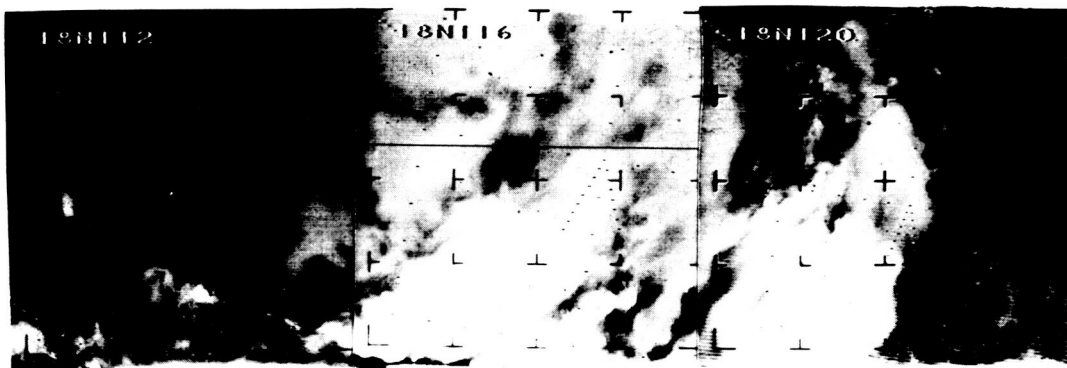
Cirrus canopy indeterminate

Cirrus canopy

The amount and thickness (transparency) of Cirrus coverage will be entered in the remarks section of the Data Log Section of the Nimbus II Users' Catalog. Examples of tropical quasi-circular cloud features are illustrated in Figure 9-18.



(a) Less than  $6^{\circ} \times 6^{\circ}$  in Extent (N)  
No Significant Cirrus Canopy



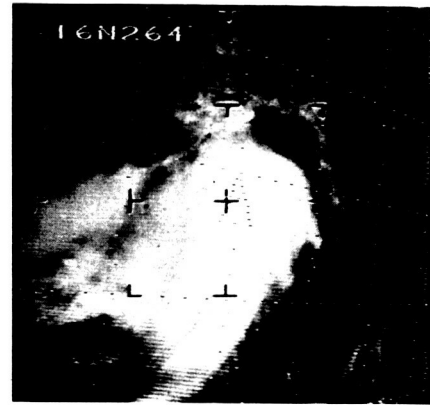
(b) Equal to or Greater than  $6^{\circ} \times 6^{\circ}$  in Extent (N)  
No Significant Cirrus Canopy

Figure 9-18—Quasi-Circular Cloud Features





(c) Moderately Intense Perturbation  
Full Cirrus Canopy



(d) Intense Perturbation (Tropical Disturbance)  
Less than  $6^{\circ} \times 6^{\circ}$  in Extent, Full Cirrus Canopy

(N)



(e) Upper Level Vortex



(f) Tropical Disturbance (N)  
Less than  $6^{\circ} \times 6^{\circ}$  in Extent, No  
Significant Cirrus Canopy

Figure 9-18 (Cont.)—Quasi-Circular Cloud Features

### 9.2.2 Major Cloud Bands

a. A major cloud band is defined here as a linear and continuous arrangement of clouds, usually very much longer than wide. These bands can include low, middle, and/or high clouds, and most often are associated with surface fronts in middle latitudes or areas of convergence in the tropics. Also, the bands may or may not be associated with cloud vortices. However, to fit into this category, the cloud vortex is not present in the specific picture or sector being classified.

b. A major band is also frequently slightly curved or distorted by a bend or bulge in the band. The distorted band may be associated with a surface frontal wave (developing wave) in mid-latitudes, or with a perturbed area in the tropics.

#### 9.2.2.1 Extratropical Cloud Bands (D)

##### 9.2.2.1.1 Pre-frontal Instability or Squall Line (Figs. 9-19 and 9-20) (G)

A cloud band observed ahead of a frontal band may be a squall line. The instability line ahead of the frontal band is often differentiated from the frontal band by the scalloped edges of the instability clouds and the presence of massive cloud blobs with a curved alignment.

When severe weather is associated with instability lines or squall lines, the related clouds assume a distinctive and massive cloud "blob" appearance. The long line of banded cumulus development is usually not present.

##### 9.2.2.1.2 Post-frontal Instability Line or Secondary Front (Fig. 9-21) (G)

In general, this cloud band parallels a cold frontal band and is located behind it; that is, it is the westernmost cloud band or one of several such bands. The bands may be separated by an area of striated cloud, or by a completely clear area.

At times, there is sufficient wind shift and/or weather associated with the post-frontal instability line to warrant the insertion of a secondary cold front on the surface synoptic chart.

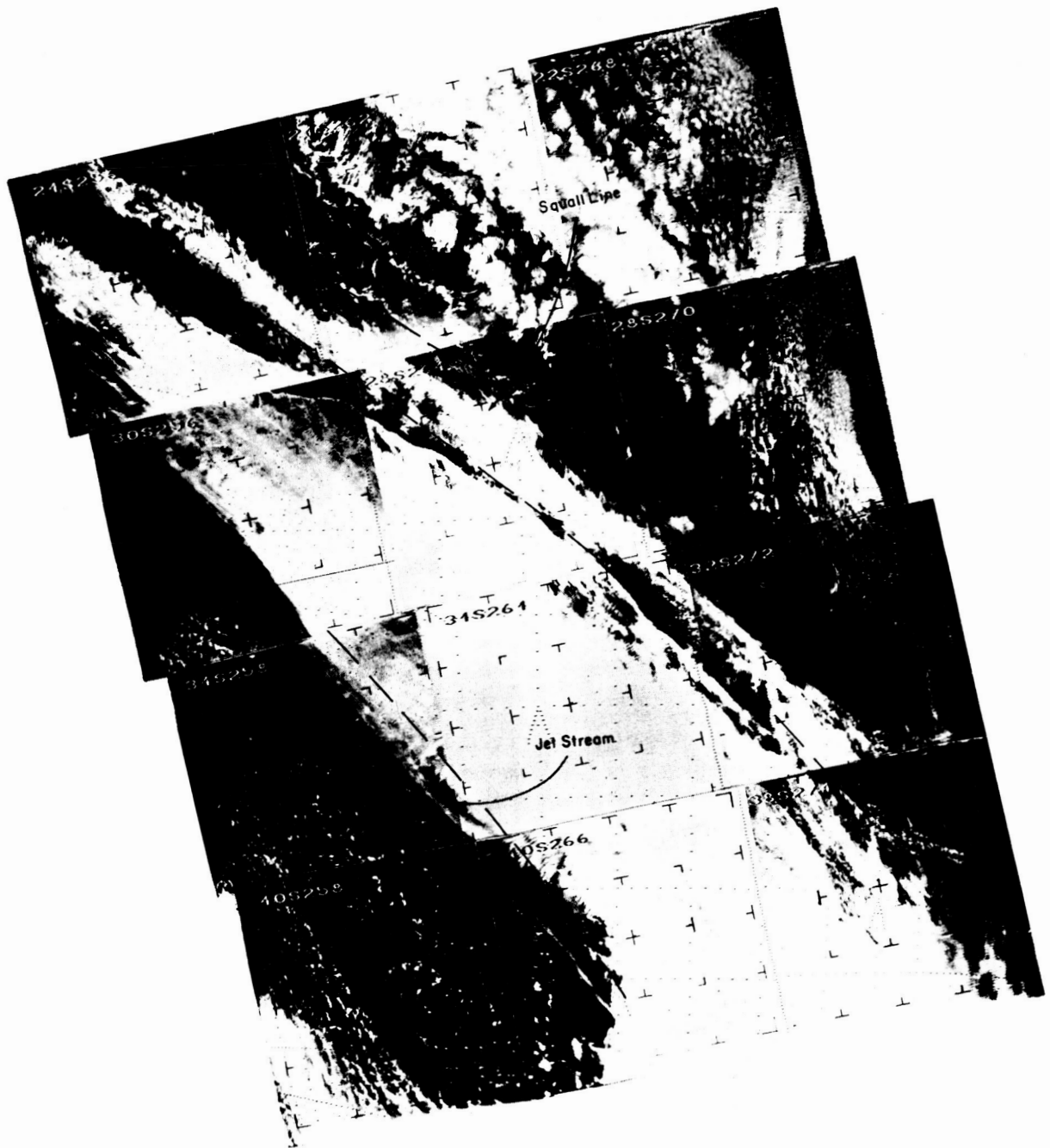
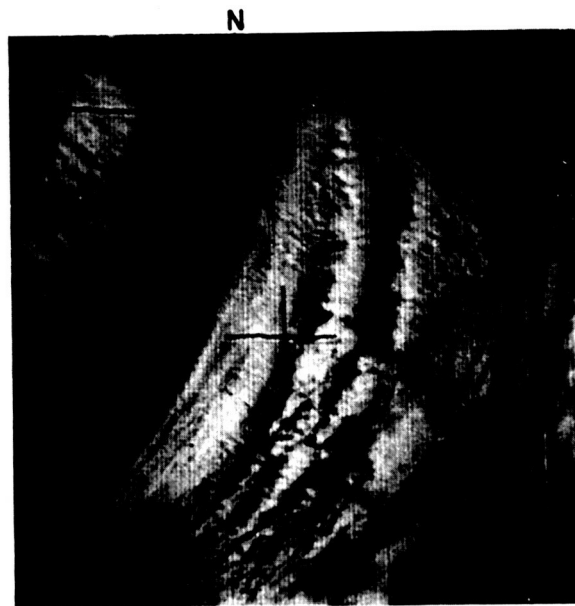


Figure 9-19—Pre-Frontal Instability Line or Squall Line, and Indication of a Jet Stream Associated with a Frontal Band (N)



(a) Instability Line Ahead of Cold Front



(b) Instability Line Cloud Band and Frontal Cloud Band

Figure 9-20—Pre-Frontal Instability

#### 9.2.2.1.3 Tropospheric Inversion Band (Fig. 9-22) (G)

The spreading out and merging of cumulus or stratocumulus clouds, produced by low level convective activity in the cold air behind a cold front, often produces cloud bands. The vertical cloud growth is inhibited, and horizontal spreading and merging take place, promoted by a strong lower tropospheric inversion. Positive differentiation of such bands from secondary cold fronts and post-frontal instability lines is often difficult.

#### 9.2.2.1.4 Frontal Bands (Fig. 9-23) (G)

A major frontal band is usually associated with an existing or recently dissipated cold or occluded front. The identification of the type of frontal band solely from a satellite picture is often difficult. Therefore, when the following five classes of frontal bands are cited, it is usually on the basis of correlating the satellite data with current synoptic data.

Warm Front – This is usually a relatively wide cloud band and is probably a cloud mass pertaining to the eastern edge of a vortex.

Cold Front – This is usually a relatively narrow band of clouds.

Occluded Front – A wide band of clouds, usually associated with a cloud vortex.

Stationary Front – Usually, identification is made on the basis of correlation with current synoptic data, or from past history. (Data from the same area 12-24 hours earlier.)

Triple Point of an Occluded Front – This is a wide cloud mass which depicts the point of intersection of the warm and cold fronts of an occluded frontal system. The triple point is usually associated with a cloud vortex to its west, and with a 500 mb short wave trough. The cloud band becomes narrower as one moves away from the triple point to either the south or northwest. Striated broken areas of cumuliform clouds may exist to the west or southwest of the triple point cloud mass.

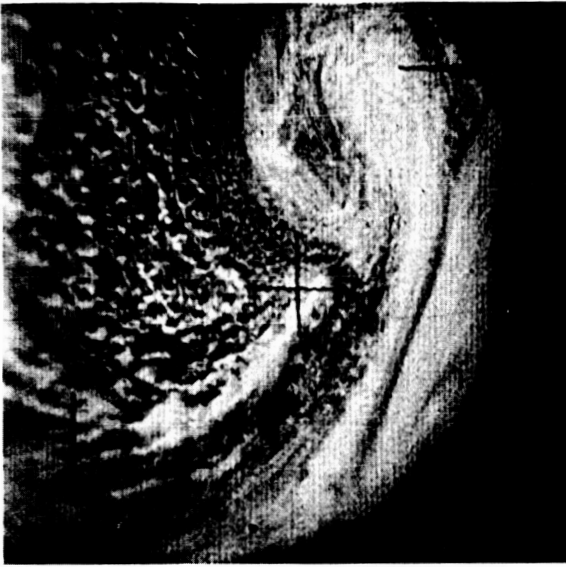


Figure 9-21—Post-Frontal Instability Line

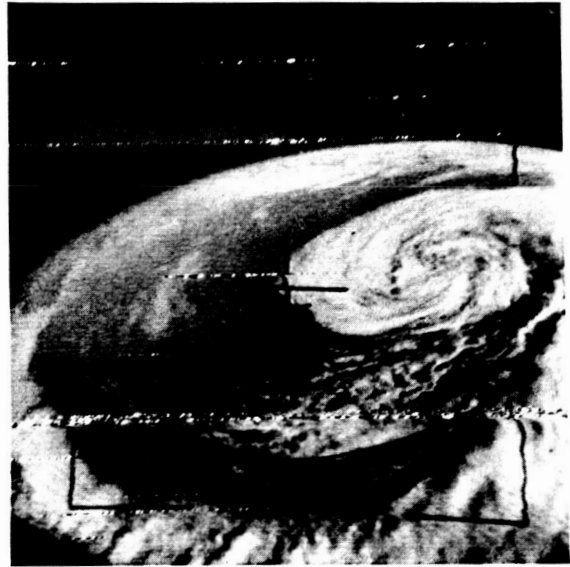


Figure 9-22—Tropospheric Inversion Band



Figure 9-23—Frontal Band (N)



Figure 9-24—Cirrus Bands Indicating Where Jet Stream Crosses Low Level Cloudiness

The following two types of frontal cloud bands can usually be identified on the basis of their appearance in a picture:

Indication of a Jet Stream Associated with a Frontal Band (Fig. 9-24) – A jet stream cloud band is frequently in evidence in the same picture as a frontal cloud band. Jet stream clouds usually appear as single or multiple, long, narrow, parallel bands of cirrus clouds, at times made visible against any lower clouds by the shadows they cast. The location of the jet stream cloud band, relative to the major frontal band, varies with the stage of development of the major synoptic system. In general, the jet stream cloud band may be several hundred miles poleward of a frontal wave, parallel to the major frontal band. As the system develops, the jet stream often crosses the frontal band near the point of occlusion (triple point).

Frontal Wave, Open or Developing Wave (Fig. 9-25) – A frontal wave is usually evidenced by a broadening or poleward bulging of the frontal band, which is often difficult to distinguish among other cloudiness. A frontal wave is, at times, accompanied by slightly curving parallel bands poleward of the frontal band, and/or by a more reflective area of higher and deeper clouds just east of the wave crest. Vortical cloud patterns are not in evidence. A weak closed cyclonic circulation may or may not be associated with the location of the wave on the surface synoptic chart.

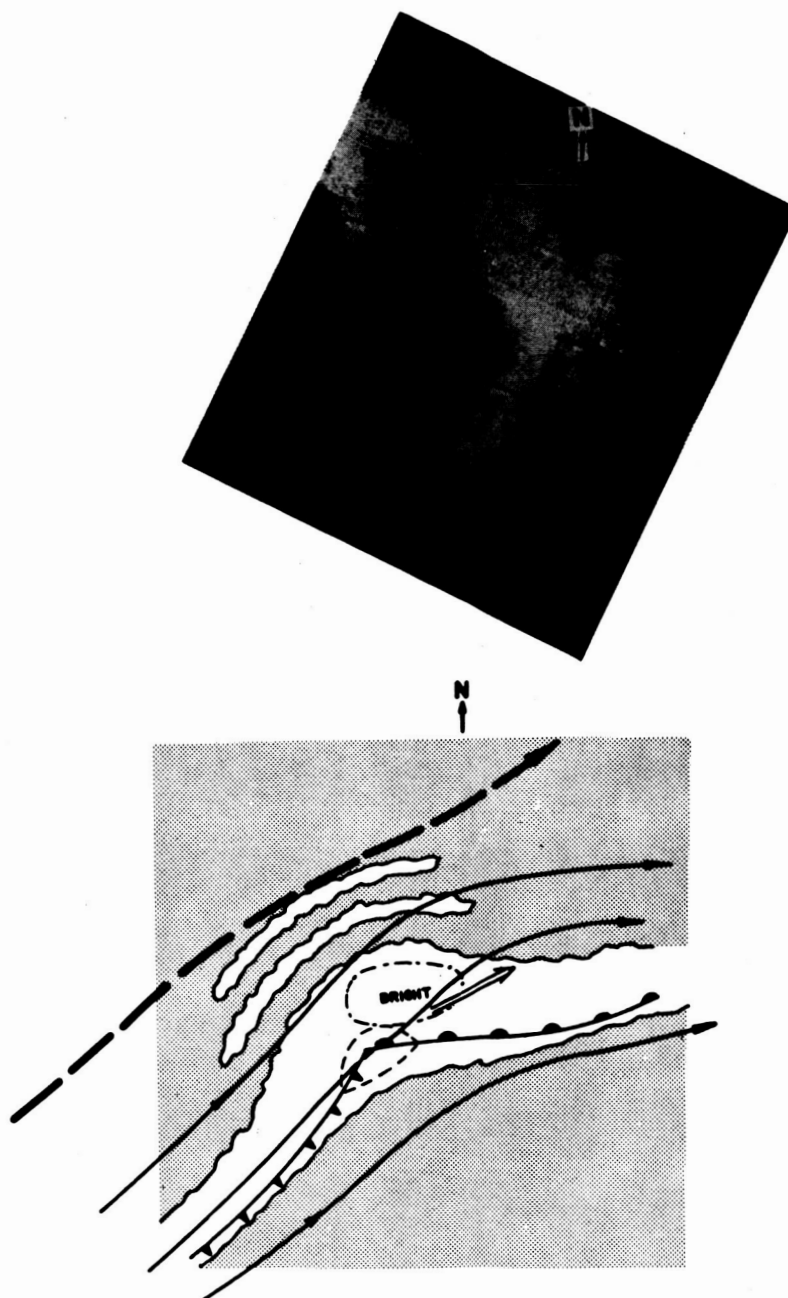
This classification also includes the so-called "pre-occlusion stage," which generally has a greater poleward bulging of the frontal band. Vortical cloud patterns are not in evidence. A closed cyclonic circulation is usually in evidence on surface synoptic charts, but has not yet reached the 500 mb level. A 500 mb short wave trough may be present, northwest of the wave.

#### 9.2.2.2 Tropical Cloud Bands (D)

Tropical cloud bands are often associated with areas of wind convergence and/or horizontal shear, or with mid-latitude cold fronts which have moved into the tropics.

##### 9.2.2.2.1 Mid-latitude Cold Front in Tropical Region (Fig. 9-26) (G)

These are extensive bands of cloudiness in lower latitudes, indicating the remaining effects of the penetration of a cold front. These cloud bands frequently



☐ — CLOUD

▒ — LAND AND OCEAN

#### FIGURE LEGEND

DASHED LINES — LOWER TROPOSPHERE FLOW    DOUBLE SHAFT ARROW — DIRECTION OF SYSTEM MOVEMENT  
 HEAVY DASHED LINES — TROPOPAUSE LEVEL FLOW  
 SOLID LINE — MIDDLE TROPOSPHERE FLOW

Figure 9-25a—Frontal Wave



N

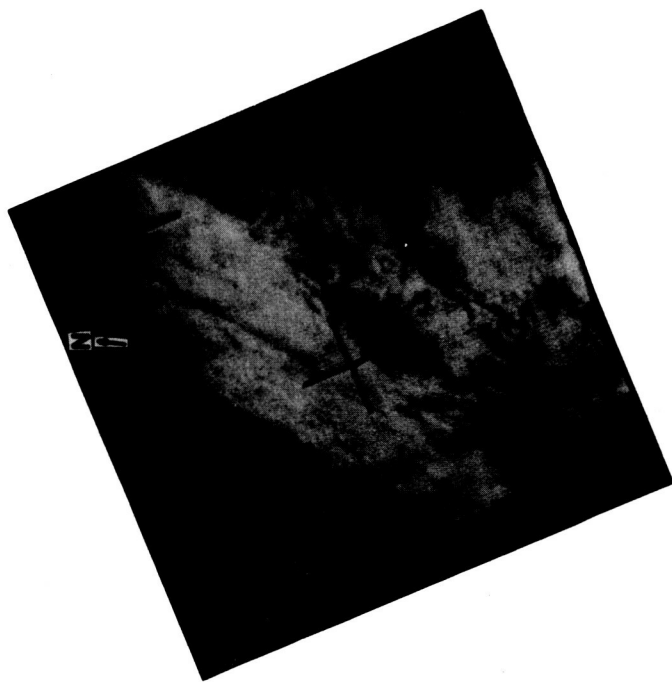
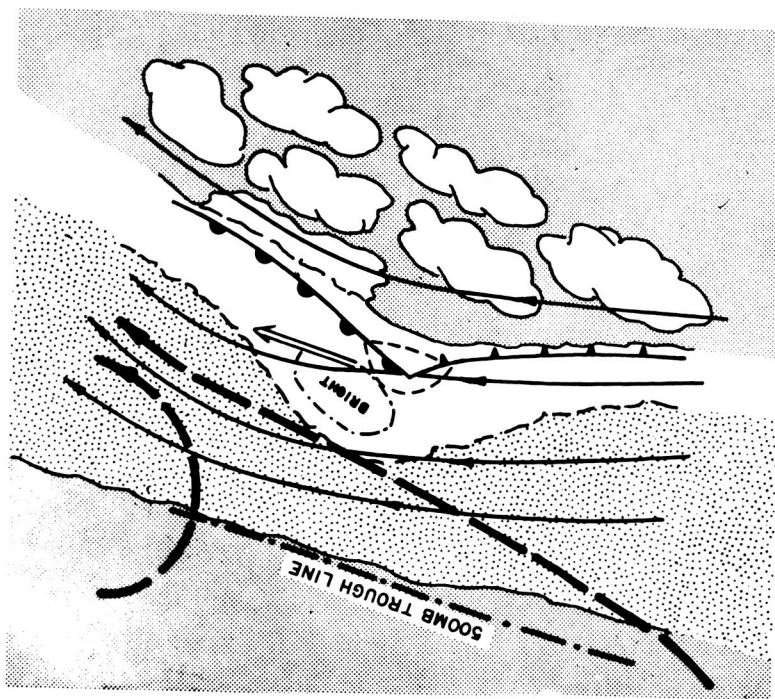


FIGURE LEGEND



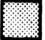

- |   |                  |   |                                    |
|---|------------------|---|------------------------------------|
|  | — CLOUD          |  | — LESS REFLECTIVE CLOUD            |
|  | — LAND AND OCEAN |  | DOT-DASH LINE — TROUGHS AND RIDGES |
| DASHED LINES — LOWER TROPOSPHERE FLOW   |                  | DOUBLE SHAFT ARROW — DIRECTION OF SYSTEM MOVEMENT                                   |                                    |
| HEAVY DASHED LINES — TROPOPAUSE LEVEL FLOW  |                  |   |                                    |
| SOLID LINE — MIDDLE TROPOSPHERE FLOW  |                  |   |                                    |

Figure 9-25b—Cloud-Masked Frontal Wave

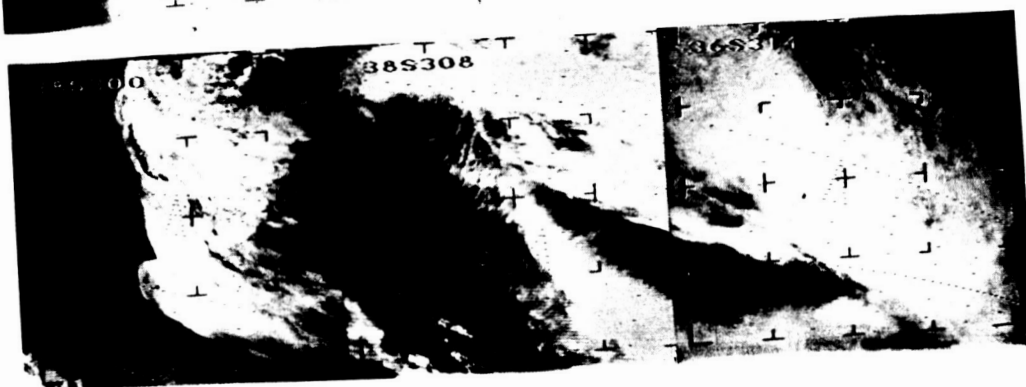
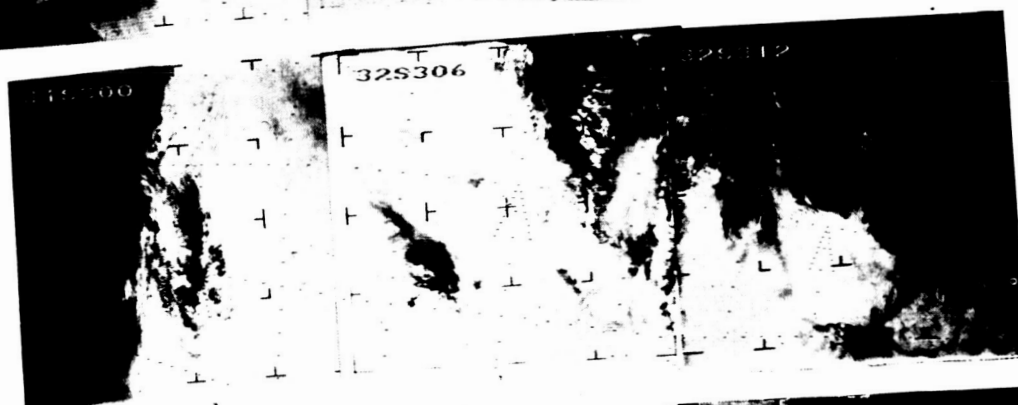


Figure 9-25c—Frontal Wave (Southern Hemisphere) (N)



(a) Cloud Band Associated with Mid-Latitude Cold Front Moving into Tropics



(b) Frontal Cloud Band at Low Latitudes

Figure 9-26—Mid-Latitude Cold Fronts in Tropical Regions

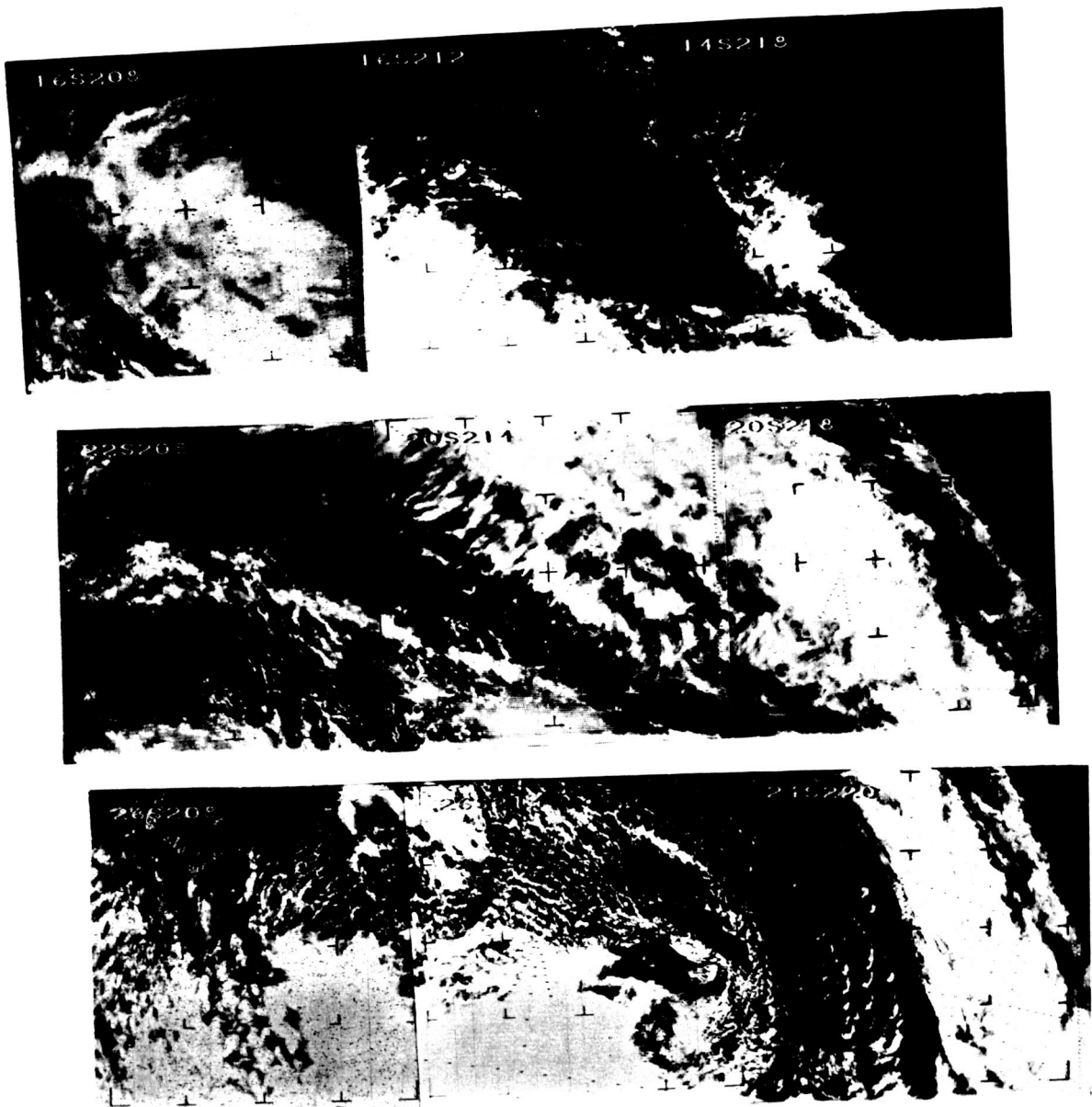


Figure 9-26 (Cont.)—Mid-Latitude Cold Fronts in Tropical Regions (N)

remain as significant features for several days after such convergence or shear lines cease to represent surface air mass boundaries. They frequently become quasi-stationary in areas of sparse synoptic data and hence may not show up on surface synoptic charts. This category is provided primarily to maintain historical continuity.

#### 9.2.2.2.2 Area or Lines of Convergence (Fig. 9-27) (G)

These are convergence lines or zones of heavy bands of cloudiness which are located primarily over tropical oceanic areas and are associated with monsoonal troughs and intertropical convergence (ITC) zones.

#### 9.2.2.2.3 Perturbed Tropical Cloud Band (Fig. 9-28) (G)

An apparent distortion of a major cloud band is often the first indication of the formation of a tropical storm. The distortion is in the form of a bending, folding, or bulging of the cloud band. These perturbed cloud bands may be the early stages of an easterly wave or easterly perturbation.

### 9.2.3 General Cloud Features (Neither Vortical Nor Major Bands)

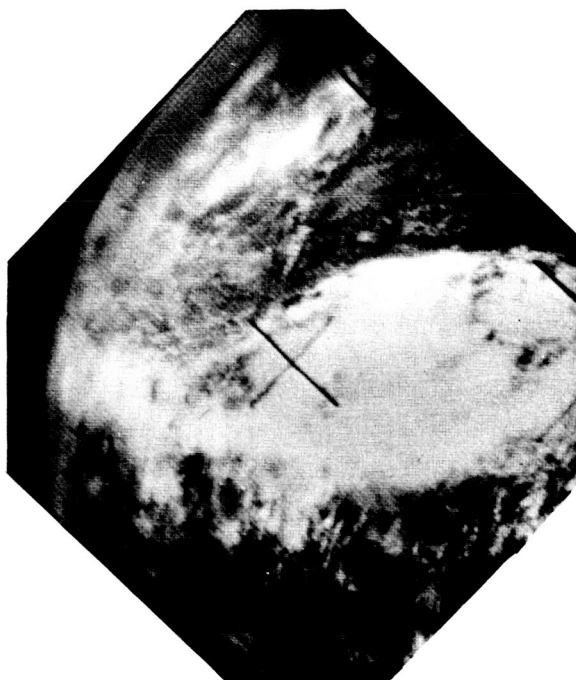
The satellite data depict cloud features which are neither vortical in character nor major cloud bands. These cloud features vary in size, shape, and coverage. They may be isolated or areas of clouds of more or less homogeneous characteristics. The divisions into stratiform cloud features and cumuliform cloud features are used in order to account for miscellaneous clouds which vary widely in character but are similar in type.

#### 9.2.3.1 Minor Cloud Lines or Parallel Bands (D)

These are lines, parallel lines, or minor bands of clouds of various widths, lengths, spacings and apparent cell sizes. These clouds may be oriented parallel, perpendicular or at other angles to the wind flow.

##### 9.2.3.1.1 Cloud Streets (Fig. 9-29) (G)

These parallel lines of cumuliform clouds, frequently oriented parallel to the wind flow, are found (1) in trade wind areas of the tropics, (2) associated

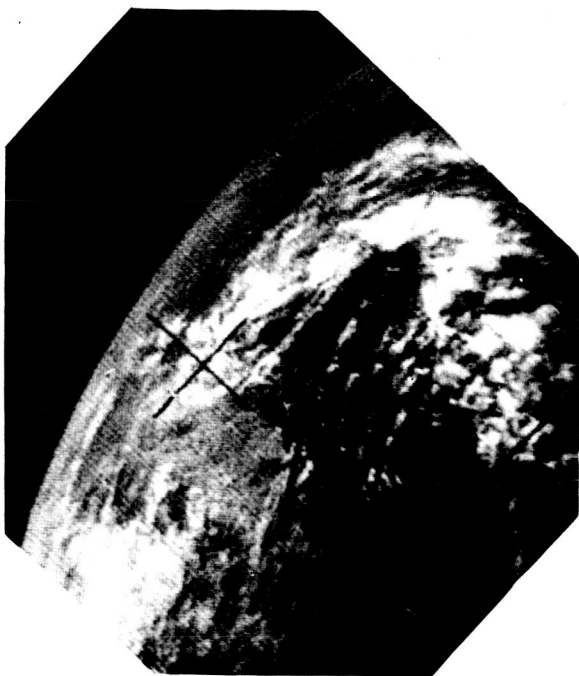


(a) Cloud Band Associated with Area of Convergence in Tropical Synoptic Scale Flow Pattern

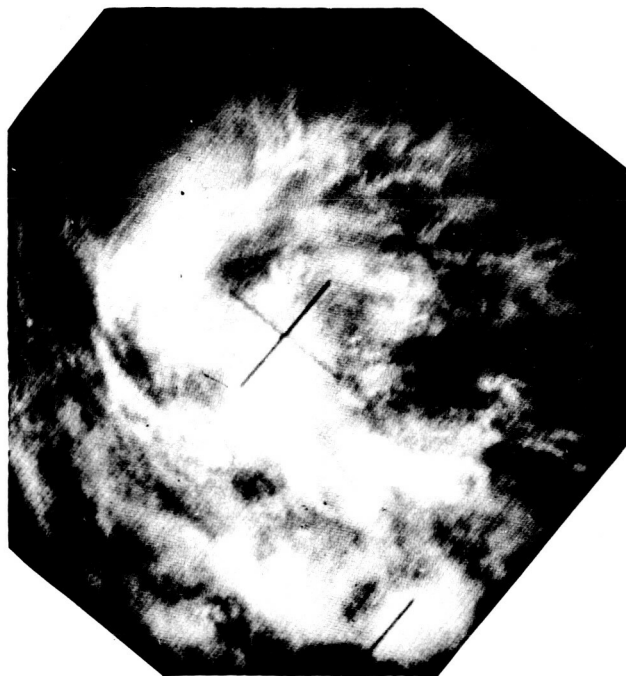


(b) Area of Convergence (N)

Figure 9-27—Line and Area of Convergence



(a) Formation of an Easterly Perturbation, "Bending" Pattern



(b) Formation of an Easterly Perturbation, "Folding" Pattern

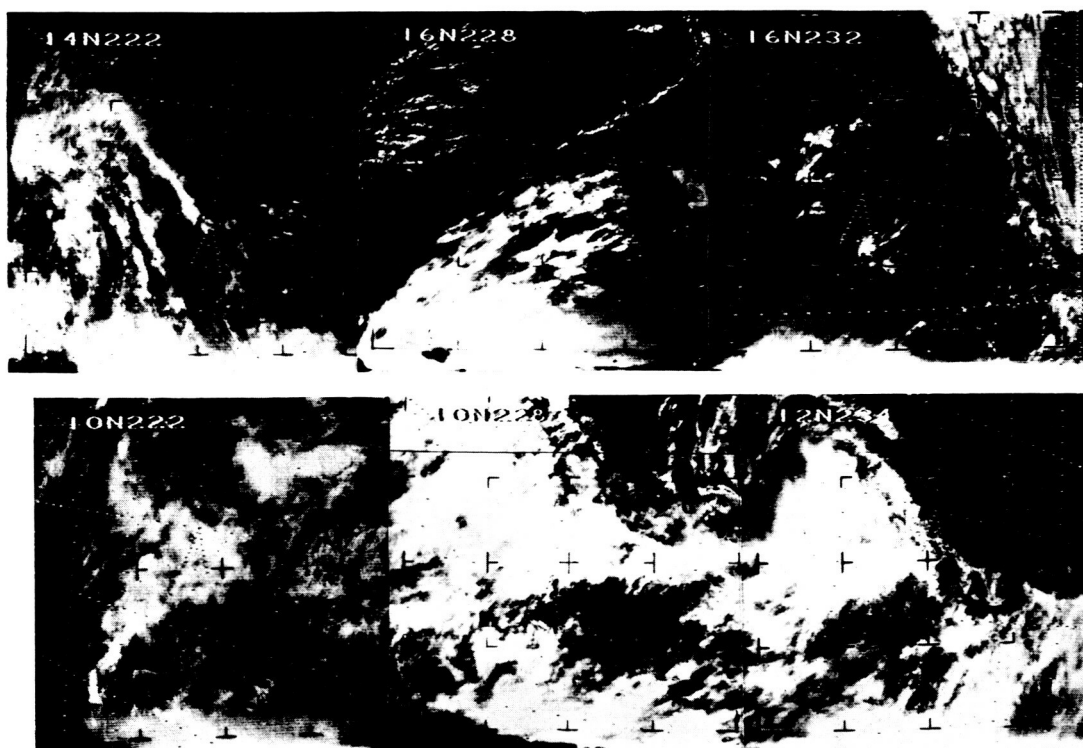


Figure 9-28—Perturbed Tropical Cloud Bands

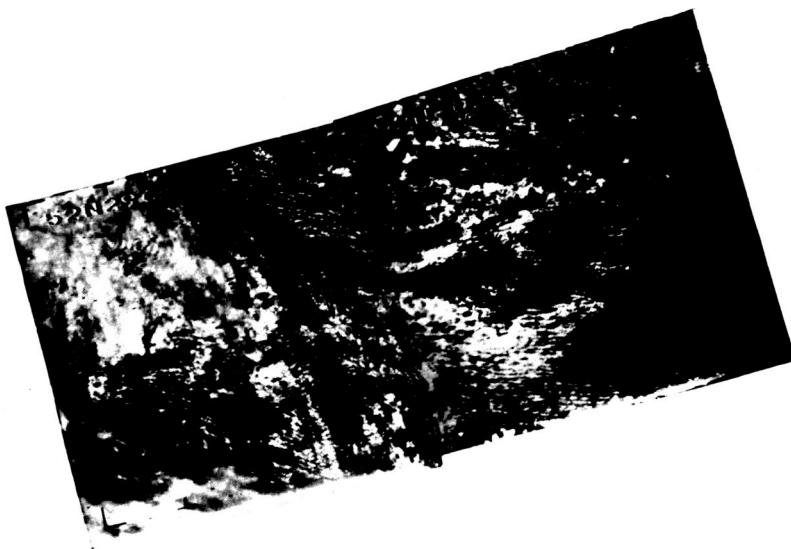


Figure 9-29—Cloud Streets (N)



Figure 9-30—Billow Clouds (N)



with low level inflow into major tropical storms or, (3) in association with circulations about extratropical cyclones, as well as in other types of situations. In many cases however, the cloud lines are not oriented parallel to the wind flow. Cloud streets observed contiguous to shorelines often provide an indication of offshore or onshore flow.

**Onshore Flow (C)** – In summer, when the land is warmer than the water, these clouds are usually found over land starting downwind from the shoreline. In winter when the water is warmer than the land, these clouds frequently form over the water and often extend across the shoreline to over the land where they are suppressed.

**Offshore Flow (C)** – In summer, these clouds tend to form over land and may extend across the shoreline to over the water surface where they are suppressed. In winter the clouds tend to form over water downwind from the shoreline.

#### 9.2.3.1.2 Billow Clouds (Fig. 9-30) (G)

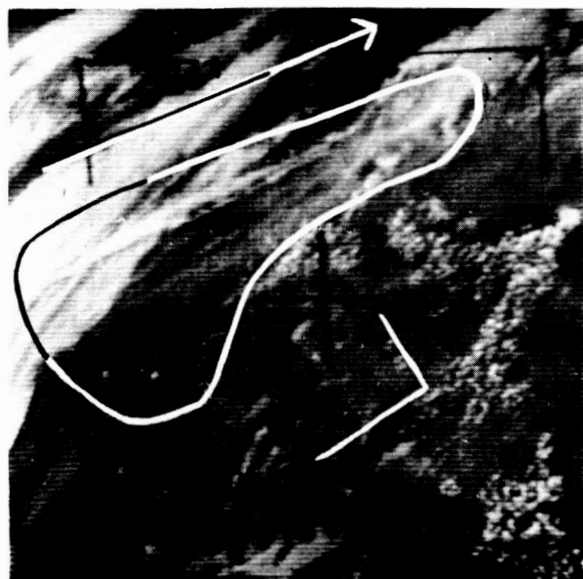
These are parallel lines of either cumuliform or stratiform clouds oriented perpendicular to the wind flow or shear. The clouds are in almost continuous bands as opposed to globular patterns. They are produced by disturbances within the air stream, often at inversions. It is often difficult to distinguish billow clouds from terrain-induced mountain wave clouds, except in cases in which the terrain and wind direction are known.

#### 9.2.3.1.3 Indication of a Jet Stream (Fig. 9-31) (G)

Long, relatively narrow cirriform cloud bands frequently indicate a jet stream just poleward of their location. They are easily identified, especially when they cast shadows on lower level cloud masses. This classification is used for jet stream clouds which appear without associated frontal cloud bands.

#### 9.2.3.1.4 Large Single Straight Lines (Fig. 9-32) (G)

These are large, single relatively straight lines of cumuliform clouds which are observed downstream from islands. These are probably thermally produced clouds resulting from air flow onto land that is significantly warmer than the surrounding water.



(a)



(b) Coast of Argentina (N)

Figure 9-31—Indication of a Jet Stream

#### 9.2.3.1.5 Crest Patterns (Fig. 9-33) (G)

These are predominantly cumuliform clouds over mountain or hilltop ridges. These cloud forms can frequently be distinguished from cloud streets by their close correlation with the topography. They are low clouds, usually 1000 to 3000 feet above the hilltops, oriented perpendicular to the wind flow. They may at times be difficult to distinguish from mountain wave clouds, but tend to dissipate as they move away from the associated topography and so to extend less distance downwind.

#### 9.2.3.1.6 Terrain Induced Wave Clouds (Fig. 9-34) (G)

These are forms of orographic cloudiness, over or downwind from hills or mountain ridges. They form in the crests of vertical waves produced by air flow over mountain barriers. These clouds must be related to the local geography and topography in order to be properly identified.

Lee Waves (Fig. 9-35) (C) – These are approximately parallel bands of straight or slightly curved stratiform appearing clouds over or downwind from hills or ridges, at altitudes not significantly greater than 10,000 feet above the terrain.

Mountain Waves (Isolated Lenticular Clouds) (Fig. 9-36) (C) – These clouds are usually small. When transparent, the lenticular clouds are not visible in satellite pictures. However, the large thick lenticular clouds are discernible and appear much like white circular cumulonimbus, often surrounded by cumuliform clouds of lesser development. They are found at levels at or above 20,000 feet, with thicknesses over 1500 feet.

Fibrous Plumes (Fig. 9-37) (C) – These are banded or fibrous stratiform streaky cirrus clouds. These clouds are usually at heights of 20,000 feet or higher over or downstream from hilltops or mountains.

#### 9.2.3.2 Cumuliform Cloud Features (D)

##### 9.2.3.2.1 Cellular Cloud Patterns (G)

These cellular appearing clouds, often in small geometrical patterns such as circular arcs, ellipses, etc., surrounding hollow clear areas, are characteristic of cumuliform development to the rear of mid-latitude oceanic cyclones as well as in the eastern portion of subtropical oceanic areas. Cellular cloud



CRETE

Figure 9-32—Large Single Straight Cloud Lines  
Downstream from Island



Figure 9-33—Crest Pattern Over the  
Rocky Mountains (N)

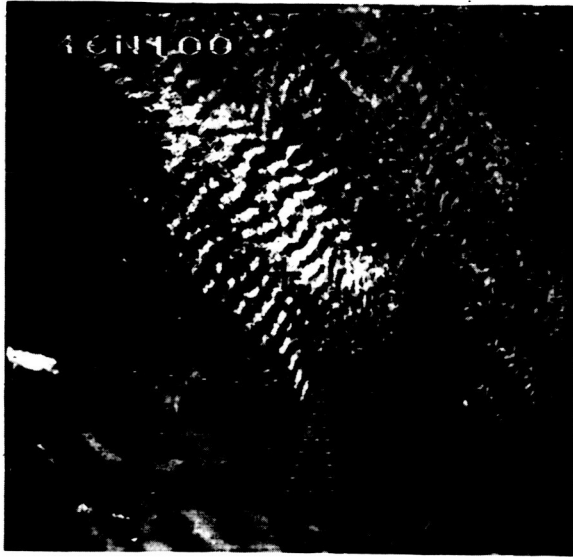


Figure 9-34—Terrain Induced Wave Clouds Over Mongolia (N)

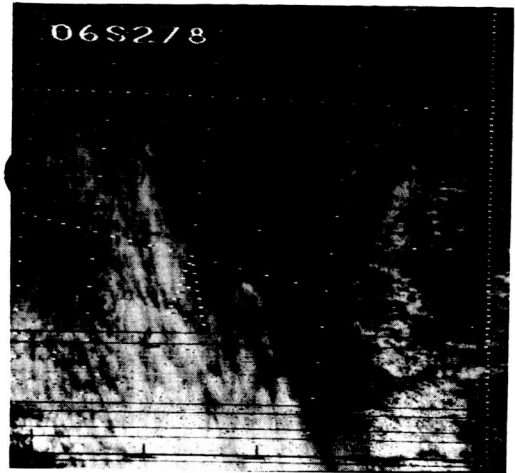


Figure 9-35—Lee Waves Over the Andes Mountains (N)



Figure 9-36—Lenticular Cloud at 35.0 N, 118.8 W Over the Tehachapi Mts. of California

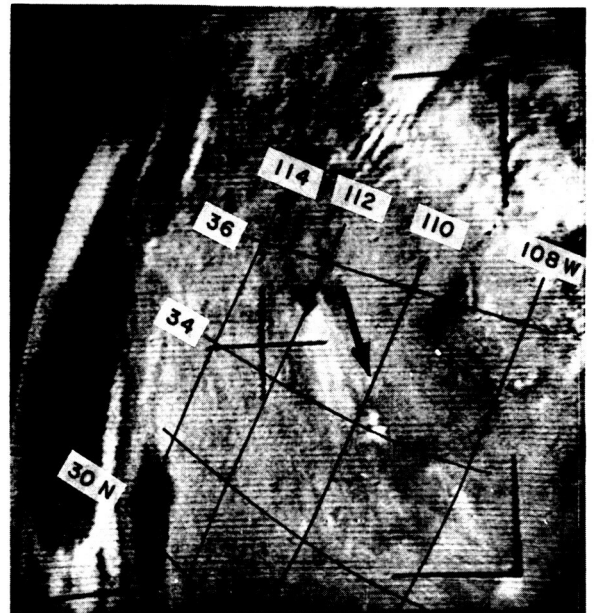


Figure 9-37—Fibrous Plumes. Initial Formation is Over the San Francisco Peaks, New Mexico

patterns are also observed over land, usually in a less organized manner. The diameters of the cells range from 20-50 n. mi. The cloud patterns often provide some identification of the low-level wind speeds and vertical shear. This is especially true when the cloud field is composed of low level cumuliform clouds with spacing between cloud elements (at TIROS resolution) greater than the smallest dimension of the cloud elements.

The classification of cellular cloud patterns, presented in the original study for this classification scheme, was based on a study of a small sample of southern hemisphere cases. A further study (Reference 43) was based on 103 northern hemisphere cases (TIROS IV and V data). The purpose of the study was to determine whether or not information about surface wind velocities in extratropical oceanic latitudes could be obtained from satellite pictures of low-level cumuliform clouds, rather than the development of a classification scheme for cellular cloud patterns. Nevertheless, some of the classes of cellular cloud patterns developed in the study are used in the following categorization:

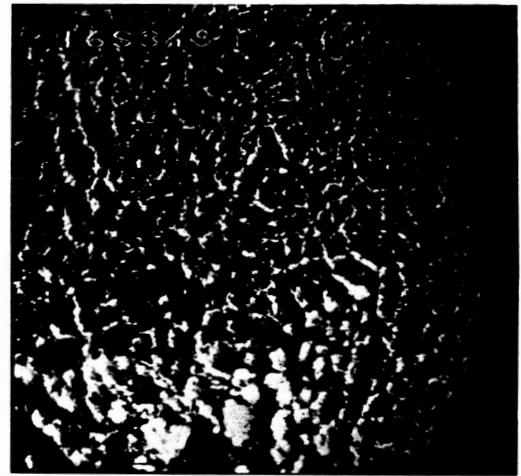
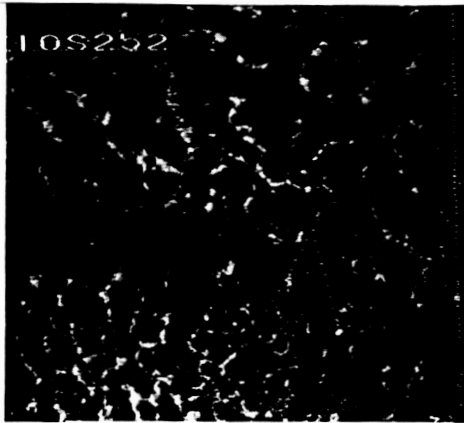
Polygonal Cells (Figs. 9-38 and 9-42a) (C) – Essentially regular polygonal cells, or circular areas of clouds surrounding a cloud free area. These cloud patterns occur with low level wind speeds of less than 20 knots. Towards the higher end of the speed range, the polygonal cells may become distorted into ellipses which tend to line up in a chain-like manner.

Scallops (Vermiculated) (Figs. 9-39, 9-42b and 9-42c) (C) – Chain-like cloud patterns with the crosswind links missing, or a double arrangement of cloud bands with a scalloped appearance. Cloud patterns in this class may appear in highly elliptical or oblong patterns. The scalloped pattern occurs primarily in the 20-25 knot low level wind speed range.

Linear Alignment of Cloud Elements (Blown-out Ellipses and Rows) (Fig. 9-40) (C) – These are either ellipses, not joined together, in a chain with open ends, or at higher wind speeds, parallel rows of non-continuous, short segmented, undefined cloud elements. These cloud patterns occur primarily with low level wind speeds greater than 13 knots.

Chaotic (Figs. 9-41 and 9-42c) (C) – No geometrical pattern discernible in the cloud field. This class tends to occur with low level windspeeds less than 30 knots.

Cloud Filled Cells (Figs. 9-42a and 9-42b) (C) – Circular or elliptical cells with interior cloudiness. To date, these cloud patterns have been observed primarily in tropical regions. Information on their relationship to low level wind speed is not presently available.



(a) Regular Polygonal Cells (N)

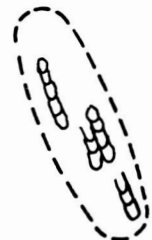
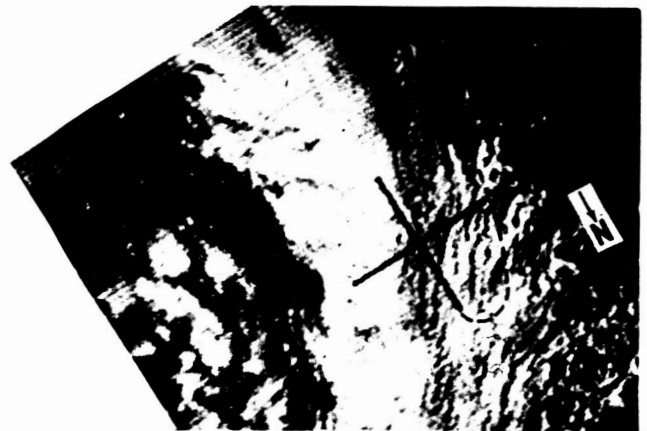
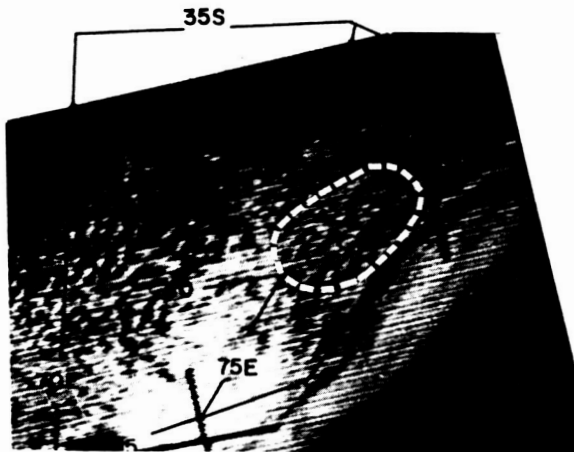
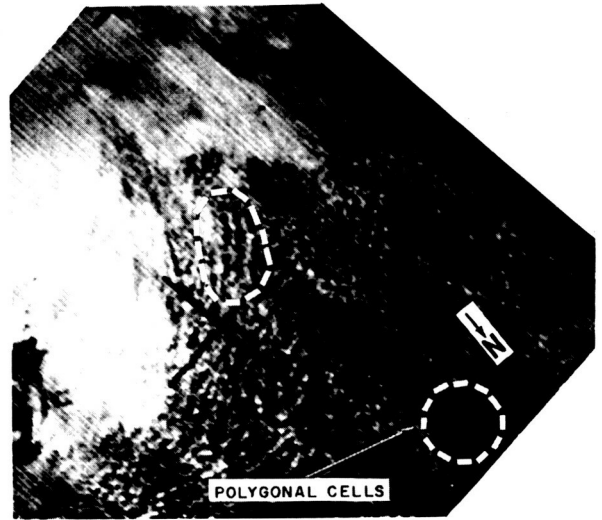
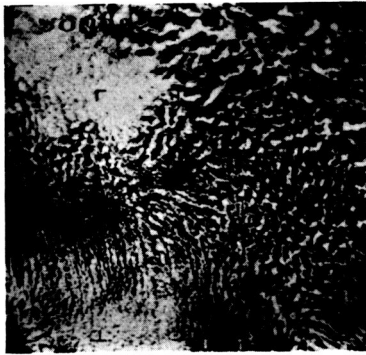


Figure 9-38—Polygonal Cells and Elliptical Chains



(a) Vermiculated (N)

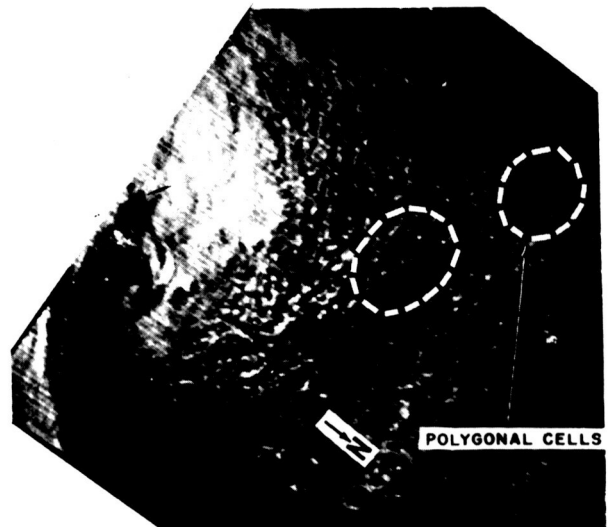
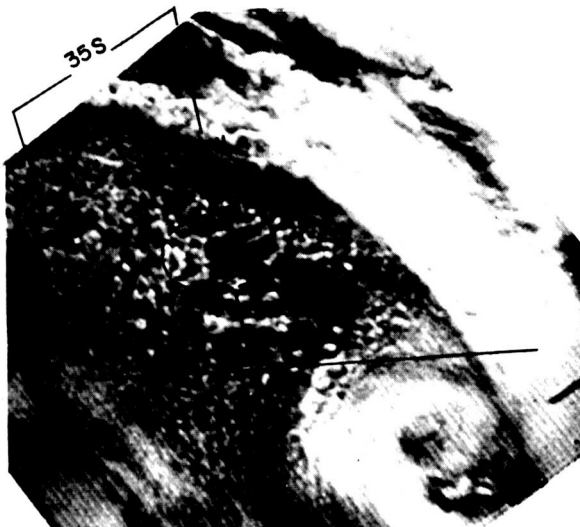
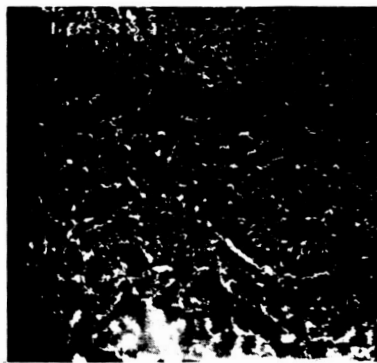
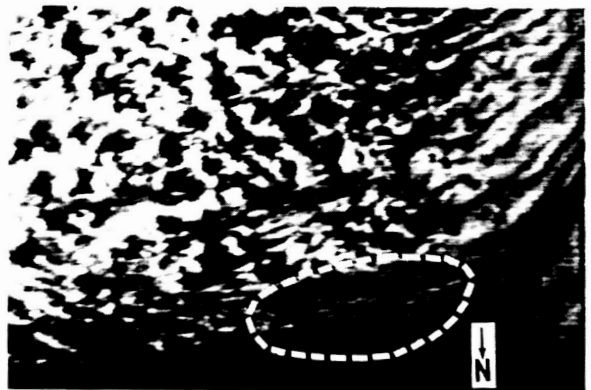
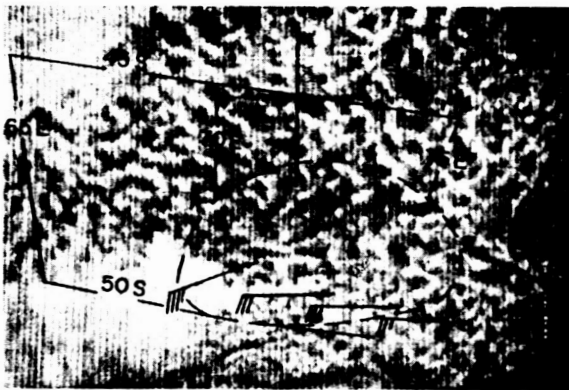


Figure 9-39-Vermiculated and Highly Elliptical Cells



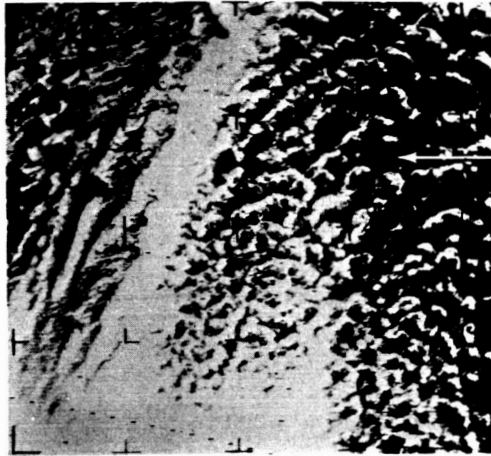


(a) Blown-Out Ellipses (N)

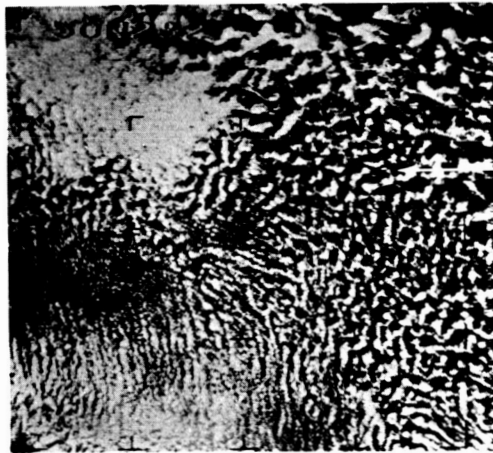


(b) Rows

Figure 9-40—Linear Alignment of Cloud Elements (Blow-Out Ellipses and Row Cloud Patterns)

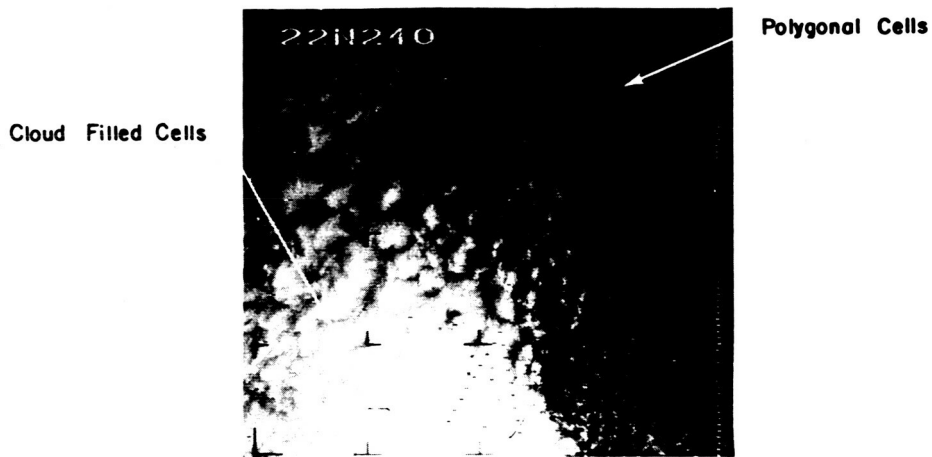


(a) Chaotic Pattern

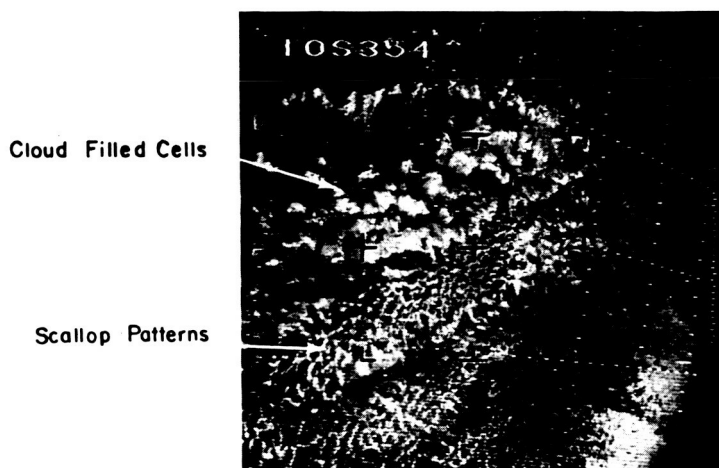


(b) Chaotic Pattern Over  
Southeastern Quebec, Canada

Figure 9-41—Chaotic Patterns (N)



(a) Cloud Filled Cells and Polygonal Cells



(b) Cloud Filled Cells and Scallop Patterns

Figure 9-42—Mixed Cellular Cloud Patterns (N)



(c) Scallop and Chaotic Patterns  
Over Quebec, Canada

Figure 9-42 (Cont.)—Mixed Cellular Cloud Patterns (N)

Actiniform (Fig. 9-43) – These are radiating or dendritic cellular cloud patterns. They usually are observed in areas of persistent subsidence inversions and appear to be related to cold ocean currents which may serve to intensify the inversions.

Mixed Cellular Cloud Patterns (Fig. 9-42) (C) – In some cases, more than one type of cellular cloud pattern is observed in the same picture or sector. This class is established to indicate that two or more identifiable cellular patterns are observed in the same picture. This class will be used under such circumstances rather than the group classification "Cellular Cloud Patterns," which will be used when the class of cellular cloud pattern is not known or determinable.

Large scale cellular bands, having longitudinal dimensions greater than approximately 180 n. mi., are occasionally associated with vortical clouds and/or frontal bands. These are usually altocumulus clouds rather than low-level cumuloniform bands and are usually observed in the same picture or sector as vortical clouds and/or frontal bands. These large scale cellular bands appear to have no preference as to the low level wind speed range. For these reasons a separate class has not been established for this class of cellular cloud patterns.

#### 9.2.3.2.2 Solid Cells (G)

These are isolated, random or evenly spaced cumulus, stratocumulus, altocumulus, or cumulonimbus clouds. Stratocumulus and altocumulus cloud patches, and cumulus clouds one-half mile or larger in diameter are visible in Nimbus AVCS pictures. Towering cumulus or cumulonimbus clouds may extend above and be identifiable against a lower continuous cloud deck.

Cumulonimbus Cloud Masses (Fig. 9-44) (C) – These are very white massive "blobs" of fully developed cumulonimbus clouds which are indicative of severe weather such as squall lines or thunderstorms. They are usually of medium size, unbroken, and of uniform appearance; often separated or completely isolated from other cloud cover, and measure up to 100 to 200 miles in length. Although each pattern is seen as a large unit (massive cloud blob) with little internal detail, the sharply defined borders, the scalloped appearance along portions of the border, and the overall intense brightness are indications of their convective nature. Squall lines rarely appear as a long line of cumulus development. A contiguous clear area is usually associated with a severe storm cloud pattern. The size of the clear area varies within wide limits.

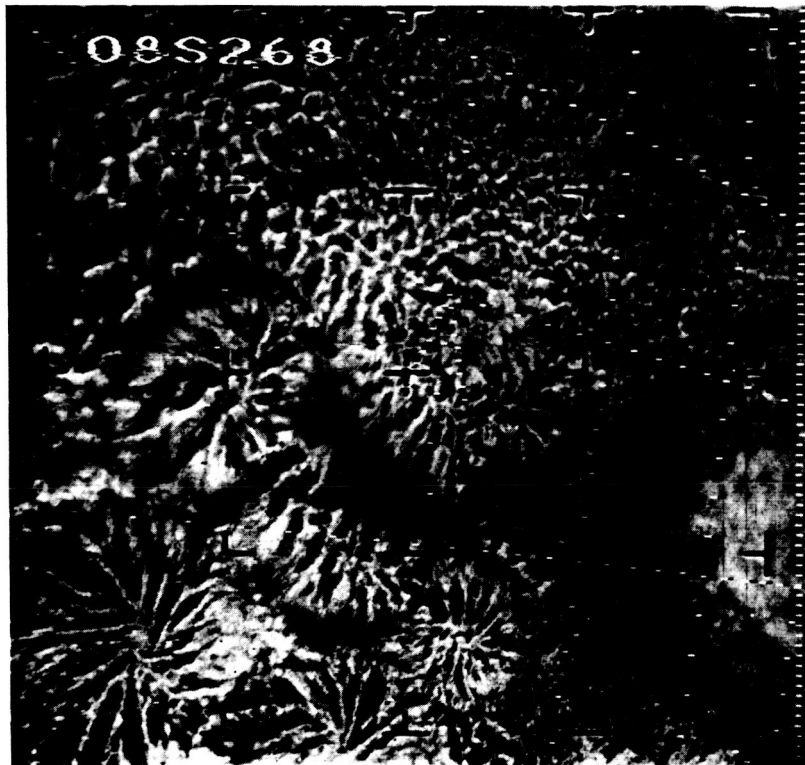
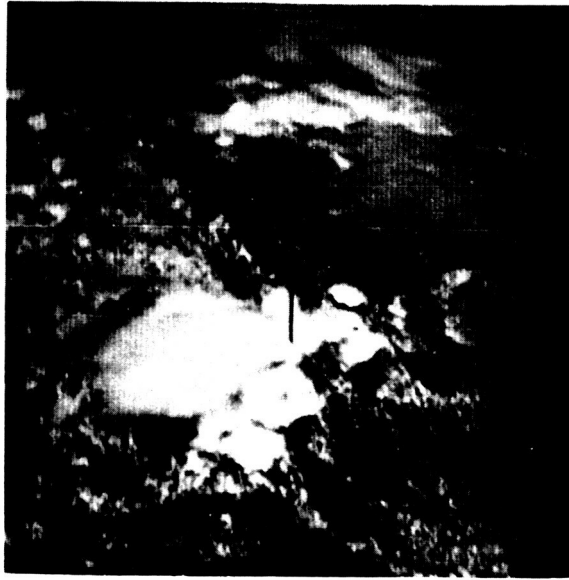
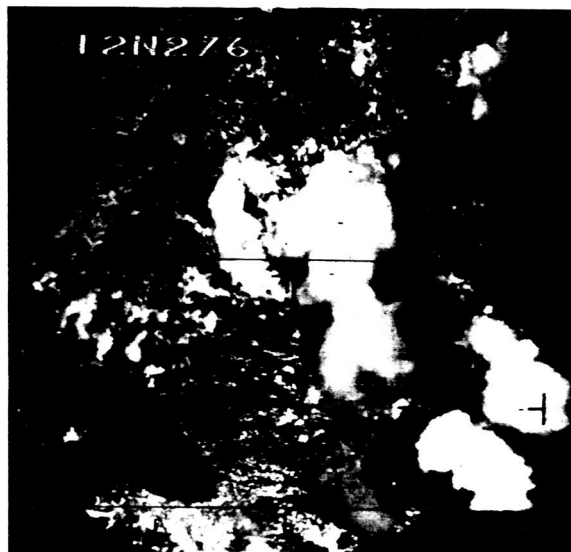


Figure 9-43—Actiniform Cloud Patterns (N)



(a)



(b) (N)

Figure 9-44—Cumulonimbus Cloud Masses

Cumulonimbus Clouds (Fig. 9-45) (C) – When not deeply imbedded in other clouds, these clouds appear as bright blobs 5 to 20 miles in diameter, or in patches up to 50 miles or more across. The larger sizes are clusters of cumulonimbus clouds, the apparent size enhanced by degradation and the formation of dense cirrus anvils.

Towering Cumuli (Fig. 9-46) (C) – Scattered towering cumuli, often within a field of smaller cumuli or cirrus, appear as a spotted or mottled sheet. The individual cumuli are usually up to two miles in diameter and are spaced five to ten miles apart. One usually sees the larger cluster rather than the individual cloud.

Cirriform Anvils (Fig. 9-47) (C) – These cirriform plumes are frequently associated with isolated cumulonimbus clouds in subtropical and temperate areas. The plumes extend in the direction of the wind or shear at levels of the order of 300 mb. Cirrus anvils may also be observed to blend with large cumulonimbus cloud masses, making them appear as single, large bright cloud masses.

#### 9.2.3.2.3 Unorganized Fair Weather Cumuliform Clouds (G)

These are small cumuliform clouds in random arrays. When contiguous to a land-water boundary, they may indicate onshore or offshore wind flow.

Onshore Flow (Fig 9-48b) (C) – The direction of flow can often be identified from low level cumuliform clouds contiguous to shorelines or coastlines. In summer, when the land is warmer than the water, these clouds are over land starting downwind from the shoreline. In winter, when the water is warmer than the land, these clouds form over the water and often extend across the shoreline to over the land where they are suppressed.

Offshore Flow (Fig. 9-48c) (C) – The direction of flow can also often be identified from low level cumuliform clouds contiguous to a shoreline or coastline in summer. These clouds form over land and extend across the shoreline to over the water surface, where they are suppressed. In winter the clouds form over water downwind from the shoreline.

Figure 9-49 illustrates unorganized fair weather cumuliform clouds which are not contiguous to shorelines.





Figure 9-45-Cumulonimbus Clouds (N)

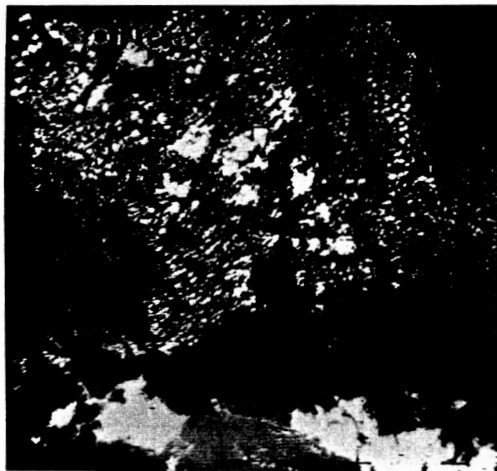


Figure 9-46-Towering Cumuli with  
Cumulonimbus Clouds (N)

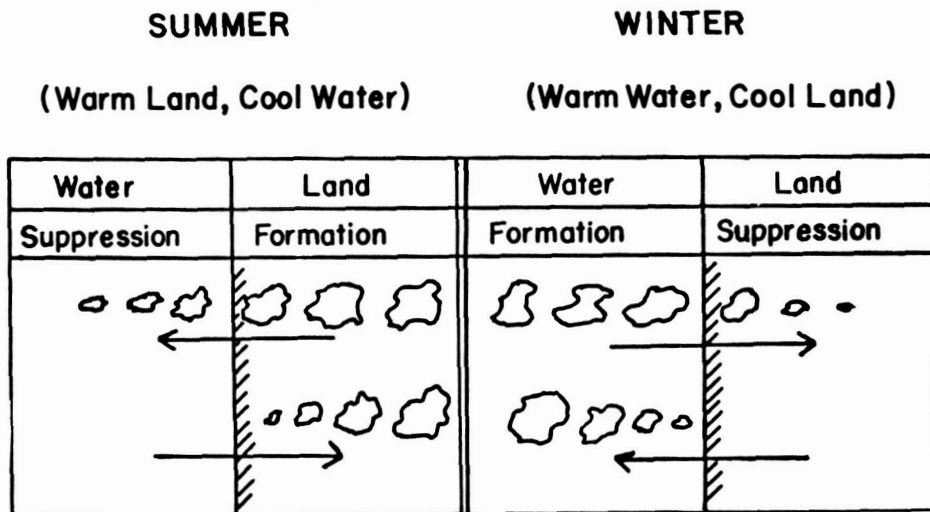


(a) (N)



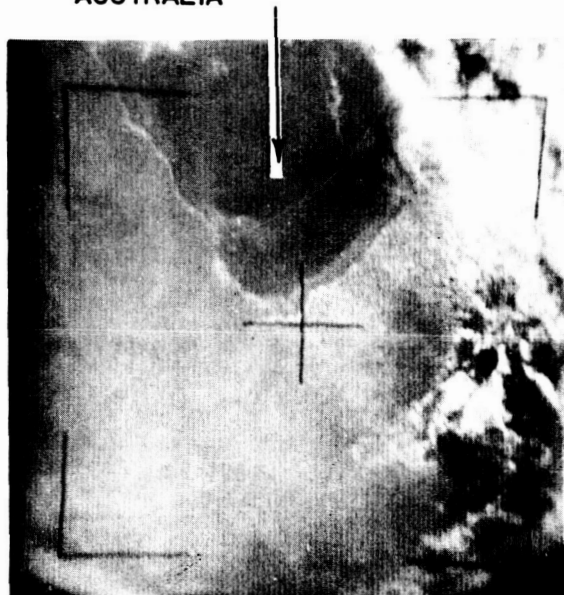
(b)

Figure 9-47—Cumulonimbus with  
Cirrus Anvils

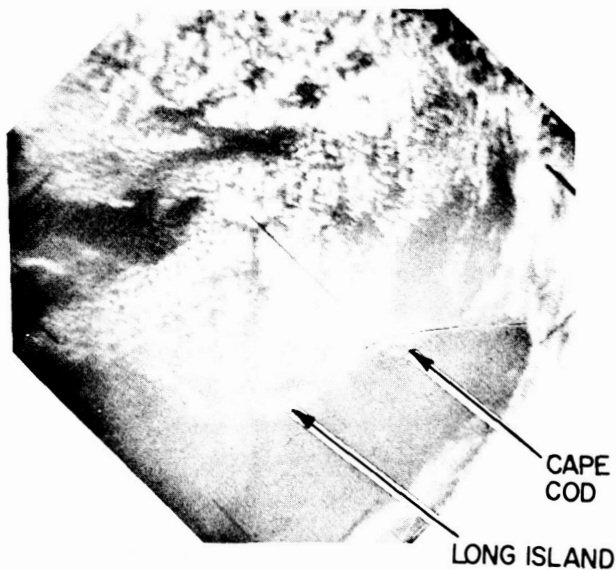


(a) Wind Direction Shown by Arrows in Relation to Cumulus Cloud Formation and Suppression Over Adjacent Land and Water Areas

GULF OF CARPENTARIA, NORTHERN AUSTRALIA



(b) Onshore Flow (Summer)



(c) Offshore Flow (Summer)

Figure 9-48—Cumuliform Clouds Indicating Onshore and Offshore Flow

### 9.2.3.3 Stratiform Cloud Features (D)

This division includes cirrus, altostratus, stratus, or apparent sheets of clouds which in certain geographical areas, are often atmospheric pollutants and obscurations.

#### 9.2.3.3.1 Atmospheric Pollutants (Fig. 9-50) (G)

These are sheets of stratiform appearing, non-fibrous, nonbanded, dark gray or gray cloud forms or obscurations. These cloud forms or obscurations are frequently haze, smoke, dust or smog over land or sea. The type of pollutant occasionally can be identified by correlating the phenomenon with a knowledge of the geographical area and the current synoptic data. The basis for assigning the type of pollutant should be noted in the remarks section of the appropriate documents.

#### 9.2.3.3.2 Stratus or Fog (G)

These clouds, often weakly fibrous or streaky in appearance, are observed in valleys or areas of land-water interface; in the stable eastern portion of subtropical anticyclones, and in general, in areas of atmospheric stability. They may appear as bright as cumulus or cumulonimbus clouds.

Coastal Stratus or Fog (Fig. 9-51) (C) – This is an area of stratus clouds or fog located only over land or only over water, and terminating approximately at the coastline.

Penetrating Stratus or Fog (Fig. 9-52) (C) – This is an area of stratus clouds or fog located primarily over water, which penetrates the coastlines and extends over land; or of low stratus or fog primarily over land, which penetrates the coastline and extends over water.

Sea Stratus or Fog (Fig. 9-53) (C) – This is an area of stratus clouds or fog over the open ocean.

Land Stratus or Fog (Fig. 9-54) (C) – This is an area of stratus clouds or fog over land.

Valley Stratus or Fog (Fig. 9-55) – This is an area of stratus clouds or fog in a valley whose shape correlates with that of the valley.

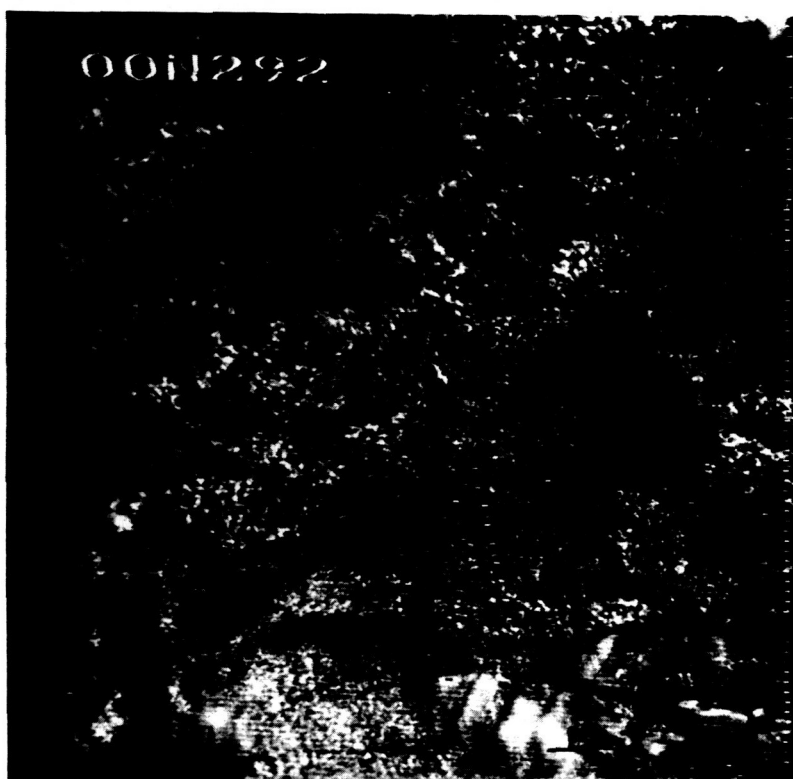


Figure 9-49—Unorganized Fair Weather Cumuliform Clouds, Not Associated with Shorelines (Over Northern Brazil) (N)

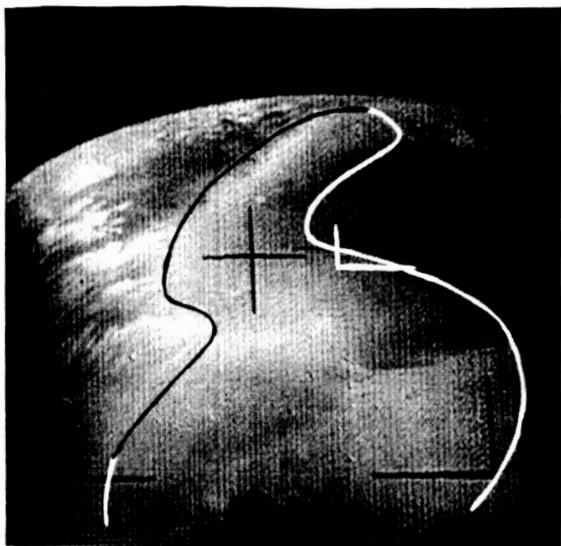


Figure 9-50—Atmospheric Pollutant Stratiform  
Appearing Neither Banded nor Fibrous-Dust



Figure 9-51—Coastal Stratus or Fog Along  
the Coast of Chile (N)

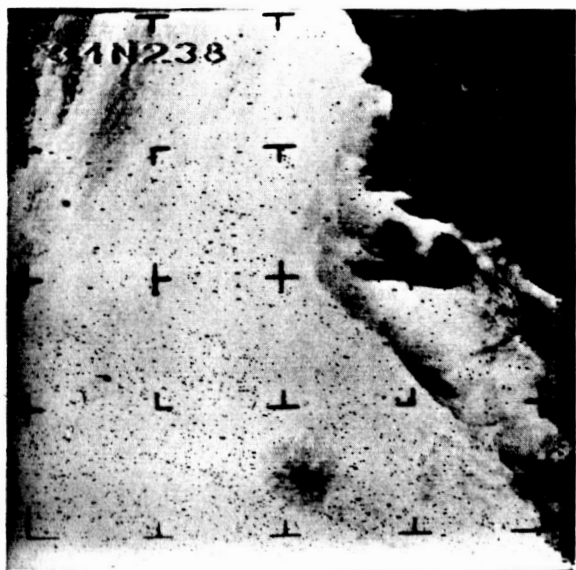


Figure 9-52—Stratus or Fog Penetrating the  
Coastline of California (N)



Figure 9-53—Sea Stratus or Fog Off the  
Coast of Northern California (N)



Figure 9-54—Land Stratus or Fog  
(Over Sweden) (N)



Figure 9-55—Valley Stratus or Fog (Over  
Northern Siberia) (N)

#### 9.2.3.3.3 Middle or High Stratiform Clouds (G)

These are cirrus, cirrostratus, altocumulus, or altostratus clouds banded, nonbanded, striated or fibrous in appearance. Extreme areas of these clouds are usually associated with vortical clouds or major cloud bands.

Middle Clouds (Fig. 9-56) (C) – These are altostratus or altocumulus clouds which often occur in combination with each other or with clouds at a lower level, in two or more levels. It is usually not possible to distinguish separate layers or the individual cloud types.

High Clouds (Fig. 9-57) (C) – These are cirrus or cirrostratus clouds which are visible when thick, except against a background of lower cloud masses. When these clouds appear in bands or striations indicating the presence of a jet stream, they are classified as jet stream cirrus and placed in a different category (see Section 9.2.3.1.3). They are also put into a different category (see Section 9.2.3.2.2) when they appear as anvils associated with cumulonimbus clouds.

Fibrous Cirrus (Fig. 9-58) (C) – These are fibrous elements of cirrus clouds which do not appear to form a continuous cloud layer.

#### 9.2.3.3.4 Medium Resolution Infrared Radiometer (MRIR) and High Resolution Infrared Radiometer (HRIR) (D)

The visible contrasts noted in nighttime HRIR and in Channel 2 MRIR data are temperature contrasts, and not the contrasts in reflectivity seen in television pictures. Cloud vortices and major cloud bands are well depicted in Nimbus I HRIR data and TIROS Channel 2 MRIR data. It is assumed that these and perhaps other features will be well depicted in Nimbus II HRIR and MRIR data, and will be appropriately classified. Classification of the data content of MRIR data will be made on the basis of Channel 2 (10-11 microns) supplemented by data from the other channels, especially the albedo channel, Channel 5 (0.2-4.0 microns).

Several cloud patterns which belong to the category, "General Cloud Features," are visible in Nimbus I HRIR data. The chief exception is that of low clouds. It is assumed that a similar situation will exist in Nimbus II data. It is also believed that most "General Cloud Features" may not be visible in Nimbus II MRIR data. The division, "Infrared Radiometer," is established for these reasons. MRIR Nimbus data which cannot be unambiguously identified will almost always be placed in this division. The division "Infrared Radiometer," will also be used as a last resort for HRIR data which cannot be assigned a specific classification.



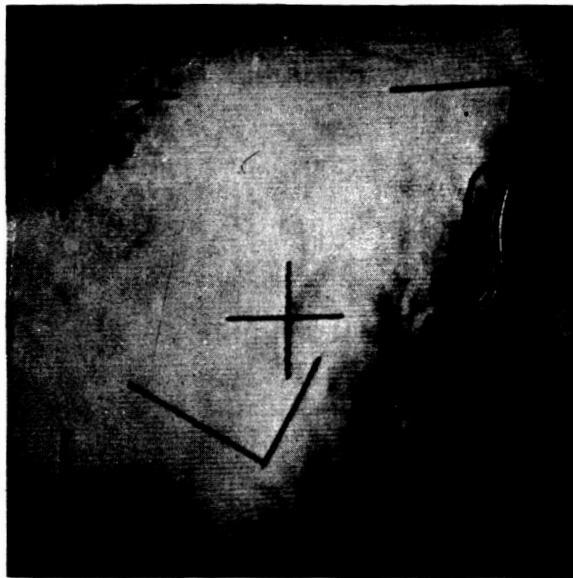


Figure 9-56(a)—Stratiform Cloud Appearing  
Neither Banded Nor Fibrous-Alto-Stratus

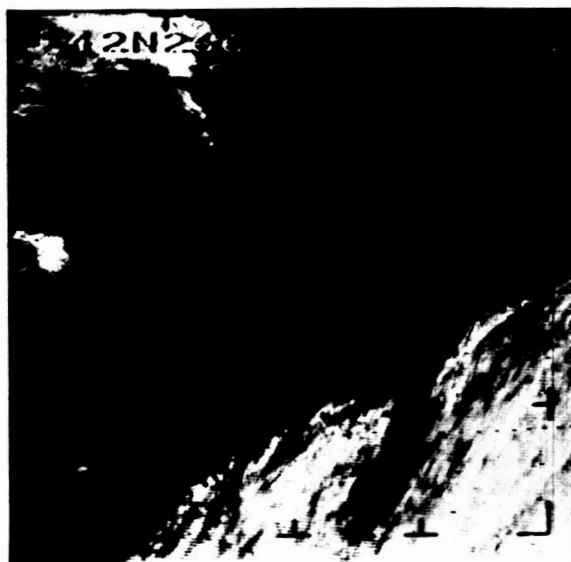


Figure 9-56(b)—Middle Stratiform Clouds (N)

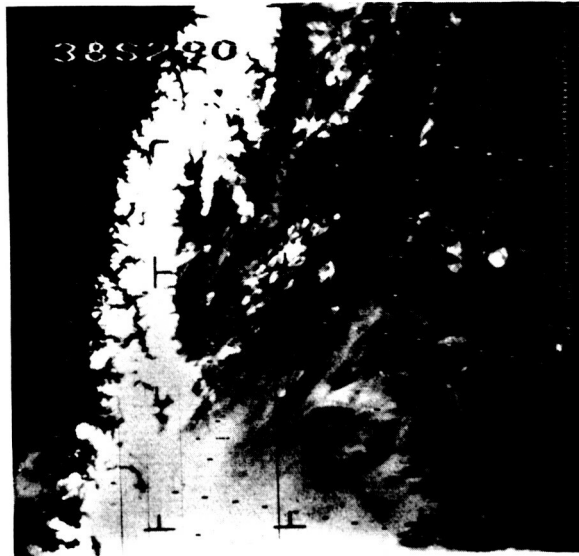


Figure 9-57—High Stratiform Cloud Over Argentina and the Snow Covered Andes Mountains (N)

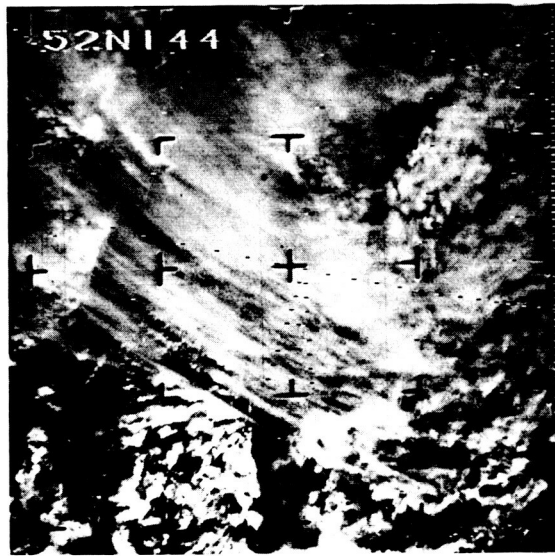


Figure 9-58—Fibrous Cirrus with Towering  
Cumulus and Altocumulus Clouds (N)

Since the brightness of HRIR and Channel 2 MRIR data is related to temperature, brightness provides an indication of cloud top height. Although the interpretation of the brightness of HRIR and MRIR data is subjective, it is believed that such interpretation will be useful to the researcher. The following table relates brightness and temperature of MRIR and HRIR positive film data to cloud height and terrain.

<u>HRIR and Channel 2 MRIR Brightness (Positive)</u>	<u>Relative Temperature</u>	<u>Frequent Implication</u>
White	Very cold	High clouds, polar or high level terrain, ice or snow
Off-white	Cold	Middle clouds
Gray	Cool	Low clouds, indefinite terrain
Black	Warm	Ocean, land, or below film range
Visible and identifiable	Varies with nature of landmark	Landmarks

Low level clouds are usually only dimly visible, or at times not even discernible, in MRIR and HRIR data. Since low level clouds are usually in the same temperature and brightness range as the terrain, the observation of identifiable landmarks by the analyst is the only assurance that low clouds do not exist. It is also possible to mistake ice or snow in polar areas and high mountain regions for middle-to-high clouds. Recent investigations indicate that cirrus clouds generally are not visible, unless very thick, when they exist in the absence of other cloudiness. A picture will be placed in the category "indistinguishable features," whenever a clear distinction cannot be made between (1) low level clouds and the terrain, (2) between clouds and snow or ice fields, or (3) clouds above a continuous undercast. An appropriate entry will be made in the remarks section of the Data Log Section of the Nimbus II Users' Guide to indicate the probable classification to the data.

The following groups, under the division, Infrared Radiometer, will be used to classify MRIR and HRIR data which display distinguishable and/or identifiable features but are not vortical cloud patterns, major cloud bands or discernible general cloud features.

## **Infrared Radiometer (D)**

**Low Level Clouds (Fig. 9-59) (G) – Large area of smooth gray or dark gray clouds.**

**Medium Level Clouds (Fig. 9-59) (G) – Large area of smooth off-white clouds.**

**Random Patterns (G)**

**Low and/or Middle Clouds (Fig. 9-60) (C) – Unorganized gray and/or off-white clouds.**

**Mostly Open High Clouds (Fig. 9-61) (C) – 20 percent to 50 percent of the image depicts white clouds.**

## **9.3 HRIR Data**

With the exception of Figures 9-59 through 9-61, Nimbus and TIROS television pictures have been used to illustrate the various categories of data content classification and their subdivisions. This approach was based on the assumption that the various cloud features could be illustrated and initially understood much better from television pictures than from HRIR data. Nimbus I HRIR data which depict vortical cloud features, major cloud bands and/or general cloud features are presented in this subsection for illustrative purposes. A detailed treatment of the interpretation of Nimbus I HRIR data is contained in a recent study (Reference 44).

The meteorological interpretation of the HRIR data presents no great problems to persons previously skilled in the interpretation of satellite pictures, provided the analyst keeps in mind the fact that the visible contrasts are those of temperature and not of reflectivity. At first this requires a distinct effort because of the great resemblance between HRIR strips and many satellite TV pictures, especially in the cloud features and patterns now so familiar from the satellite pictures. Perhaps the chief new problem is the fact that low clouds, which would be among the significant features in a satellite picture, may be only dimly visible or at times not even discernible in the HRIR data.

Otherwise, it appears that most of the principles developed for interpretation of the satellite TV cloud pictures are generally valid when dealing with the HRIR data. Vortices, cloud patterns associated with short wave troughs, major or active frontal bands, tropical storms, and other similar major features can

Low level clouds

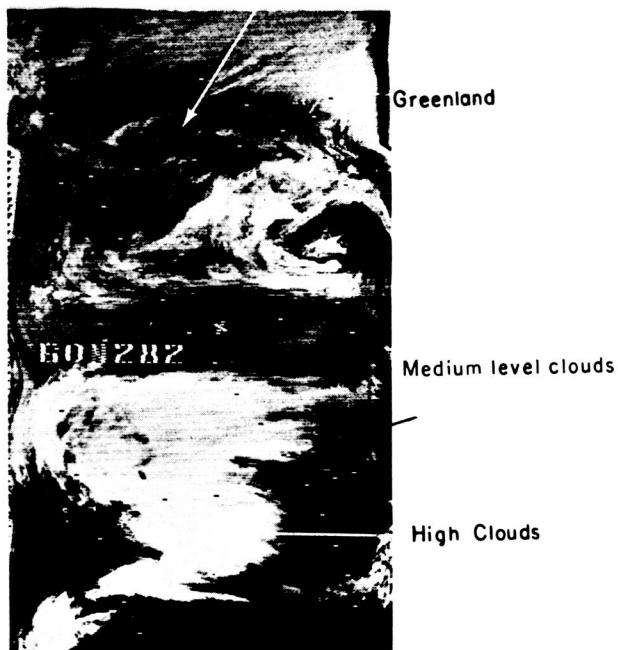


Figure 5-59—Low and Middle Level Clouds  
(Nimbus I HRIR Data)

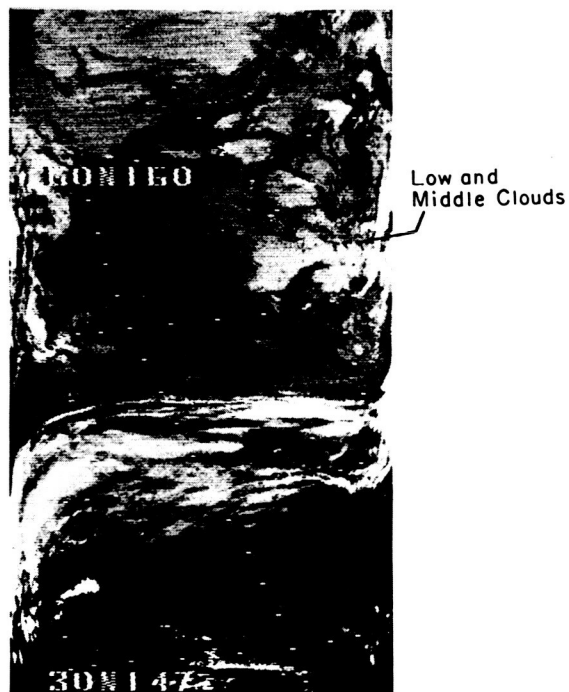


Figure 9-60—Random Pattern Low and Middle  
Clouds (Nimbus I HRIR Data)

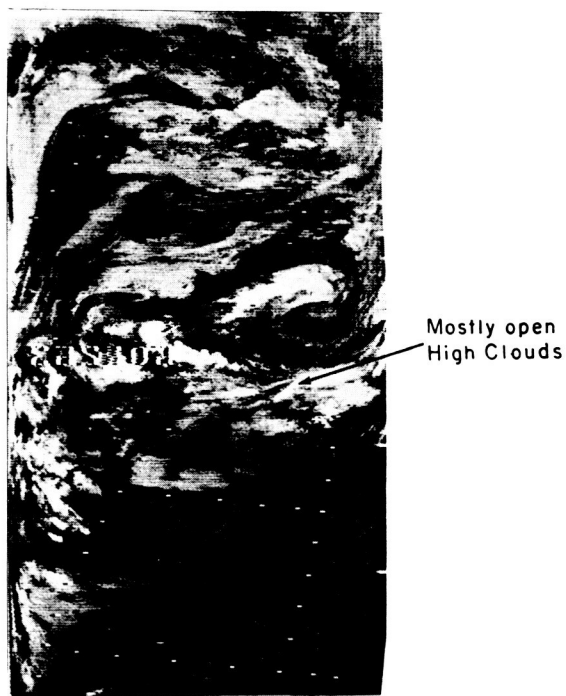


Figure 9-61—Mostly Open High Clouds  
(Nimbus I HRIR Data)

usually be clearly seen and identified. In many cases, it appears that such identification is significantly aided by the relative de-emphasis of the low cloud features in the HRIR data. Even far smaller details such as lee waves and billow clouds can often be identified.

In the following illustrative examples, rectified HRIR data and conventional meteorological data are in some cases presented with the photofacsimile recording of the HRIR data. This is done to illustrate the concept that descriptive classifications can often be made without recourse to other data. It also points up the frequent desirability and/or requirement for additional information, and in some cases limited research, to substantiate or confirm interpretative HRIR classifications.

Figures 9-62 and 9-63 depict an extratropical cloud vortex over northeastern Canada, a cold frontal band over Labrador and the eastern United States, hurricane Dora near the east coast of Florida, a cloud mass over northern Montana and high narrow cloud bands over southwestern United States and Mexico. Surface and 500 mb synoptic maps for the same period are shown in Figures 9-64 and 9-65.

Figures 9-66 and 9-67 show a mature extratropical cloud vortex over the Sea of Okhotsk with a frontal band extending from north of the center of the vortex to the southeast, then south and southwest. Surface and 500 mb maps for the same period are shown in Figures 9-68 and 9-69.

Figures 9-70 and 9-71 depict typhoon Wilda, with an extensive cirrus canopy, centered near  $17^{\circ}\text{N}$ ,  $143^{\circ}\text{E}$ , and an apparent small scale upper level tropical vortex near  $29^{\circ}\text{N}$ ,  $144^{\circ}\text{E}$ . A second major upper level tropical vortex is visible near  $20^{\circ}\text{N}$ ,  $155^{\circ}\text{E}$ . Surface and 300 mb streamline patterns are shown in Figures 9-72 and 9-73.

Figure 9-74 shows an apparent upper level tropical vortex centered near  $30^{\circ}\text{N}$ ,  $165^{\circ}\text{W}$ , and a major frontal cloud band to the northwest. The details of the vortex are obscured by a high cloud shield which is typical for many upper level tropical vortices.

Figures 9-75 and 9-76 show a major cloud band over the western United States with an apparent frontal wave, a jet stream cloud band over northern Idaho and Montana and another just west of California, lee wave clouds to the east of the Sierra Nevadas, and a large patch of clouds over southwestern Canada. The surface synoptic map for the same time period is shown in Figure 9-77.



High Narrow Cloud Bands

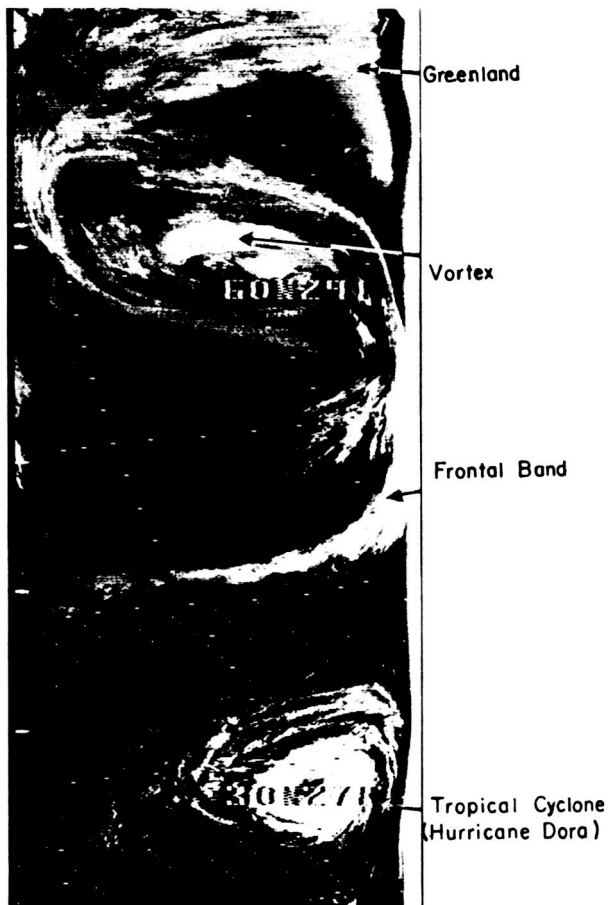


Figure 9-62—HRIR Data for Orbits 174 and 175, 9 September 1964.



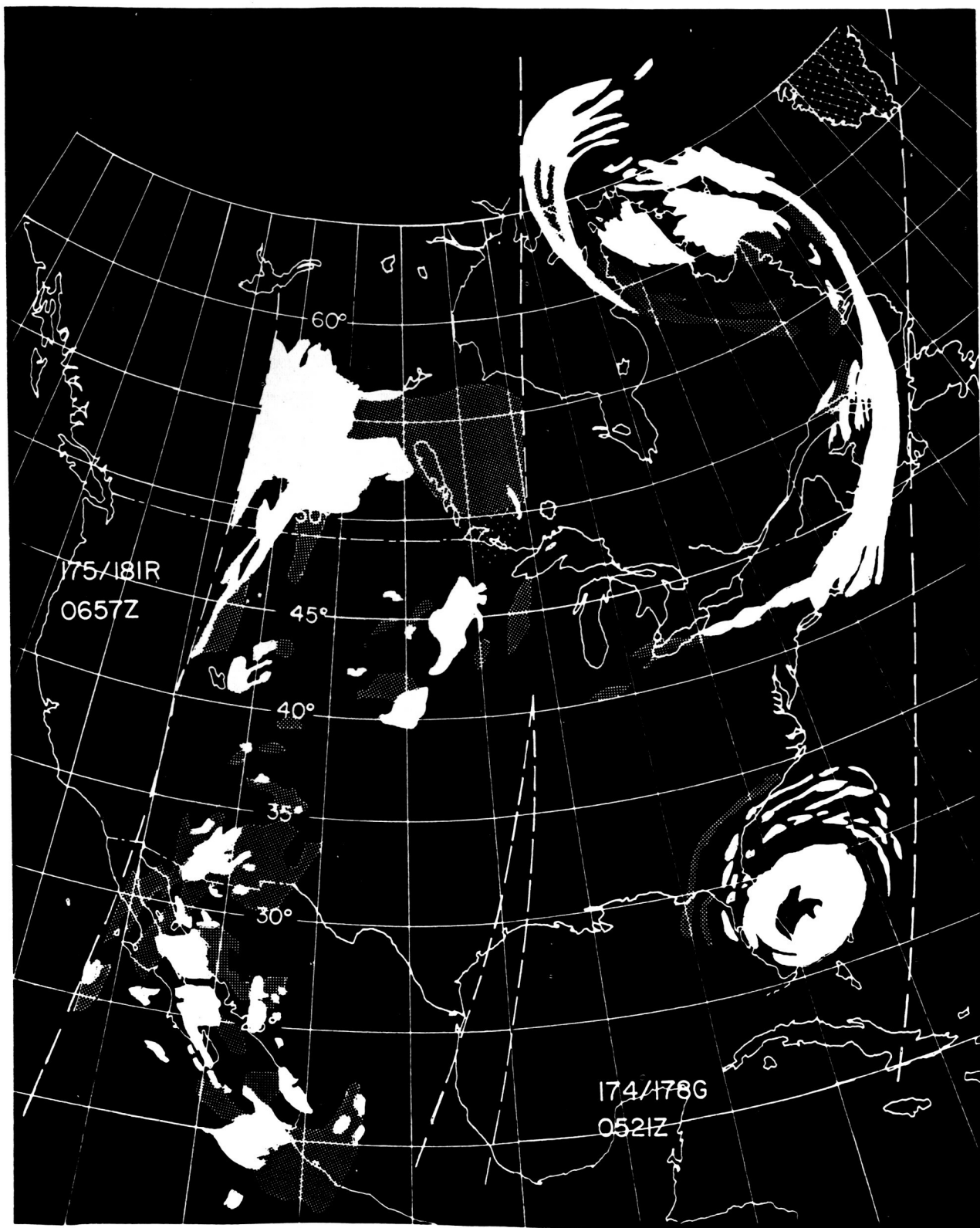


Figure 9-63—Rectified HRIR Data for 9 September 1964 (See Reference 44 for Shading Convention for Rectified HRIR Data)

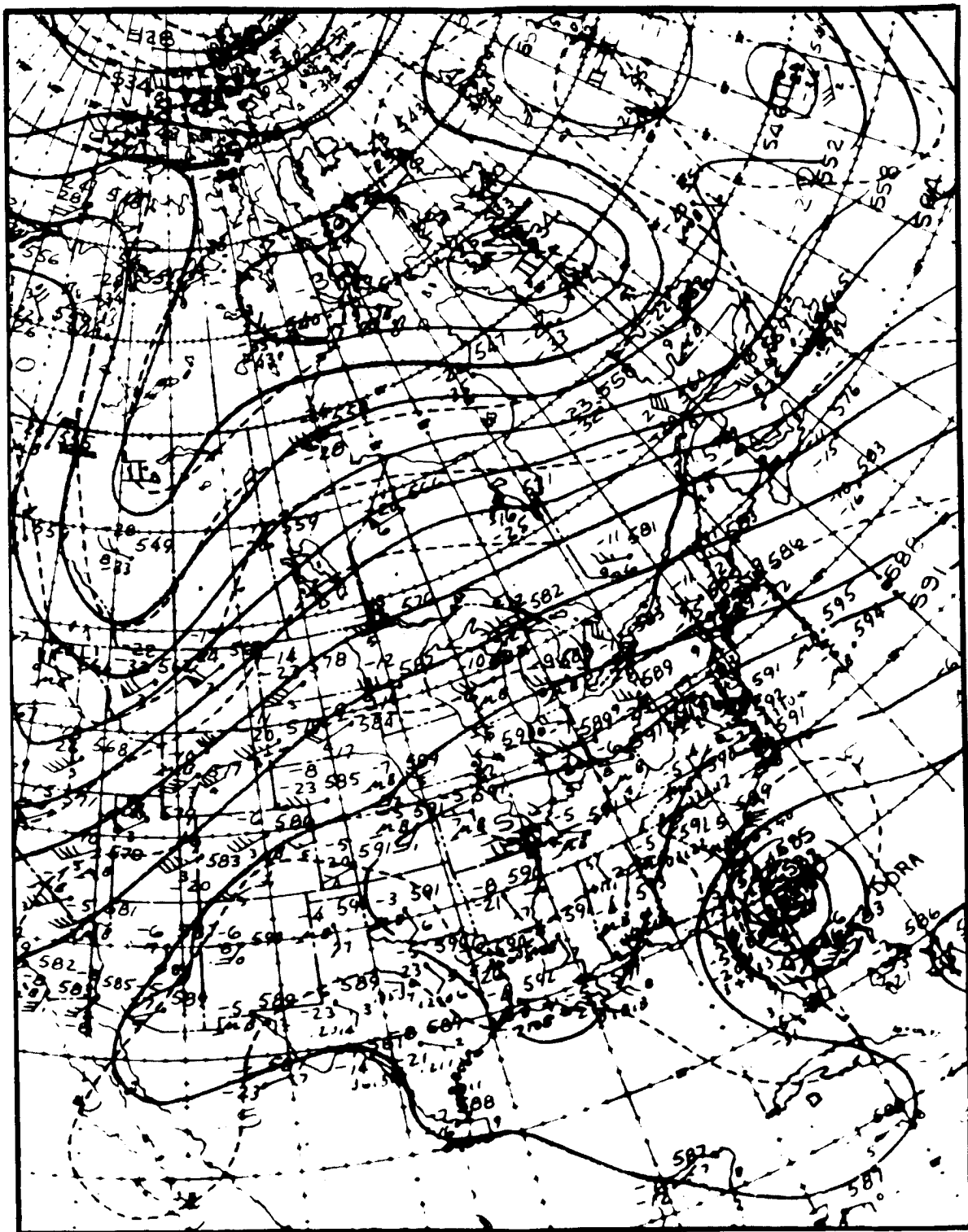


Figure 9-64—NMC 500 mb Analysis, 1200 UT, 9 September 1964

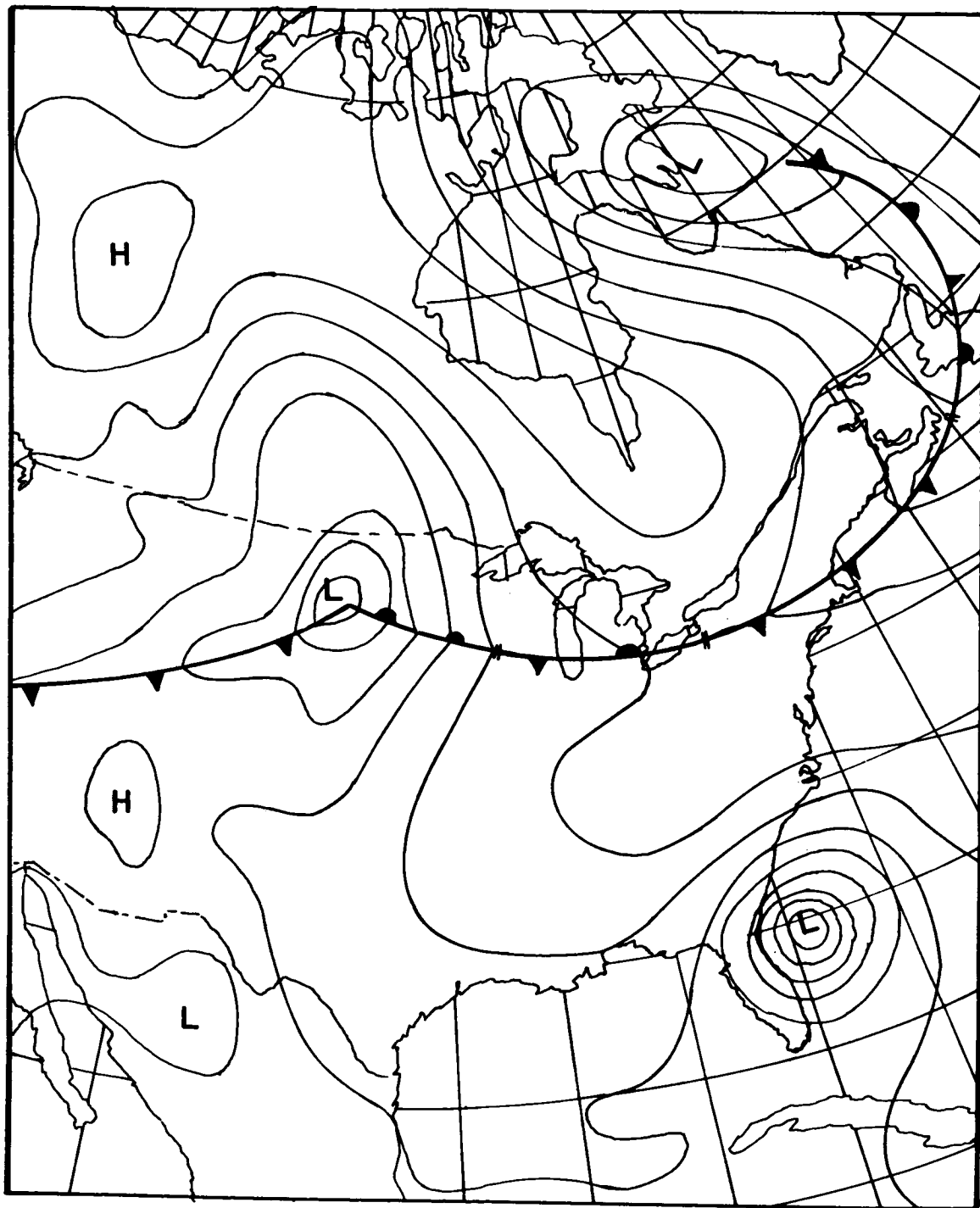


Figure 9-65—NMC Surface Analysis, 1200 UT, 9 September 1964

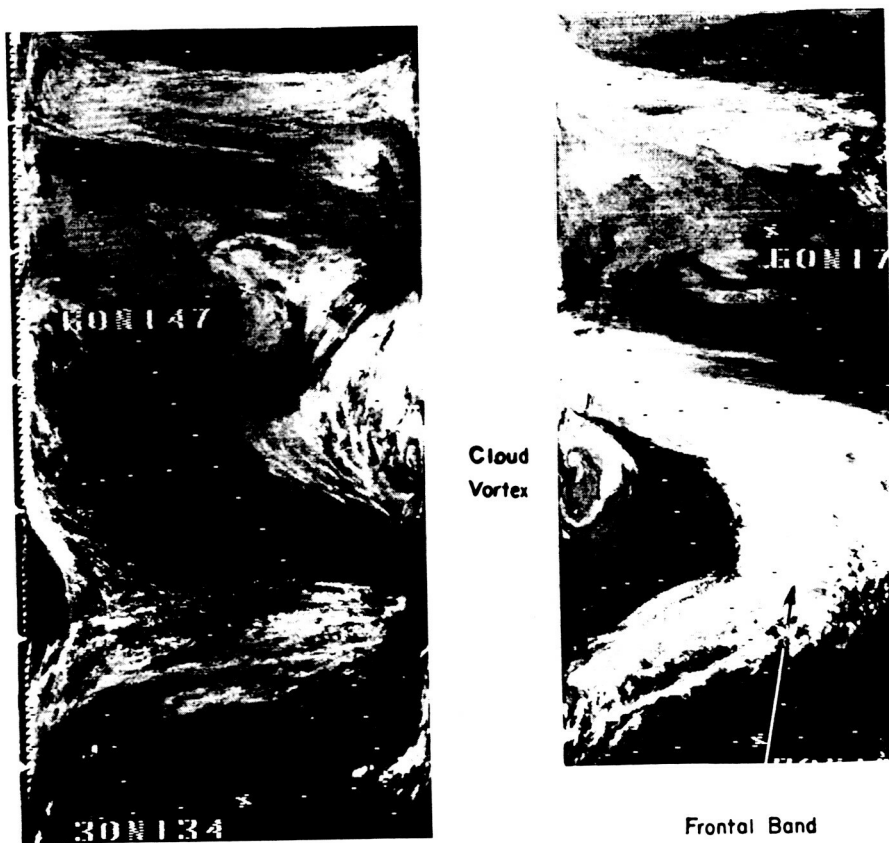


Figure 9-66—HRIR Strips for 14 September 1964

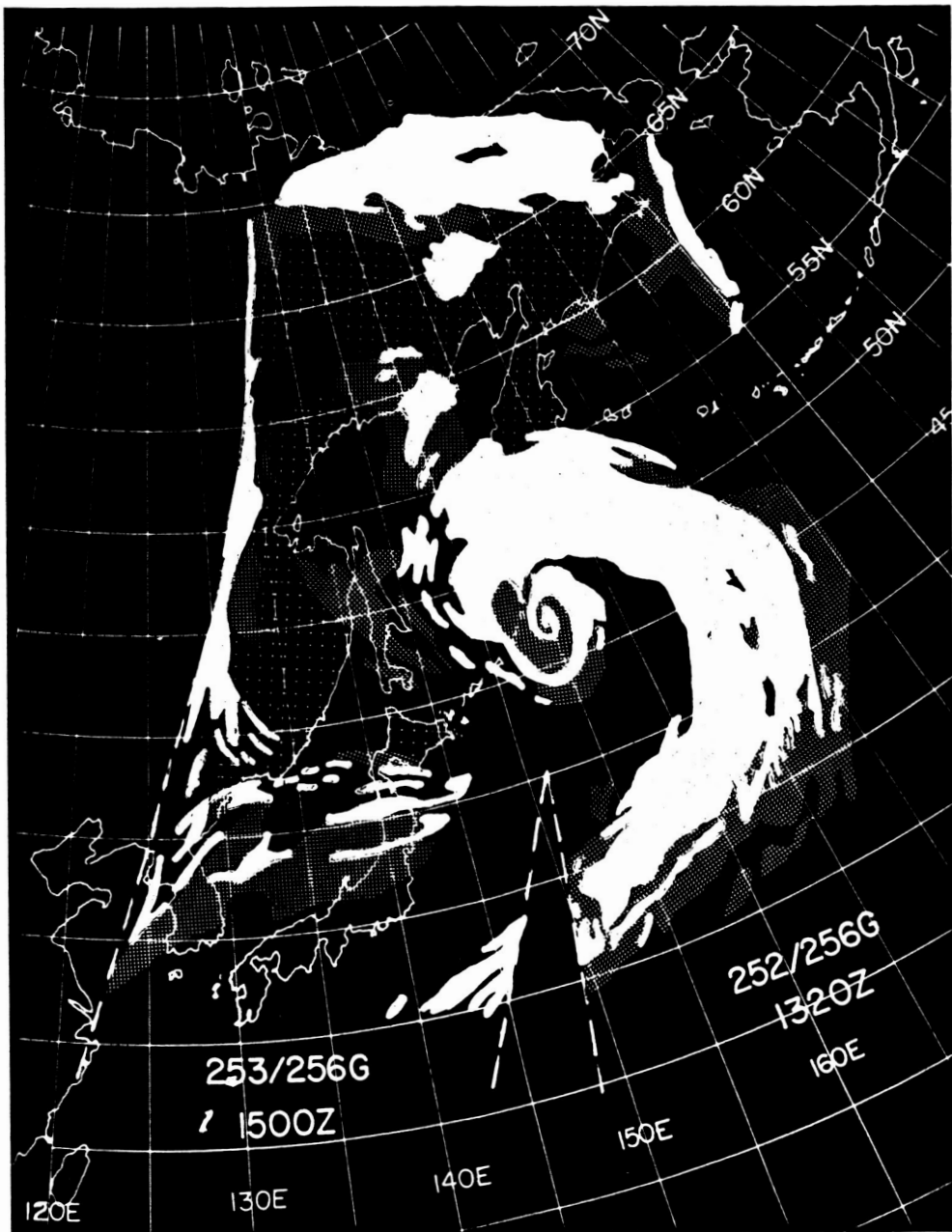


Figure 9-67—Rectified HRIR Data for 14 September 1964

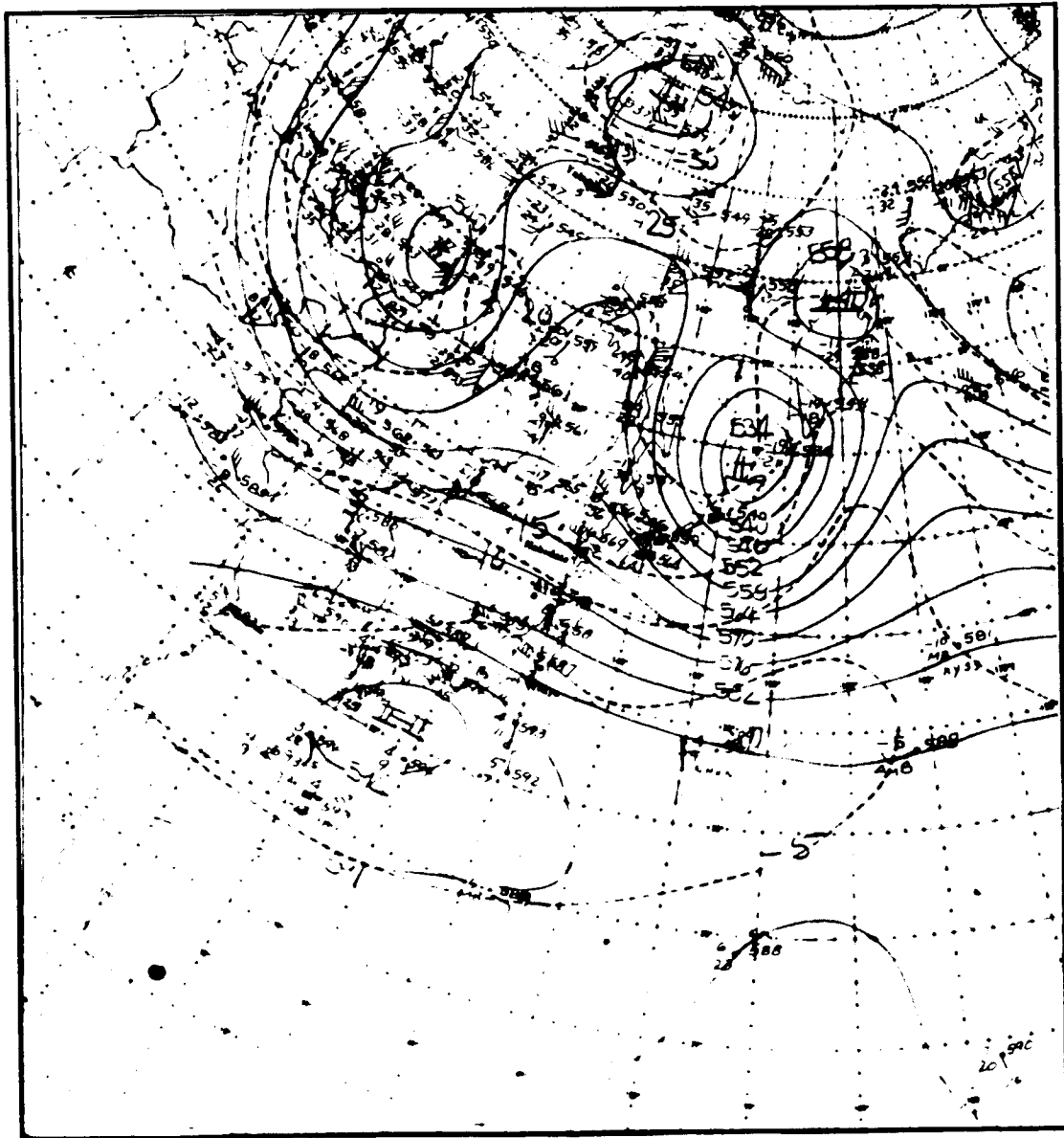


Figure 9-68—NMC 500 mb Analysis, 1200 UT, 14 September 1964

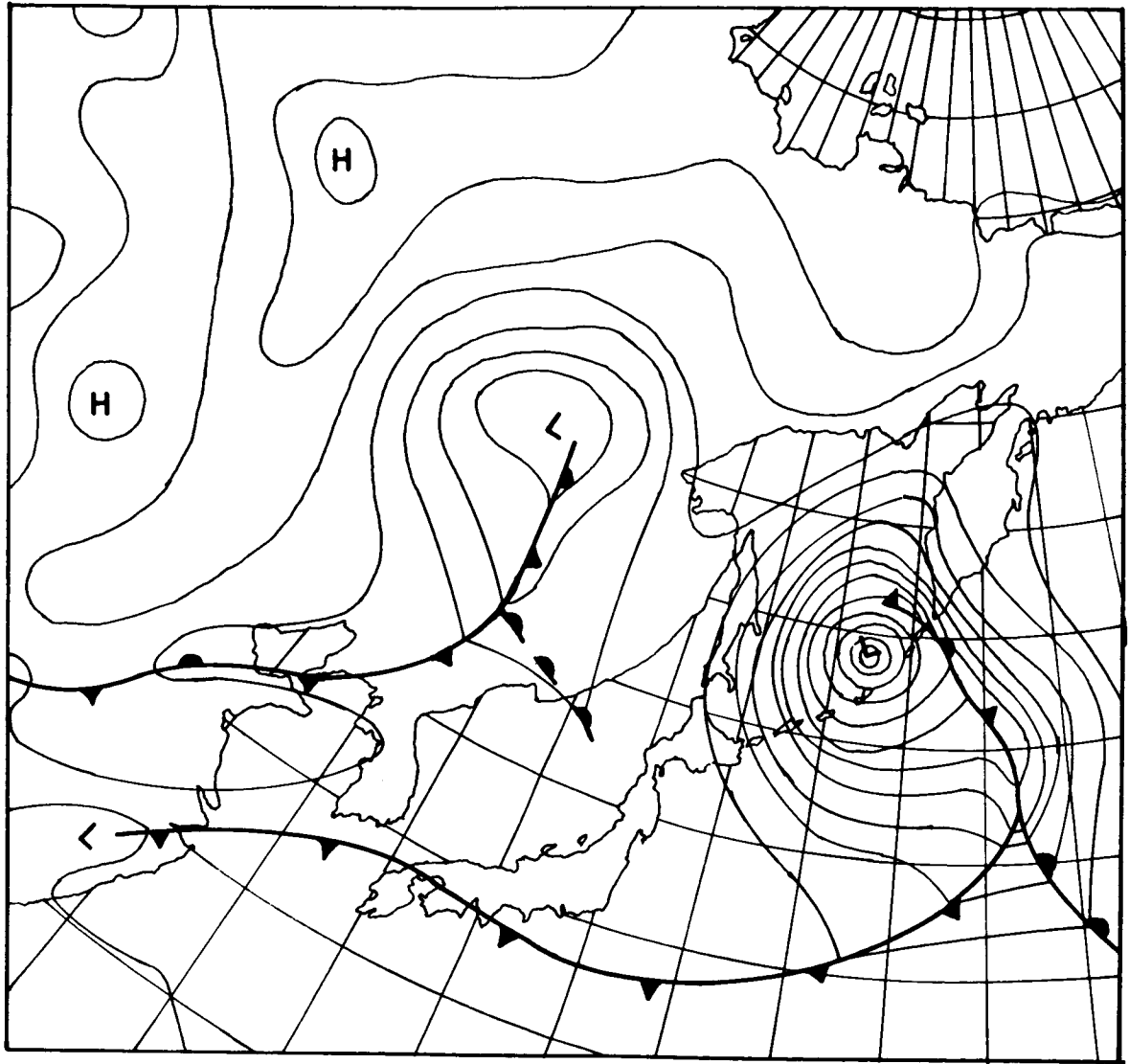


Figure 9-69—NMC Surface Analysis, 1200 UT, 14 September 1964



326



325



324

Figure 9-70—HRIR Photofacsimile Strips (Unrectified) Orbits 324, 325 and 326, 19 September 1964

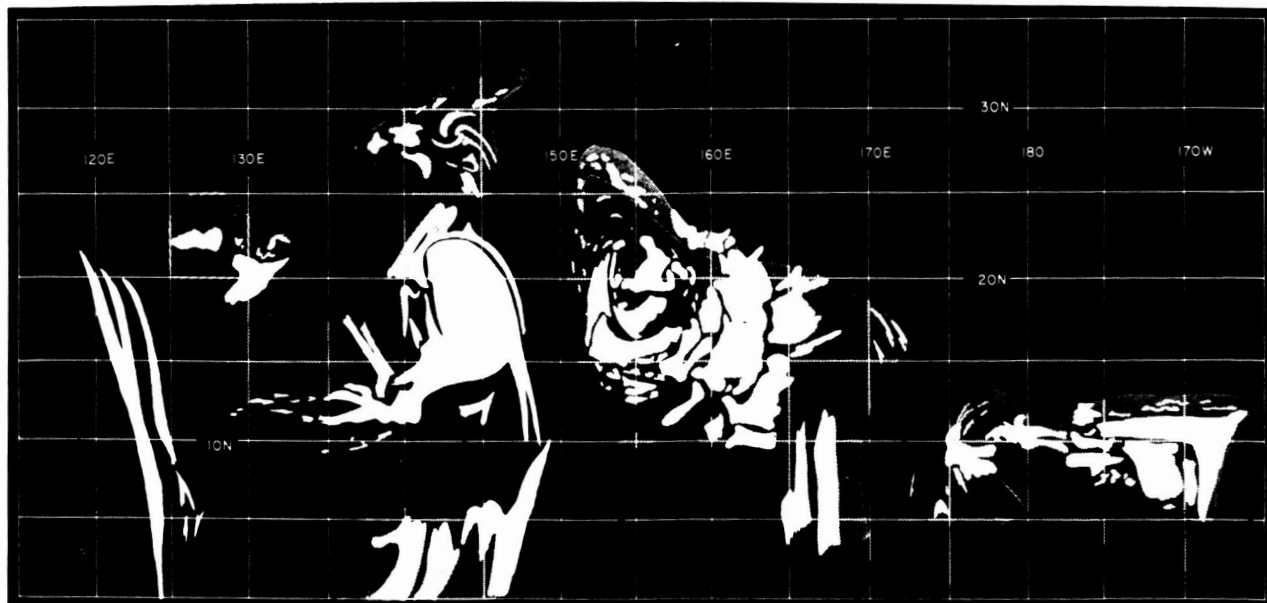


Figure 9-71—HRIR Representation (Rectified) Orbits 324, 325 and 326, 19 September 1964



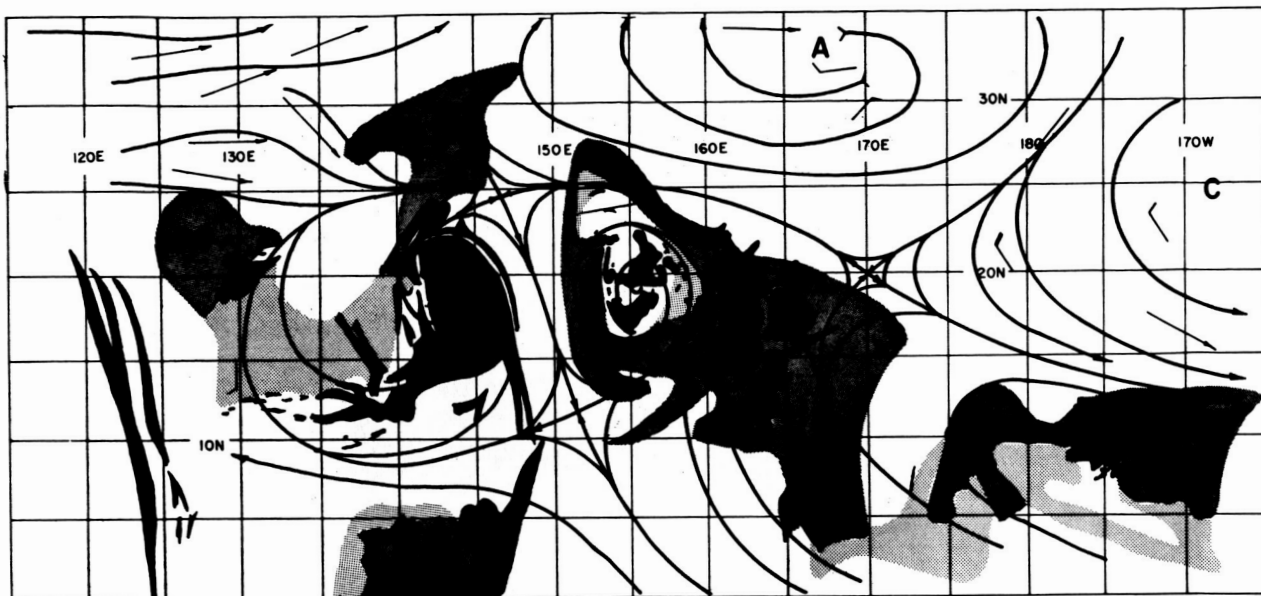


Figure 9-72—HRIR Revised 300 mb Streamline Analysis, 1200 UT, 19 September 1964

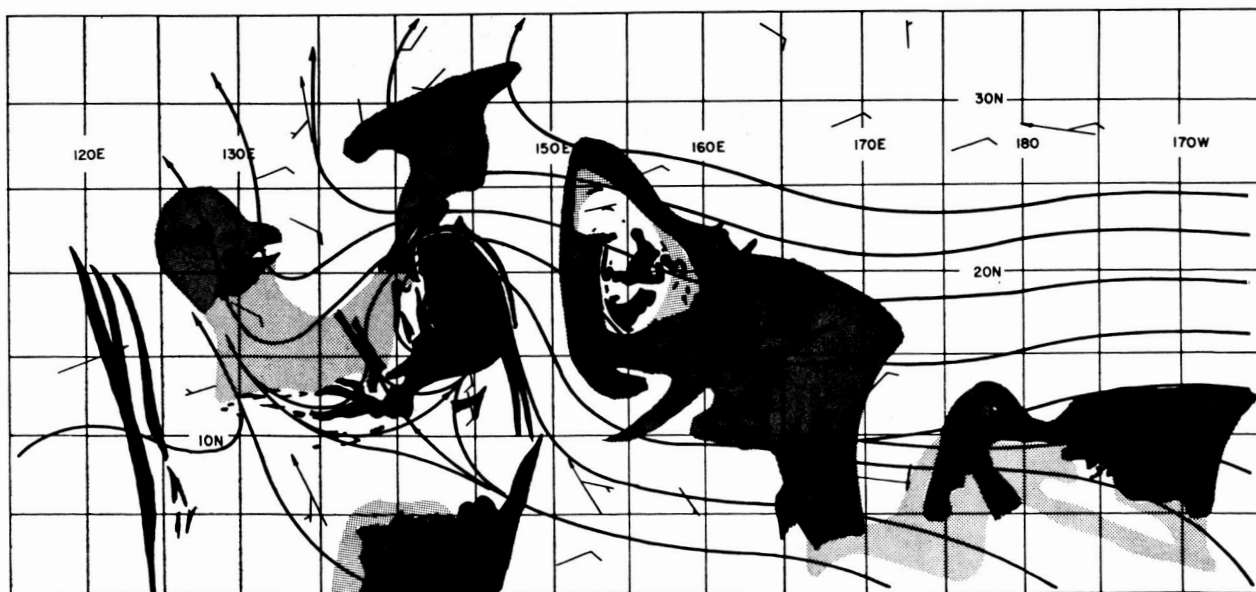


Figure 9-73—HRIR Revised Surface Streamline Analysis, 1200 UT, 19 September 1964

Frontal Band



Upper Level Vortex

Figure 9-74—HRIR Observation of an Upper Level Vortex Over the Tropical North Pacific. Orbit 353, about 1105 UT, 21 September 1964

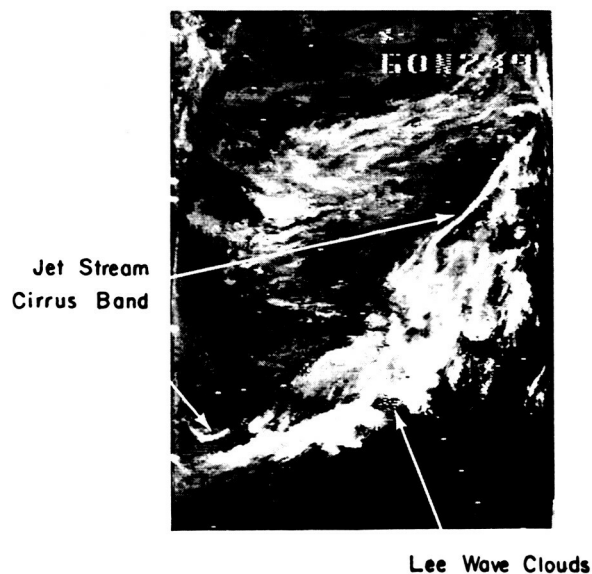


Figure 9-75-Nimbus I HRIR - A Portion of Orbit 44 Over Western North America at Approximately 0800 UT, 31 August 1964

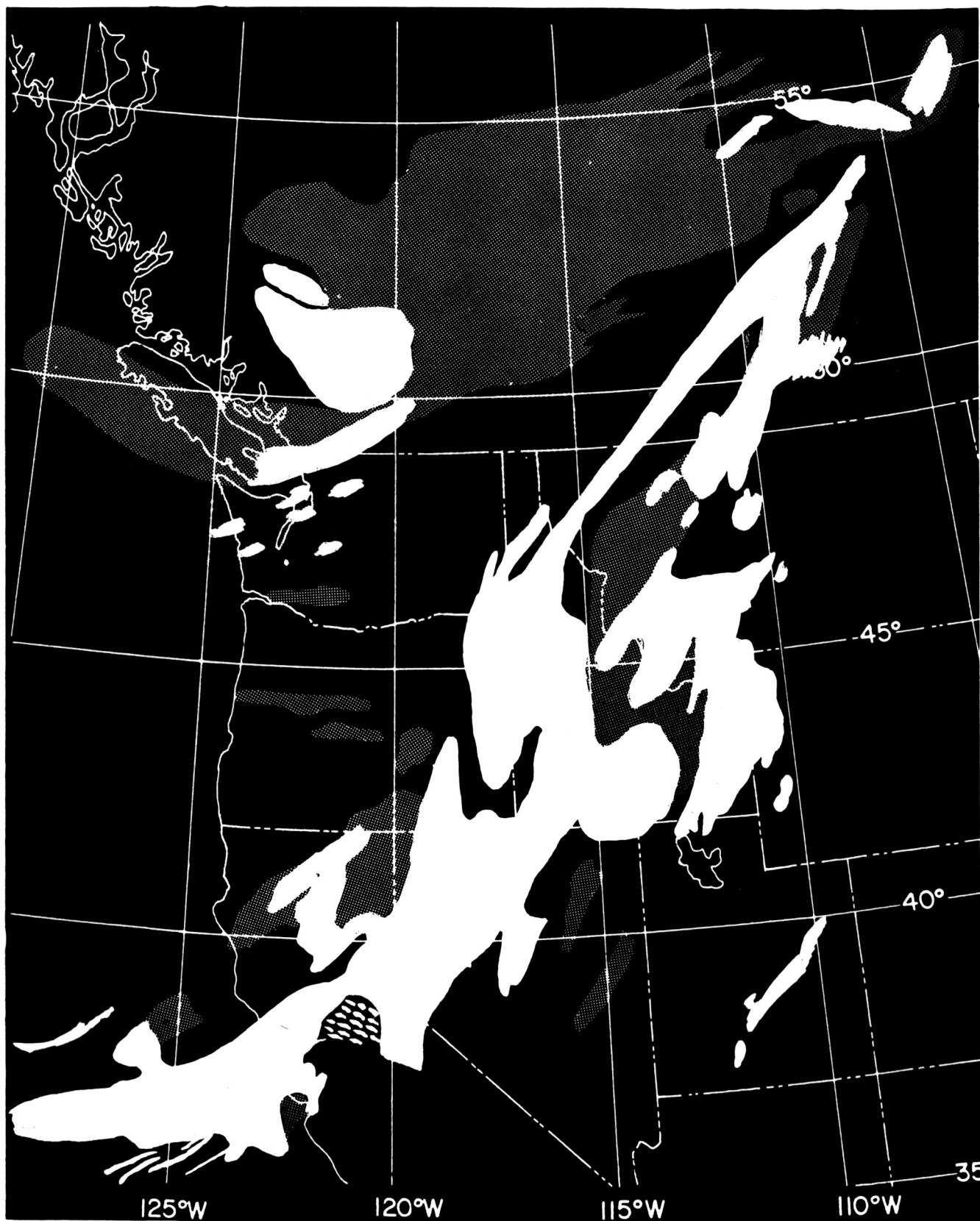


Figure 9-76—A Rectified Map of Cloud Cover as Depicted by HRIR on a Portion of Orbit 44



Figures 9-78 through 9-81 depict a cloud band apparently related to a front extending from the eastern Great Lakes southeastward across the Middle Atlantic States. Distinct variations in HRIR brightness indicate that the cloud top within this band extends to widely different levels. An area of higher clouds, near the horizon, is connected to the northwest end of this band (upper left edge of the picture). A second area of higher clouds is visible along the eastern horizon of the picture. An area of somewhat bright but parallel lines, suggestive of wave or billow clouds, can be seen in the vicinity of  $39^{\circ}$ - $40^{\circ}$ N,  $78^{\circ}$ - $80^{\circ}$ W. Surface reports (Fig. 9-80) indicate that the faint grey area which extends across central New England into New York State depicts scattered cirrus clouds with lower broken to overcast clouds. A number of landmarks (Fig. 9-79) are identified in the clear area northeast of the frontal band, over northeastern New England and southeastern Canada.

Figure 9-82 shows a vortical cloud near Baffin Island with a frontal band extending south to east, passing east of Newfoundland then extending westward to the east coast of the United States just south of  $40^{\circ}$ N. Hurricane Ethel and the eastern edge of Hurricane Dora are visible in the lower portion of the picture. An area of apparent post frontal cellular clouds appears as a general gray mass with no evidence of the cellular structure. Greenland is also visible in the picture.

Figure 9-83 depicts cloud patterns associated with a short wave trough.

Figures 9-84 through 9-88 illustrate mosaics of contiguous orbits.

Significant features visible in Figures 9-84 and 9-85 include:

1. Post-frontal cellular clouds near  $55^{\circ}$ N,  $10^{\circ}$ - $30^{\circ}$ W.
2. Low stratus or fog appearing as untextured areas of uniform, flat, light gray tone near  $55^{\circ}$ N, between  $102^{\circ}$  and  $112^{\circ}$ E and east and northeast of this area.
3. Frontal cloud bands appear as:
  - a. Low level clouds near  $57^{\circ}$ N,  $45^{\circ}$ E.
  - b. Low level cloudiness with higher level scattered to broken streaky cloudiness from  $68^{\circ}$ N,  $90^{\circ}$ E to  $62^{\circ}$ N,  $110^{\circ}$ E.
  - c. Extensive high level cloudiness near  $58^{\circ}$ N,  $30^{\circ}$ E.
4. Short wave troughs near  $60^{\circ}$ N,  $30^{\circ}$ E and  $50^{\circ}$ N,  $100^{\circ}$ E.

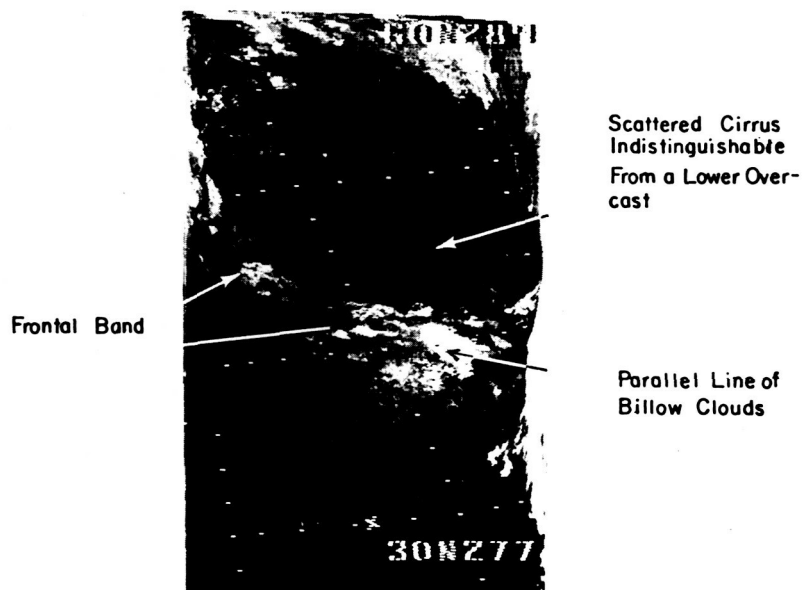


Figure 9-78—HRIR Picture of Eastern North America on Orbit 335 at 0530 UT, 20 September 1964

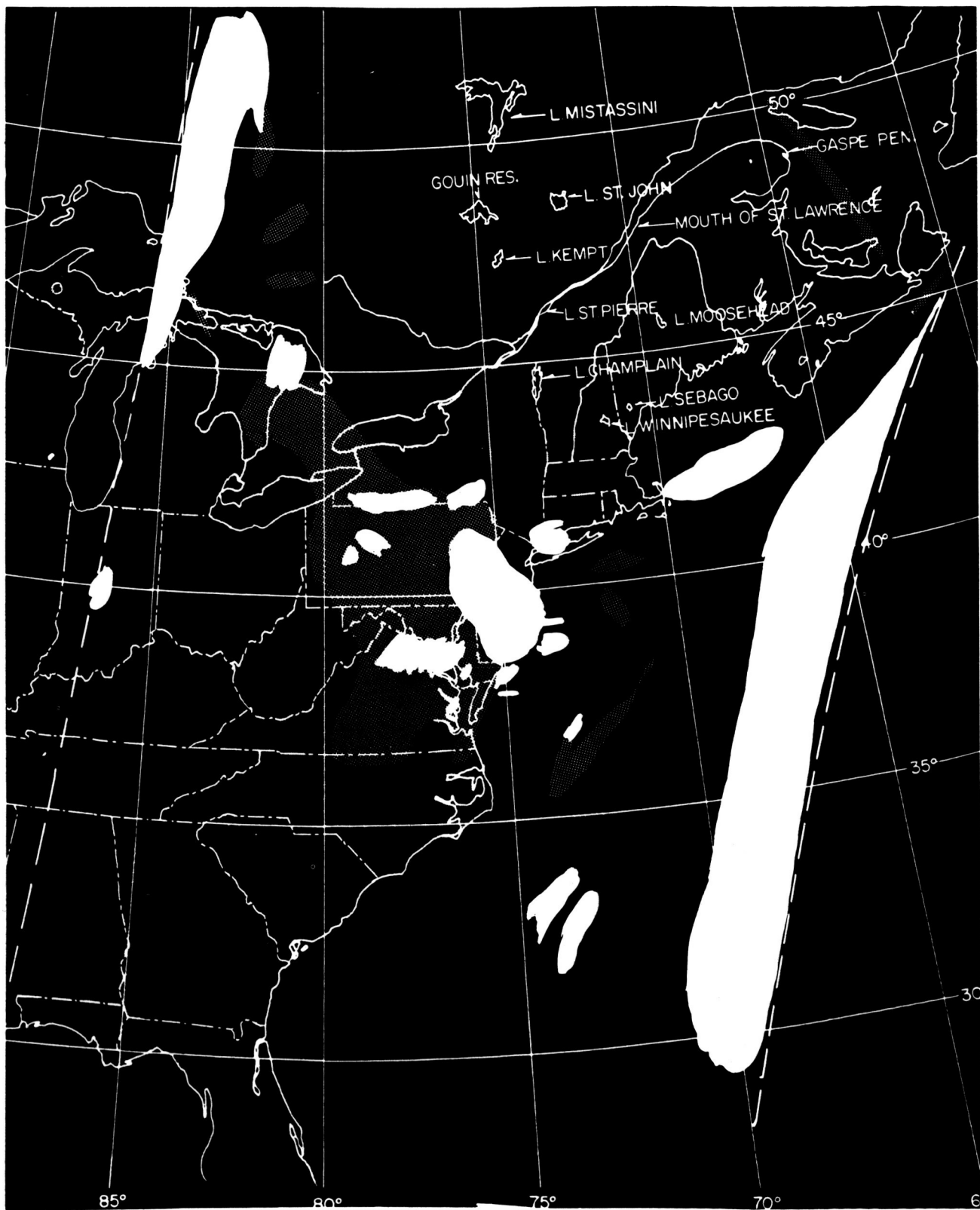


Figure 9-79—Rectified Map of Cloud Cover as Seen by HRIR on Orbit 335  
at 0530 UT, 20 September 1964



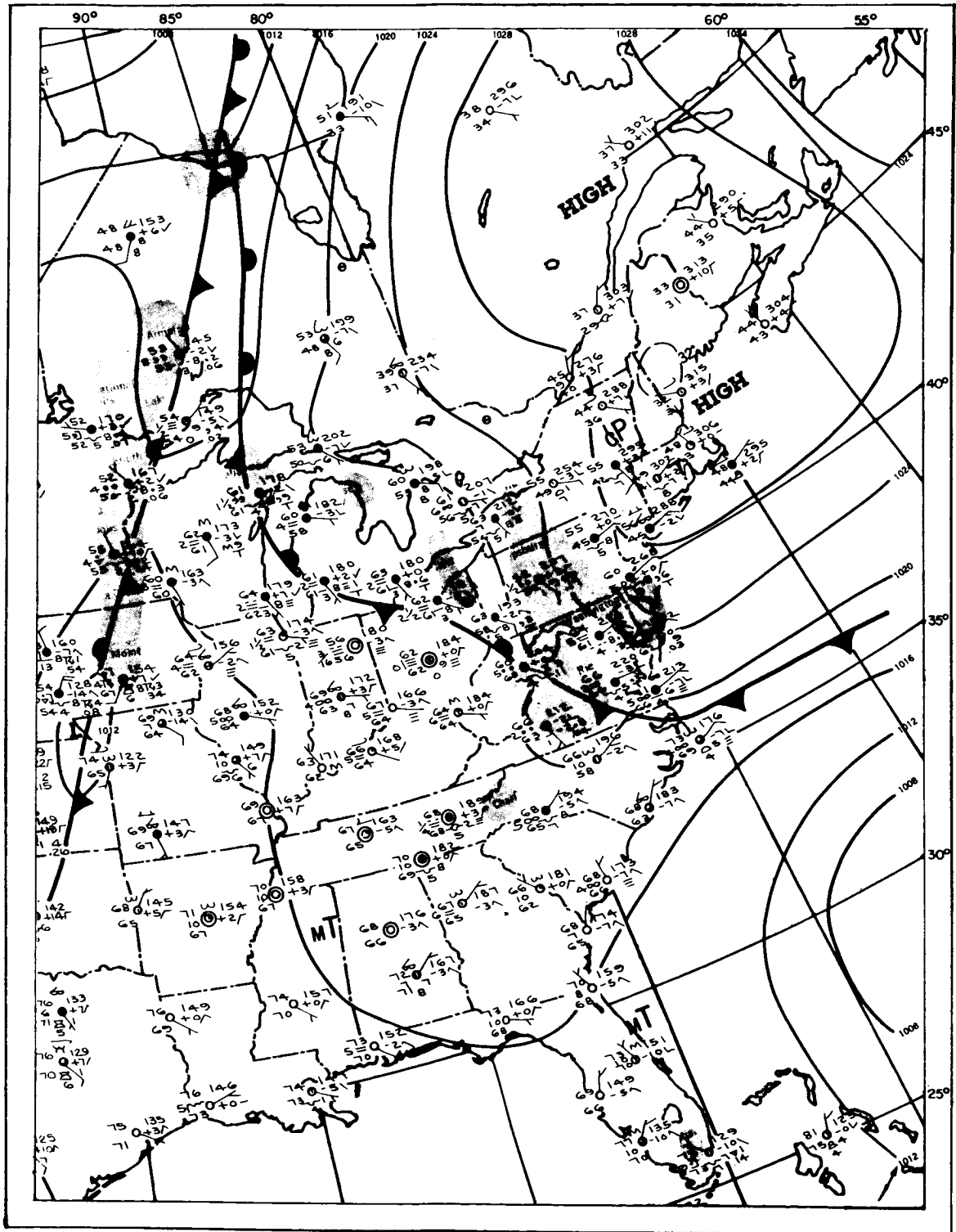


Figure 9-80—Surface Weather Map at 0600 UT, 20 September 1964

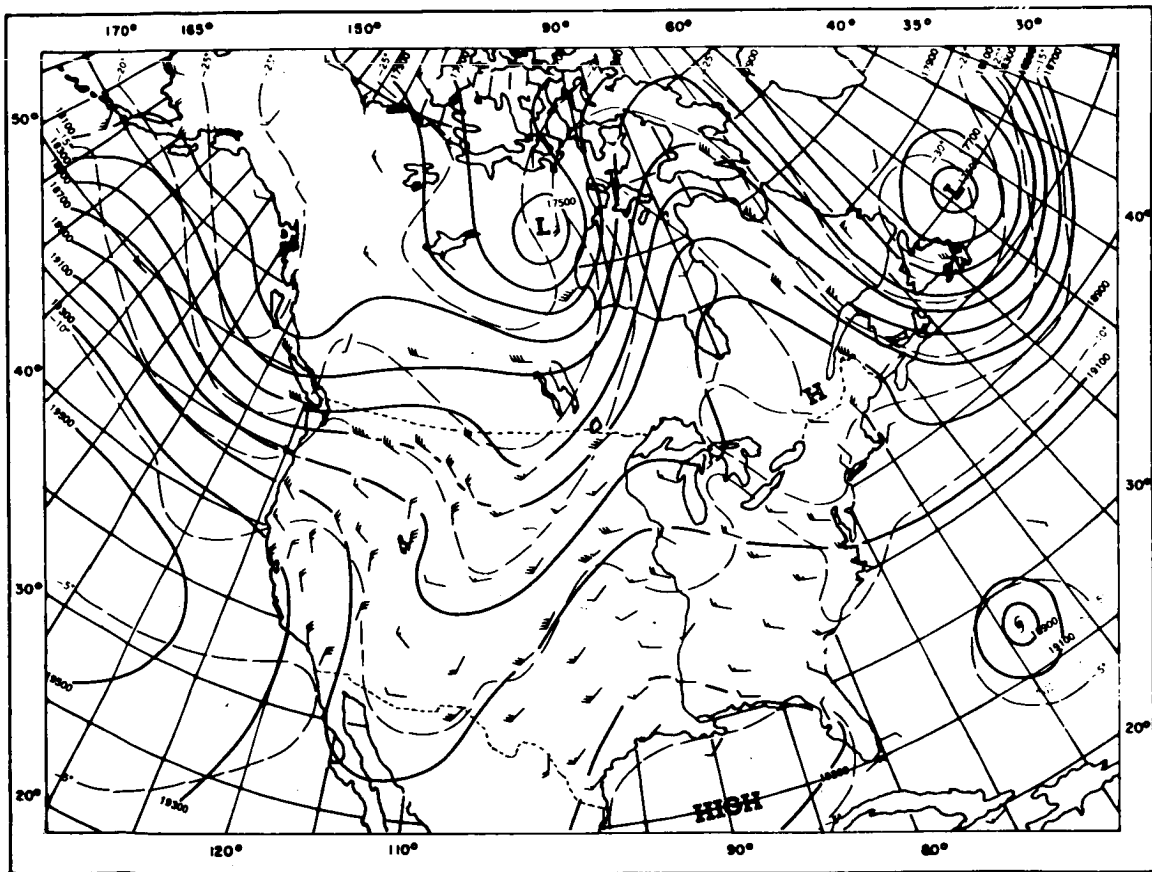


Figure 9-81-500 mb Map at 0000 UT, 20 September 1964

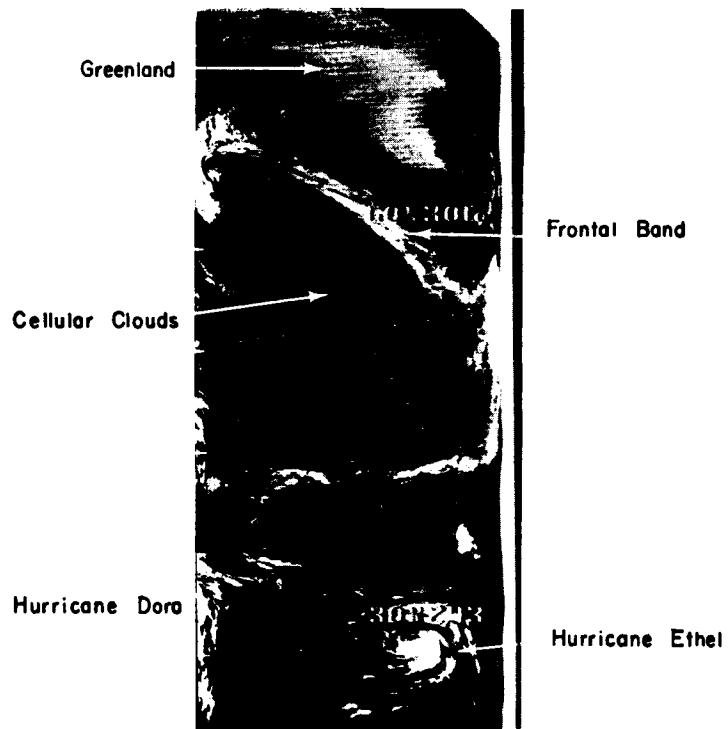


Figure 9-82—Cellular Cumulus (near 50°N, 300°E) May Appear as Only a General Gray Mass in the HRIR, Hurricane Ethel, Hurricane Dora, Frontal Band and Vortex

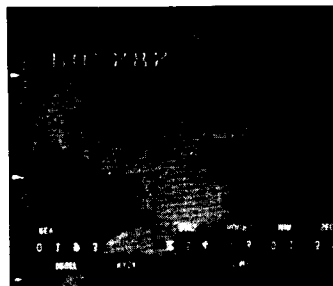


Figure 9-83—HRIR View of a Well Developed Short Wave Trough



Figure 9-84—HRIR Mosaic of Eurasian Area for 16-17 September 1964

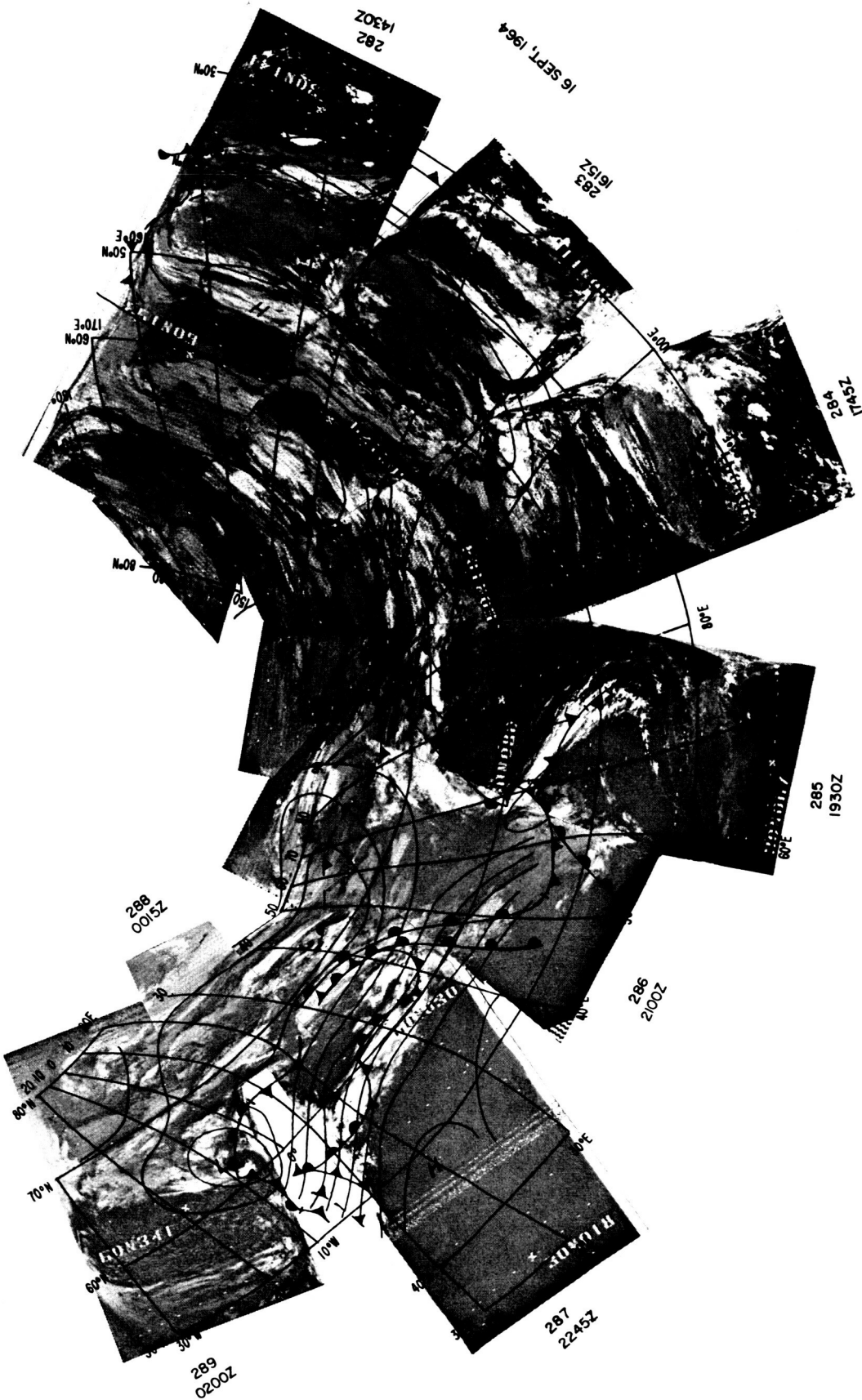


Figure 9-85—HRIR Mosaic with NMC 500 mb Analysis (0000 UT, 17 September 1964 West of About 110°E; 1200 UT, 16 September to the East), and Russian Frontal Analysis for 0000 UT, 17 September 1964

5. Landmarks and clear areas:

- a. Lake Baikal ( $54^{\circ}\text{N}$ ,  $108^{\circ}\text{E}$ ).
- b. Pamir Highlands (near  $37^{\circ}\text{N}$ ,  $72^{\circ}\text{E}$ ).
- c. Tibetan Plateau (near  $32^{\circ}\text{N}$ ,  $90^{\circ}\text{E}$ ).

The following significant features are in evidence in Figures 9-86 and 9-87:

1. Vortical cloud patterns near  $60^{\circ}\text{S}$ ,  $180^{\circ}$ ,  $68^{\circ}\text{S}$ ,  $170^{\circ}\text{W}$  with a frontal band extending northward to  $45^{\circ}\text{S}$ ,  $180^{\circ}$  and near  $45^{\circ}\text{S}$ ,  $140^{\circ}\text{W}$  with a frontal band extending northward to  $30^{\circ}\text{S}$ ,  $140^{\circ}\text{W}$ .
2. A short wave trough near  $50^{\circ}\text{S}$ ,  $45^{\circ}\text{E}$ .
3. A frontal wave near  $45^{\circ}\text{S}$ ,  $95^{\circ}\text{E}$ .
4. Large clear area over southern Australia, near  $30^{\circ}\text{S}$ ,  $120^{\circ}\text{E}$ .

Principal features depicted in Figure 9-88 are:

1. A bright, slightly vortical cloud centered near  $55^{\circ}\text{S}$ ,  $160^{\circ}\text{E}$  with a frontal band extending northward.
2. A "crescent-shaped" vortical cloud (Class A) centered near  $63^{\circ}\text{S}$ ,  $160^{\circ}\text{E}$ .
3. Part of a "hooked-shaped" vortical cloud (Class B) centered near  $55^{\circ}\text{S}$ ,  $125^{\circ}\text{E}$ , visible at  $55^{\circ}\text{S}$ ,  $130^{\circ}\text{E}$ .
4. A frontal wave near  $50^{\circ}\text{S}$ ,  $120^{\circ}\text{E}$ .
5. The Andes Cordillera of South America running north-south along  $70^{\circ}\text{W}$  near  $30^{\circ}\text{S}$  with a long band of apparent cirrus clouds extending northwest-southeast across the mountains.

#### 9.4 Terrestrial Features

Terrestrial features or land forms are often observed in satellite data. Since terrestrial features are of interest to a variety of researchers, they will be identified and cataloged. However, priority is given to cloud features. In the unlikely event that man-made objects are observed, they will not be cataloged.

Terrestrial features are divided into six divisions. These divisions were selected on the basis of ease of recognition and identification, and frequency of occurrence in satellite pictures. Since they are in common usage and familiar to most people, further description is considered unnecessary. The names and/or identification of terrestrial features will be listed in the remarks section of

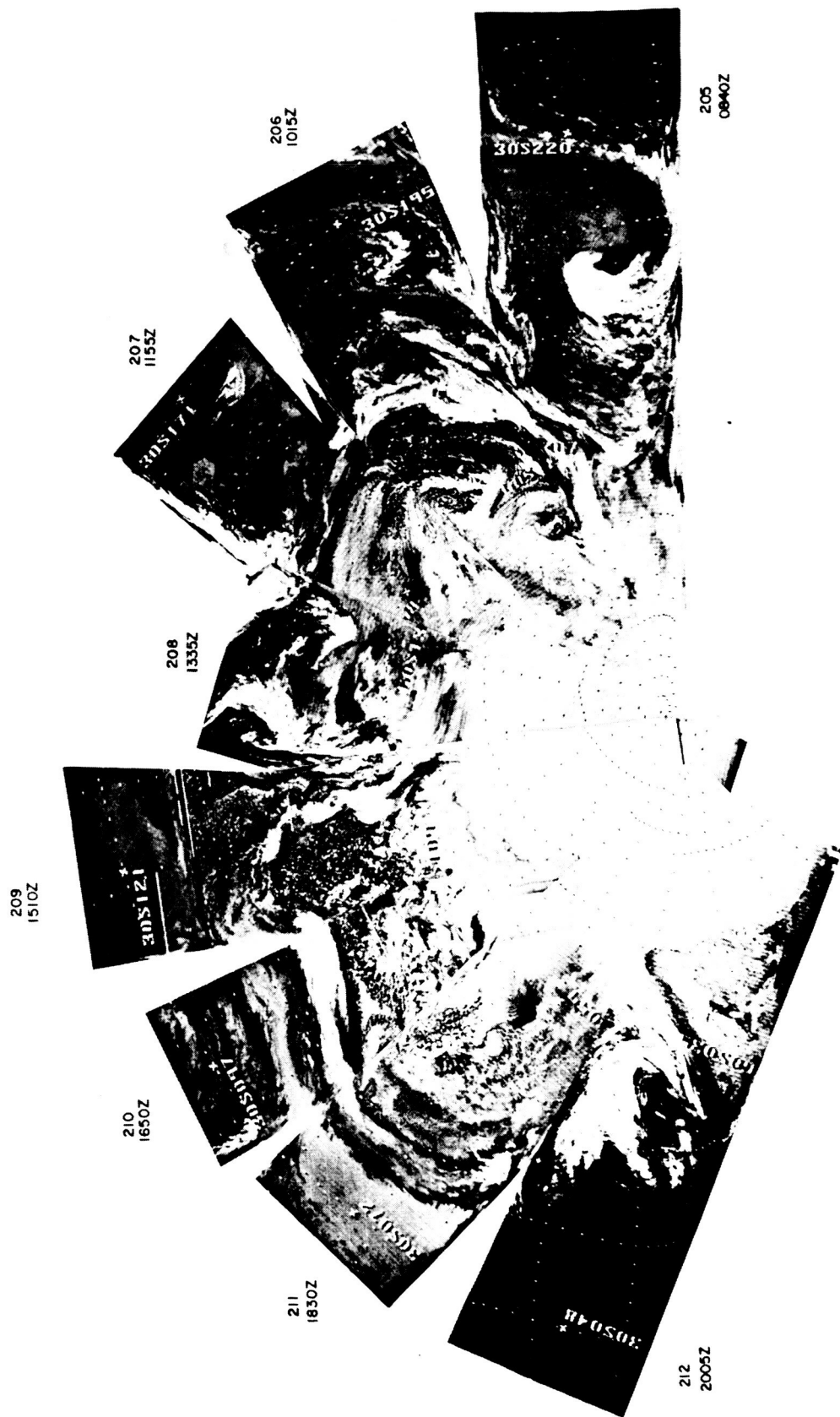
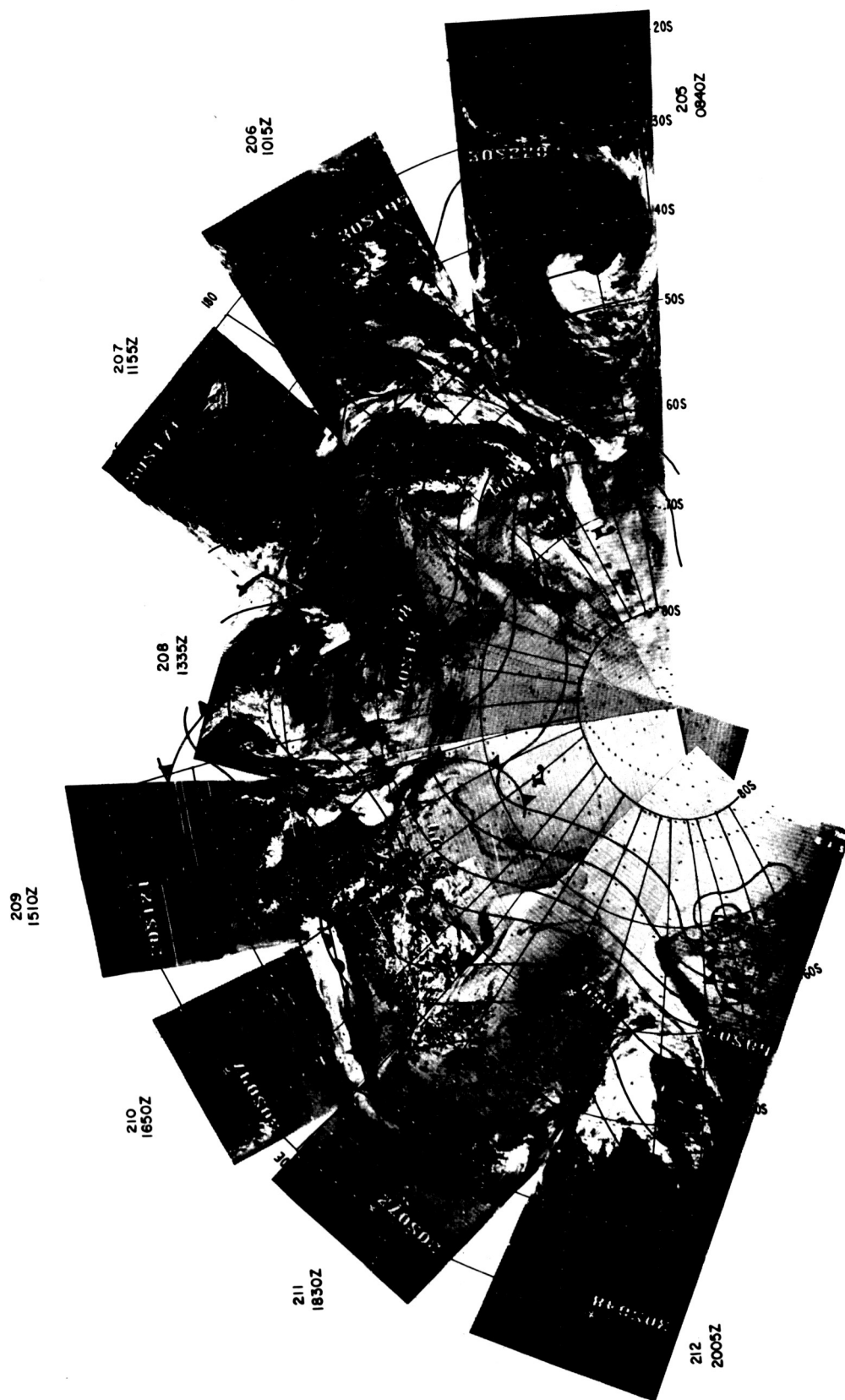


Figure 9-86—HRIR Southern Hemisphere Mosaic for 11 September 1964





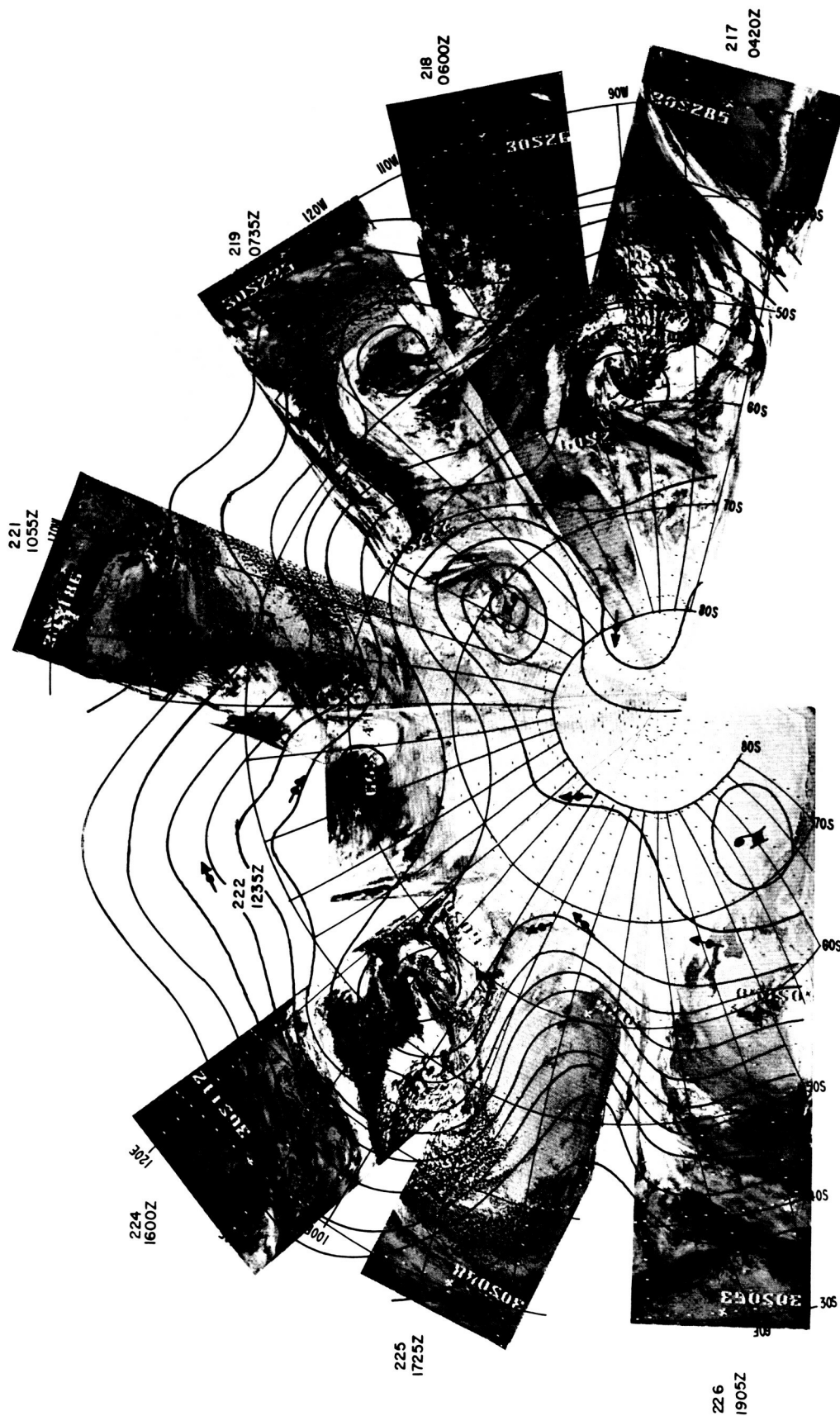
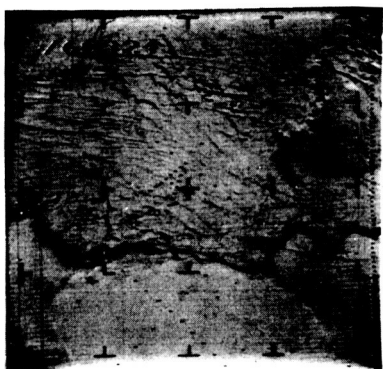


Figure 9-88—HRIR Mosaic for 12 September 1964, with 500 mb Data (0000 UT, 13 September) West of 180°, and 500 mb Data (0000 UT, 12 September) East of 180°. Analysis Drawn Combining HRIR and Conventional Data



Ice Fields and Ice Packs  
(Antarctic Region) (N)



Ice Floes and Ice Bergs  
(Antarctic Region) (N)

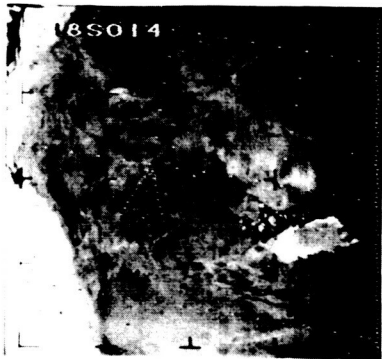


Lake and Mountains with Snowfield  
(USSR) (N)

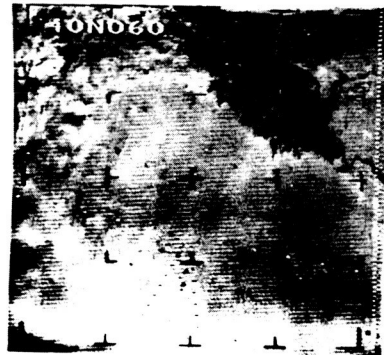


Lake and Mountains with Snowfield  
(USSR) (N)

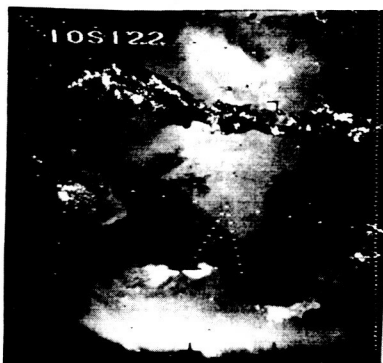
Figure 9-89—Selected Terrestrial Features



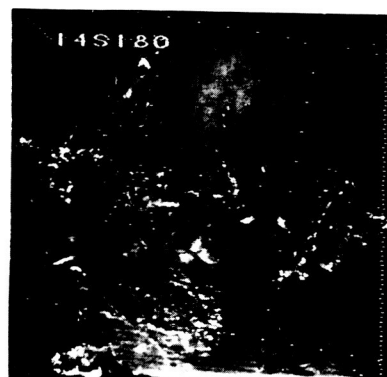
Alkali Flat  
(Southwest Africa) (N)



Turkmen and Uzbek Republics  
(USSR) (N)

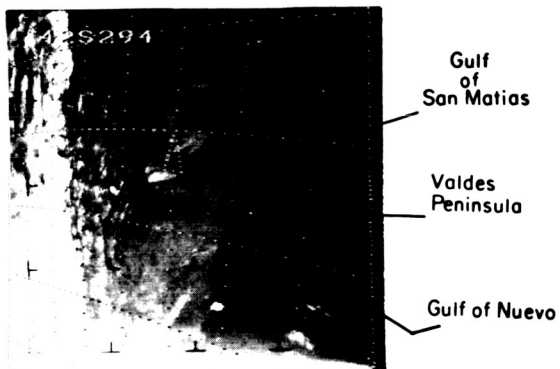


Sun Glint and Indonesian Islands  
(N)

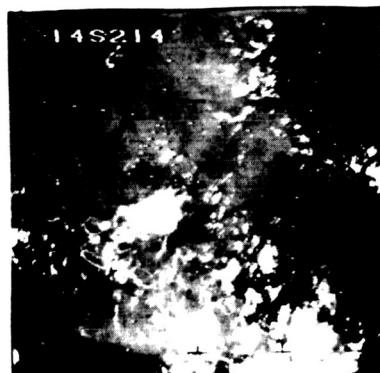


Sun Glint Over the South Pacific  
Ocean Near the Fiji Islands (N)

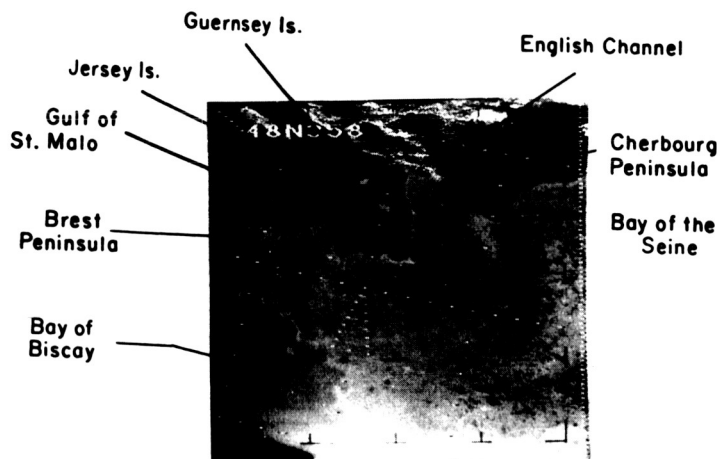
Figure 9-90—Selected Terrestrial Features



Coastline of Argentina (N)



Islands and Atolls  
Tuamotu Archipelago (N)



Coastline of Northwest France (N)



Canadian Rocky Mountains  
(Snowfield) (N)

Figure 9-91-Selected Terrestrial Features



Ice Cap and Fiords  
Northeast Greenland (N)



Ice Cap  
Southern Greenland (N)

Figure 9-92—Selected Terrestrial Features

appropriate documentation. Selected terrestrial features are illustrated in Figures 9-89 through 9-92. The terrestrial features that are most frequently observed and identified are listed below.

#### 9.4.1 Water Body

- Gulf

- Strait, channel or canal

- Sea or ocean

  - Ocean currents

  - Ocean wave patterns

  - Ice floes or icebergs

  - Ice fields or ice packs

- River or stream

  - Flooded

  - Frozen

  - Partly frozen

  - Delta

  - Flood plain

- Lake

  - Frozen

  - Partly frozen

#### 9.4.2 Desert

- Sand

- Sand dunes

- Alkali flats (salt flats, salt pans)

- Dry river bed (arroyo or wadi)

- Dry lake (playa)

- Oasis

#### 9.4.3 Mountain

- Peak or dome

- Range or system

- Volcano

- Glacier

  - Valley (Mountain glacier or ice streams) – Streams of ice that flow downward through valleys

Piedmont (intermont) – Glacier on a plain at the base of a mountain  
Ice sheet or Ice cap – Broad, irregular, cake-like ice masses that  
generally blanket the terrain (Ice cap – A small ice sheet).

Snow field

#### 9.4.4 Coastline

Rugged  
Beach or bar  
Peninsula or cape  
Bay, estuary or lagoon  
Coastal plain  
Fiord (Fjord) or ria

#### 9.4.5 Other Geomorphology

Plain  
Plateau or table land  
Valley, gorge or canyon  
Swamp or marsh  
Fault or other lineament  
Island or atoll  
Basin or depression

#### 9.4.6 Miscellaneous

Sun glints  
Underwater features  
Ice or snow field  
Forest or vegetation  
Forest fire

##### Cloud Amount

Open	<20% Coverage
Mostly open	20% to 50% coverage
Mostly covered	50% to 80% coverage
Covered	>80% coverage

## 9.5 Indistinguishable Features

There are cases in which a clear distinction cannot be made between clouds and terrain, clouds and snow or ice fields, or clouds above a continuous undercast. This category is established to indicate to researchers, experimenters and other users the questionable value of the pictures and at the same time to provide a classification for retrieval. It should be noted that in cases in which features cannot be identified or distinguished because of atmospheric pollutants or other identifiable obscurations visible in the picture, the picture will be categorized under "General Cloud Features" (atmospheric pollutants). This category will not be used to classify pictures of tropical vortical cloud features in which the distinction cannot be made between a cirrus canopy and other clouds. Pictures of this nature will be classified under the appropriate tropical cyclone group.

### 9.5.1 Indistinguishable Features – Clear Distinction Cannot be Made Between Clouds and Terrain, Clouds and Snow or Ice Fields and/or Cloud Fields

9.5.1.1 Inadequate Distinction Between Clouds and Terrain (D)

9.5.1.2 Inadequate Distinction Between Clouds and Snow/Ice Fields (D)

9.5.1.3 Inadequate Distinction Between Clouds and Lower Undercast (D)

## 9.6 Pictures of Poor Quality or No Discernible Features

This category is established in order to account for data acquired by the Nimbus II satellite, which is considered to be of no value to researchers, experimenters and other users other than spacecraft engineers. It is assumed that there will be no requests for retrieval of data in this category. The poor quality of the picture is related to the condition of the data transmitted from the satellite to the ground station and/or to data degradation in transmission from the DAF stations to the Nimbus Data Handling Facility or in initial reproduction. In general, it is not possible to improve the quality of these pictures by more sophisticated photographic processing techniques. Sectors with all data missing, or no discernible features, as well as sectors with excessive lines, excess noise breaks or dots, will be placed in this category. A coded entry (see



Section 9.9.2) will be made in the remarks section of the Data Log Section of the Nimbus II Monthly Catalogs, indicating the reason for placing the picture in this category. Pictures with identifiable features, but containing some missing data, missing or incorrect grids, limited engineering errors or other minor discrepancies, will be classified on the basis of their data content and a coded entry (see Section 9.8) made in remarks section of the Data Log Section of the Catalogs to indicate the discrepancy.

It should be noted that whenever the reason for non-discernibility is related to atmospheric pollutants or other identifiable obscurations, they will be given the appropriate classification under the category, "General Cloud Features" (atmospheric pollutants).

#### 9.7 Classification and Cataloging Descriptors for Nimbus C Satellite

<u>Alpha Descriptor</u>	<u>Numerical Descriptor</u>	<u>Data Content</u>
VRTC	1000	Vortical Cloud Features
VXCL	1100	Extratropical Vortical Cloud Features
VXFR	1110	Frontal Vortices
VXFB	1111	Class A
VXFQ	1112	Class B
VXFM	1113	Class C
VXFD	1114	Class D
VXFT	1115	Class E
VXNO	1120	Nonfrontal Vortices
VXNL	1121	Class I
VXNW	1122	Class II
VXNS	1123	Class III
VXNT	1124	Class IV
VXNM	1125	Class V
VTCT	1200	Tropical Vortical Cloud Features
VTSM	1210	Tropical Cyclone, less than $4^{\circ} \times 4^{\circ}$ in extent
VTSA	1211	Cirrus canopy indeterminate eye visible
VTSB	1212	Cirrus canopy indeterminate eye not visible
VTSC	1213	Cirrus canopy, eye visible
VTSD	1214	Cirrus canopy, eye not visible
VTSE	1215	No cirrus canopy, eye visible
VTSF	1216	No cirrus canopy, eye not visible
VTSQ	1217	With associated squall line

<u>Alpha Descriptor</u>	<u>Numerical Descriptor</u>	<u>Data Content</u>
VTMM	1220	Tropical Cyclone, $4^{\circ} \times 4^{\circ}$ to $6^{\circ} \times 6^{\circ}$ in extent
VTMA	1221	Cirrus canopy indeterminate, eye visible
VTMB	1222	Cirrus canopy indeterminate, eye not visible
VTMC	1223	Cirrus canopy, eye visible
VTMD	1224	Cirrus canopy, eye not visible
VTME	1225	No cirrus canopy, eye visible
VTMF	1226	No cirrus canopy, eye not visible
VTMQ	1227	With associated squall line
VTLR	1230	Tropical Cyclone, greater than $6^{\circ} \times 6^{\circ}$ in extent
VTLA	1231	Cirrus canopy indeterminate, eye visible
VTLB	1232	Cirrus canopy indeterminate, eye not visible
VTLC	1233	Cirrus canopy, eye visible
VTLD	1234	Cirrus canopy, eye not visible
VTLE	1235	No cirrus canopy, eye visible
VTLF	1236	No cirrus canopy, eye not visible
VTLQ	1237	With associated squall line
VTLQ	1240	Quasi-circular cloud features, less than $6^{\circ} \times 6^{\circ}$ in extent
VTTA	1241	No cirrus canopy
VTTB	1242	Cirrus canopy indeterminate
VTTC	1243	Cirrus canopy
VTXQ	1250	Quasi-circular cloud features, $6^{\circ} \times 6^{\circ}$ or greater in extent
VTXA	1251	No cirrus canopy
VTXB	1252	Cirrus canopy indeterminate
VTXC	1253	Cirrus canopy
BAND	2000	Major Cloud Bands
BXCL	2100	Extratropical Cloud Bands
BXSQ	2110	Pre-frontal instability or squall line
BXPF	2120	Post-frontal instability line or secondary front
BXIB	2130	Tropospheric Inversion band
BXFR	2140	Frontal bands
BXFW	2141	Warm front
BXFC	2142	Cold front
BXFV	2143	Frontal wave
BXFO	2144	Occluded front
BXFP	2145	Triple point of an occluded front
BXFS	2146	Stationary front

<u>Alpha Descriptor</u>	<u>Numerical Descriptor</u>	<u>Data Content</u>
BXFJ	2147	Indication of a jet stream associated with a frontal band
BTCL	2200	Tropical Cloud Bands
BTFR	2210	Mid-latitude cold front in tropical region
BTIC	2220	Area or line of convergence
BTPT	2230	Perturbed tropical cloud band
GNRL	3000	General Cloud Features
GLPB	3100	Minor Cloud Lines or Parallel Bands
GLJT	3110	Indication of a jet stream
GLLS	3120	Large single straight lines
GLBL	3130	Billow clouds
GLCR	3140	Crest patterns
GLST	3150	Cloud streets
GLSN	3151	Onshore flow
GLSF	3152	Offshore flow
GLTR	3160	Terrain induced wave clouds
GLTL	3161	Lee waves
GLTM	3162	Mountain wave
GLTF	3163	Fibrous plumes
GCUM	3200	Cumuliform Cloud Features
GCSC	3210	Solid cells
GCSM	3211	Cumulonimbus cloud masses
GCSN	3212	Cumulonimbus clouds
GCST	3213	Towering cumuli
GCSA	3214	Cumulonimbus with cirriform anvils
GCCC	3220	Cellular cloud patterns
GCCP	3221	Polygonal cells
GCCS	3222	Scallops (vermiculated)
GCCL	3223	Linear alignment (blown-out ellipses)
GCCR	3224	Chaotic
GCCA	3225	Cloud filled cells
GCCF	3226	Actiniform
GCCM	3227	Mixed cellular cloud patterns
GCFW	3230	Unorganized Fair Weather Cumuliform Clouds
GCFN	3231	Onshore flow
GCFE	3232	Offshore flow
GCFO	3233	Fair weather cumuliform clouds not contiguous to shorelines
GSTR	3300	Stratiform Cloud Features
GSPL	3310	Atmospheric pollutants

<u>Alpha Descriptor</u>	<u>Numerical Descriptor</u>	<u>Data Content</u>
GSPH	3311	Haze
GSPG	3312	Smog
GSPK	3313	Smoke
GSPD	3314	Dust
GSFG	3320	Stratus or fog
GSFL	3321	Land stratus or fog
GSFC	3322	Coastal stratus or fog
GSFV	3323	Valley stratus or fog
GSFP	3324	Penetrating stratus or fog
GSFS	3325	Sea stratus or fog
GSMI	3330	Middle or high stratiform
GSMH	3331	Middle clouds
GSMH	3332	High clouds
GSMF	3333	Fibrous cirrus
GIRD	3400	Infrared Radiometer
GILO	3410	Low level clouds
GIMI	3420	Medium level clouds
GIPT	3430	Random pattern clouds
GIPL	3431	Low and middle clouds
GIPO	3432	Mostly open high clouds
GIDT	3440	Daytime HRIR
TRRN	4000	Terrestrial Features
TWTR	4100	Water Body
TWGF	4110	Gulf
TWCH	4120	Strait, channel or canal
TWSE	4130	Sea or ocean
TWSC	4131	Ocean current
TWSW	4132	Ocean wave pattern
TWSB	4133	Ice fields or ice packs
TWSP	4134	Ice floes or icebergs
TWRV	4140	River or stream
TWRF	4141	Flooded
TWRZ	4142	Frozen
TWRP	4143	Partly frozen
TWRD	4144	Delta
TWRL	4145	Flood plain
TWLK	4150	Lake
TWLF	4151	Frozen
TWLP	4152	Partly frozen
TWLS	4153	Snow covered

<u>Alpha Descriptor</u>	<u>Numerical Descriptor</u>	<u>Data Content</u>
TCST	4200	Coastline
TCMT	4210	Mountainous, rugged
TCBR	4220	Beach or bar
TCPA	4230	Peninsula or cape
TCA Y	4240	Bay, estuary or lagoon
TCCP	4250	Coastal plain
TCFD	4260	Fiord (Fjord) or ria
TMNT	4300	Mountain
TMPK	4310	Peak or dome
TMRG	4320	Range or system
TMVL	4330	Volcano
TMGL	4340	Glacier
TMGV	4341	Valley glacier (mountain glacier or ice stream)
TMGP	4342	Piedmont glacier (intermont glacier)
TMGI	4343	Ice sheet or ice cap
TMSF	4350	Snow field
TDES	4400	Desert
TDSD	4410	Sand
TDDU	4420	Sand dunes
TD AK	4430	Alkali flats (salt flats, salt pans)
TDLK	4440	Dry lake (playa)
TDRV	4450	Dry river bed or dry wash (arroyo, wadi)
TDOA	4460	Oasis
TGEO	4500	Other Geomorphology
TGPN	4510	Plain
TGTB	4520	Plateau or tableland
TGVY	4530	Valley, gorge or canyon
TGSW	4540	Swamp or marsh
TGIL	4550	Island or atoll
TGBN	4560	Basin or depression
TGFT	4570	Fault or other lineament
TQUA	4600	Miscellaneous
TQGL	4610	Sun glints
TQDN	4620	Underwater features
TQSF	4630	Ice or snow field
TQVG	4640	Forest or vegetation
TQVF	4641	Forest fire
TQCL	4650	Cloud amount
TQCO	4651	Open

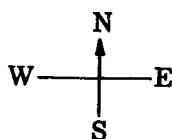
<u>Alpha Descriptor</u>	<u>Numerical Descriptor</u>	<u>Data Content</u>
TQCS	4652	Mostly open
TQCB	4653	Mostly covered
TQCV	4654	Covered
INDF	5000	Indistinguishable Features
INDT	5100	Inadequate Distinction Between Clouds and Terrain
INDS	5200	Inadequate Distinction Between Clouds and Ice/Snow Field
INDC	5300	Inadequate Distinction Between Cloud Fields
POOR	6000	Picture of Poor Quality or no Discernible Features

### 9.8 Phenomenon Continuation Code

Each four-digit data content descriptor is followed by an entry of a single Alphabetical character, the alphabet representing the phenomenon continuation code. The code indicates that all significant features of the phenomenon described by the preceding descriptors are contained within the sector or that some of the significant features of the phenomenon are contained in other sectors and/or swaths. Figure 9-93 indicates the sequence in which sectors and swaths will be analyzed and illustrates the phenomenon Continuation Code.

<u>Sequence</u>	<u>Code</u>	
0	A	All significant features are contained in this sector
1	B	Some significant features are contained in the preceding sector
2	C	Some significant features are contained in the next swath
3	D	Some significant features are contained in the next sector
4	E	Some significant features are contained in the preceding swath
12	F	Some significant features are contained in the preceding sector and next swath
13	G	Some significant features are contained in the preceding sector and next sector
14	H	Some significant features are contained in the preceding sector and preceding swath
23	I	Some significant features are contained in the next swath and next sector

<u>Sequence</u>	<u>Code</u>	
24	J	Some significant features are contained in the next swath and preceding swath
34	K	Some significant features are contained in the next sector and preceding swath
123	L	Some significant features are contained in the preceding sector, next swath and next sector
124	M	Some significant features are contained in the preceding sector, next swath and preceding swath
134	N	Some significant features are contained in the preceding sector, next sector and preceding swath
234	O	Some significant features are contained in the next swath, next sector and preceding swath
1234	P	Some significant features are contained in the preceding sector, next swath, next sector, and preceding swath
	Q	The phenomenon is too complex for description by this coding system.



<u>Swath 3</u>	<u>Swath 2</u>	<u>Swath 1</u>
Next Swath	Current Swath	Preceding Swath
	1	
	Preceding Sector	
	Current Sector	
2	0	4
	Next Sector	
	3	

Figure 9-93--Sector and Swath Analysis Sequence

## 9.9 Codes for Remarks Section of Data Log

Section 9.9.1 contains the data content confirmation code for entries in the remarks section of the Data Log Section of the Nimbus II catalog.

Section 9.9.2 contains the quality control code for entries in remarks section of the Data Log Section of the Nimbus II Catalog.

Section 9.9.3 contains the Cloud Amount Code for entries in the remarks section of the Data Log Section of the Nimbus II Catalog.

Any additional remarks required will be in abbreviated plain language format. Each abbreviation, contraction, and/or code entry will be separated from other entries by a blank space.

The order of entry in the remarks section of the Data Log Section of the Nimbus II Catalog is as follows:

- (a) Data Content Confirmation
- (b) Quality Control Code
- (c) Cloud Amount Code
- (d) Abbreviations and Contractions

### 9.9.1 Data Content Confirmation Code

The data content confirmation code consists of a one digit numeral (0-6) followed by a single alphabetical character. The numeral indicates the data content descriptor of the sector to which the confirmation code applies. The letter indicates that the feature described by the descriptor was or was not confirmed by conventional meteorological data or topographical, geographical or geomorphological data. Normally, the data classification procedures will include routine reference to various available meteorological analyses, provided daily to NDUC by the National Meteorological Center. The confirmation obtained by these procedures would apply largely to major cloud features such as frontal bands, vortices and clouds of considerable areal extent. Similarly, references will be made to various world atlases for topographical, geographical or geomorphological data in those instances where required. The confirmation code is an optional one and will be required only for those situations differing significantly from reasonably positive data confirmation, such as those described by Codes C, D and E.



### Numerical Code

- 0 - All descriptor mnemonics of the sector
- 1 - First descriptor mnemonic of the sector
- 2 - Second descriptor mnemonic of the sector
- 3 - Third descriptor mnemonic of the sector
- 4 - Fourth descriptor mnemonic of the sector
- 5 - Fifth descriptor mnemonic of the sector
- 6 - Sixth descriptor mnemonic of the sector

### Alphabetical Code

- A - Descriptive category - confirmation not required.
- B - Classification confirmed by conventional meteorological data.
- C - Classification confirmed by conventional meteorological data; however, conventional data place phenomena in a significantly different but nearby location.
- D - No conventional meteorological data available to confirm classification.
- E - Classification differs from that in available conventional meteorological data. However, analyst is confident of classification.
- F - No attempt made to confirm classification by conventional meteorological data.
- G - Small scale general cloud features - confirmation by conventional meteorological data not possible.
- W - Classification confirmed by topographical, geographical or geomorphological data.
- X - Topographical, geographical or geomorphological data not available to confirm classification.
- Y - Classification differs from that in available topographical, geographical or geomorphological data; however, analyst is confident of classification.
- Z - No attempt to confirm classification by topographical, geographical or geomorphological data.

### 9.9.2 Quality Control Codes

#### Code

- EE - Engineering Error - flutter and wow, sync tear, pulldown, noise lines, breaks, dots, etc.
- AE - Apparent Attitude Error (Attitude appears to deviate more than 3° from nominal in at least one of the three axes).

### Code

- NL - No Legend (index display).
- EL - Erroneous Legend (index display) - overprint of picture, incorrect time, incorrect orbit number, etc.
- XG - Partial or incomplete grid.
- EG - Erroneous grid.
- CG - Grid off center.
- OG - Grid index omitted.
- DG - Double grid.
- NG - No grid.
- PE - HRIR Phasing Error (shift) - sync pulses visible on picture or earth's horizon not centered on picture.
- PI - Picture Image Retained (picture contains part of the image of another picture).
- PC - Poor film contrast.
- PU - Picture underexposed.
- PO - Picture overexposed.
- PP - Partial picture (some data missing).
- PR - Faulty Photographic Processing.
- DD - All daytime data.
- MD - Mixed data (day and night data).
- ND - All nighttime data (only for MRIR entries).
- XX - No data.
- NS - No gray scale wedge.
- ES - Erroneous gray scale wedge.
- XS - Partial or incomplete gray scale wedge.
- QS - Gray scale wedge of poor quality.
- TM - Time Marks (time ticks) - missing, incomplete, in wrong place, or otherwise in error.

### 9.9.3 Cloud Amount Code

A cloud amount code entry can be made in the remarks section of the Data Log Section of the Nimbus II Users' Catalog to indicate the total amount of cloudiness in a picture or sector in which the amount of cloudiness is not indicated by a descriptor in the Data Content Section.

### Code

- O - Open - <20% cloudiness
- MOP - Mostly open - 20% to 50% cloudiness
- MCO - Mostly covered - 50% to 80% cloudiness
- C - Covered - >80% cloudiness

## APPENDIX A

### DIGITAL HRIR DATA PROCESSING

The Nimbus Meteorological Radiation Tape-HRIR will be a basic repository for radiation data from the Nimbus High Resolution Infrared Radiometer. This tape will contain data in binary mode at a density of 800 bits per inch.

The first file on this tape contains a BCD label. The label consists of fourteen words of BCD information followed by an end-of-file. The remaining files on this tape contain formatted HRIR data in the format described on the following pages. The first record in this data file is a documentation record which describes the data to be found in the succeeding records. This first record contains seventeen words (see Table A-1). The remaining records in the file will be of variable length, but this length will be consistent within the file (see Table A-2). The length (L) of the data record can be computed as follows:

$$L = (\text{SWATHS PER RECORD}) \times (\text{WORDS PER SWATH}) \\ + (\text{NUMBER OF NADIR ANGLES}) + 7$$

Ninety degrees are added to all latitudes and attitude data to eliminate negative signs.

Table A-3 defines the flags which appear in the data records.

TABLE A-1

## NMRT-HRIR Documentation Record Format

<u>Word No.</u>	<u>Quantity</u>	<u>Units</u>	<u>Scaling</u>	<u>Remarks</u>
1	Dref	-----	B = 35	Number of days between 0 hour on 9/1/57 and zero hour on day of launch.
2	Date	MMDDYY	B = 35	Date of interrogation for this orbit, i.e., 2/5/64 would be (020504)8. Only the last digit of year is used.
3	Nimbus Day	-----	B = 35	Start time for this file of data
4	Hour	Z hour	B = 35	
5	Minute	Z minute	B = 35	
6	Seconds	Z seconds	B = 35	
7	Nimbus Day	-----	B = 35	End time for this file of data
8	Hour	Z hour	B = 35	
9	Minute	Z minute	B = 35	
10	Seconds	Z seconds	B = 35	
11	Mirror Rotation Rate	Deg/Sec	B = 26	Rotation rate of radiometer mirror
12	Sampling Frequency	Samples/Sec	B = 35	Digital sampling frequency per second of vehicle time
13	Orbit Number	-----	B = 35	Orbit Number
14	Station Code	-----	B = 35	DAF Station identification code
15	Swath Block Size	-----	B = 35	Number of 35-bit words per swath
16	Swaths/Record	-----	B = 35	Number of swaths per record
17	Number of Locator Points	-----	B = 35	Number of anchor points per swath for which latitudes and longitudes are computed.

**TABLE A-2**  
**NMRT-HRIR Data Record Format**

<u>Word No.</u>	<u>Quantity</u>	<u>Units</u>	<u>Scaling</u>	<u>Remarks</u>
1D	Nimbus Day	-----	B=17	Start time for this record of data
1A	Hour	Z hour	B=35	
2D	Minutes	Z minute	B=17	
2A	Seconds	Z seconds	B=35	
3D	Roll Error	Degrees	B=14	Roll error at time specified in words one and two.
3A	Pitch Error	Degrees	B=32	Pitch error at time specified in words one and two.
4D	Yaw Error	Degrees	B=14	Yaw error at time specified in words one and two.
4A	Height	Kilometers	B=35	Height of spacecraft at time specified in words one and two.
5D	Detector cell Temperature	Degrees K	B=17	Measured temperature of detector cell at time specified in words one and two.
5A	Electronics Temperature	Degrees K	B=35	Measured temperature of electronics at time specified in words one and two.
6D	24 V Supply	Volts	B=14	Measured voltage at time specified in words one and two.
6A	20 V Supply	Volts	B=32	Measured voltage at time specified in words one and two.
7D	Reference Temperature A	Degrees K	B=17	Measured temperature of housing at time specified in words one and two.
7A	Reference Temperature B	Degrees K	B=35	
8	Nadir Angle	Degrees	B=29	Nadir angles corresponding to each locator point, and measured in the plane of the radiometer
.				
.				
N	Nadir Angle	Degrees	B=29	

The above data constitutes what is essentially the documentation portion of a data record. This data will be followed by several blocks of data with each block representing a swath. The number of these blocks in a record as well as the size of each block is specified in the documentation record represented on the previous page.

TABLE A-2 (Continued)

## NMRT-HRIR Data Record Format (Continued)

<u>Word No.</u>	<u>Quantity</u>	<u>Units</u>	<u>Scaling</u>	<u>Remarks</u>
(N+1)D	Seconds	Z Seconds	B = 8	Seconds past time in words 1A & 2D for beginning of this swath.
(N+1)A	Data Population	-----	B = 35	Number of data points in this swath.
(N+2)D	Latitude	Degrees	B = 11	Latitude of subsatellite point for this swath
(N+2)A	Longitude	Degrees	B = 29	Longitude of subsatellite point for this swath, positive westward 0 to 360°.
N+3	Flags	-----	-----	Reserved for flags describing this swath
(N+4)D	Latitude	Degrees	B = 11	Latitude of viewed point for the first anchor spot
(N+4)A	Longitude	Degrees	B = 29	Longitude of viewed point for first anchor spot, positive westward 0 to 360°.
.				
.				
.				
MD	Latitude	Degrees	B = 11	Latitude and longitude for
MA	Longitude	Degrees	B = 29	Mth anchor spot
(M+1)D	HRIR Data	-----	B = 14	HRIR measurements. Tag and
(M+1)A	HRIR Data	-----	B = 32	prefix reserved for flags.
.				
.				
.				
K(A or D)	HRIR Data	-----	B = 32 - 14	Last HRIR data measurement

All remaining or unused portions of a swath data block are set to zero, giving a swath block size as specified in the documentation record. The above data on this page is repeated for the number of swaths in each record.

TABLE A-3

## DEFINITION OF FLAGS DESCRIBING EACH HRIR SWATH

<u>FLAG</u>	<u>BIT</u>	<u>DEFINITION</u>	<u>YES</u>	<u>NO</u>
1	35	Summary flag. All checks defined by flags 2 thru 12 are satisfactory. (each flag is zero)	0	1
2	34	Consistency check between sampling rate, vehicle time, and ground time is satisfactory	0	1
3	33	Vehicle time is satisfactory	0	1
4	32	Vehicle time has been inserted by flywheel	1	0
5	31	Vehicle time carrier is present	0	1
6	30	Vehicle time has skipped	1	0
7	29	Vehicle time frame sync interrupt by hardware did not occur.	1	0
8	28	Sync pulse recognition was satisfactory	0	1
9	27	Dropout of data signal was detected	1	0
10	26	Ground time has a new pattern	1	0
11	25	Ground time is discontinuous	1	0
12	24	Swath size is satisfactory when compared with the theoretical swath size	0	1
13	23	End of tape was detected on the spacecraft	1	0

## FLAGS FOR INDIVIDUAL MEASUREMENTS

<u>PREFIX</u>	<u>TAG</u>	<u>DEFINITION</u>	<u>YES</u>	<u>NO</u>
S	18	The particular measurement is below the earth-space threshold	1	0
1	19	Unassigned		
2	20	Unassigned		

## APPENDIX B

### Digital MRIR Data Processing

The MRIR digital magnetic tape (output of the Telemetrics 670 Computer) is formatted for compatibility with the IBM 7094 computer system. The digital response from each radiometer sensor is stripped of sync bits and all five simultaneous responses are placed in one 36-bit IBM word with 7 bits for each data measurement and a one in the least significant bit. The time code is also stripped of all unnecessary bits and formatted into one 36-bit word expressing time to the nearest second. The following special code words are inserted to identify the various conditions described below:

1.  $(666666666666)_8$  - Identifies the next word as the Minitrack time word.
2.  $(777777777777)_8$  - Identifies end of data.
3.  $(525252525252)_8$  - Identifies data dropout. This code word is used when all five measurements are simultaneously bad. When an individual measurement is bad, the data for that measurement is set equal to the previous measurement.

The magnetic tape containing the formatted MRIR radiation data represents the primary source of radiometer data for further processing and archiving. The first step in this procedure is to examine the formatted radiometer output and create an intermediate tape which contains (1) the response from each radiometer channel for every earth-viewed scan, (2) the associated response from each channel of the radiometer while viewing space, (3) the associated response from each channel of the radiometer while viewing spacecraft housing, and (4) the time associated with each earth scan. The intermediate tape will be the basic repository for raw radiation data from the Nimbus Medium Resolution Infrared Radiometer, and also represents the primary input source of radiometer data for the second step in the data processing plan.

The Nimbus Meteorological Radiation Tape (NMRT-MRIR) for the Medium Resolution Infrared Radiometer is the output from the second step of the data processing plan. The inputs to this program are (1) the intermediate MRIR data tape, (2) pertinent telemetry data transmitted from the spacecraft, (3) the Minute Vector Tape (MVT) containing position vectors of the spacecraft at one minute intervals, and (4) miscellaneous documentation data.



During this second phase, each data measurement is converted to equivalent units of energy, latitudes and longitudes are computed for locator points, and orbital and telemetry data are computed as a function of time. These data are formatted as described below, and the Nimbus Meteorological Radiation Tape for medium resolution infrared data is produced.

The NMRT-MRIR is the basic repository for calibrated radiation data from the medium resolution infrared radiometer. This tape contains data in binary mode and a density of 800 bits per inch. The first file on each tape contains a BCD label consisting of fourteen words of BCD information followed by an end-of-file. The remaining files on this tape contain the MRIR data in the format described below. There will be one file for each orbit of data. The first record in a data file is a documentation record containing 15 words which describe the data to be found in each succeeding record (see Table B-1). The remaining data records in each file will be of variable length, but this length will be consistent within the file (see Table B-2). The length of a data record (L) can be determined as follows:

$$L = (\text{SWATHS PER RECORD}) \times (\text{WORDS PER SWATH}) + (\text{NUMBER OF NADIR ANGLES}) + 8$$

Ninety degrees are added to all latitudes and attitude errors to eliminate negative signs.

TABLE B-1

## NMRT-MRIR Documentation Record Format

<u>Word No.</u>	<u>Quantity</u>	<u>Units</u>	<u>Scaling</u>	<u>Remarks</u>
1	Nimbus Day	-----	B = 35	Start time for this file of data.
2	Hour	Z Hour	B = 35	
3	Minute	Z Minute	B = 35	
4	Seconds	Z Seconds	B = 35	
5	Nimbus Day	-----	B = 35	End time for this file of data.
6	Hour	Z Hour	B = 35	
7	Minute	Z Minute	B = 35	
8	Seconds	Z seconds	B = 35	
9	Mirror Rotation Rate	Deg/Sec	B = 26	Rotation rate of radiometer mirror.
10	Sampling Frequency	Samples/Sec	B = 23	Digital sampling frequency per second of vehicle time.
11	Orbit Number	-----	B = 35	Orbit Number.
12	Station Code	-----	B = 35	Station code for DAF ground station.
13	Swath Block Size	-----	B = 35	Number of 35-bit words per swath.
14	Swaths Per Record	-----	B = 35	Number of swaths per record.
15	Number of Locator Points	-----	B = 35	Number of anchor points per swath for which latitudes and longitudes are computed.

TABLE B-2  
NMRT-MRIR Data Record Format

<u>Word No.</u>	<u>Quantity</u>	<u>Units</u>	<u>Scaling</u>	<u>Remarks</u>
1D	Nimbus Day	-----	B = 17	Start time for this record of data.
1A	Hour	Z Hour	B = 35	
2D	Minutes	Z Minute	B = 17	
2A	Seconds	Z Second	B = 35	
3D	Roll Error	Degrees	B = 14	Roll error at time specified in words one and two.
3A	Pitch Error	Degrees	B = 32	Pitch error at time specified in words one and two.
4D	Yaw Error	Degrees	B = 14	Yaw error at time specified in words one and two.
4A	Height	Kilometers	B = 35	Height of Spacecraft at time specified in words one and two.
5A	Housing one Temperature	Degrees K	B = 32	Measured temperature of housing one at time specified in words one and two.
6D	Housing two Temperature	Degrees K	B = 14	Measured temperature of housing two at time specified in words one and two.
6A	Electronics Temperature	Degrees K	B = 32	Measured temperature of electronics at time specified in words one and two.
7D	Chopper one Temperature	Degrees K	B = 14	Measured temperature of chopper at time specified in words one and two.
7A	Chopper two Temperature	Degrees K	B = 32	Measured temperature of chopper at time specified in words one and two.
8D	GHA of SUN	Degrees	B = 14	GHA of sun at time specified in words 1 and 2.
8A	Decl of Sun	Degrees	B = 32	Declination of sun at time specified in words 1 and 2. Ninety degrees added to eliminate negative sign.
9	Nadir Angle	Degrees	B = 29	Nadir angles corresponding to each locator point and measured in the plane of the scanning radiometer.
:				
:				
N	Nadir Angle	Degrees	B = 29	Last nadir angle.

The above data constitutes what is essentially the documentation portion of a data record. These data will be followed by several blocks of data with each block representing a swath. The number of these blocks in a record as well as the size of each block is specified in the documentation record represented on the previous page.

TABLE B-2

## NMRT-MRIR Data Record Format (Continued)

<u>Word No.</u>	<u>Quantity</u>	<u>Units</u>	<u>Scaling</u>	<u>Remarks</u>
(N+1)D	Seconds	Z Seconds	B = 8	Seconds past time in words 1A & 2D for beginning of this swath.
(N+1)A	Data Population	-----	B = 35	Number of data points in this swath.
(N+2)D	Latitude	Degrees	B = 11	Latitude of subsatellite point for this swath.
(N+2)A	Longitude	Degrees	B = 29	Longitude of subsatellite point for this swath.
(N+3)D	Latitude	Degrees	B = 11	Latitude of viewed point for the first anchor spot.
(N+3)A	Longitude	Degrees	B = 29	Longitude of viewed points for the first anchor spot. Measured positive westward, 0 - 360 degrees.
(M)D	Latitude	Degrees	B = 11	Latitude and longitude of last anchor spot.
(M)A	Longitude	Degrees	B = 29	
(M+1)D	MRIR Data	-----	B = 14	MRIR Data Measurement, channel one.
(M+1)A	MRIR Data	-----	B = 32	MRIR Data Measurement, channel one.
K(A or D)	MRIR Data	-----	B = 14 - 42	Last MRIR Data Measurement, channel one.

Words M+1 through K are repeated for channels two through five respectively. All remaining or unused portions of a swath data block are set to zero, giving a swath block size as specified in the documentation record. The above data on this page is repeated for the number of swaths in each record.

## APPENDIX C

### Glossary and List of Abbreviations

#### Glossary

**ANOMALY:** Geocentric angle between an orbiting body and its perigee, measured in the direction of motion. True anomaly is the actual angle; mean anomaly is a function of time and the anomalistic period, and is equivalent to true anomaly only for a circular orbit.

**ANOMALISTIC PERIOD:** The time elapsed between successive passages of an orbiting body through perigee.

**APOGEE:** The point in an orbit which is furthest from the center of the earth.

**ARGUMENT:** Geocentric angle between an orbiting body (or a point on the orbit) and ascending node, measured in the direction of motion.

**ASCENDING NODE:** The point at which an orbiting body crosses the equator northbound; identified by time and longitude (or right ascension in celestial coordinates).

**ATTITUDE (SATELLITE):** The orientation of a satellite in space. For Nimbus attitude conventions see Section 1.3 and entries below under Pitch, Roll, and Yaw.

**BLIND ORBIT:** An orbit during which a satellite cannot be interrogated because it does not come within range of any DAF station, or when no DAF station is available due to schedule conflicts.

**DATA ACQUISITION FACILITY:** A ground station at which are performed various functions to control satellite operation and to obtain data from a satellite. Two DAFs are used for Nimbus, one at Rosman, North Carolina (Rosman), and one at Fairbanks, Alaska (Ulaska).

**DATA ORBIT:** The orbit during which data were acquired by the satellite. If the orbit number changes during a data swath (See Orbit Number, below) the Data Orbit is identified by the higher orbit number.

**DEGRADATION:** The lessening of picture image quality because of noise or any optical, electronic, or mechanical distortions in the image-forming system.

**DESCENDING NODE:** The point at which an orbiting body crosses the equator southbound; identified by time and longitude.

**EPHEMERIS:** A tabulation of spacecraft location at regular time intervals. (Plural is ephemerides.)

**FIDUCIAL MARKS:** Index marks on the face of the AVCS and APT Vidicons, which appear on all pictures.

**HEADING LINE:** The instantaneous projection of the spacecraft velocity vector on the earth's surface.

**INCLINATION:** The angle between the earth's equatorial plane and the orbital plane of a satellite. The angle is measured at the ascending node, counterclockwise from the equatorial plane, looking toward the center of the earth.

**INTERROGATION ORBIT:** The orbit during which data were played back from the satellite to a DAF station.

**NADIR:** The point on the celestial sphere opposite the zenith, i.e., the point directly "below" a satellite.

**NADIR ANGLE:** The angle measured at the satellite between a given axis or ray and the local vertical.

**NODAL PERIOD:** The time elapsing between passages of a satellite through successive ascending nodes.

**ORBIT NUMBER:** In satellite meteorology orbit number refers to a particular circuit beginning at the ascending node. The orbit number from launch to the first ascending node is designated zero, thereafter the number increases by one at each ascending node.

**PERIGEE:** The point in an orbit which is nearest the center of the earth.

**PITCH:** A parameter of satellite attitude. For Nimbus the pitch axis is perpendicular to the orbit plane.

**PRINCIPAL LINE:** The line of intersection between the principal plane and the image plane, or between the principal plane and the earth.

**PRINCIPAL PLANE:** The plane defined by the optical axis of a camera and the local vertical through the front nodal point of the camera lens.

**PRINCIPAL POINT:** The point of intersection of the optical axis of a camera with the image plane or with the earth.

**RETROGRADE ORBIT:** An orbit with an inclination angle between  $90^\circ$  and  $180^\circ$ , i.e., the satellite has a westward component of motion.

**ROLL:** A parameter of satellite attitude. For Nimbus the roll axis is the local horizontal through the satellite in the orbital plane; it coincides with the velocity vector if the orbit is circular.

**SUBPOINT TRACK:** Locus of subsatellite points on the earth, on an image, or on the celestial sphere.

**SUBSATELLITE POINT:** Intersection of the local vertical through the satellite with the earth's surface, with the image plane, or with the celestial sphere.

**TIROS:** Acronym for Television Infrared Observation Satellite.

**VIDICON:** Television camera tube.

**YAW:** A parameter of satellite attitude. For Nimbus the yaw axis coincides with the local vertical through the satellite.

#### List of Common Abbreviations

ASC	Ascending
APT(S)	Automatic Picture Transmission (System)
AVCS	Advanced Vidicon Camera System
CAMR	Camera (number identifier)
DAF	Data Acquisition Facility
DRIR	Direct Readout Infrared Radiometer
GSFC	Goddard Space Flight Center
HRIR	High Resolution Infrared Radiometer
MRIR	Medium Resolution Infrared Radiometer
NASA	National Aeronautics & Space Administration
NDHF	Nimbus Data Handling Facility
NDHS	Nimbus Data Handling System

NDUC	Nimbus Data Utilization Center
NESC	National Environmental Satellite Center
NMRT	Nimbus Meteorological Radiation Tape
NTCC	Nimbus Technical Control Center
NWRC	National Weather Records Center
PIG	Plotter Information Generator
SIP	Sensory Information Processor
SSDC	Space Science Data Center
STADAN	Space Tracking and Data Acquisition Network
UT	Universal Time



## REFERENCES

1. Stampfl, R. A. and H. Press, "Nimbus Spacecraft System." Aerospace Engineering, 21, 16-28, July 1962.
2. Goldshlak, L. and R. B. Smith, "Nimbus Backup Gridding: AVCS and HRIR." Technical Report No. 1, Contract No. NAS 5-3253, ARACON Geophysics Co., Concord, Mass., January 1964.
3. "TIROS VII Radiation Data Catalog and Users' Manual." Goddard Space Flight Center, Greenbelt, Maryland, Volume 1 thru 4.
4. "TIROS IV Radiation Data Catalog and Users' Manual." Goddard Space Flight Center, Greenbelt, Maryland, 15 December 1963. 250 pp.
5. "TIROS II Radiation Data Users' Manual." Goddard Space Flight Center, Greenbelt, Maryland, 15 August 1961. 57 pp.
6. "TIROS III Radiation Data Users' Manual." Goddard Space Flight Center, August 1962. 71 pp.
7. Bandeen, W. R., R. A. Hanel, John Licht, R. A. Stampfl, and W. G. Stroud. "Infrared and Reflected Solar Radiation Measurements from the TIROS II Meteorological Satellite." J. of Geophys. Res., 66, 3169-3185, October 1961.
8. Hanel, R. A., W. R. Bandeen, and B. J. Conrath. "The Infrared Horizon of the Planet Earth." J. of the Atmos. Sciences, 20, 73-86, March 1963.
9. Bandeen, W. R., B. J. Conrath and R. A. Hanel. "Experimental Confirmation from TIROS VII Meteorological Satellite of the Theoretically Calculated Radiance of the Earth Within the 15 Micron Band of Carbon Dioxide." J. of the Atmos. Sciences, 20, 609-614, November 1963.
10. Nordberg, W., W. R. Bandeen, G. Warnecke, and V. Kunde. "Stratospheric Temperature Patterns Based on Radiometric Measurements from the TIROS VII Satellite." Space Research V, North-Holland Publishing Co., 1964.
11. Bandeen, W. R., V. Kunde, W. Nordberg, and H. P. Thompson. "TIROS III Meteorological Satellite Radiation Observations of a Tropical Hurricane." TELLUS, XVI, 1964.
12. Deacon, E. L., "Water Vapor over the Sahara and TIROS III Observation." J. of Atmos. Sciences, 20, 614-615, November 1963.

13. Fritz, Sigmund, and Jay S. Winston. "Synoptic Use of Radiation Measurements from Satellite TIROS II." Monthly Weather Review, 90, 1-9, January 1962.
14. Fritz, S., P. Krishna Rao, and M. Weinstein. "Satellite Measurements of Reflected Solar Energy and the Energy Received at the Ground." J. of Atmos. Sciences, 21, 141-151, March 1964.
15. Furukawa, P. M., P. A. Davis, and W. Viezee. "An Examination of Some TIROS II Radiation Data and Related Studies." Final Report, Contract No. AF 19(628)-322, Stanford Research Institute, Menlo Park, California, July 1962.
16. Greenfield, S. M. and W. W. Kellogg. "Calculations of Atmospheric Infrared Radiation as seen from a Meteorological Satellite." J. of Meteor., 17, 283-289, June 1960.
17. Hanel, R. A. and D. Q. Wark. "TIROS II Radiation Experiment and Its Physical Significance." J. Opt. Soc. Am., 51, 1394-1399, December 1961.
18. King, Jean I. F., "Meteorological Inferences from Satellite Radiometer." J. of Atmos. Sciences, 20, 245-250, July 1963.
19. Larsen, S.H.H., T. Fujita, and W. L. Fletcher. "Evaluation of Limb Darkening from TIROS III Radiation Data." Research Paper No. 18, Mesometeorology Project, Department of Geophysical Sciences, The University of Chicago, August 1963.
20. Pedersen, Finn and Tetsuya Fujita. "Synoptic Interpretation of TIROS III Measurements of Infrared Radiation." Research Paper No. 19, Mesometeorology Project, Department of Geophysical Sciences, The University of Chicago, October 1963.
21. Larsen, S.H.H., T. Fujita, and W. L. Fletcher. "TIROS III Measurements of Terrestrial Radiation and Reflected and Scattered Solar Radiation." Research Paper No. 20, Mesometeorology Project, Department of the Geophysical Sciences, The University of Chicago, October 1963.
22. London, Julius, "Satellite Observations of Infrared Radiation." Scientific Report No. 1, Contract No. AF 19(604)-5955, College of Engineering, New York University, New York 53, N.Y., December 1959.

23. London, Julius, Katsuyuki Ooyama, and Herbert Viebrock. "Satellite Observations of Infrared Radiation." Report No. 2, Contract No. AF 19(604)-5955, College of Engineering, New York University, New York 53, N.Y., July 1960.
24. London, Julius, Katsuyuki Ooyama, and Herbert Viebrock. "Satellite Observations of Infrared Radiation." Final Report, Contract No. AF 19 (604)-5955, College of Engineering, New York University, New York 53, N.Y., October 1961.
25. Möller, Fritz and Ehrhard Raschke. "Evaluation of TIROS III Radiation Data." Interim Report No. 1 (July 1963) and Final Report (March 1964) NASA Research Grant Ns G-305, Ludwig-Maximilians-Universität, Meteorologisches Institut, München, Germany.
26. Nordberg, W., W. R. Bandeen, B. J. Conrath, V. Kunde, and I. Persano. "Preliminary Results of Radiation Measurements from the TIROS III Meteorological Satellite." J. of the Atmos. Sciences, 19, 20-30, January 1962.
27. Prabhakara, C., and S. I. Rasool. "Evaluation of TIROS Infrared Data." 234-246 in Proceedings of the First International Symposium on Rocket and Satellite Meteorology, Washington, D.C., April 1962, edited by H. Wexler and J. E. Caskey, Jr., North-Holland Publishing Co., Amsterdam, 1963.
28. Rasool, S. I., "Cloud Heights and Nighttime Cloud Cover from TIROS Radiation Data." J. of the Atmos. Sciences, 21, 152-156, March 1964.
29. Wark, D. Q., G. Yamamoto, and J. H. Lienesch. "Methods of Estimating Infrared Flux and Surface Temperatures from Meteorological Satellites." J. of the Atmos. Sciences, 19, 369-384, September 1962. (Also "Infrared Flux and Surface Temperature Determinations from TIROS Radiometer Measurements." Meteorological Satellite Laboratory Report No. 10 (1962) and Supplement thereto (1963), U. S. Weather Bureau, Washington, D.C.)
30. Wexler, R., "Satellite Observations of Infrared Radiation." First Semi-annual Technical Summary Report, Contract No. AF 19(604)-5968, Allied Research Associates, Inc., Boston, Mass., December 24, 1959.
31. Wexler, R., "Satellite Observations of Infrared Radiation." Second Semi-annual Technical Summary Report, Contract No. AF 19(604)-5968, Allied Research Associates, Inc., Boston, Mass. June 30, 1960.

32. Wexler, R., "Interpretation of Satellite Observations of Infrared Radiation." Scientific Report No. 1, Contract No. AF 19(604)-5968, Allied Research Associates, Inc., Boston, Mass., April 20, 1961.
33. Wexler, R., "Interpretation of TIROS II Radiation Measurements." Final Report, Contract No. AF 19(604)-5968, Allied Research Assoc., Inc., Boston, Mass., May 31, 1962.
34. Wexler, Raymond and Paul Sherr. "Synoptic Analysis of TIROS III Radiation Measurements." Final Report, Contract No. AF 19(628)-429, ARACON Geophysics Co., Concord, Mass., January 31, 1964.
35. Bandeen, W. R., M. Haley, and I. Strange, "A Radiation Climatology in the Visible and Infrared from the TIROS Meteorological Satellites." Paper presented at the International Radiation Symposium, I.U.G.G., Leningrad, August, 1964 (available in document X-651-64-218, Goddard Space Flight Center, Greenbelt, Maryland; also published as NASA TN D-2534).
36. Feinberg, Paul, "The MRIR-PCM Telemetry System - A Practical Example of Microelectric Logic Design," NASA TN D-2311, Goddard Space Flight Center, Greenbelt, Maryland.
37. "Handbook of Geophysics." Revised Edition, The MacMillan Co., New York, 1960.
38. Stampfl, R. A. and W. G. Stroud. "The Automatic Picture Transmission (APT) TV Camera System for Meteorological Satellites." NASA TN D-1915, November 1963.
39. Goldshlak, L. "APT Users' Guide." Scientific Report No. 1, Contract No. AF 19(628)-2471, Allied Research Associates, Inc., Concord, Mass., June 1963.
40. "APT Users' Guide," National Weather Satellite Center, Washington, D.C., 1965.
41. Goldshlak, L. and W. K. Widger, Jr. "The Nimbus II Data Code Experiment." Technical Note No. 1, Contract No. NAS5-10114, ARACON Geophysics Div., Allied Research Associates, Inc., Concord, Mass., January 1966.
42. Smith, R. B. "Manual Gridding of DRIR Facsimile Pictures." Technical Note No. 7 under Contract No. NAS5-3253, ARACON Geophysics Div., Allied Research Associates, Inc., Concord, Mass., November 1965.

43. Merritt, E. S. and C. W. C. Rogers. "Meteorological Satellite Studies of Mid-latitude Atmospheric Circulation (U)." Final Report, Contract No. N62306-1584, ARACON Geophysics Co., Concord, Mass., 1965.
44. Widger, W. K., Jr., J. C. Barnes, E. S. Merritt, and R. B. Smith. "Meteorological Interpretation of Nimbus High Resolution Infrared (HRIR) Data." Final Report, Contract No. NAS5-9554, ARACON Geophysics Co., Concord, Mass., August 1965.